MAXIMIZING HYDROCARBON RECOVERY OF A MATURE FIELD HAVING BOTTOM WATER DRIVE RESERVOIR USING VARIOUS IOR/EOR TECHNIQUES

By

MANISH KUMAR

School of Engineering Studies

Under the Guidance of

Dr. Pushpa Sharma, UPES.

Dr. D. K. Gupta, UPES.

Dr. R. K. Shamra, RESERVOIL

Submitted

In Partial Fulfillment for the Requirement of the Degree of

DOCTOR OF PHILOSOPHY

to

UNIVERSITY OF PETROLEUM AND ENERGY STUDIES

DEHRADUN-248007

August 2018

ACKNOWLEDGEMENTS

I take this opportunity to express my gratitude to my Internal Guide, Professor Dr. Pushpa Sharma without whose guidance, constant persuasion and incredible support, I would not be able to overcome all the hurdles through the journey of research work for Ph. D. I am very privileged to have a guide who has paid all attention to my research work in spite of his busy schedule. I have been able to enhance my technical knowledge, skills in paper writing and scientific research work only because of you. You have always been there for taking care of small things. I will be always indebted for all your noble deeds.

I would like to extend my heartful gratitude to my Internal Co-Guide, Dr. D. K. Gupta, Professor who guided me throughout my research work. His constant support and encouragement helped me to overcome all the obstacles. His insights and enthusiasm have been inspirational for me at all times. I have always received valuable suggestions and comments which has improved my research work. I will be always grateful for giving me new insight in research work.

Constant encouragement and invaluable suggestions made by External Guide, Dr. R.K. Sharma, Director-Reservoil, has made this work possible.

I would like to extend my gratitude towards Oil India Limited management for allowing me to carry out research work at UPES, Dehradun and granting permission to access data for doing this research work.

I take this occasion to thank the management of University of Petroleum and Energy studies, for providing me this golden opportunity for doing my research work. I particularly offer my deepest regards and sincere thanks to Dr. S. J. Chopra, Chancellor, Dr Deependra Kumar Jha, Vice chancellor, and Dr. Kamal Bansal, Dean, College of Engineering studies for providing me facilities, valuable suggestions and constant motivation during my entire research work. Special thanks to Dr. S. K. Gupta, Dr. S. K. Nanda, Dr. R. P.Soni, Dr. Parichay Kumar Das, Dr. Ashutosh Pandey and Dr. Vijay Parthsarthy for their valuable comments and suggestions, and helping me in understanding the flow of research work, and aligning things together in a comprehensive manner.

Also, I am grateful to Center for Continuing Education (CCE) and their entire team for guiding me in workflow for doing part time Ph.D. Special thanks to Mr. Rahul Sharma, Mr. Saurav Negi, Ms. Dimpy Daniel, Mr. Afaq Ahmed and Ms. K Deepa from CCE for their support and help.

I would like to thank all faculty members of Department of Petroleum Engineering and Earth Sciences, Dehradun for their support and help.

I am thankful to my mother, father, elder brothers and sisters for their constant support throughout the research work. I have always received unconditional support from them. Without your support and affection, I have not been able to pursue my research work.

My unequivocal gratitude and praise to the Almighty God by whom and through whom all things consist, for the life, grace, favor, strength, wisdom, and understanding to come this far in life and continue onwards. All glory be to God on high, And thanks forever!

Last, but not the least, my better half Mrs. Madhuri Kishore, daughter Miss Manshi Vidyarthi and son Vatsal Vidyarthi hold special mention for their unconditional love and understanding during research work for making of this thesis complete.

Manish Kumar
03.08.18
(Manish Kumar)

This thesis is dedicated to

Almighty GOD

Respected Teachers

And

My Parents–Smt. Duleshwari Devi and Shri Motilal Vidyarthi

DECLARATION

I, Manish Kumar hereby declare that the work presented in the thesis "**MAXIMIZING HYDROCARBON RECOVERY OF A MATURE FIELD HAVING BOTTOM WATER DRIVE RESERVOIR USING VARIOUS IOR/EOR TECHNIQUES**", to the best of my knowledge and belief, is original and my own work carried out at **UNIVERSITY OF PETROLEUM AND ENERGY STUDIES**, and has not been submitted elsewhere for a degree, also it contains no material previously published or written by another person except where due acknowledgement has been made in the text.

Manish Kumar
03/08/18

Manish Kumar

Chief Reservoir Engineer

Oil India Limited

Guwahati, Assam

UPES

www.upes.ac.in

THESIS COMPLETION CERTIFICATE

This is to certify that the thesis entitled **"MAXIMIZING HYDROCARBON RECOVERY OF A MATURE FIELD HAVING BOTTOM WATER DRIVE RESERVOIR USING VARIOUS IOR/EOR TECHNIQUES"** by Mr. Manish Kumar in partial completion of the requirements for the award of the Degree of Doctor of Philosophy in Engineering is an original work carried out by him under our supervision and guidance.

It is certified that the content of the thesis, in full or parts have not been submitted to any other Institute or University for the award of any other degree or diploma.

Internal Guide

Pushpa Sharma
03/08/2018

Dr. Pushpa Sharma

Professor
Department of Petroleum Engineering & Earth Sciences
University of Petroleum and Energy Studies
Dehradun- 248007, India

Internal Co-Guide

03/08/18

Dr. D. K. Gupta

Professor & HOD
Department of Petroleum Engineering & Earth Sciences
University of Petroleum and Energy Studies
Dehradun- 248007, India

Reservoil

A-31, Sudershan, sector- 17, Vashi, Navi Mumbai – 400705
Tel: +91-22-27659419, FAX: +91-22-27660782,
Email: reservoil@vsnl.com, visit us at www.reservoil.com

THESIS COMPLETION CERTIFICATE

This is to certify that the thesis entitled **"MAXIMIZING HYDROCARBON RECOVERY OF A MATURE FIELD HAVING BOTTOM WATER DRIVE RESERVOIR USING VARIOUS IOR/EOR TECHNIQUES"** by Mr. Manish Kumar in partial completion of the requirements for the award of the Degree of Doctor of Philosophy in Engineering is an original work carried out by him under our supervision and guidance.

It is certified that the content of the thesis, in full or parts have not been submitted to any other Institute or University for the award of any other degree or diploma.

External Guide

Dr. R K Sharma

Director :
Reservoil
Navi Mumbai, India
26Th July 2018

RESERVOIL * NAVI MUMBAI *

ABSTRACT

Oil deposits are often found in association with a communicating gas or water zone. The production of the oil often leads to unwanted production of water which lowers the recovery. In order to achieve maximum production for economic benefit best completion suited for the reservoir needs to be established. Today, advanced technologies of horizontal drilling and application of advanced well completion such as inflow control devices (ICD) turns the development of unswept oil into a reality. Additionally, maximum production can be achieved with more oil wells, but few optimal numbers of wells with proper well spacing reduces economic cost and increase recovery.

In this research, recovery maximization of bottom water drive reservoir has been done using primary, secondary and tertiary recovery methods.

For evaluating all the possibilities under primary, secondary and tertiary recovery, a reservoir with bottom water drive was selected. Initially, reservoir characterization was carried out using analytical studies i.e. material balance studies for determining drive mechanism index, aquifer strength determination, oil in place determination followed by determination of Water Oil Contact and transition zone thickness from capillary pressure lab data. In addition, lab data from special core analysis (SCAL) were used for determining relative permeability for different Rock types and reservoir fluid characterization using black oil PVT data. Outcome of the analytical studies were used for better understanding of reservoir architecture, which helped in numerical simulation modeling using Eclipse and Petrel software. Sixteen years of historical production and pressure data combined with a voluminous set of rock and fluid property data were utilized for history matching water, gas, and pressure behavior of forty-six wells over period of sixteen years for evaluating various development strategies under various Improved Oil Recovery (IOR)/ Enhanced Oil Recovery (EOR) options.

Under primary recovery, optimized vertical well, horizontal well and smart horizontal wells were placed in the history matched model for enhancing the recovery. Further pressure maintenance using water injection was applied on the reservoir. In tertiary recovery, simultaneous water alternate gas (SWAG) method was applied on the history matched model.

Sensitivity study has been performed on vertical well and horizontal well using different variants i.e. withdrawal rate, perforation length/ horizontal well length, offset from

water oil contact using history matched model. Optimized variant for horizontal well was further used in performing uncertainty/sensitivity study on compartment length, number of ICDs (Inflow control devices) and nozzle size of each ICD. Optimized variants for vertical and horizontal well were used in determining an optimal number of vertical and horizontal wells in a sector model. Lastly, a field development plan for mature field having bottom water drive reservoir was proposed by utilizing optimized variants for vertical, horizontal and smart horizontal wells with ICD for tapping unswept oil. Further pressure maintenance scheme and SWAG process were deployed. Techno economic feasibility study was carried out for best vertical well, horizontal well, horizontal well with ICD and various field development strategies.

TABLE OF CONTENTS

LIST OF TABLES

LIST OF FIGURES

NOMENCLATURE

ABBREVIATION	DESCRIPTION
CCE	Constant composition expansion
CVD	Constant volume depletion
EOH	End of History
EOP	End of Prediction
EOR	Enhanced Oil Recovery
EOS	Equation of State
FDP	Field development plan
FWL	Free water level
FZI	Flow zone indicator
GOR	Gas oil ratio
HCPV	Hydrocarbon pore volume
hp	Perforation thickness (feet)
ICD	Inflow control device
IRR	Internal rate of return
lab	Laboratory
LWD	Logging while drilling
MM	Million Metric
NPV	Net present value
OCS	Oil collecting station
res	Reservoir
RFT	Reservoir formation tester
RQI	Rock quality index
SCAL	Special Core Analysis
STOIIP	Stock Tank Oil Initially in Place
SWAG	Simultaneous Water and Gas
THP	Tubing head pressure
TVDSS	True vertical depth below sea level
WOC	Water Oil Contact
h	Formation thickness (feet)
B_o	Formation volume factor of oil
ϕ	Porosity (Fraction)
σ	Interfacial tension (dynes/cm)
μ_o	Oil viscosity (cP)
θ	Contact angle (degrees)
K	Permeability (mD)
K_h	Horizontal permeability (mD)

ABBREVIATION	DESCRIPTION
K_o	Oil permeability (mD)
K_v	Vertical permeability (mD)
P_c	Capillary pressure
r_e	Drainage radius (feet)
r_w	Wellbore radius (feet)
B_o	Formation volume factor of oil
ρ_w	Water density(lbm/ft^3)
ρ_o	Oil density (lbm/ft^3)
Σ	Interfacial tension (dynes/cm)
ϕ_e	Effective porosity
μ_o	Oil viscosity(cP)
$J(S_w)$	J Function
r	Pore throat radius
C_t	Total compressibility
scm	Standard Cubic Meter
BCM	Billion Cubic Meter
MMm^3	Million Cubic Meter
m^3/d	Meter cube per day

CHAPTER 1

INTRODUCTION

1.1 OVERVIEW

Average recovery factor for world oil ranges from 20 to 40 percent (NCBI website). This percentage includes mainly easy oil. As shown in Figure 1.1, more oil can be recovered over easily found oil which is dependent on modern technology, better management of reservoir and optimal/ economic development strategies. In last decades, it has been observed that big discoveries are decreasing. Big discoveries have peaked between the year 1960 and 1970 (Ivanhoe, 1997), and therefore decline in discoveries has been seen. Most of the world oil reserves are from thirty big fields which are considered to be one-half of world oil reserves. Development of these big fields involves new technology with economics taken into consideration along with better reservoir management (Black and LaFrance, 1998; Al-Attar, 2004).

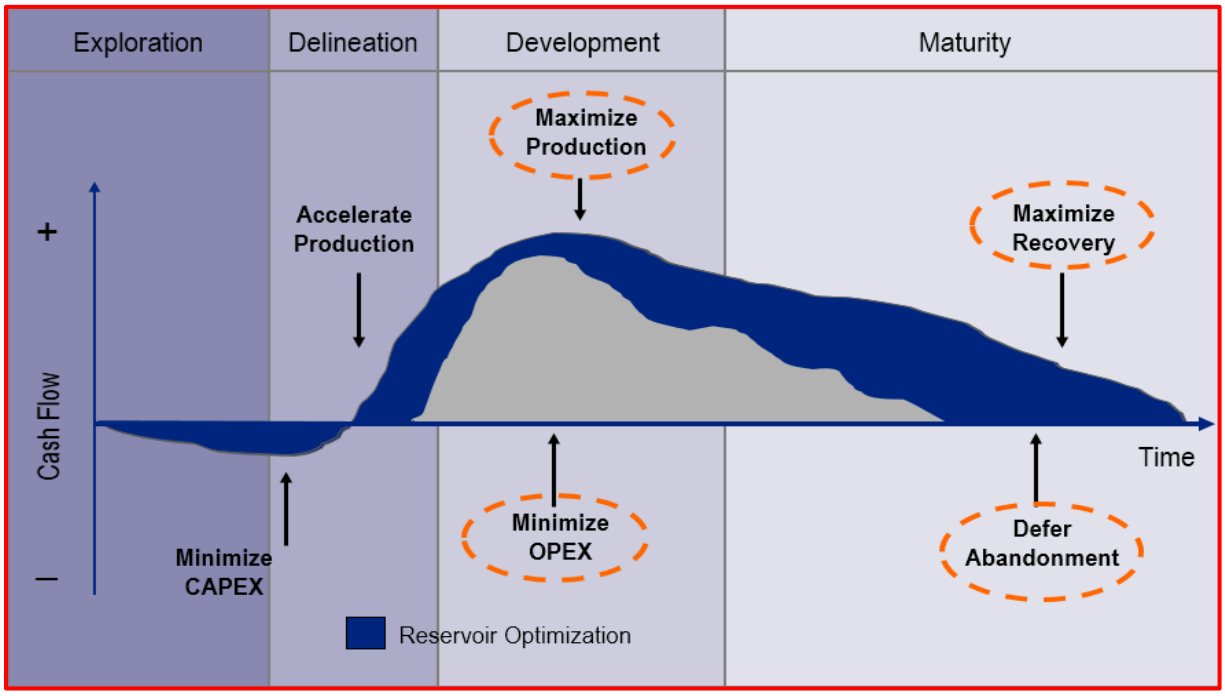

Figure 1.1: Exploration & Production cycle (source: PETROTEL website)

For mature fields, a large production history is available along with large amount of geoscientific data, even then the possibility of unforeseen results can't be ignored while predicting the performance of reservoir at well level or field level. Some of the parameters

associated for such unforeseen results are connected with geological uncertainties and fluid dynamics inside the reservoir which leads to left out oil inside the reservoir.

Knowing in advance all these, utmost care should be taken while well planning and field operations. LWD (Logging while drilling) /MWD (Measurement while drilling) gives real time data which can be utilized for changing the course of well for identification of sweet spot. Anticipating the above, it is necessary to adopt flexibility in well planning. Data gathered from previous wells and knowledge gained from that can be effectively utilized for optimizing future wells.

Most of the giant fields worldwide are in their mature stage and a large amount of oil is left inside, which needs to be recovered. In an era of increased oil price, small oilfields were abandoned by big companies due to uneconomical operating conditions, but the same may be attractive for small sized companies. Viewing above, development of mature field is attractive and at the same time challenging also. In this research work, various methods have been deployed for developing mature field with more emphasis on various development strategies deployed at well level firstly and at the end at field scale.

Oil fields when produced for certain time are termed as mature fields or brown fields. More precisely, a mature field is that field whose production has started declining after reaching plateau period. Another definition could be where the field has reached economic limit of production under given circumstance of oil prices after primary and secondary recovery has been done.

Revitalization of mature field can be done on well level or reservoir level. As maximum number of wells are drilled in a structure, various well development practices viz. stimulation, recompletion in the same zone or higher up, acquisition of additional data, surveillance or implementation of artificial lift methods in an optimal manner are taken into account.

Further, injectors are drilled for pressure maintenance or displacement of fluid which targets secondary and tertiary methods of recovery. Before going for drilling injector for the above purpose, location of unswept oil needs to be identified first. Allocations of reserve for such cases are challenging due to lots of uncertainties and problems are associated with the estimation of residual oil saturation (S_{or}).

Hence, the priority in development of mature field is to ascertain how much oil is left inside. This is an important factor regarding the application of tertiary recovery methods

because there is an adverse relation between acceleration of production and increase of ultimate recovery.

Development of mature field is dependent on efficacy of deployed strategies. In ageing fields, less revenue is generated for recovering additional oil. This factor is disadvantageous. Looking from another angle, a mature field has lots of geoscientific data, information and experience, which is collected over years of production.

Creating field development plans to optimize the recovery efficiency of hydrocarbons is one of the main tasks of the reservoir group, and numerical simulation of reservoir fluid flow is the standard tool for conducting these studies.

Numerical simulation is based on well-known physical principles of law of conservation of mass and Darcy law for fluid flow in porous media. The goal is to solve these equations and achieve the description of pressures and saturations through the lifecycle of a field. In a general way, one can classify two distinct solution methods i.e. finite difference and streamlines.

In the finite difference method, the reservoir is discretized into cells of finite volumes, pressures and saturations and is solved for this computational mesh. Streamline methods offer another approach to high-resolution simulation. For streamlines, pressure is initially solved for the computational mesh, generating a potential field. From the studied potential field, streamlines are calculated which are instantaneous curves tangent to the velocity field which represents the direction of flow. These are the lines drawn in the flow field so that at a given instant, they are tangent to the direction of flow at every point in the flow field. Since the streamlines are tangent to the velocity vector at every point in the flow field, there can be no flow across a streamline. Mathematically, these lines are obtained analytically by integrating the equations defining lines tangent to the velocity field (NPTEL website). Along these streamlines, which are one-dimensional spaces, the saturation equation is solved, and the results are remapped to the grid.

In the following sections, well/ reservoir application to revitalize mature field having bottom water drive will be discussed.

1.2 MOTIVATION/NEED FOR THE RESEARCH

Recovery maximization has been addressed by many researchers using various tools and techniques. The available researches focused on just one of the specific parameter/issue

of mature field development and didn't provide a holistic framework for mature field development. With emerging technologies, efficiency of operation and proper characterization, more oil can be recovered. In this research work various well completion techniques will be deployed in three-dimensional reservoir model which will maximize the recovery. Additionally, well spacing, pressure maintenance and simultaneous water alternate gas injection will also be deployed in the model with the optimized parameters for vertical, horizontal and smart horizontal wells for maximum oil production.

1.3 RESEARCH OBJECTIVES

The main objective of the present research work is to maximize recovery from a bottom water drive reservoir by evaluating the following:

- To evaluate production behavior of vertical well, horizontal well and horizontal well with advanced well completion i.e. inflow control device by varying different parameters (offset from Water Oil Contact, Production rate, Perforation/ horizontal well length, compartment length, Nozzle sizes and number of Nozzles in case of ICD) in a history matched three-dimensional numerical reservoir simulation model.
- To find optimum number of vertical and horizontal wells in a sector model using optimized parameters for vertical and horizontal well.
- To develop a field development plan for maximizing recovery with favorable economics using primary, secondary and tertiary recovery mechanisms using optimized parameters.

1.4 RESEARCH METHODOLOGY

Present research work has been carried out in two stages. The first part deals with analytical studies (material balance studies, determination of contacts using RFT data and transition zone thickness using capillary pressure data, analysis of lab data for SCAL studies and reservoir fluid characterization of black oil) followed by numerical reservoir modeling.

Thereafter, in present research work, following steps have been considered:

A. Reservoir Characterization
B. Numerical Modeling
C. Dynamic Modeling
D. Field development

There is a big advantage of numerical methods when compared to analytical methods. The primary reason being numerical methods consider heterogeneity of reservoir, fluid flow dynamics inside the reservoir, spatial variation of porosity, permeability, facies and saturation functions (relative permeability and capillary pressure).

Analytical studies are important and necessary for proper reservoir characterization which aids in conceptualizing three-dimensional numerical simulation model.

1.5 CONTRIBUTION OF RESEARCH

It is a common industry practice to reduce water coning in oil reservoirs by perforating vertical wells as far above the oil water contact (OWC) as possible and to produce the wells at or below the critical oil rate (Ansari and Johns, 2006; Bahadori, 2010). Determination of offset and withdrawal rate for recovery maximization and favorable economics is always crucial in case of bottom water drive reservoirs. In case of horizontal well, horizontal well length also plays an important role in maximizing recovery. Considering above, it is pertinent to determine the range of values for which, maximum recovery will be obtained.

In case of horizontal wells, water breakthrough is dependent on heterogeneity of the reservoir along the horizontal well length. For this, ICD is needed to maintain uniform contact movement by providing proper pressure differential throughout the horizontal well length.

Number of optimal vertical and horizontal wells has severe impact on economics and hence needs to be addressed carefully.

The optimized variant for vertical/horizontal /smart horizontal wells and well spacing needs to be incorporated in a full field model to evaluate different development strategies for maximizing recovery. Additionally, pressure maintenance is also needed for reservoir with decline in pressure which results in liberation of free gas and thus causes lifting of fluids to the surface. Lastly, EOR technique such as SWAG application may increase the recovery further.

This research will help in determination of optimum variants for:

- Vertical well (Withdrawal rate and offset from WOC)
- Horizontal well (withdrawal rate, horizontal well length and offset from WOC)
- Smart horizontal well ICD (Compartment length and Nozzle sizes)
- Number of vertical/ horizontal wells required for a given sector

Additionally, optimized parameters for vertical/horizontal and smart horizontal wells will be deployed for enhancing recovery from mature field. Application of secondary recovery (pressure maintenance) and tertiary recovery (SWAG) mechanism will also be done in the model for further increasing the recovery.

1.6 OUTLINE OF THESIS CHAPTER

There are eight (8) chapters in the thesis and their brief details are as follows:

Chapter-1 This chapter gives an overview of mature field production problems, ways, and means to overcome water production and increase recovery efficiency. The methodology adopted to enhance production has also been given, followed by contribution of research.

Chapter-2 This chapter gives an overview of concepts used in the research work, current practices in improved oil recovery/ Enhanced oil recovery (IOR/EOR) and research gap identified. It has been observed that an IOR/EOR option has been done in earlier research work but the integrated effect has not been highlighted.

Chapter-3 This chapter gives an overview of the field in terms of its location, structure contour map, stratigraphy, geology, fluid contents, production behavior, production problems and possible measures to maximize production.

Chapter-4 This chapter gives information on input for reservoir simulation study i.e. relative permeability, capillary pressure, PVT analysis, dynamic data (pressure and production history) and porosity permeability transform. Additionally, analytical studies have also been carried out to understand the dynamics of the reservoir such as contact determination from core and well log data, transition zone thickness determination, material balance studies to characterize the reservoir.

Chapter-5 This chapter gives information on Numerical Modeling, which integrates geophysical, geological and dynamic recurrent data to make a representative model for fluid flow behavior inside the reservoir.

Chapter-6 This chapter gives information on Dynamic Modeling. Geological Model is initialized using equilibration method. Aquifer modeling has been carried out to replicate the pressure behavior in the reservoir followed by history matching and performance prediction at well level and field scale.

Chapter-7 This chapter gives information on results and discussion of sensitivity cases performed on vertical well, horizontal well and smart horizontal well followed by well spacing optimization for vertical and horizontal wells. Optimized variants for vertical well, horizontal well and smart horizontal well is used in field development and planning.

Chapter-8 This chapter discusses on conclusion, recommendations and future research possibilities based on the present study.

CHAPTER 2
LITERATURE REVIEW

2.1 OVERVIEW

Extensive research has been carried out and numerous research papers, books and articles have been published on maximizing oil and gas recovery (Bailey et al. (2004), Carpenter C. (2015), SPE website, Anietie et al. (2018), Kumar et al. (2017), Gamal et al. (2016), Maalouf et al., (2017), etc.). Although there are many studies and research work in the area of recovery maximization in different types of reservoir (sandstone, carbonate, etc.) with different reservoir fluid characteristics and depositional environment, there is more scope to improve the emerging technology in field of Enhanced Oil Recovery (EOR)/ Improved Oil Recovery (IOR).

The main objective of reservoir engineers is to develop the field in an optimal and economical manner using proper reservoir management and characterization. This issue is complex in nature as a large number of variables are associated in this process i.e. location of well, number of wells, artificial lift methods, deployment, selection and number of rigs required.

Hydrocarbon reservoirs are intricate in nature and preparing a representative model for the reservoir is difficult. Reservoir behavior can be predicted using a dynamic simulation model. A dynamic simulation model can predict correctly depending on the heterogeneity captured by static model. Dynamic reservoir simulation is always a better choice for field development and planning using various development strategies, which make the entire workflow more realistic. (Mezzomo and Schiozer, 2003).

Recovery maximization from a well in bottom water drive reservoir can be done using optimizing the variants for different well types (vertical, horizontal well, smart horizontal wells). Well spacing has also major impact on economics and hence needs careful attention. Beyond primary and secondary recovery, tertiary recovery mechanisms are also practiced to increase the recovery factor.

2.2 PRIMARY RECOVERY

2.2.1 Using Vertical Well / Horizontal Well

Dikken (1990) first presented and modeled the pressure drop in horizontal well and its effect on the performance of horizontal well. Cho (2003) studied for integrated optimization

on long horizontal well length, Fan and Fang (1997) developed a model for optimal horizontal well length using a coupled model of reservoir and wellbore hydraulics.

In 2003, Joshi S.D. study showed that horizontal wells can be used in variety of primary, waterflooding and EOR projects. In addition, it was showed that horizontal wells can be used for reducing hydrocarbon finding cost and reduce operating cost (Joshi, 2003).

Kalla and White (2007) built a polynomial response model for optimizing completion length, tubing head pressure (THP) and diameter of tubing for a well in a partial penetrating gas reservoir with uncertain properties. Reservoir engineering application included experimental design and response models which improve study efficiency. These designs should consider more levels i.e. excluding high and low values for approximating nonlinear response for oil and gas reservoir. The polynomial response model was used to model gas well with water coning where eleven (11) geological factors were varied while doing optimization.

Determining good well locations and completion of production and injection wells is important to optimally develop and produce a reservoir (Fahim Forouzanfar and A. C. Reynold, 2013).

Popa (2013) developed a new approach for identification and placement of horizontal wells using fuzzy logic. The output of the system allowed generation of quality maps which revealed target areas with substantial potential of horizontal drilling.

In 2013 Pordel et al. developed a generalized Inflow Performance Relationship (IPR) for an oil reservoir taking into account the reservoir and well parameters in which a well is drilled horizontally.

Further in 2013 Pang et al. has also proposed a better model of designing perforation and optimizing long horizontal wells. The study showed that optimization of perforation length is made up of three factors; the heel toe section filtration difference will dominate perforation optimization when the horizontal well length is short, and on the other hand, pressure drawdown will have significant effect on perforation especially when the horizontal well has fully penetrated the reservoir or the pressure drawdown is big enough to obtain homogenized production influx profile, perforation density should be lower in high-permeability section than that in low-permeability stripe.

Dosunmu and Osisanya (2015) showed that horizontal well productivity is significantly affected by oil viscosity, horizontal permeability and well diameter.

Al Qahtani et al., (2015) showed noble ideas of taking full advantage of long horizontal well if it is produced from both ends i.e. from heel as well as toe.

Menouar (2013) showed that formation damage should be accessed properly for estimation of effective horizontal well length for predicting the performance of well. Other parameters to be considered are the invasion depth, damage permeability or the anisotropy ratio.

2.2.2 Smart Horizontal Well using Inflow Control Devices (ICD)

In the last decade, many papers have been published which addresses different aspects of inflow control devices (ICD) technology. Majority of the research work uses case study where practical problems have been addressed and benefits of installation of ICD is emphasized. It may be noted that ICD technology cannot be applied universally to each and every oilfield (Birchenko et al., 2008).

In the last decade installations of ICD have been carried out in hundreds of wells which are now being considered as mature well completion technology. Well modelling software can be used for predicting steady-state performance of ICD (Ouyang, 2009; Johansen and Khoriakov, 2007). Majority of the reservoir simulators include basic functionality for modeling of ICD, but some of them propose practical means for capturing effects of annulus flow (Wan et al., 2008; Neylon et al., 2009).

Historically, the most common method for designing ICD completions has been to use steady-state or pseudo steady-state (i.e. static) analytical modeling using data at one or more points in time (Ellis et al., 2009). The perceived advantages of this approach were speed and simplicity. However, static modeling ignores several aspects of the problem, which may substantially influence the design results. There are significant advantages of three-dimensional (3-D) dynamic or numerical models over static model.

Leung et al. (2010) study showed the effect of reliable data obtained from Logging While Drilling (LWD) in carbonate reservoir for managing production. Dynamic reservoir simulation in near well can infer location for by passed oil, which may be utilized for drilling infill locations. Analysis of LWD data is needed for identification of fracture intensity, which may be used for dealing with fluid losses.

Oil recovery is increased by appropriate selection of ICD, which also stops flow of unwanted production of water and gas. Results obtained from fields and simulation studies show that production of oil, gas and water are very much dependent on the type of ICD and number of ICD used (Mojaddam et al., 2012).

Moradi Dowlatabad et al. (2015) showed that Autonomous Inflow Control Devices (AICD) completions are more appropriate to reduce the production of the unwanted fluids and increase oil recovery than ICD. The results showed that although both of the AICD and ICD completions significantly reduce the oil production variations comparing with Open-hole completion, AICD completion perform much better than the ICDs to manage the effect of the reservoir uncertainties on oil recovery.

Sadana et al. (2016) prepared a prototype for ICD with modification, where ICD annulus is packed with a porous Polytetrafluoroetheylene (PTFE) sleeve that exhibits water-sensitive control functions. Flow testing through porous PTFE sleeve shows about 200% increase in differential pressures for 70% brine cuts compared to 0% Water Cut, which means it can restrict flow when the brine cut increases.

Wanga et al. (2016) showed that for weakly heterogeneous reservoirs, ICD cannot obtain remarkable effect contrast to openhole completion, but for strongly heterogeneous reservoirs, the IOR effect of ICD is considerable.

Magzoub et al. (2015) proposed a solution for enhancing production and water breakthrough using dual multilateral completion in place of application of ICD near heel area of horizontal well.

Kolchanova (2014) showed that application of expanded LWD suite where rock natural radioactivity spectrum is derived using three-component analysis of Thorium, Potassium and Uranium helps in determining the nature of rocks radioactivity and to effectively drill horizontal wells.

2.2.3 Well Spacing

Well spacing is the maximum area of the resource reservoir that can be efficiently and economically drained by one well. The relevance of well spacing is to prevent waste, avoid unnecessary expenditure on wells and to protect the rights of reserves owners. There are two views on optimization of well spacing, first one is economic ultimate recovery and the second one is physical ultimate recovery (Tabatabaei, 2007). Same amount of oil can be recovered

using less number of wells if well spacing is optimized properly. Recovery is increased if number of wells can be increased, but the incremental recovery obtained reduces by increasing well numbers. Economic calculation using Net Present Value (NPV) and Internal Rate of Return (IRR) method should be done for optimizing number of wells. This will save money and economics of the project will also become favorable.

Wells spacing is a function of well drainage radius, which depends on the heterogeneity of the reservoir, permeability of the reservoir, drive mechanism and API gravity of oil. If the permeability of the reservoir is on the higher side then it is a better practice to space out wells rather than drilling wells close to one another and ending up with the production interference. In case of water drive reservoirs it is generally better to optimize well spacing so that the oil production does not leave too much of left out oil due to coning in between two producers.

Well spacing can be different in a single reservoir depending upon the heterogeneity. Well spacing studies need to be done on priority while generating a field development plan with the help of well test data available and the geological model to optimize ultimate recovery of any oil/gas field and data from any new well drilled should also be used to update geological model and simulate the same.

Tokunaga and Hise (1966) introduced a relationship for the present worth of an oil field, which is expressed as a function of the well spacing. The derivative of this function was used to find the point of maximum present worth, which is designated as the optimum spacing. The two most important limitations to the method are that oil recovery and production rate must be independent of the well spacing.

Davis and Shepler (1969) verified that the well spacing originally used to develop a petroleum field, in general, is not the most suitable spacing. The ideal well spacing is dependent on individual reservoir architecture and characteristics. Hence it is important to consider static model uncertainties and dynamics of the fluid flow for technological and economic scenario.

Pedroso and Schiozer (2000) research showed a methodology for optimizing the number of producer wells and their location in a reservoir during field development phase.

As per thumb rule, oil wells are developed on 40-acres spacing and gas wells are developed on 160-acres spacing (Chodhury Amanat, 2003).

Khasanov et al. (2013) developed a mathematical model to determine both rentable/profitable oil thickness and optimum horizontal well spacing in oil rims with massive gas cap. Within this model, dimensionless criteria for rentable thickness and optimal horizontal well pattern width, which includes filtration and volumetric parameters of reservoir, well and infrastructure costs and oil price at wellhead was made. The main advantage of the proposed method to determine optimal well spacing is that it does not require multiple numerical simulations. The disadvantage is limitation of well production rate model and simplicity of the economic model. Limitations of economic model are: (i) wells are drilled in the first year (ii) infrastructure costs are independent of oil production peak.

Key factors influencing performance of reservoirs include controllable and uncontrollable factors. Uncontrollable factors include porosity, water saturation, net-to-gross thickness, initial pressure, permeability and fluid properties. The most relevant parameters among the controllable factors are optimizing well spacing, well design variations, well placement, surface facilities design, completion technologies and operating conditions (Abdul-Latif et al., 2015).

Well spacing depends on geomechanics, petrophysics, stimulation design, hydraulic-fracture geometry and reservoir fluids. These factors are combined by use of numerical simulation to study their effects on the well spacing (Wilson, 2016).

Awotunde and Naranjo (2014) proposed to solve well placement optimization problem for minimum well spacing (minimum distance between any two wells that a company or an asset team considers technically safe) which can successfully determine optimal well locations without violating any of the constraints.

2.3 SECONDARY RECOVERY (PRESSURE MAINTENANCE)

When primary energy is not sufficient for lifting of fluids to separator, then secondary recovery methods are deployed in form of fluid injection, mainly water or gas (Archer and Wall, 2012). When volumetric withdrawal rate of production is balanced by injection rate in such a way that average reservoir pressure is kept constant, then this method is termed as pressure maintenance. In order to minimize the cost of injection, rate is kept sufficient so that average reservoir pressure is above bubble point pressure. Level of pressure maintenance can be determined from Figure 2.1 (Archer and Wall, 2012) below for determining the capability of self-flow to be produced on the surface under high Water Cut.

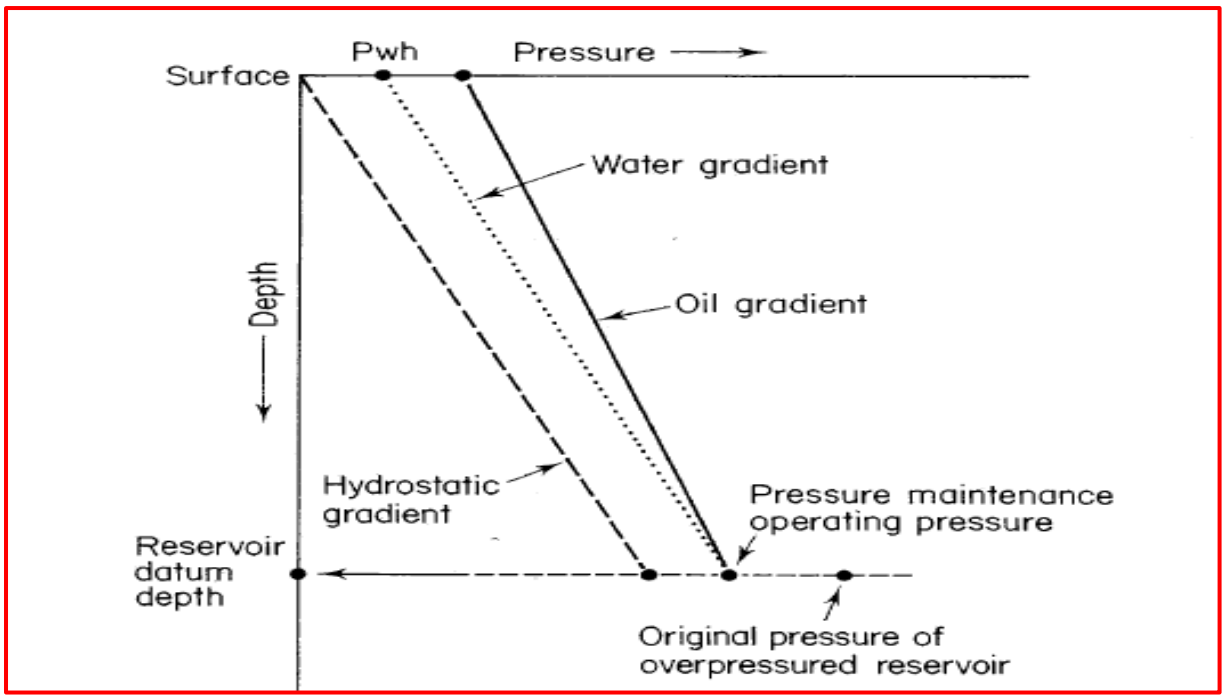

Figure 2.1: Operating pressure for natural flow in originally over pressured undersaturated oil reservoir under pressure maintenance (Archer and Wall, 2012)

When injection rate of fluid at reservoir condition balances fluid withdrawal rate then, this process is termed as complete voidage replacement. In practice, any fraction of voidage could be replaced if it provides an optimum recovery scheme. Proper design of a secondary recovery scheme is best performed after a period of primary recovery in order to observe the dynamic response of the reservoir. The displacement of oil by water or gas under immiscible conditions occurs both microscopically and macroscopically in a reservoir. On the micro scale, it is considered that the distributions of trapped oil in pores are swept by displacing fluid.

The equation used in order to calculate volume changes in the reservoir is:

$$\Delta V = V_1 C_t \Delta P \tag{2.1}$$

Above equation is a variation of a part of the material balance equation listed below:

$$V_2 = V_1 (1 + C_t \Delta P) \tag{2.2}$$

In this equation, following parameters are used

$$\Delta V = V_2 - V_1 \tag{2.3}$$

V_2 = Reservoir volume, after depletion

V_1 = Reservoir volume, before depletion

This change in volume is the amount of oil produced at the surface, and the recovery factor is therefore given by $\Delta V/V_1$. After petroleum is produced for a little bit of time,

reduction in the reservoir pressure is observed. This can be problematic as the primary drive mechanism starts losing its potential because fluid starts moving in the direction of low pressure. In order to mitigate this effect, injection wells are used to inject gas or water to keep the pressure drop at a low level.

$$\Delta P = P_1 - P_2 \tag{2.4}$$

P_2 = Reservoir pressure, after depletion

P_1 = Reservoir pressure, before depletion

Compressibility is given by:

$$C_t = C_f + \sum_{i=g,0,w} S_i C_i \tag{2.5}$$

$$C_f \equiv \frac{1}{\emptyset}\frac{d\emptyset}{dp} \tag{2.6}$$

$$C_i \equiv \frac{1}{V_i}\frac{dV}{dp} \tag{2.7}$$

In this equation, $\emptyset$ symbolizes the porosity, C_t is total compressibility, C_f is formation compressibility, symbol S and C is used for saturation and compressibility of an individual component. This is important as the porosity works as the storage space for fluids in the rock.

Flewitt (1975) developed a model in carbonate reservoir utilizing normalized original wireline porosity logs with potential production of 100,000 barrels per day through 188 active wells. By combining the use of production data and pulsed neutron logs, a separate water front and pressure response was identified within discrete environmental units. This new reservoir description helped in dynamic reservoir simulation modeling and quantification of reservoir performance behavior. It was also inferred that pattern water flooding has more impact on recovery than original peripheral bottom water drive.

Mezzomo and Schiozer (2003) formulated a process for optimizing primary recovery development strategies, which encompasses only vertical producer wells. This methodology helps in the decision-making process, looking to maximizing profits and minimizing the risks associated with the investment..

Temizel et al. (2016) inspected the possibility of a reversal of the typical scenario where injection rate for pressure maintenance is based on hydrocarbon production. Trigger obtained from production rate might be useful for managing voidage replenishment ratio, which may be used for big reservoirs.

2.4 TERTIARY RECOVERY (ENHANCED OIL RECOVERY)

Recovery of hydrocarbon happens using two major processes viz. primary recovery and secondary recovery. Primary recovery happens by virtue of existing energy in the hydrodynamic system or by using artificial lift mechanism, while, secondary recovery refers to the production of hydrocarbon by virtue of external energy into the system by water/gas injection (Lyons and Plisga, 2005). Enhanced oil recovery (EOR) is the implementation of various techniques for increasing the amount of crude oil that can't be extracted from an oil field using primary and secondary recovery techniques.

Simultaneous Water and Gas Injection (SWAG) is an EOR process in which water and gas are mixed together and this resulting mixture is injected in the wellbore. SWAG process incorporates the effects of microscopic sweep efficiency obtained from miscible gas injection and frontal stability obtained from waterflooding (Meshal and Adel, 2007).

SWAG combines the benefits of frontal stability obtained from water flooding and microscopic sweep efficiency obtained from miscible gas injection with better economics (Fabusuyi Oluwatosin John, 2015).

Christensen et al. (2001) defined the SWAG method as simultaneous injection of both water and gas at the same time into an interval or the entire formation thickness. This process can be performed using two different techniques: Conventional SWAG technique and modified SWAG technique (Algharabi et al., 2007).

In a Conventional SWAG technique, gas and water are mixed at the surface. However, in a modified SWAG technique, water and gas are injected together through a single well bore and no mixing is done at the surface. The two phases are pumped separately using a dual completion injector and are selectively injected into the formation. Usually, water is injected into the upper portion whereas gas is injected at the bottom of the formation (Mazen, 2008).

According to the Helfferich (1981), a SWAG process is a multi-component and multiphase displacement of oil-water by solvent-water. The fundamental mathematical description of the mass conservation equation is similar to different EOR methods (Rouzbeh Ghanbarnezhad et al., 2010). The purpose of SWAG injection is to allow deeper penetration of the gas into the lower part of the reservoir and reduce the residual oil saturation (Shehadeh et al., 2010).

Chen et al. (2016) study showed that immiscible gas is not as effective as water injection in maximizing oil recovery from reservoir, which is evident from the model analysis, coupled with results from special core analysis.

2.5 RECOVERY MAXIMIZATION

Bailey et al. (2004) made a model for risk and decision analysis. This tool, when applied to a field for optimizing Net Present Value (NPV), showed that value maximization can be done in planning short term and long term horizons as well as foundation for making the most of asset value.

Carpenter (2015) showed that for thin oil-rim reservoirs, well placement, well type, well path and the completion methods evaluation leads to minimize the well count, enhance the well performance and improve the ultimate recovery per well.

2.6 GAP IN LITERATURE AND RESEARCH DOMAIN

Recovery maximization has been addressed by many authors in the research papers using various tools and techniques. The available researchers are focusing just one of the specific parameters/issues of the mature field developments and have not provided a holistic framework for mature field development. With emerging technologies, efficiency of operation and proper characterization, more oil can be recovered. In this research work recovery maximization will be carried out at three levels. Firstly, at well level, recovery will be maximized using vertical/horizontal and smart horizontal wells by optimizing variants like offset, withdrawal rate, horizontal well length, nozzle sized and compartment length. Secondly, well spacing will be optimized for vertical and horizontal wells with optimized variants obtained from the sensitivity analysis of vertical and horizontal well. Lastly, a field development plan with various scenarios will be made for maximizing the recovery and favorable economics.

It is also observed that no significant work has been done for recovery maximization from bottom water drive reservoirs in our country. An attempt has been made to carry out sensitivity analysis followed by field development plan, which will help to develop a strong base for advance research in this area.

2.7 CHAPTER SUMMARY

This chapter reviewed the literature on well placement, well spacing in the category of primary recovery, water injection for pressure maintenance under secondary recovery and application of SWAG under tertiary recovery category. Different methodologies have been adopted to maximize recovery in the literature. Different theories are applicable under different conditions. Application of horizontal/vertical well has been carried out since many years where one aspect has been studied individually i.e. horizontal well length in case of horizontal wells and perforation length in case of vertical well, determination of critical rate and breakthrough time for vertical and horizontal well for a given offset from WOC. Combination of all these has not been applied to a heterogeneous reservoir in order to find the best combination of withdrawal rate, offset from WOC, horizontal well length/perforation length. In case of long length of horizontal well in heterogeneous reservoir, permeability variation is an important step which needs attention. Application of inflow control device after optimizing compartment length and nozzle sizes with optimized offset and withdrawal rate will aid in maximizing recovery apart from maintaining uniform contact movement for avoiding premature water breakthrough.

Application of water injection and SWAG technique are also helpful in supplementing the reservoir with energy and increasing the recovery.

CHAPTER 3
OVERVIEW OF FIELD

3.1 FIELD OVERVIEW

The Makum/North Hapjan field (Figure 3.1, DGH India website) is located on the southern flank of the upper Assam basin high and represents a prograding sequence of deltaic to shoreface sands interbedded with shale/coal source beds. The Upper Assam Basin (Figure 3.2, DGH India website) is a composite foreland basin which is located between the eastern Himalayan foot hills and the Assam - Arakan thrust belt. The basin is terminated to the northeast by the Mishimi Hills block and to the Southwest and partly disrupted by the Shillong plateau basement uplift.

The generalized stratigraphic column for the Upper Assam Shelf is shown in Figure 3.3 (Raju and Mathur,1995). The main reservoir units for the area are the lower Eocene Tura Sandstone Formation, a stacked sequence of deltaic progradational sand units and the Lower Oligocene Barail Sandstone Formation, a delta front sequence capped by thin coal layers. Hydrocarbon source is the Upper Eocene Kopili and Upper Oligocene Barail Coal-Shale Formation, both interbeds of limy shales and lignite beds.

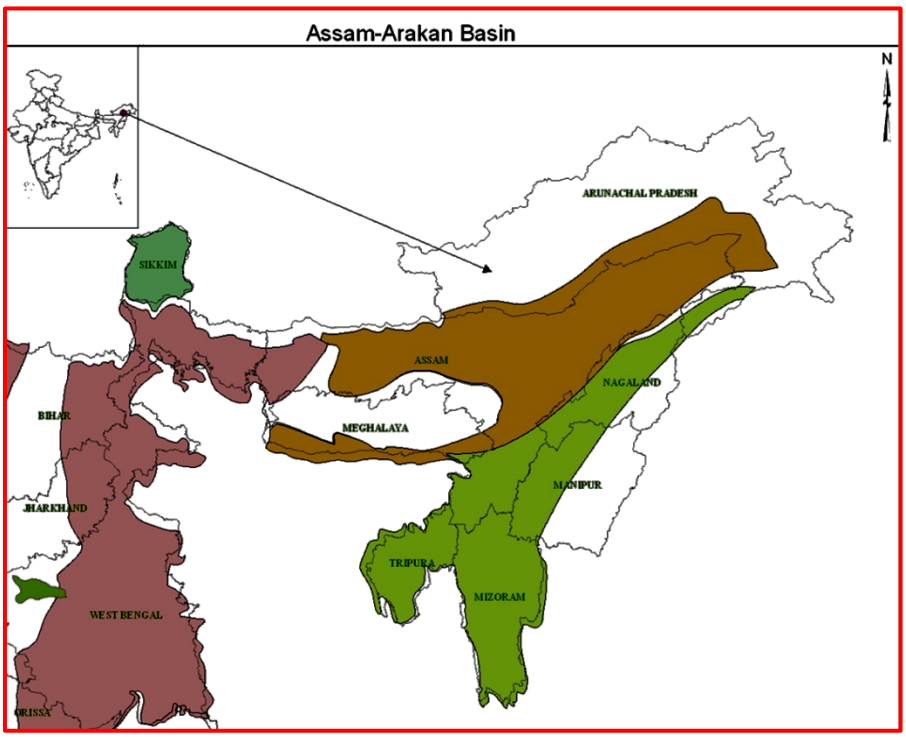

Figure 3.1: Assam Arakan Basin (Source: DGH India website)

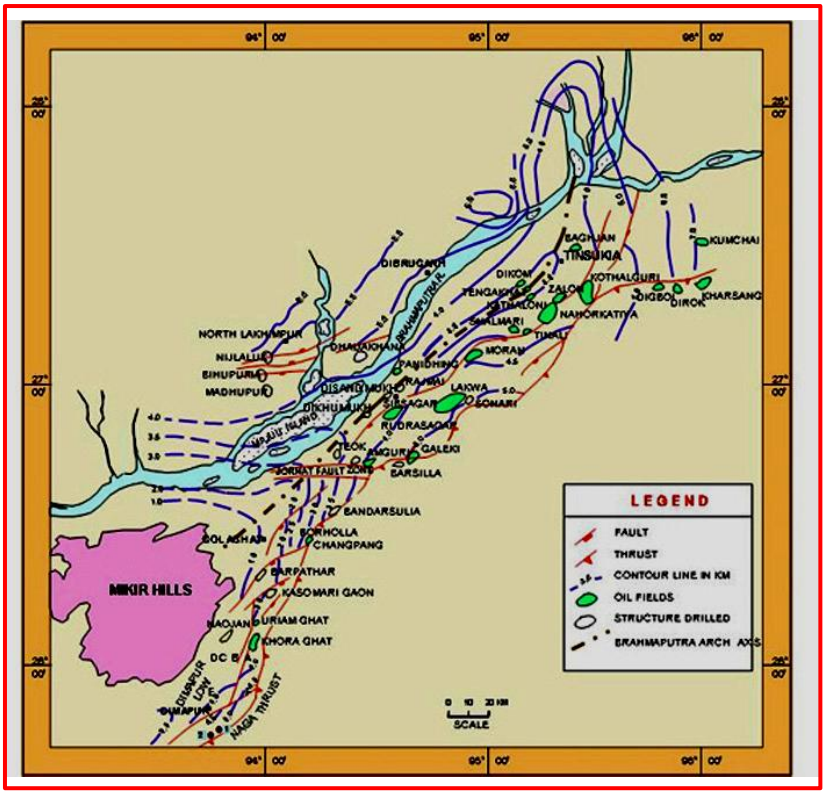

Figure 3.2: Study Area (Source: DGH India website)

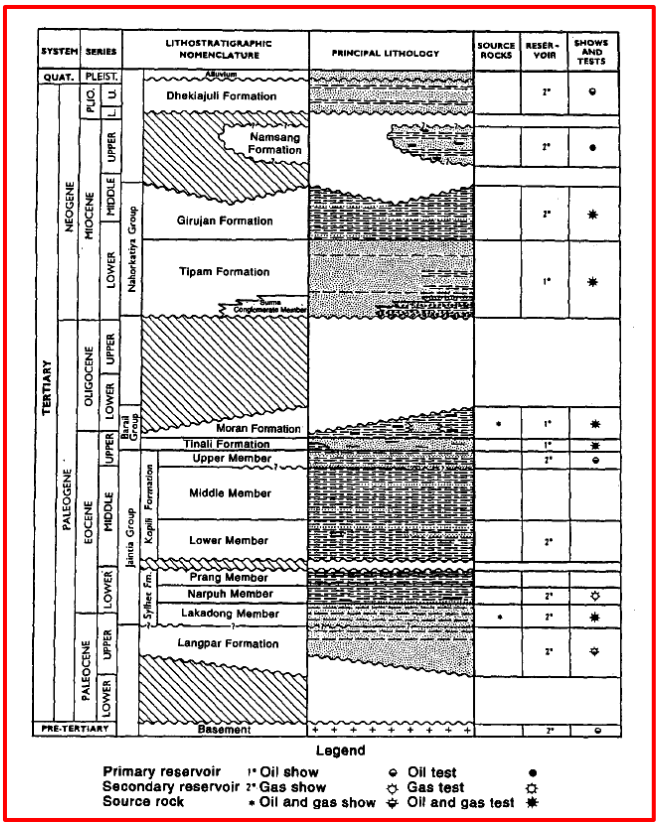

Figure 3.3: Generalized stratigraphic succession of the study area Source: Raju and Mathur (1995)

3.2 RESERVOIR DESCRIPTION

This field is one of the most prolific producers of Upper Assam Basin, India. It is a faulted anticline, about 35 sq. km in size at the Arenaceous Top level, with the major axis of the structure trending in NE-SW direction. The structure is bisected by eight major NE-SW normal faults heading towards southeast, with a maximum throw of 200 m while there are six NE-SW trending normal faults heading towards northeast with a throw of 80 m, except one with a throw of more than 200 m. A depth contour map on top of Oligocene sand reservoir has been prepared and presented as Figure 3.4 (Oil India Limited internal report, 2014). This reservoir is oil-bearing with an initial gas cap and a strong bottom water drive. The original oil-water margin was at around 2568 m True Vertical Depth below Sea Level (TVDSS) while the original gas-oil margin was at 2522 m TVDSS. The oil pay thickness of the structure in Oligocene sand reservoir ranges from 12 m to 35.5 m. The gas pay of the gas cap zone ranges from 0 to 27 m. The reservoir porosity ranges from 18% to 24%, whereas the permeability varies from 100 mD to 500 mD.

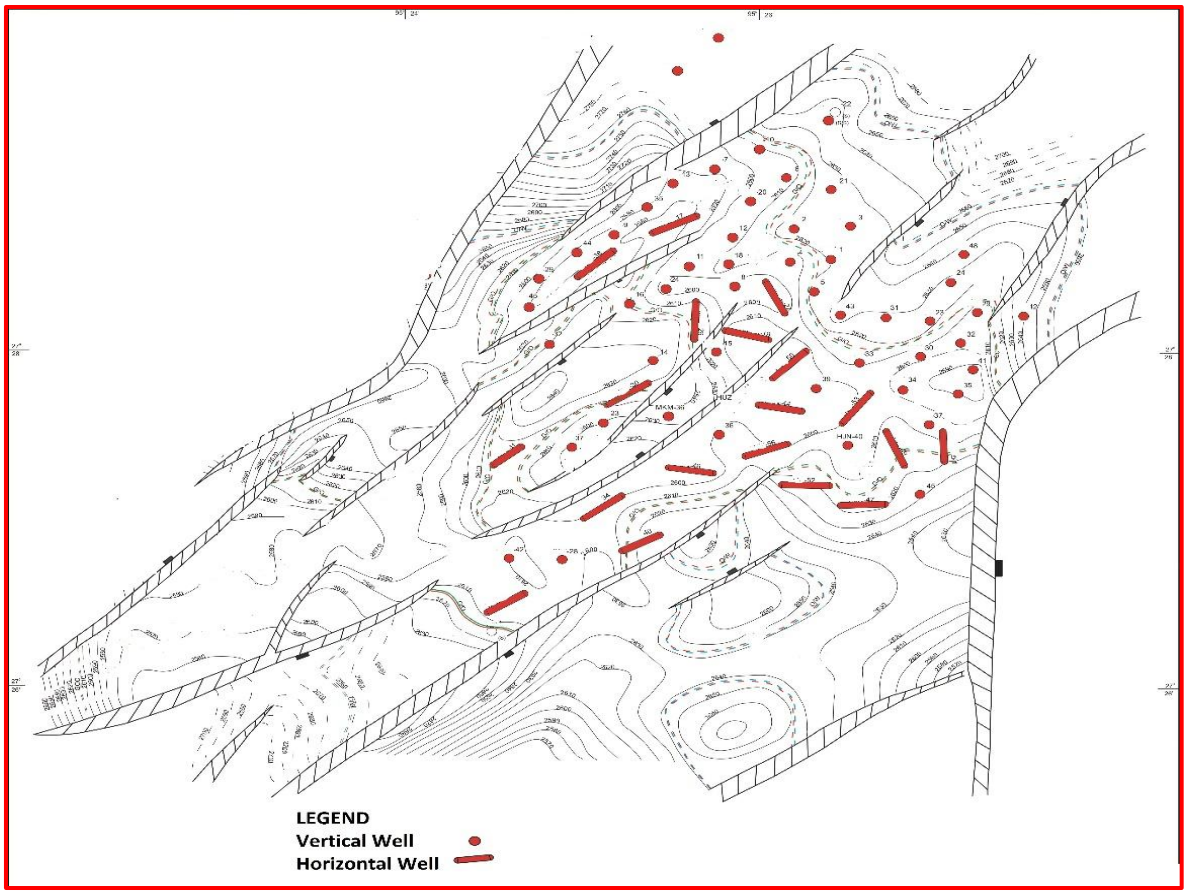

Figure 3.4: Depth contour map on top of Oligocene sand (Source: Oil India Limited internal report, 2014)

Majority of the production comes from horizontal wells. This reservoir has bottom water drive with active support. Currently, this field is experiencing problems such as high Water Cut, cessation of flow due to high Water Cut. High Water Cut in the vertical well is mainly due to formation of cone.

3.3 CHAPTER SUMMARY

This chapter gives an overview of field in terms of its location, structure contour map, stratigraphy and geology.

CHAPTER 4

RESERVOIR CHARACTERIZATION

In this chapter, inputs for reservoir simulation study have been described in term of relative permeability, PVT analysis, dynamic data (pressure history, production history) and porosity permeability transform. Additionally, analytical studies have also been performed for better understanding of the dynamics of reservoir such as material balance studies, contact determination and transition zone thickness determination for characterizing the reservoir.

4.1 POROSITY PERMEABILITY TRANSFORM

Porosity permeability transform was characterized using SCAL data from two (2) wells. Figure 4.1 shows scattered data not following any trend. The poor fit of the data distribution was organized by Rock Quality Index i.e. $RQI = 0.0314 * \left[\frac{K}{\phi}\right]^{0.5}$ limits with corresponding permeability relationship assigned to each grouping (Amaefule, 1993).The relationships are defined applying different flow zone index coefficient. The Flow Zone Index (FZI) (Amaefule, 1993) relationship is defined by:

$$K = 1014\,(FZI)^2 \left(\frac{\phi_E^{\,3}}{(1-\phi_E)^2}\right) \tag{4.1}$$

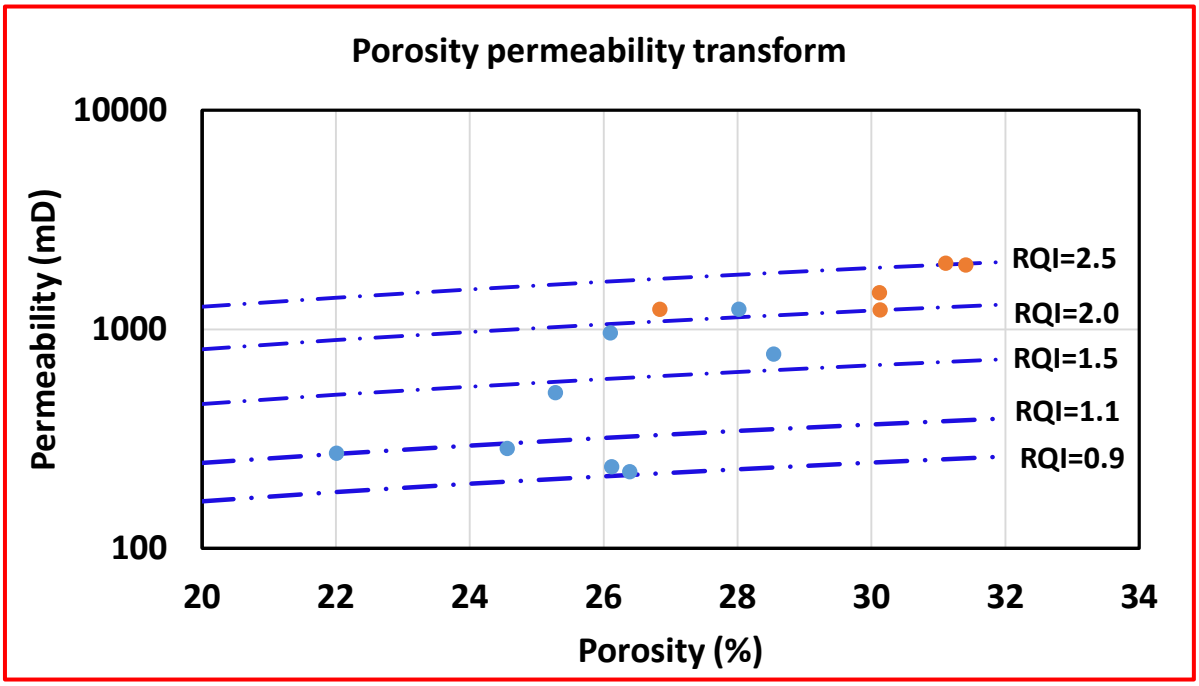

Figure 4.1: Porosity permeability relationship

Data used for plotting porosity permeability transform in Figure 4.1 above and permeability data generated using Rock Quality Index (RQI) using various values of porosities have been presented in Annexure-I.

4.2 SPECIAL CORE ANALYSIS STUDIES

When two or more immiscible fluids flow simultaneously through a porous medium, they compete and do not move at equal velocity. This results on the one hand from interactions between the fluids and the rock, and on the other from interactions among the fluids themselves. The concept of relative permeability is an attempt to extend Darcy's law for single phase flow of fluid through porous media to account for simultaneous flow of several phases. In this regime, the flow of each phase is governed by the microscopic pressure gradient of each phase and the fraction of overall permeability that is associated with it.

In addition, it is necessary to define residual saturations, which normally indicate the smallest saturation for a given phase to become mobile. Relative permeability for a given fluid is a fraction i.e. between zero and one. Since the wetting phase does not flow at or below its irreducible saturation, it follows that its relative permeability is zero in that saturation range. Likewise, for the non-wetting phase, its relative permeability is zero for saturations equal /below the residual value. For two phase flow in porous media, the relative permeability of both wetting and non-wetting phases is usually plotted versus the wetting phase saturation. These curves are called as relative permeability curves. This curve can be generated by using some correlations like Corey correlation (Ahmed, T., 2010)**.**

However, in a 3-Phase flow situation, the oil relative permeability would be a function of both water and gas saturations.

The so-called *Stone Models* (Stone, 1970) may be used for the construction of 3-Phase relative permeability curves. A variety of other models exists, but these have been the most commonly used models. For the purpose of illustration, Stone's Model 1 and Stone's Model 2 have been described below.

For ***Stone's Model 1***, normalized saturations of oil, water and gas are defined as below:

$$S_{oD} = \frac{S_o - S_{or}}{1 - S_{wir} - S_{or}} \tag{4.2}$$

$$S_{wD} = \frac{S_w - S_{wir}}{1 - S_{wir} - S_{or}} \tag{4.3}$$

$$S_{gD} = \frac{S_g}{1 - S_{wir} - S_{or}} \tag{4.4}$$

Where S_{oD}, S_{wD} and S_{gD} are normalized saturations of oil, water and gas. S_{or} is the minimum residual oil saturation and S_{wir} is irreducible water saturation. Then we define the functions β_w and β_g.

$$\beta_w = \frac{K_{row}}{1 - S_{wD}} \tag{4.5}$$

$$\beta_g = \frac{K_{rog}}{1 - S_{gD}} \tag{4.6}$$

The 3-Phase oil relative permeability (K_{ro}) as constructed by Stone´s Model 1 may now be defined as:

$$K_{ro} = S_{oD}\, \beta_w\, \beta_g \tag{4.7}$$

Where K_{ro} is 3-Phase relative permeability of oil, K_{rog} is relative permeability of oil w.r.t. gas, K_{rg} is relative permeability of gas, K_{row} is relative permeability of oil w.r.t. water, K_{rw} is relative permeability of water.

It may be noted that above formulas assume that end point relative permeability is one. If this is not the case, the relative permeability formula must be modified accordingly.

Stone's Model 2 does not require the estimation of S_{or}, as it attempts to estimate it implicitly by its formulation.

The model simply is:

$$K_{ro} = \left(K_{rog} + K_{rg}\right)(K_{row} + K_{rw}) - (K_{rw} + K_{rg}) \tag{4.8}$$

In this model, S_{or} is defined at the point where slope of K_{ro} becomes negative. The two models of Stone predict different k_{ro}*'s* in many cases, and one should be very careful in selecting which model to use in each situation. In this research work, ***Stone Model 2*** has been used.

4.2.1 Relative Permeability

Relative permeability and capillary pressure data (Annexure-II) from well M-5 and well M-8 were considered for generation of saturation function as input to reservoir simulation. Relative permeability of oil-water for four samples has been plotted in Figure 4.2 through Figure 4.5.

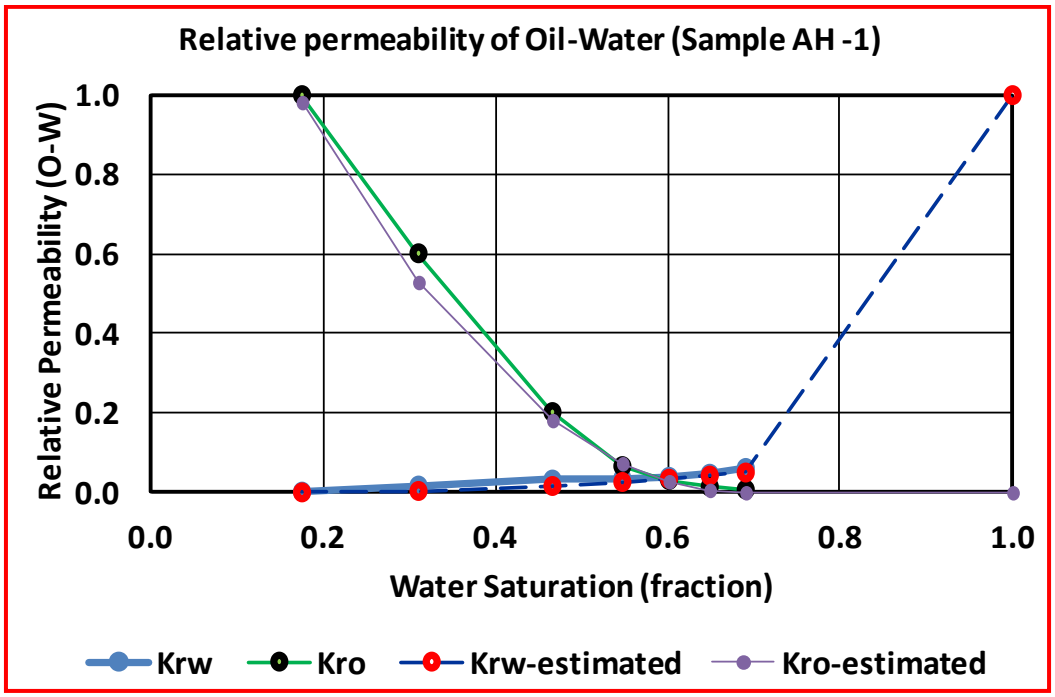

Figure 4.2: Relative permeability of Oil-Water (Sample AH-1)

It can be seen from relative permeability (Oil-Water) graph of sample AH-1 that connate water saturation (S_{wc}) is 0.17 and residual oil saturation (S_{or}) is 0.31. Relative permeability of water at maximum saturation is 0.05 and relative permeability of oil at maximum saturation is 1.

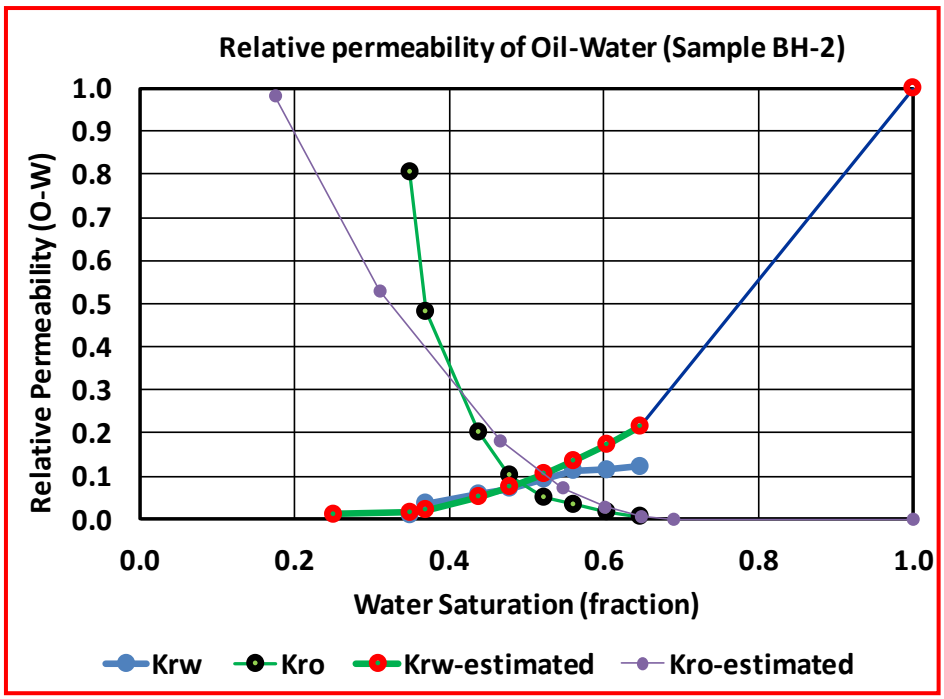

Figure 4.3: Relative permeability of Oil-Water (Sample BH-2)

It can be seen from relative permeability (oil-water) graph of sample BH-2 that S_{wc} is 0.25 and S_{or} is 0.33. Relative permeability of water at maximum saturation is 0.24 and relative permeability of oil at maximum saturation is 1.

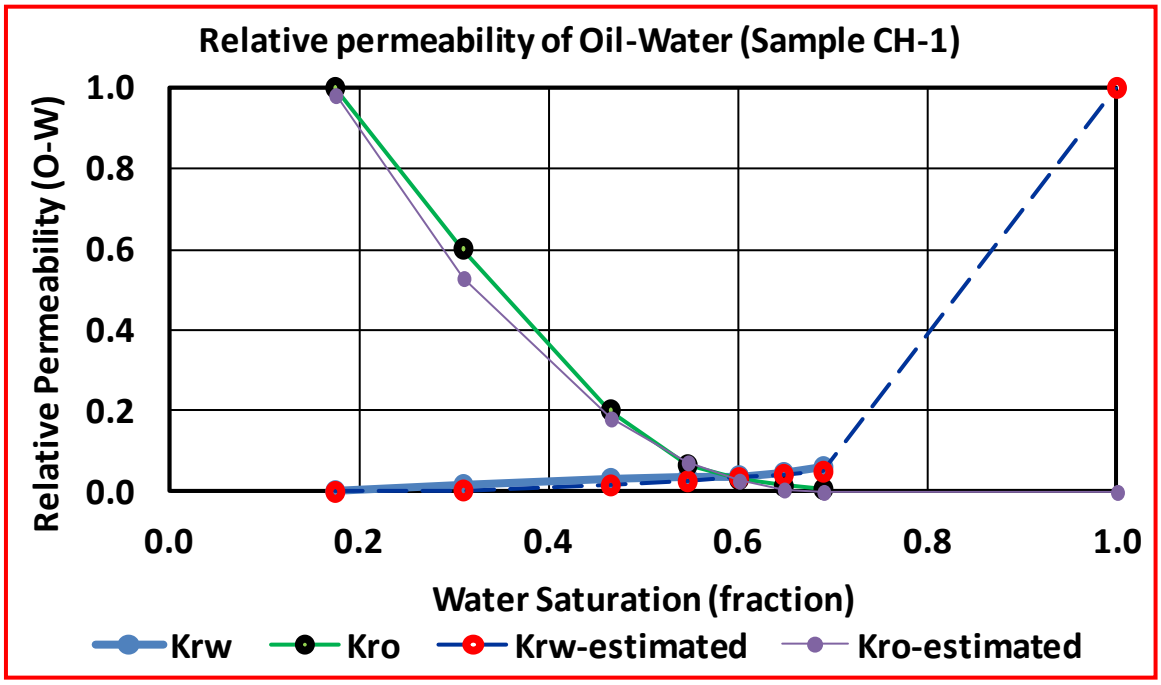

Figure 4.4: Relative permeability of Oil-Water (Sample CH-1)

It can be seen from relative permeability (Oil-Water) graph of sample CH-1 that S_{wc} is 0.14 and S_{or} is 0.32. Relative permeability of water at maximum saturation is 0.14 and relative permeability of oil at maximum saturation is 1.

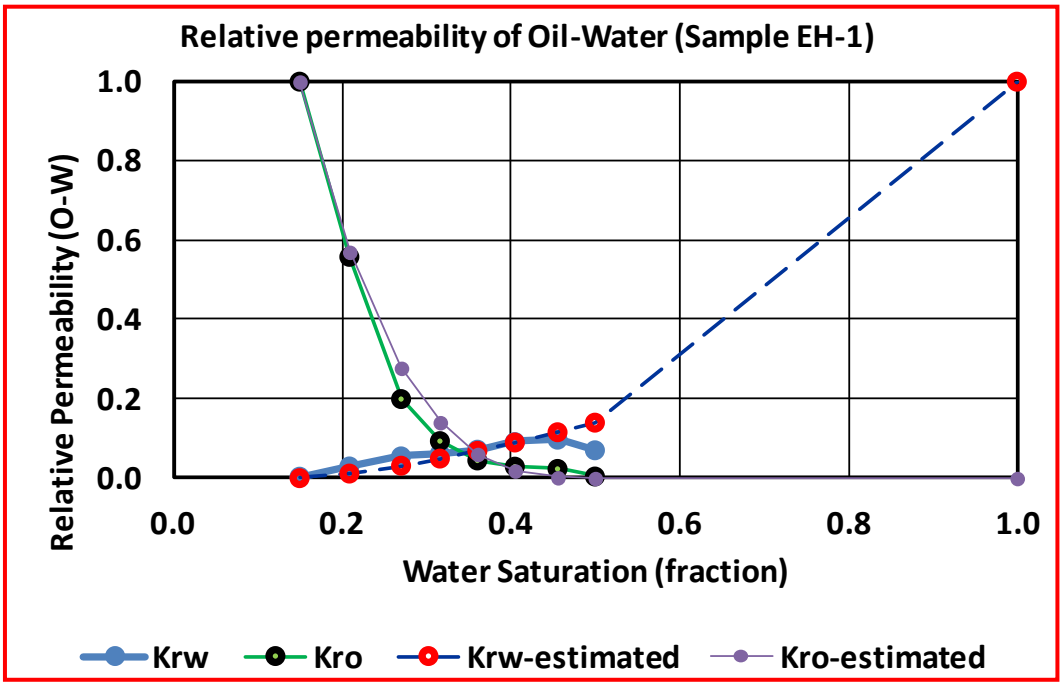

Figure 4.5: Relative permeability of Oil-Water (Sample EH-1)

It can be seen from relative permeability (oil-water) graph of sample EH-1 that S_{wc} is 0.14 and S_{or} is 0.50. Relative permeability of water at maximum saturation is 0.14 and relative permeability of oil at maximum saturation is 1. Corey exponents along with saturation end points have been estimated for all the core samples and is given in Table 4.1.

Table 4.1: Corey exponent for oil-water relative permeability curve

Core	Porosity (%)	Air Permeability (mD)	RQI	FZI	N_o	N_w	K_{rwe}	K_{roe}	S_{wc} (fraction)	S_{or} (fraction)
AH-1	27.93	330	1.079	2.785	2.03	2	0.05	1	0.17	0.31
BH-2	21.6	457	1.444	5.242	2.61	1.9	0.24	1	0.25	0.33
CH-1	29.63	651	1.471	3.495	4.06	1.7	0.14	1	0.14	0.32
EH-1	29.14	597	1.421	3.456	3.04	1.4	0.14	1	0.14	0.5

Relative permeability of Oil-Gas for 4 samples has been plotted in Figure 4.6 through Figure 4.9.

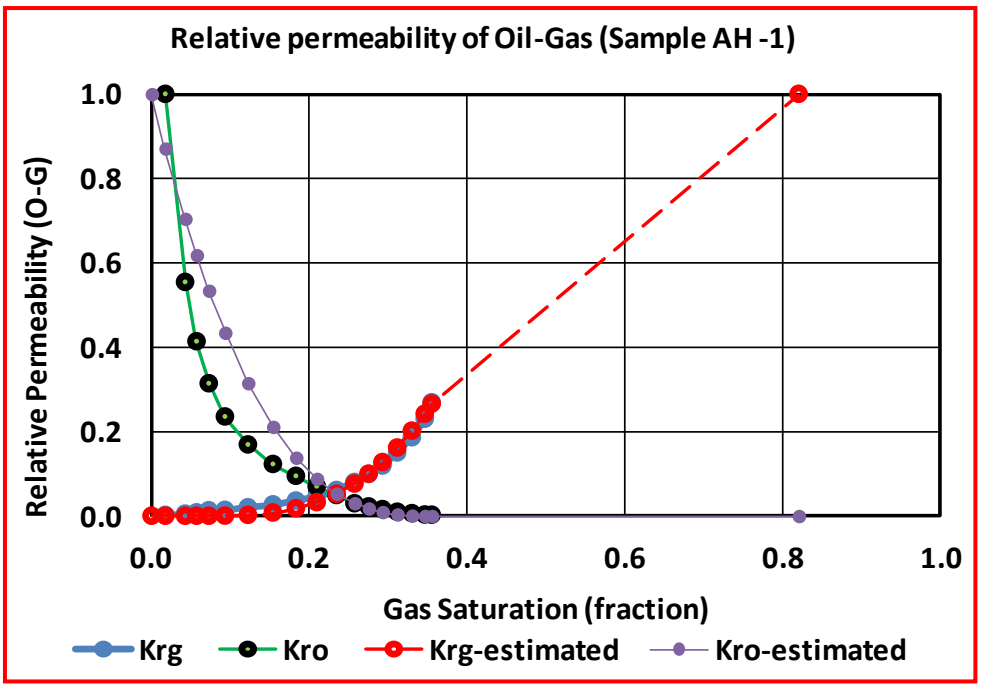

Figure 4.6: Relative permeability of Oil-Gas (Sample AH-1)

It can be seen from relative permeability (Oil-Gas) graph of sample AH-1 that connate water saturation is 0.17 (Figure 4.2), critical gas saturation is 0.06 and residual oil saturation is 0.46. Relative permeability of gas at maximum saturation is 0.28 and relative permeability of oil at maximum saturation is 1.

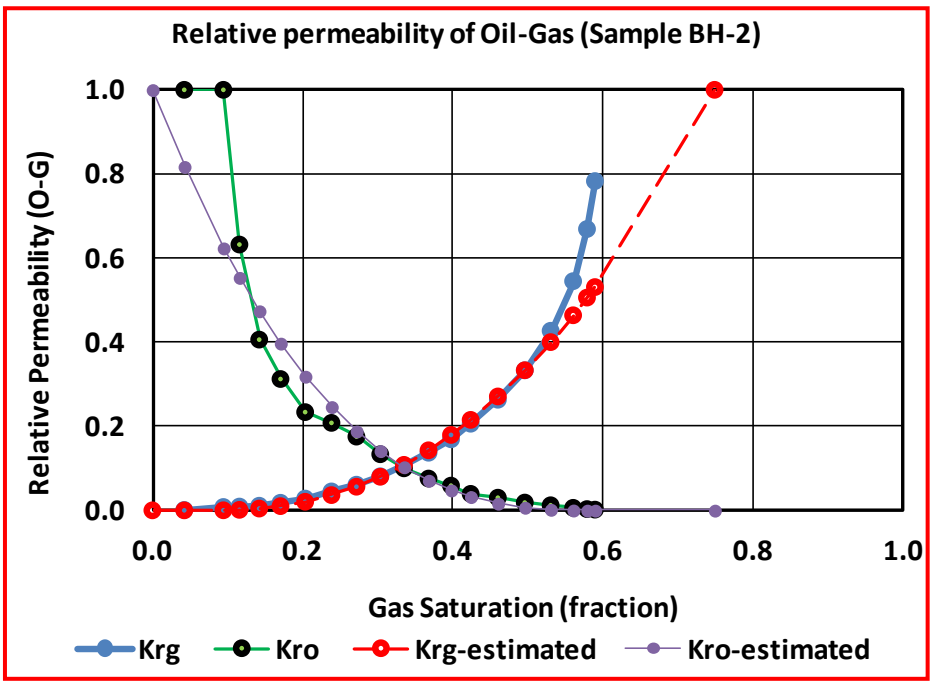

Figure 4.7: Relative permeability of Oil-Gas (Sample BH-2)

It can be seen from relative permeability (Oil-Gas) graph of sample BH-2 that connate water saturation is 0.25 (Figure 4.3), critical gas saturation is 0.08 and residual oil saturation is 0.16. Relative permeability of gas at maximum saturation is 0.53 and relative permeability of oil at maximum saturation is 1.

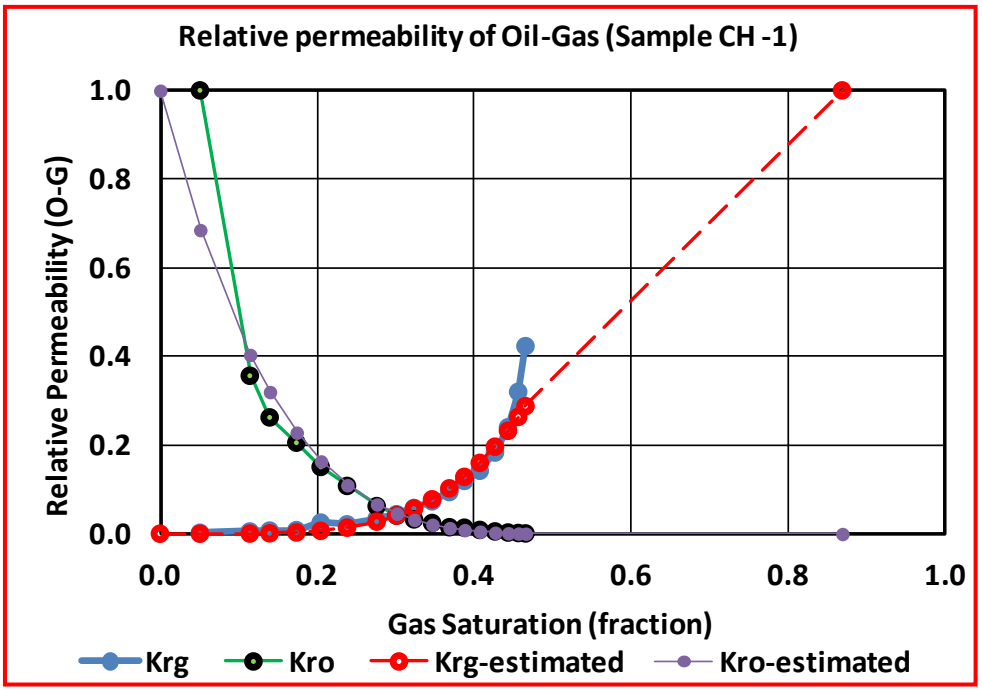

Figure 4.8: Relative permeability of Oil-Gas (Sample CH-1)

It can be seen from relative permeability (Oil-Gas) graph of sample CH-1 that connate water saturation is 0.13 (Figure 4.4), critical gas saturation is 0.04 and residual oil saturation is 0.32 . Relative permeability of gas at maximum saturation is 0.59 and relative permeability of oil at maximum saturation is 1.

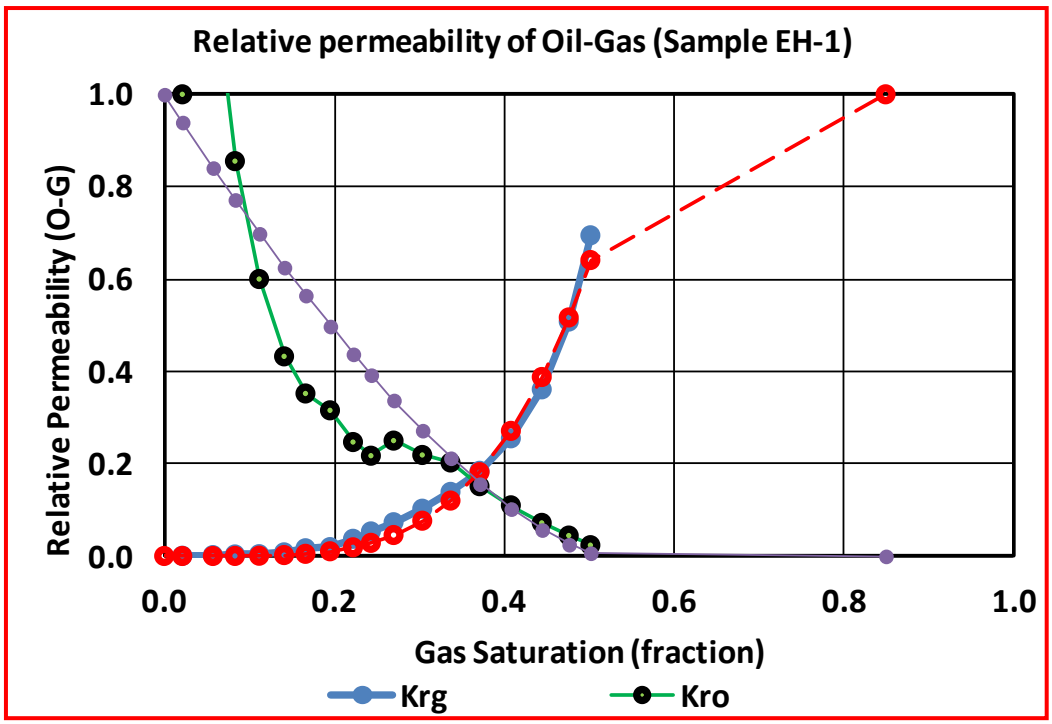

Figure 4.9: Relative permeability of Oil-Gas (Sample EH-1)

It can be seen from relative permeability (Oil-Gas) graph of sample EH-1 that connate water saturation is 0.15 (Figure 4.5), critical gas saturation is 0.04 and residual oil saturation is 0.33 . Relative permeability of gas at maximum saturation is 0.74 and relative permeability of oil at maximum saturation is 1. Corey exponents along with saturation end points have been estimated for all the core samples and is given below in Table 4.2.

Table 4.2: Corey exponent for Oil-Gas relative permeability curve

Core no.	Porosity (%)	Air Perm (mD)	RQI	FZI	N_o	N_g	K_{rge}	K_{roe}	S_{wc}	S_{org}	S_{gc}
									(fraction)		
AH-1	27.93	330	1.079	2.785	2.79	3.1	0.28	1	0.17	0.46	0.06
BH-2	21.6	457	1.444	5.242	2.7	2.3	0.53	1	0.25	0.16	0.08
CH-1	29.63	651	1.471	3.495	3.88	4	0.59	1	0.13	0.32	0.04
EH-1	29.14	597	1.421	3.456	1.48	3.8	0.74	1	0.15	0.33	0.04

4.2.2 Capillary Pressure:

Capillary pressure lab data from two wells M-5 and M-8 were measured at laboratory conditions, which were converted to the equivalent water-oil at reservoir conditions using Equation 4.10, where σ is interfacial tension, θ is contact angle and r is pore throat radius.

$$P_c = \frac{2\sigma.Cos\theta}{r} \tag{4.9}$$

$$P_{c(res)} = P_{c(lab)} \frac{(\sigma\ cos\theta)_{\text{res}}}{(\sigma\ cos\theta)_{\text{lab}}} \tag{4.10}$$

The converted capillary pressures at reservoir condition were plotted for well M-8 and M-5 in Figure 4.10 and Figure 4.11 respectively.

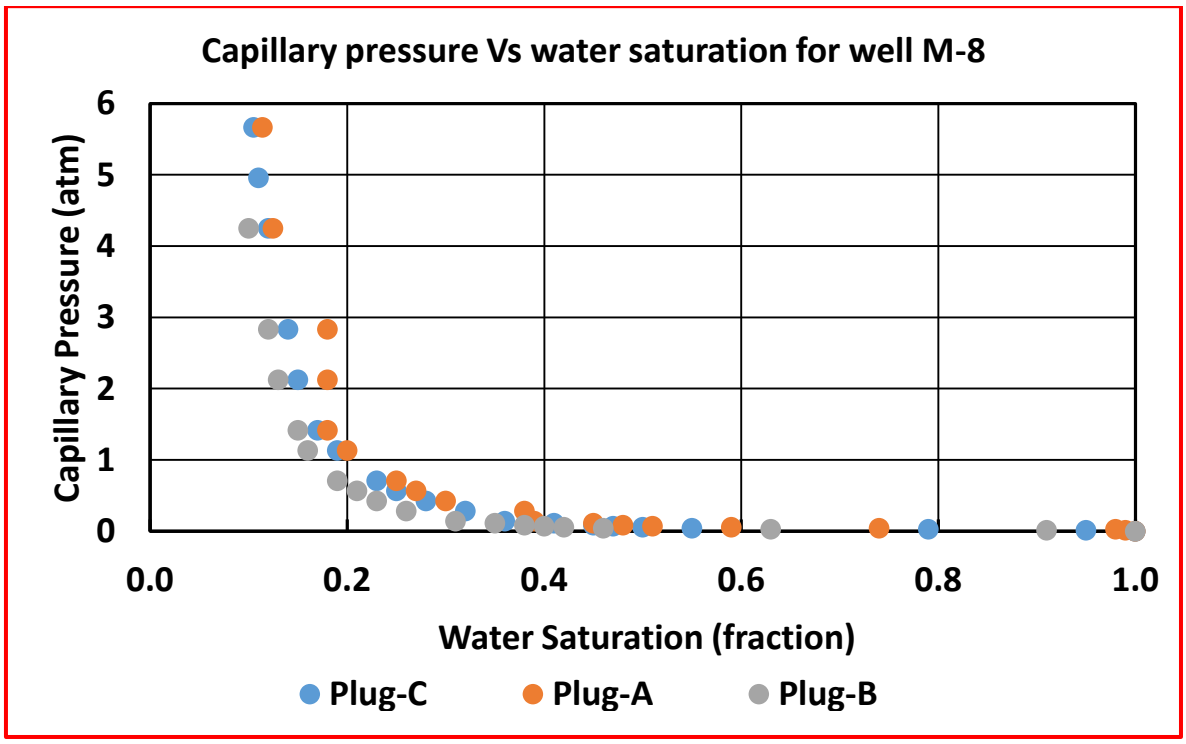

Figure 4.10: Capillary pressure Vs S_w for well M-8

Capillary pressure for three vertical core plugs were converted to reservoir condition and plotted as Figure 4.10 for well M-8. It can be seen that minimum water saturation is in the range of 0.10 to 0.18.

Capillary pressure for four vertical core plugs were converted to reservoir condition and plotted as Figure 4.11 for well M-5. It can be seen that minimum water saturation is in the range of 0.30 to 0.50.

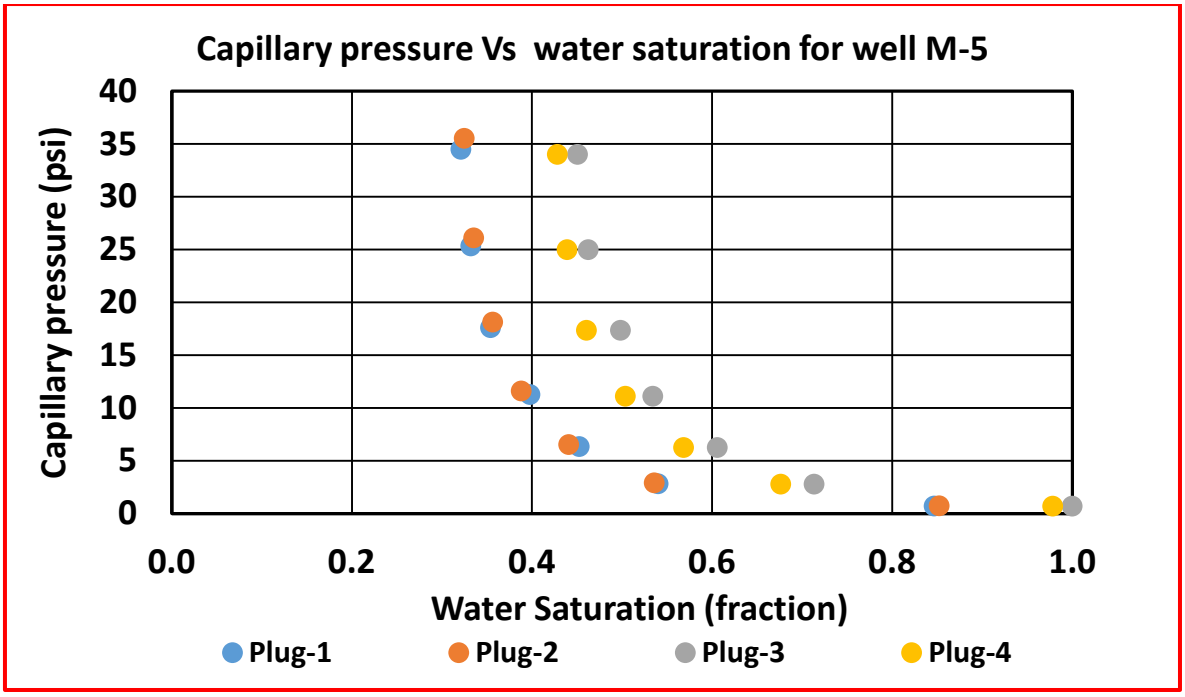

Figure 4.11: Capillary pressure Vs S_w for well M-5

Variations in pore geometrical attributes, in turn, define the existence of distinct zones (hydraulic units) with similar fluid-flow characteristics. Leverett (1941) proposed just such a dimensionless capillary pressure group, and he derived the term $\left[\frac{K}{\emptyset}\right]^{0.5}$ instead from a simple pore-space model. J-Leverett function was calculated using Equation 4.11. A least squares regression analysis was then made using the J values as the independent variable for a set of samples with similar pore size distributions to identify different trends which is also representative of different Rock types. Rock Quality Index (RQI) has been calculated for all plug from M-5 (Plug-1, Plug-2, Plug-3 and Plug-4) and M-8 (Plug-A, Plug-B and Plug-C) in Table 4.3 below.

Table 4.3: Rock quality index (RQI) for core plugs from well M-5 and well M-8

Plug	Well	Porosity (%)	Air permeability (mD)	RQI
Plug-C	M-8	31.8	1500	2.157
Plug-A	M-8	30.0	1200	1.986
Plug-B	M-8	31.5	1700	2.307
Plug-1	M-5	26.4	289	1.039
Plug-2	M-5	26.67	727	1.639
Plug-3	M-5	24.0	68	0.529
Plug-4	M-5	26.3	100	0.612

The best correlation was obtained using a power law equation form of J function (Equation 4.12). A tabulation of different values for a and n for Equation 4.12 have been given in Table 4.4. For all Rock types J function was plotted in Figure 4.12 and Figure 4.13 respectively on linear and logarithmic scale.

$$J = \frac{P_c}{\sigma\, Cos\theta}\left[\frac{K}{\emptyset}\right]^{0.5} \tag{4.11}$$

$$J(S_w) = a * {S_w}^n \tag{4.12}$$

Where a is constant and n is exponent.

Table 4.4: Coefficient for J function for various Rock types

J function	a	n
J-1	11657	-2.915
J-2	19678	-2.902
J-3	500000	-3.5
J-4	10000000	-3.964
J-5	20000000	-3.96

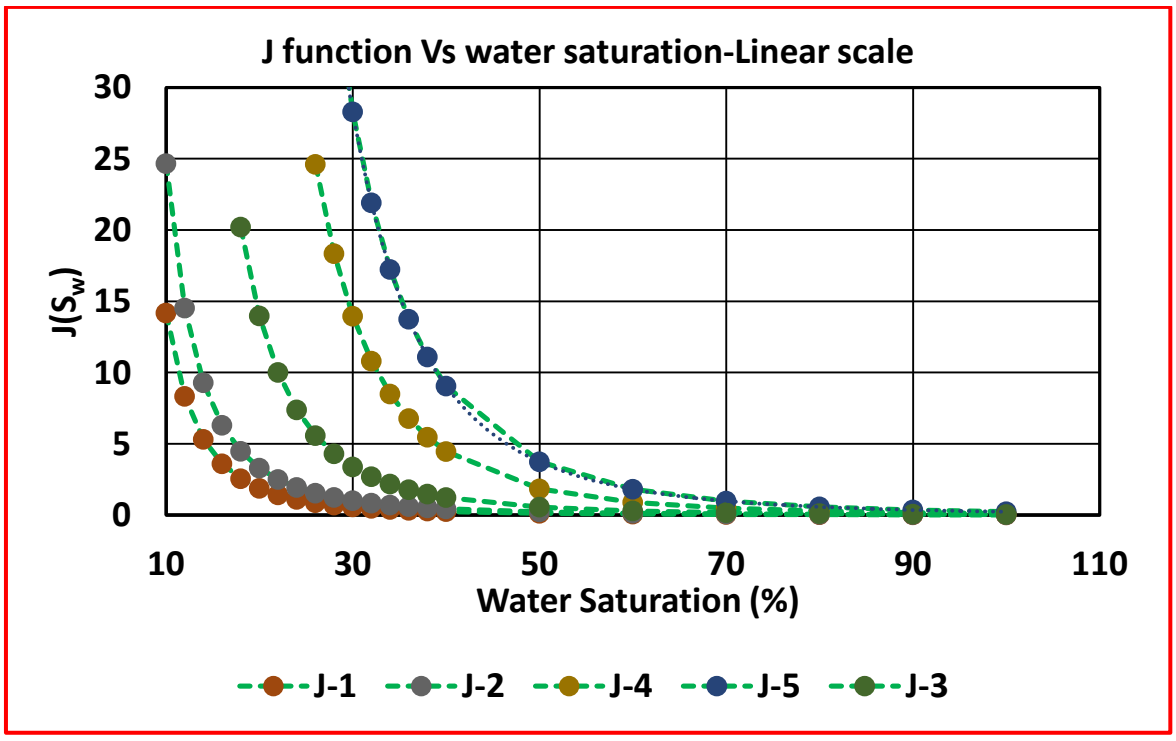

Figure 4.12: J function Vs S_w (linear scale) for various Rock types

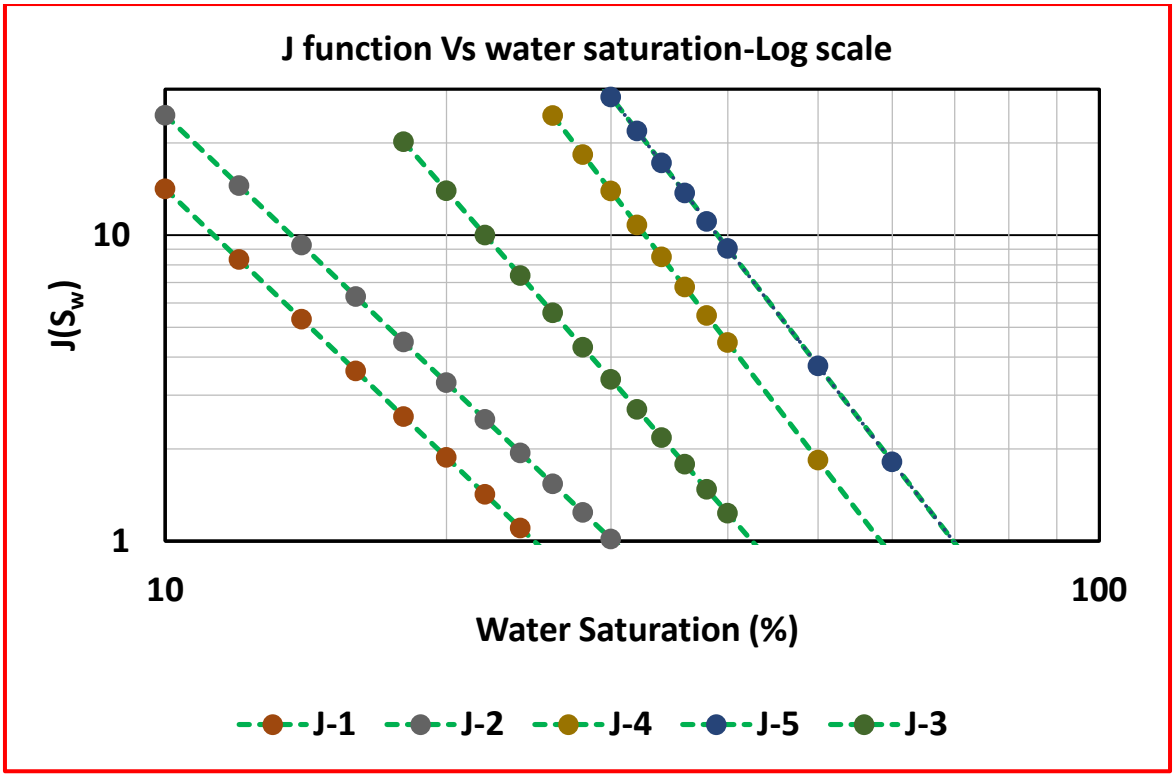

Figure 4.13: J function Vs S_w (log scale) for various Rock types

An analytical representation for individual-phase relative permeability is commonly used in numerical simulators (Ahmed, T., 2010). The most frequently used functional forms for expressing the relative-permeability are given below

Oil-Gas relative permeability curves are estimated for different Rock types using the following formulae.

$$K_{rw-estimated} = \frac{K_{rwe}\,(S_w - S_{wc})^{N_w}}{(1 - S_{or} - S_{wc})^{N_w}} \tag{4.13}$$

$$K_{ro-estimated} = \frac{K_{roe}\,(1 - S_w - S_{or})^{N_o}}{(1 - S_{or} - S_{wc})^{N_o}} \tag{4.14}$$

Where

k_{rwe} = Water relative permeability at the residual oil saturation

K_{roe} = Oil relative permeability at connate water saturation

S_{wc} = Connate water saturation

S_{or} = Residual oil saturation in the water-oil system

N_o, N_w = Exponents for relative permeability curves

Based on the five rock types determined by J function from Table 4.4, a set of five pseudo relative permeability curves were constructed. Figure 4.14 through Figure 4.18

shows the calculated relative permeability and J function for Rock types 1 to 5 for oil water system. Rock type 1 is considered the best Rock type.

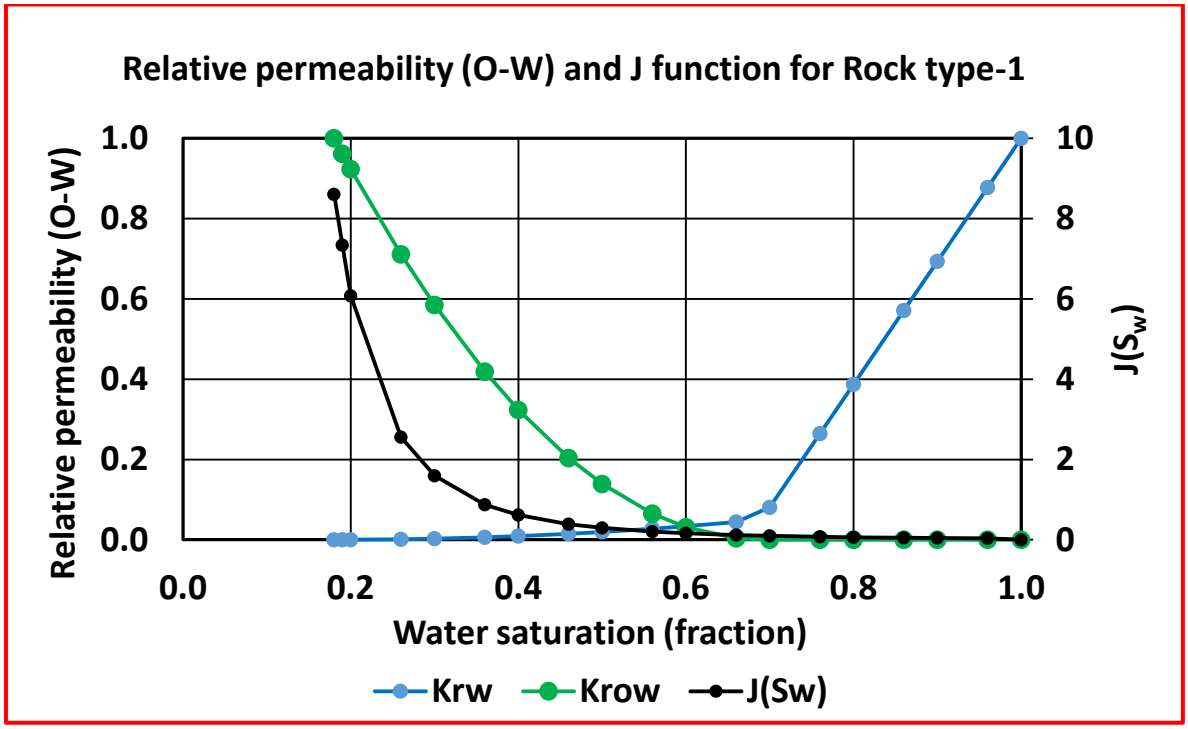

Figure 4.14: Relative permeability (Oil, Water) and J Function curve for Rock type 1

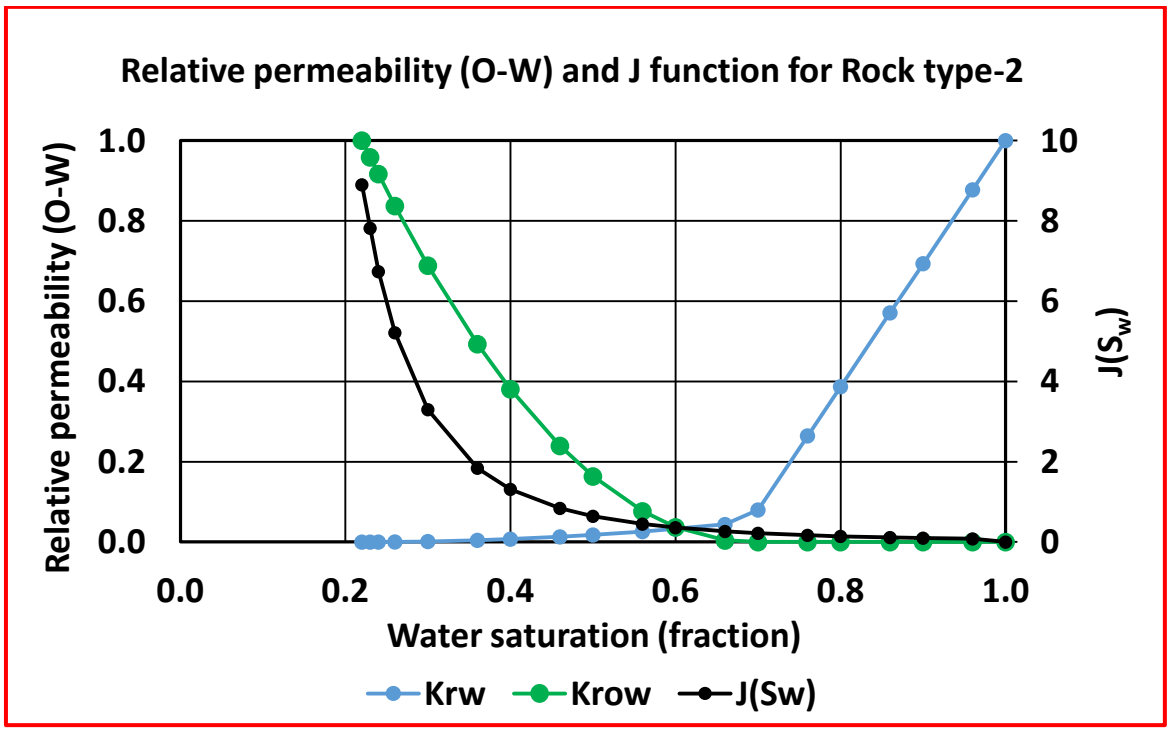

Figure 4.15: Relative permeability (Oil, Water) and J Function curve for Rock type 2

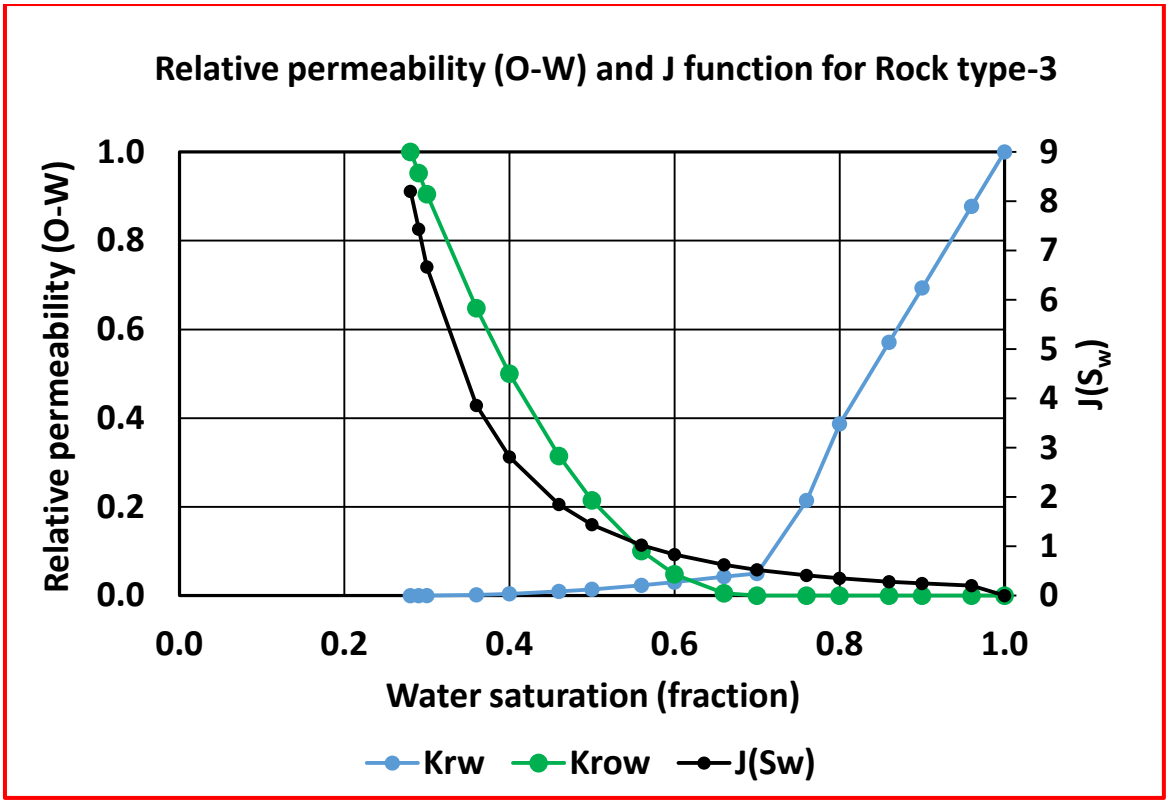

Figure 4.16: Relative permeability (Oil, Water) and J Function curve for Rock type 3

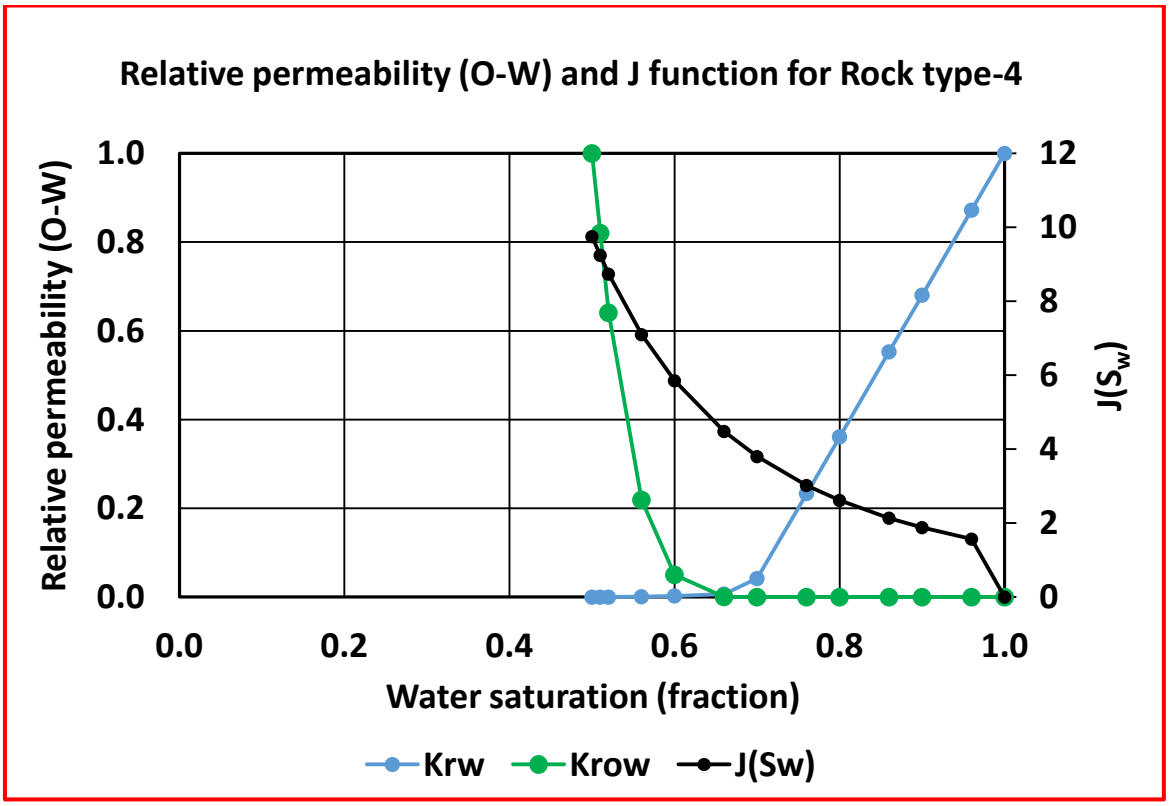

Figure 4.17: Relative permeability (Oil, Water) and J Function curve for Rock type 4

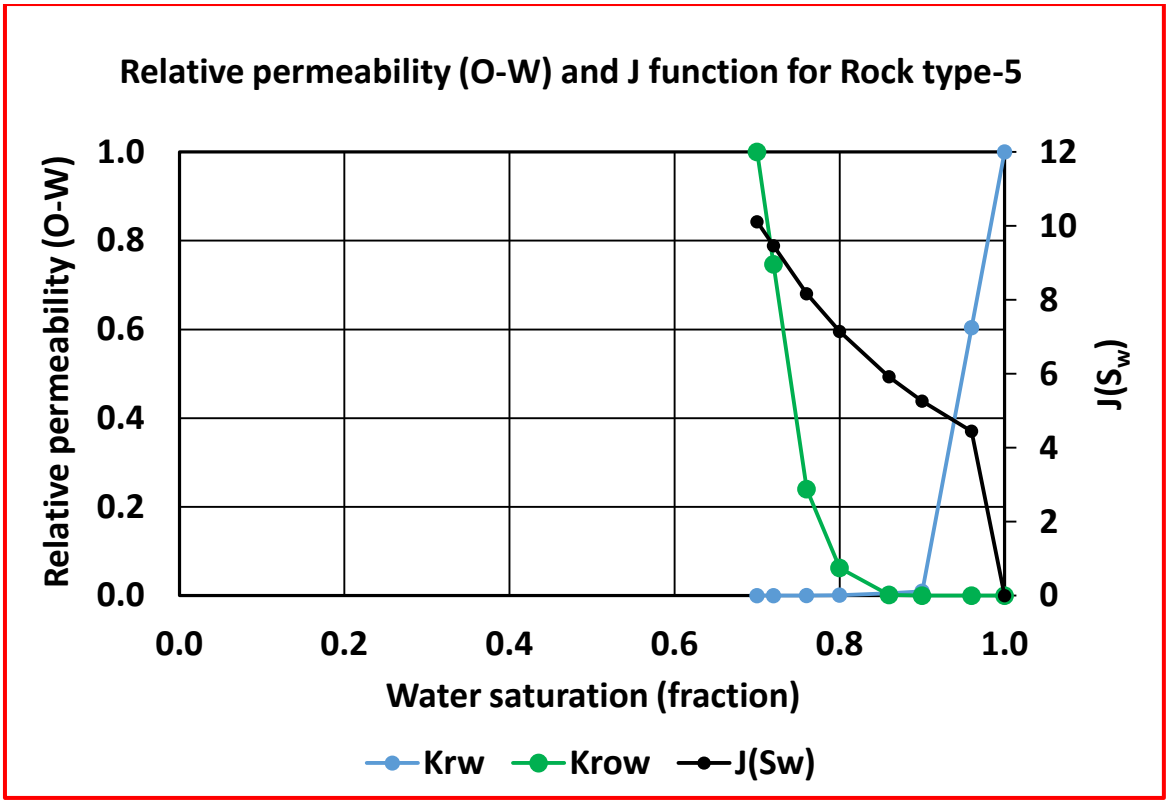

Figure 4.18: Relative permeability (Oil, Water) and J Function curve for Rock type 5

Oil-Gas relative permeability curve are estimated for different Rock types using the following formulae.

$$K_{rg-estimated} = \frac{K_{rge}\,(S_g - S_{gc})^{N_g}}{(1 - S_{org} - S_{wc} - S_{gc})^{N_g}} \tag{4.15}$$

$$K_{ro-estimated} = \frac{K_{roe}\,(1 - S_g - S_{wc} - S_{org})^{N_o}}{(1 - S_{wc} - S_{org})^{N_o}} \tag{4.16}$$

Where,

K_{rge} = Gas relative permeability at maximum gas saturation

K_{roe} = Oil relative permeability at critical gas saturation

S_{org} = Residual oil saturation in the gas-oil system

S_{gc} = Critical gas saturation

N_o, N_g = Exponents on relative permeability curves

Based on the five rock types determined by J function from Table 4.4, a set of five pseudo relative permeability curves were constructed. Figure 4.19 through Figure 4.23 shows the calculated relative permeability for Rock types 1 to 5, respectively for oil gas system. Rock type 1 is considered to be the best Rock type.

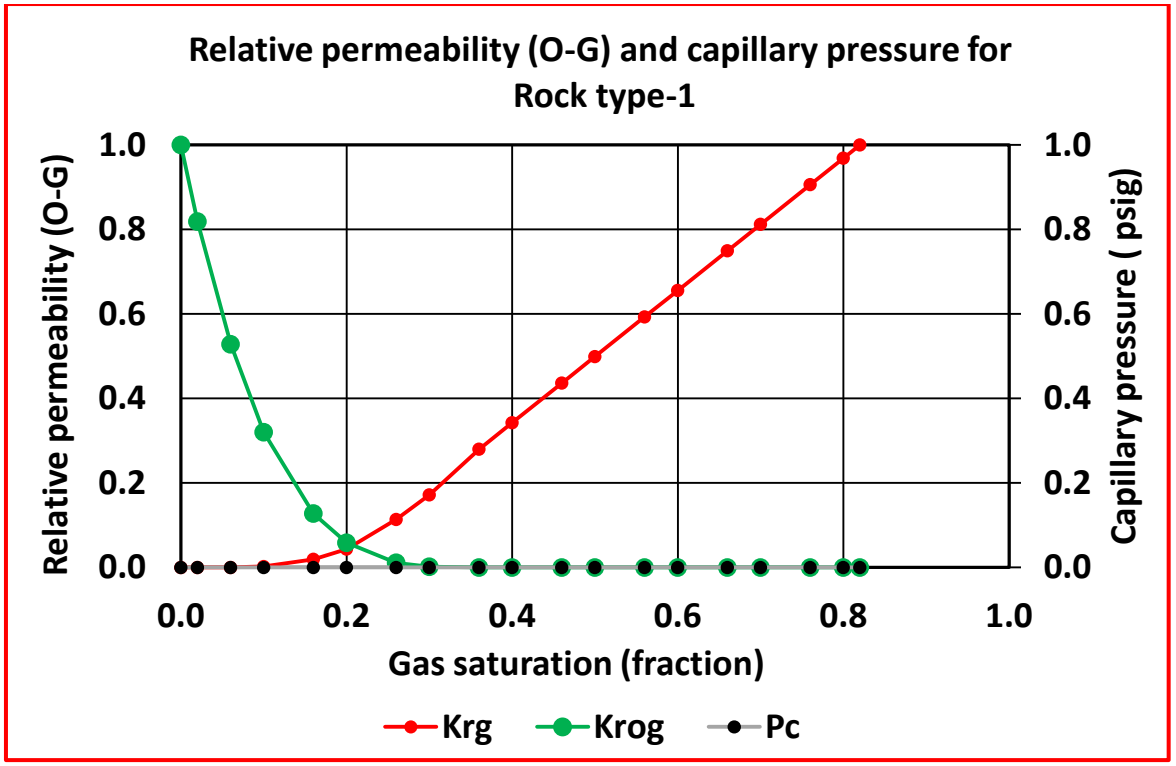

Figure 4.19: Relative permeability (Oil, Gas) and capillary pressure curve for Rock type 1

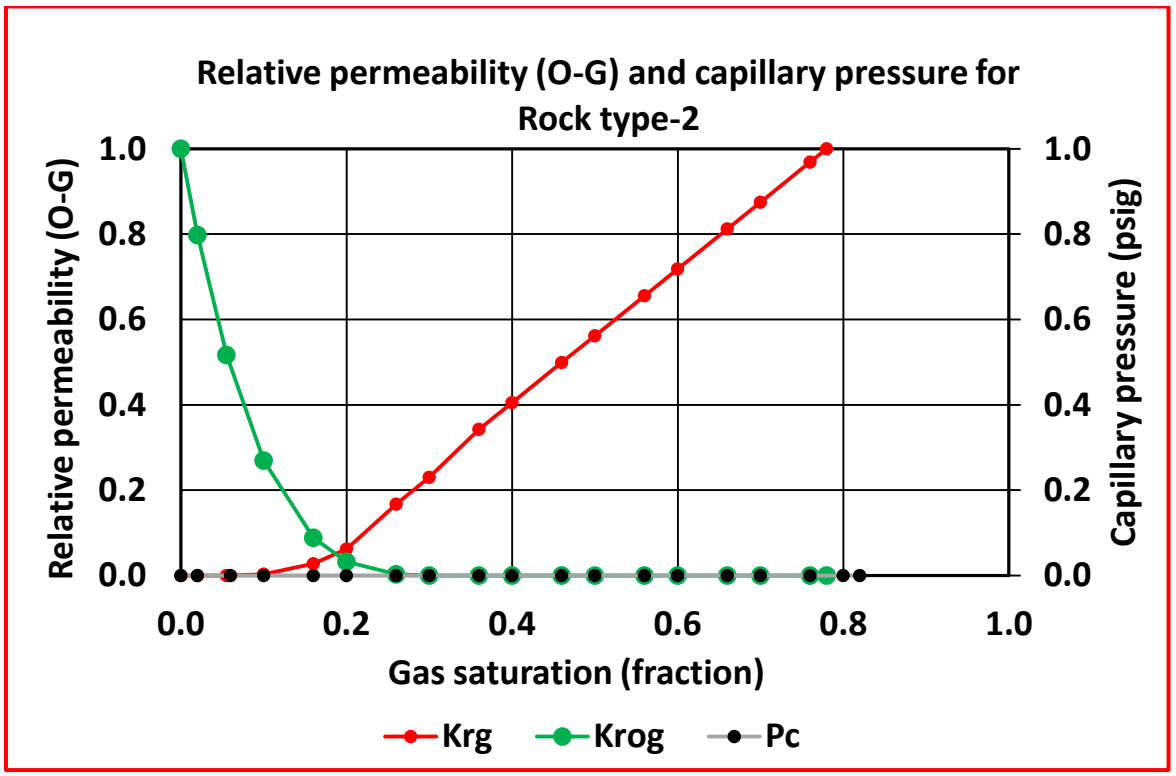

Figure 4.20: Relative permeability (Oil, Gas) and capillary pressure curve for Rock type 2

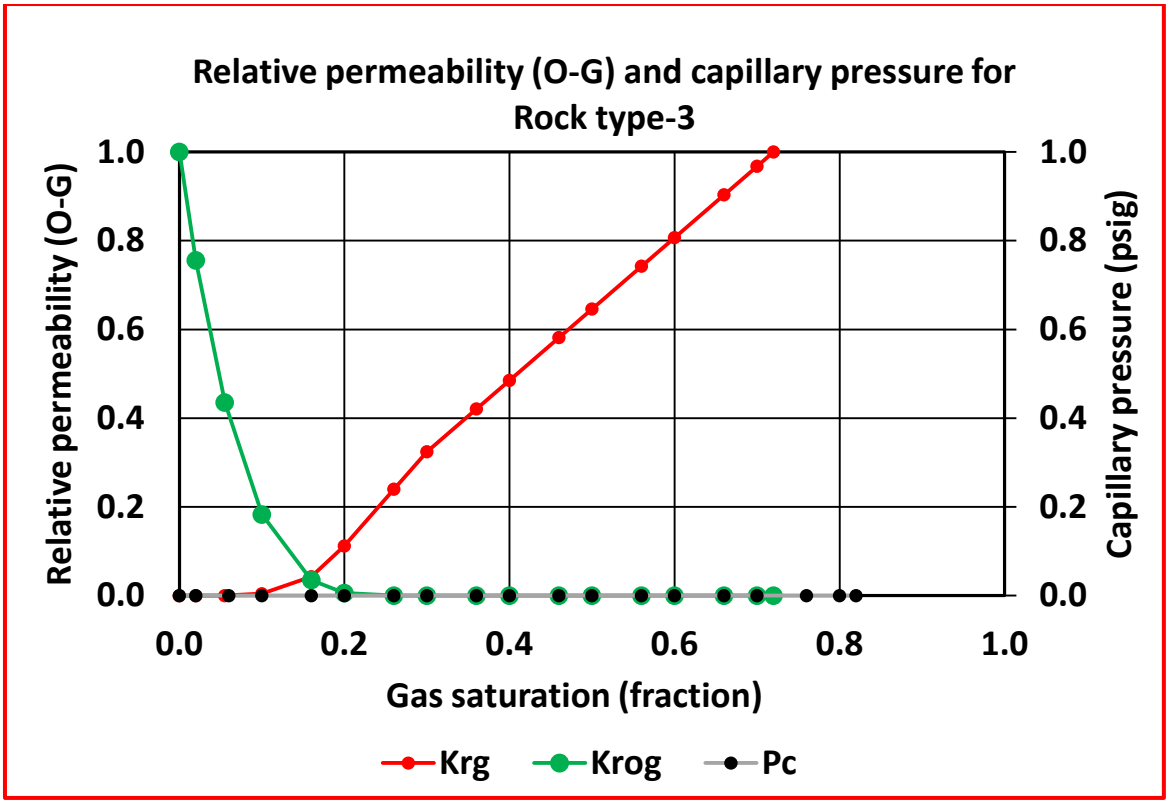

Figure 4.21:Relative permeability (Oil, Gas) and capillary pressure curve for Rock type 3

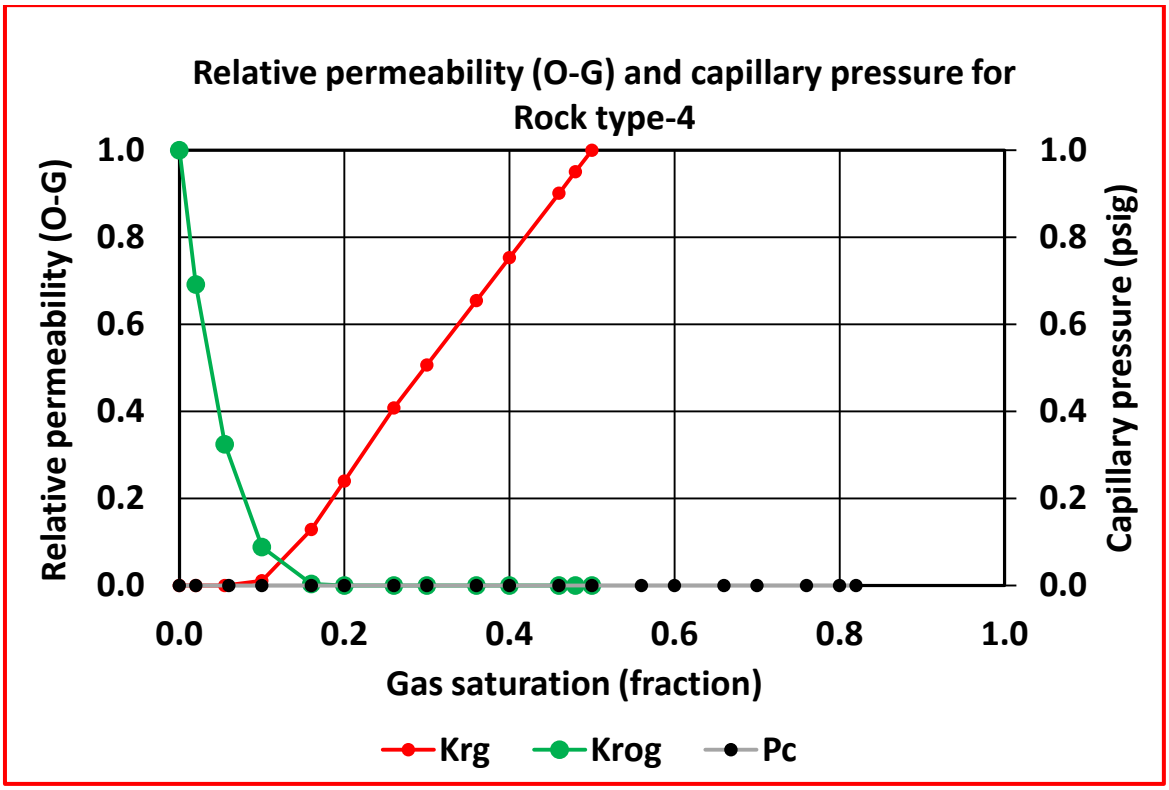

Figure 4.22: Relative permeability (Oil, Gas) and capillary pressure curve for Rock type 4

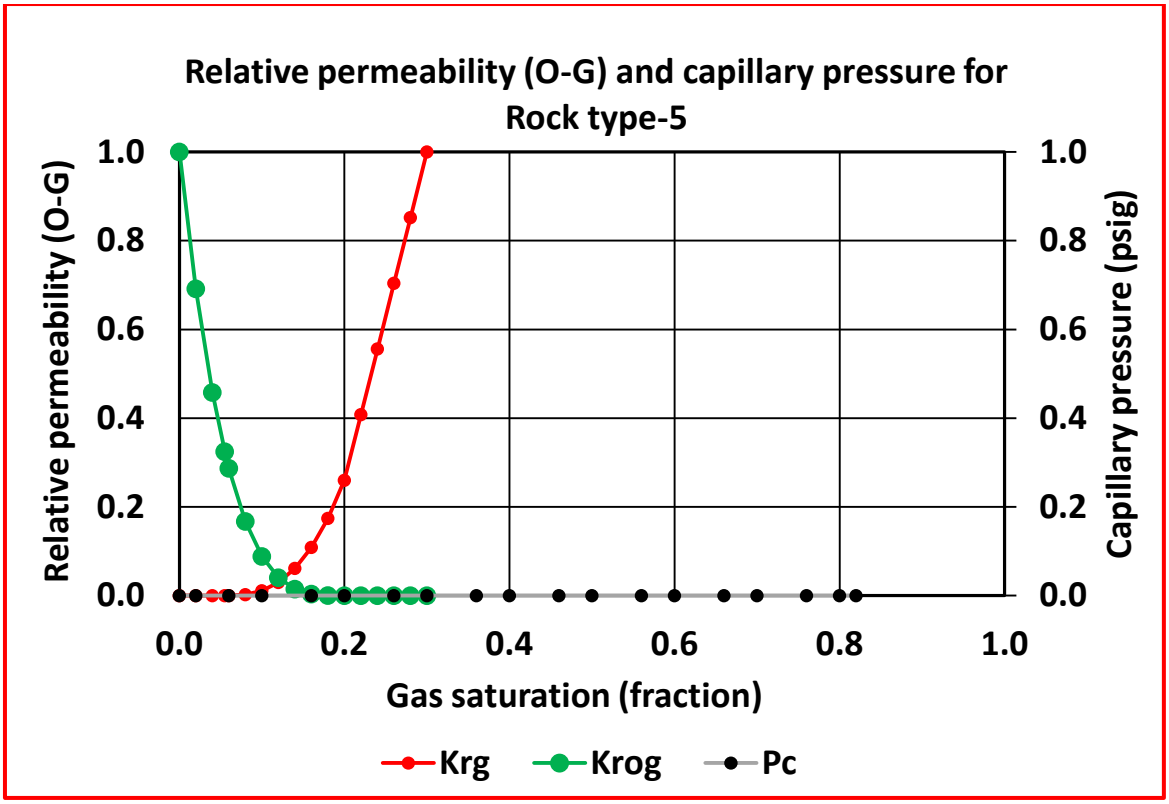

Figure 4.23:Relative permeability (Oil, Gas) and capillary pressure curve for Rock type 5

4.3 RESERVOIR FLUID CHARACTERIZATION (BLACK OIL PVT DATA)

Fluid properties, like rock properties, significantly affect fluid flow dynamics in porous media. Unlike rock properties, fluid properties exhibit significant pressure dependency. Therefore, it is often necessary in reservoir simulation to estimate these properties using correlations and/or Equations of State (EOS).

Oil properties that appear in the governing flow equations for the oil phase are density, compressibility, formation volume factor, viscosity and solubility of gas in oil. In the absence of gas, these oil properties can be treated as constants, because the compressibility of gas-free oil is very small. However, the presence of dissolved gas in oil necessitates the use of appropriate correlations to determine the variation of these properties with pressure and temperature. Theoretically, an infinite amount of gas can dissolve in oil, provided that adequate pressure is available. Accordingly, if pressure is available, it is conceivable that there will be no free gas (undersaturated reservoirs). If pressure is not sufficient, some of the gas will exist in the Free State (saturated reservoirs).

Since gas solubility in water is very small compared to oil, for most practical cases, it is assumed that constant values of these properties will come into play in the water flow equation.

4.3.1 PVT Analysis

The black oil PVT data (Constant composition experiment and differential liberation experimental lab data) from well M-2 was reviewed and validated. The original PVT data was adjusted to smooth the properties trend and to extrapolate the fluid properties to the reservoir pressure at the gas oil contact. An extrapolation of the saturation pressure was performed from the original PVT data in order to prepare the fluid properties for the material balance and reservoir simulation study. Plot of PVT properties have been shown in Figure 4.24 through Figure 4.27.

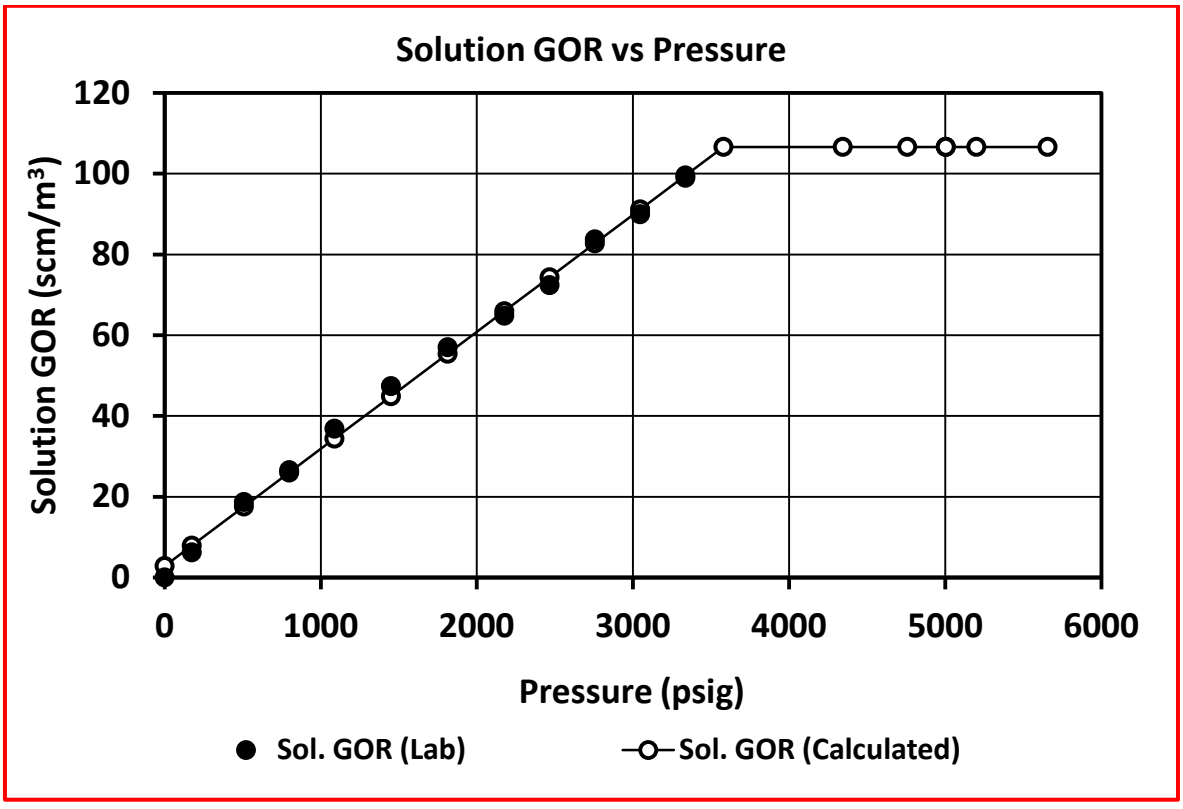

Figure 4.24: *Solution* GOR *Vs pressure*

It can be seen from Figure 4.24 that solution GOR is 110 scm/m^3 at and above bubble point pressure. Smoothing of curve has been performed above and below bubble point pressure for input in reservoir simulation studies.

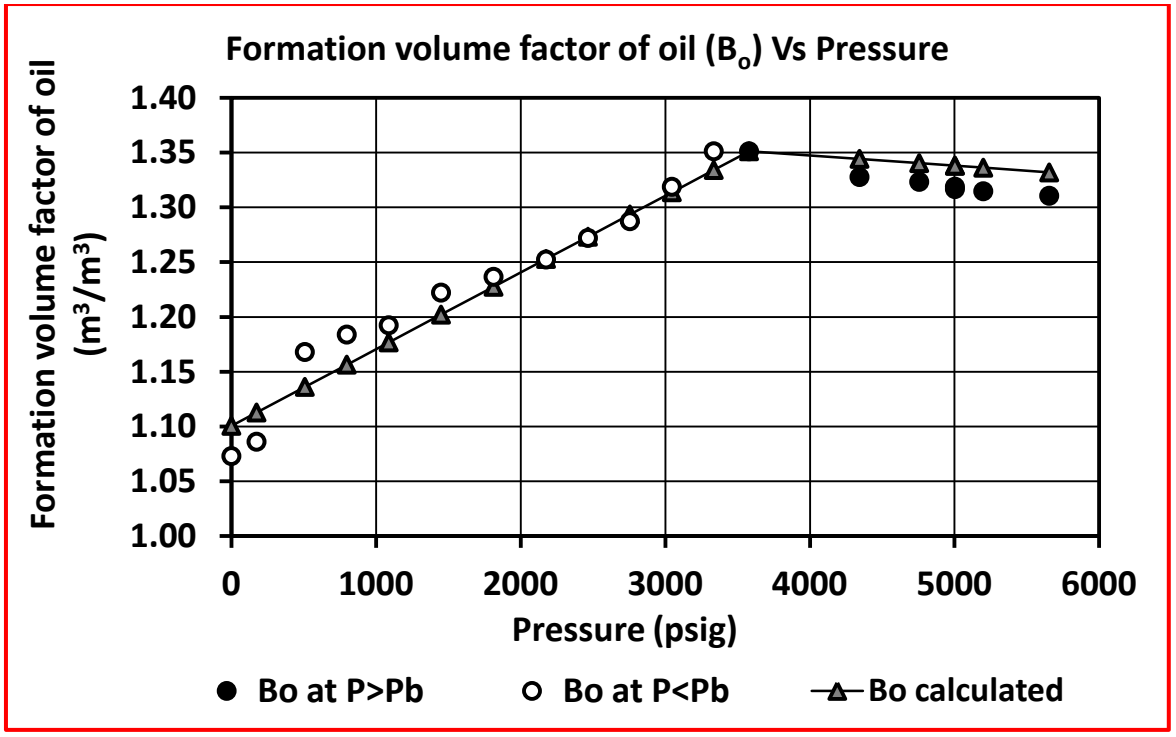

Figure 4.25: Formation volume factor of oil(B_o) Vs pressure

It can be seen from Figure 4.25 that formation volume factor of oil is 1.35 at bubble point pressure. Smoothing of curve has been performed above and below bubble point pressure for input in reservoir simulation studies.

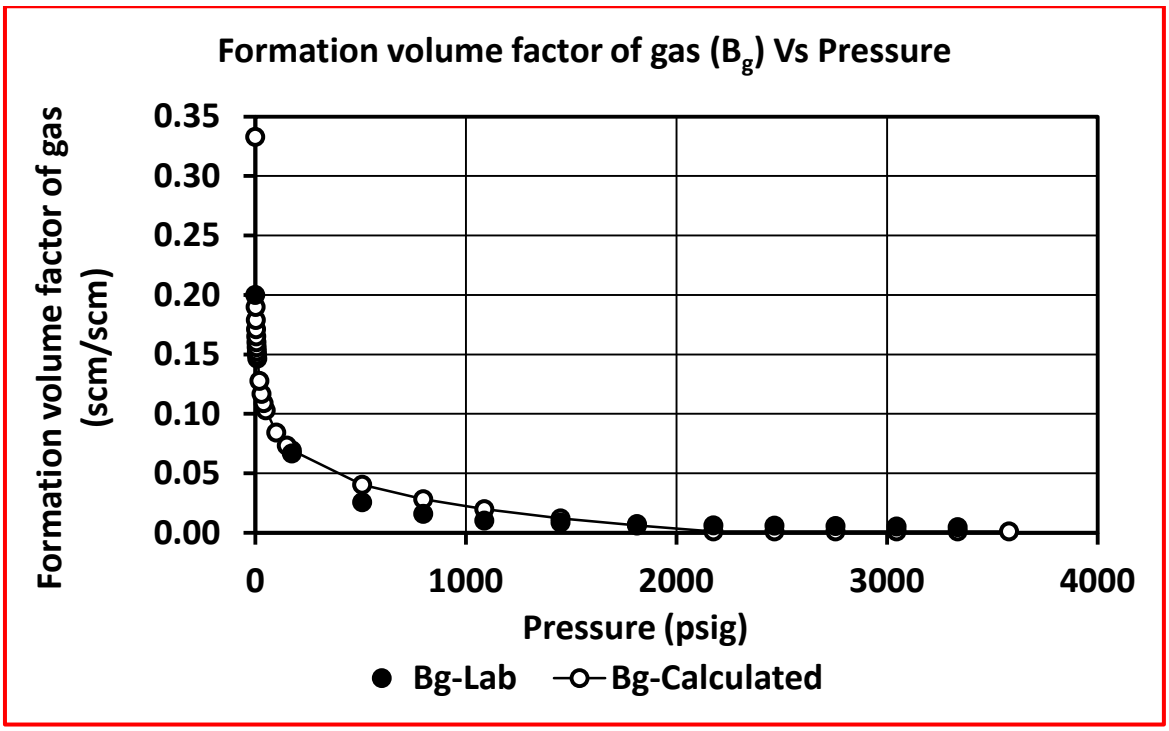

Figure 4.26: Formation volume factor of gas (Bg) Vs pressure

It can be seen from Figure 4.26 that smoothing of curve has been performed above and below bubble point pressure for input in reservoir simulation studies.

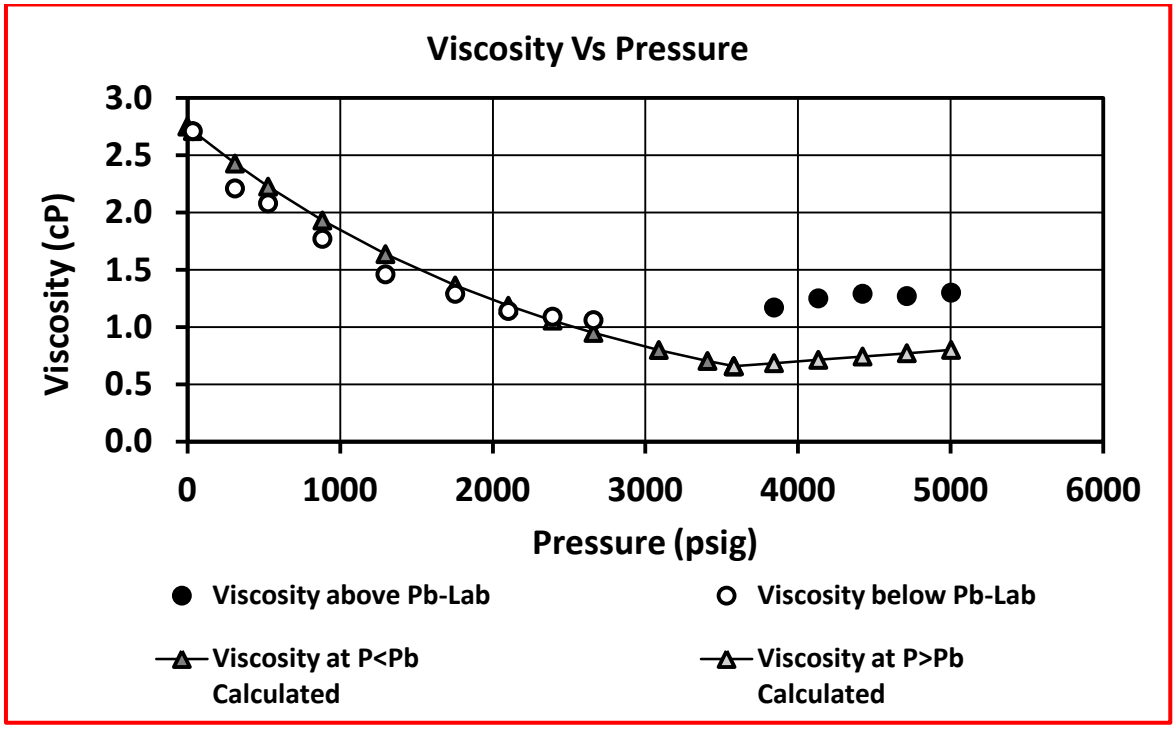

Figure 4.27: Viscosity Vs pressure

It can be seen from Figure 4.27 that viscosity of oil is 0.65 cP at bubble point pressure. Smoothing of curve has been performed above and below bubble point pressure for input in reservoir simulation.

Once the PVT data was adjusted, the oil density was calculated using material balance approach. The oil density versus pressure was calculated using the information of gas gravity, oil formation volume factor and the residual oil API gravity. The results of this calculation are presented in Table 4.5.

Sample calculation of mass of oil and gas and oil density (Table 4.5) is given below:

$$(Mass\ of\ oil\ and\ gas)_{P_i} = (Mass\ of\ oil\ and\ gas)_{P_{i-1}} +$$

$$(1.217)\{(Solution\ GOR)_{P_{i-1}} - (Solution\ GOR)_{P_i}\}\,(Gas\ gravity)_{P_{i-1}}$$

Where P_i is the pressure where calculation for mass of oil and gas is done and P_{i-1} is the lower value of pressure in Table 4.5. Calculation of mass of oil and gas at bubble point pressure (P_b) of 3580 psig is given below:

$(Mass\ of\ oil\ and\ gas)_{3580} = (Mass\ of\ oil\ and\ gas)_{3336} +$

$(1.217)\{(Solution\ GOR)_{3336} - (Solution\ GOR)_{3580}\}\ (Gas\ gravity)_{3336}$

$(Mass\ of\ oil\ and\ gas)_{3580}$= 1002.334 + (1.217)(106.6504 - 99.5744)(0.7712)

= 1002.334+6.6411=1008.975 gm

Sample calculation of oil density is given below:

$$(Oil\ Density)_P = \frac{(Mass\ of\ oil\ and\ gas)_P}{Oil\ FVF_P * 1000}$$

$$(Oil\ Density)_{3580} = \frac{(Mass\ of\ oil\ and\ gas)_{3580}}{Oil\ FVF_{3580} * 1000}$$

$$(Oil\ Density)_{3580} = \frac{1008.975}{1.3512 * 1000}$$

$$(Oil\ Density)_{3580} = 0.7467\ gm/cc$$

Table 4.5: Oil density calculation

Lab data		**Smoothed data**				**Calculated variable**	
Pressure (psig)	**Corrected relative volume**	**Sol GOR, scm/m^3**	**Gas Gravity**	**Gas Comp factor**	**Oil FVF (m^3/m^3)**	**Mass of oil and gas (gm)**	**Oil density (gm/cc)**
5656	0.985708	106.6504	All gas is in solution above bubble point pressure, hence no gas gravity and gas compressibility factor value is given		1.331889	1008.975	0.757552
5200	0.9889	106.6504			1.336202	1008.975	0.755107
5004	0.990272	106.6504			1.338056	1008.975	0.754061
5004	0.990272	106.6504			1.338056	1008.975	0.754061
4757	0.992001	106.6504			1.340392	1008.975	0.752747
4344	0.994892	106.6504			1.344298	1008.975	0.750559
3580	**1**	**106.6504**	**0.80682**	**0.966183**	**1.3512**	**1008.975**	**0.746726**
3336		99.5744	0.771245	0.976488	1.33412	1002.334	0.751307
3046		91.1644	0.736706	0.968289	1.31382	994.7937	0.757177
2756		82.7544	0.710577	0.941919	1.29352	987.521	0.763437
2466		74.3444	0.692858	0.902294	1.27322	980.4296	0.770039
2176		65.9344	0.683549	0.855006	1.25292	973.4335	0.776932
1813		55.4074	0.683748	0.794662	1.22751	964.6738	0.785879
1450		44.8804	0.697125	0.745992	1.2021	955.7426	0.795061
1088		34.3824	0.723587	0.72447	1.17676	946.498	0.804326
798		25.9724	0.75424	0.73809	1.15646	938.7784	0.811769
508		17.5624	0.793303	0.789404	1.13616	930.659	0.819127
174		7.8764	0.848714	0.908493	1.11278	920.6545	0.827346
0		0	0.881998	1.001194	1.1006	912.2	0.828821
1 psi = 0.0689476 bars							

4.4 HISTORICAL PRESSURE PRODUCTION PLOT

Pressure, production data has been collected for forty-six (46) individual wells for a period of sixteen years. Plot of the same on field scale has been given in Figure 4.28.

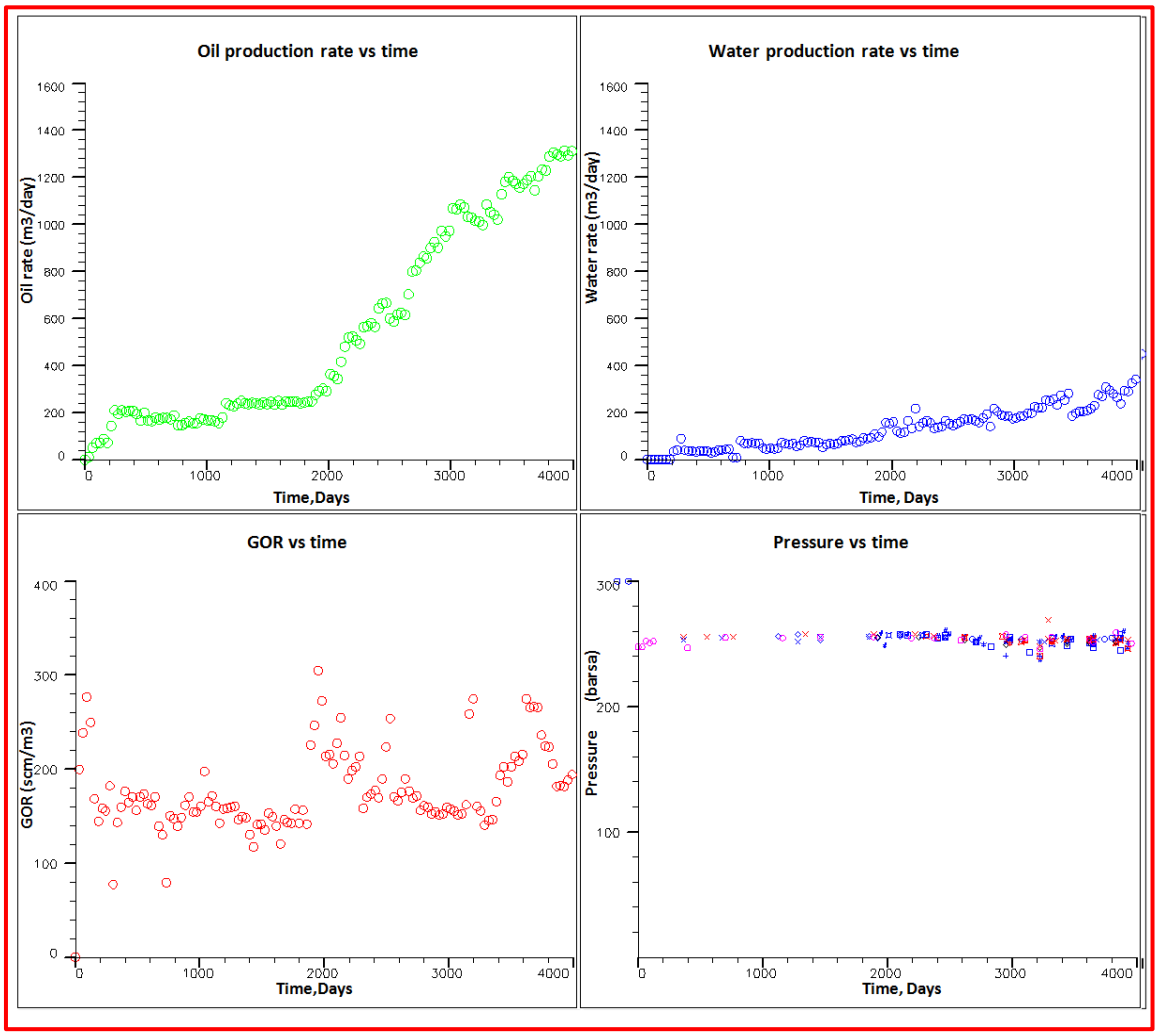

Figure 4.28: Field wise oil rate, water rate, GOR and SBHP

4.5 CONTACT DETERMINATION

Water Oil Contact determination has been done using well logs and same has been verified using Reservoir Formation Tester (RFT) data.

The basic principle of contact determination using RFT data is the intersection of the oil and water gradients. In Figure 4.29, an oil gradient of 0.33 psi/ft was estimated from three valid reservoir pressures. This oil gradient corresponds to a reservoir oil density of 0.7403 gm/cc which is close to the PVT oil density of 0.7551 gm/cc less than 2% difference. The well also shows two reservoir pressures that clearly define a water gradient of 0.44 psi/ft. The

intersection of the oil gradient line with the water gradient line permits the estimation of a Free Water Level (FWL) at 2561 m TVDSS. The results of the analysis are shown in Figure 4.29.

In Figure 4.30 Water Oil Contact has been determined using log data and a comparison has been done using contacts determined by RFT data (Figure 4.29).

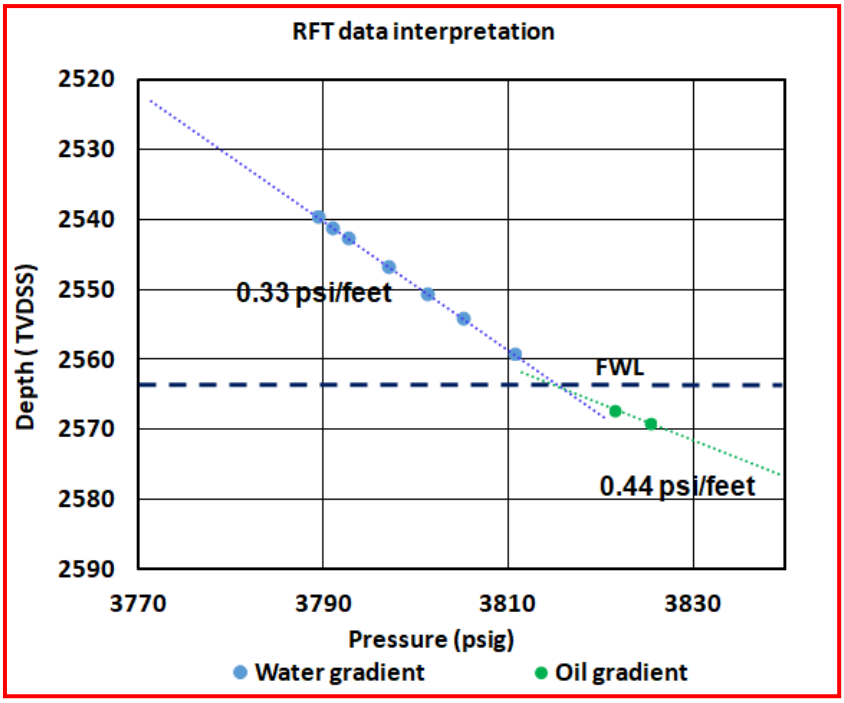

Figure 4.29: Determination of contact from RFT data

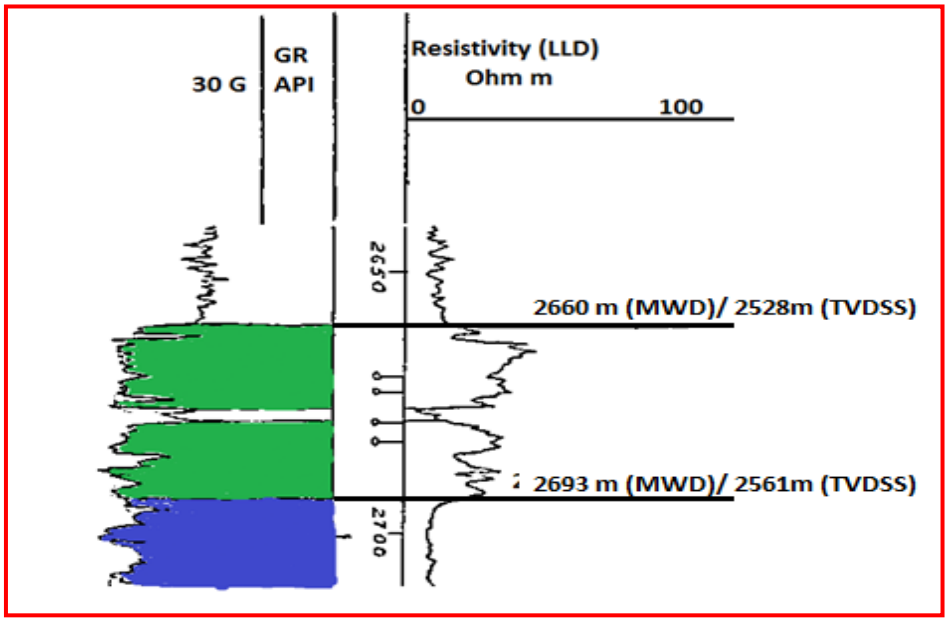

Figure 4.30: Determination of contact from log data (Source: Oil India Ltd. internal report)

In order to compare and ascertain Water Oil Contact determined from RFT data deep resistivity logs (LLD) has been used which is shown in Figure 4.30 above. An increased value of resistivity in the oil zone followed by a low resistivity value in water zone is marked in green and blue color for indicative purpose. Contact determined using well log is in Measured well depth below derrick floor (2693 m), where 132 m (Kelly bushing height w.r.t. mean sea level) has been subtracted to convert it in TVDSS depth of 2561 m.

4.6 DETERMINATION OF TRANSITION ZONE THICKNESS USING CAPILLARY PRESSURE LAB DATA

After determination of J-function for different Rock types, water saturation above FWL was determined using Equation 4.13, and plotted in Figure 4.31.

$$P_c = (\rho_w - \rho_o)gh \tag{4.13}$$

Where P_c is capillary pressure, ρ_w and ρ_o are water and oil density, g is acceleration due to gravity and h is depth. The classic method is based on Leverett's J-function approach (Leverett, 1941). Other commonly used methods include Johnson, Skelt and Harrison (Johnson, 1987; Skelt and Harrison, 1995; Skelt, 1996).

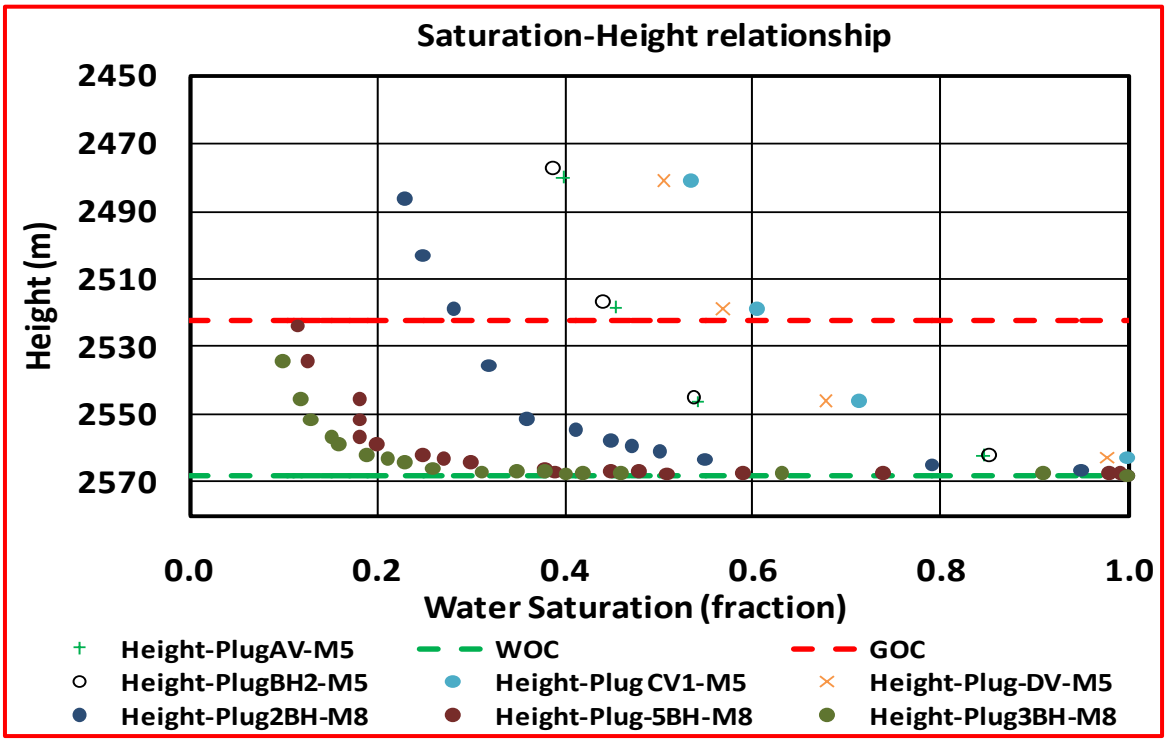

Figure 4.31: Saturation-Height relationship

It can be seen from Figure 4.31 that initial water saturation varies between 0.1 and 0.5 in the oil zone signifying existence for different Rock types.

4.7 MATERIAL BALANCE STUDIES

A reservoir tank with an initial Oil in place of 347 MMSTB with size of gas cap m = 0.34 has been constructed. A bottom drive aquifer has been defined using Fetkovich semi steady state aquifer model with an average aquifer permeability of 25 mD and the material balance analytical method has been applied. The results of the calculated oil production versus the tank pressure are shown below in Figure 4.32.

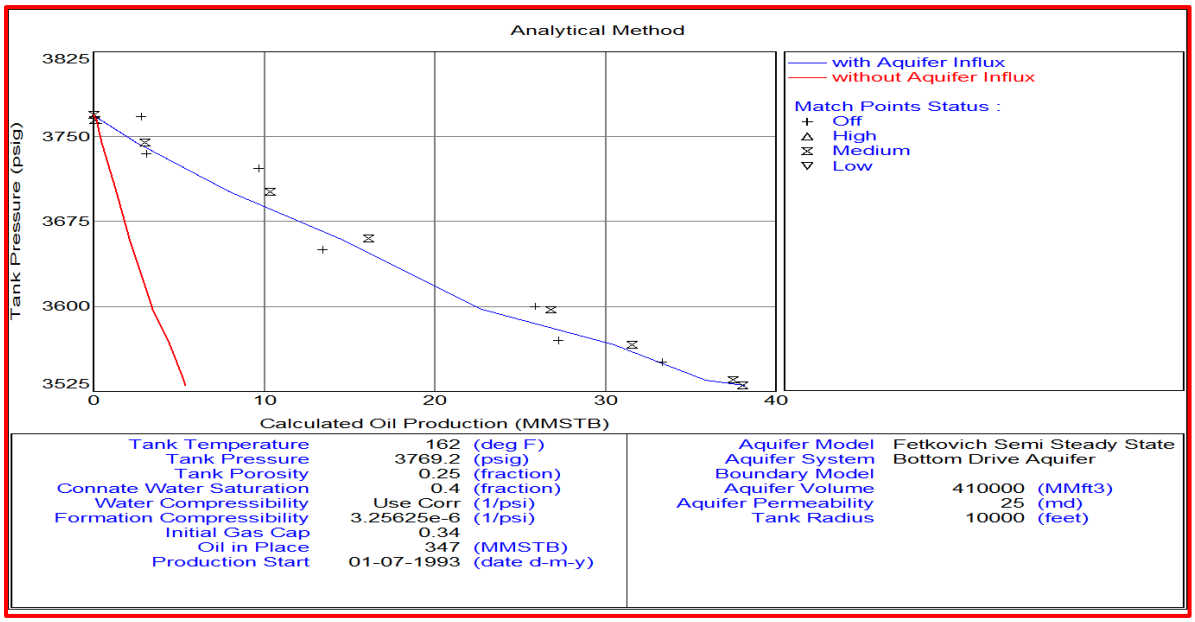

Figure 4.32: Material Balance results (Pressure Vs. Calculated oil production)

4.7.1 Fetkovich Semi Steady State Aquifer

In the semi-steady state model, the pressure within the aquifer is not kept constant but allowed to change. Material balance equation is used to find the changed average pressure in the aquifer. Based on this fact the influx is worked out to be,

$$W_e = \frac{W_{ei}}{P_i}(p_i - \bar{p})\left(1 - e^{\left(-\frac{JP_i t}{W_{ei}}\right)}\right) \tag{4.14}$$

$$J = \frac{fkh}{141.2\ \mu\ [\ln\frac{r_e}{r_o} - \frac{3}{4}]} \tag{4.15}$$

$$f = \frac{encroachment\ angle}{360^o} \tag{4.16}$$

Where W_{ei} is the maximum Encroachable water influx, J is the aquifer productivity index. p_i is the initial pressure and $\bar{p}$ is the average reservoir pressure and f is fractional encroachment angle.

Pressure and cumulative oil production have been plotted in Figure 4.32, which is matched with the fetkovitch semi steady state aquifer model. A good pressure match indicated in blue line validated the model for calculation of oil in place using Campbell plot (Figure 4.34) and drive mechanism indices represented below in Figure 4.33.

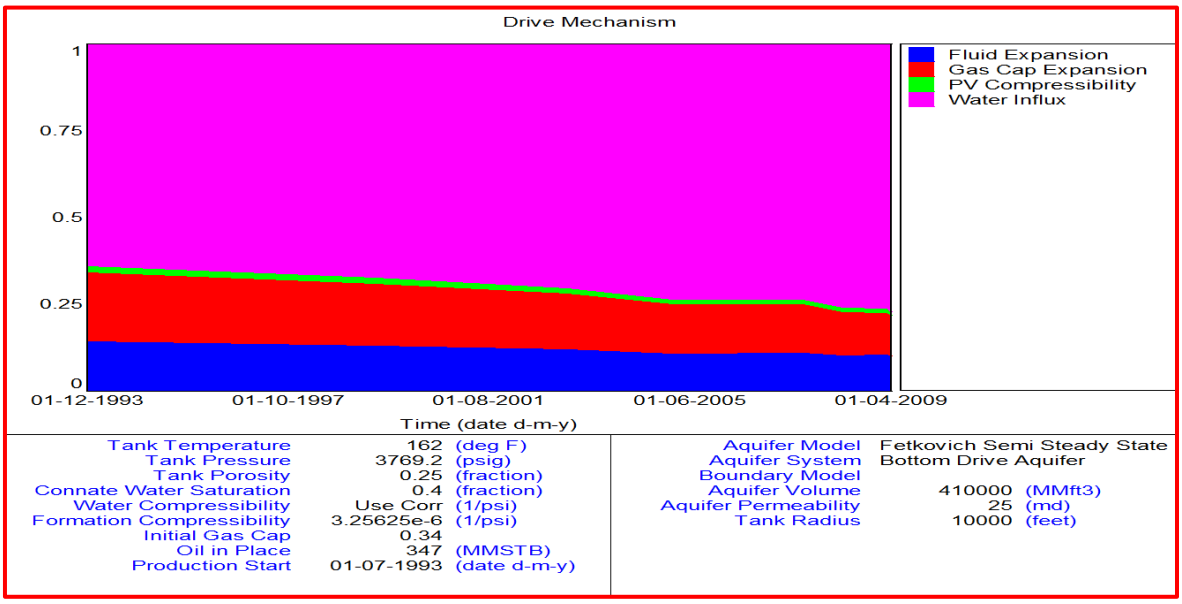

Figure 4.33: Drive mechanism index/ Energy plot

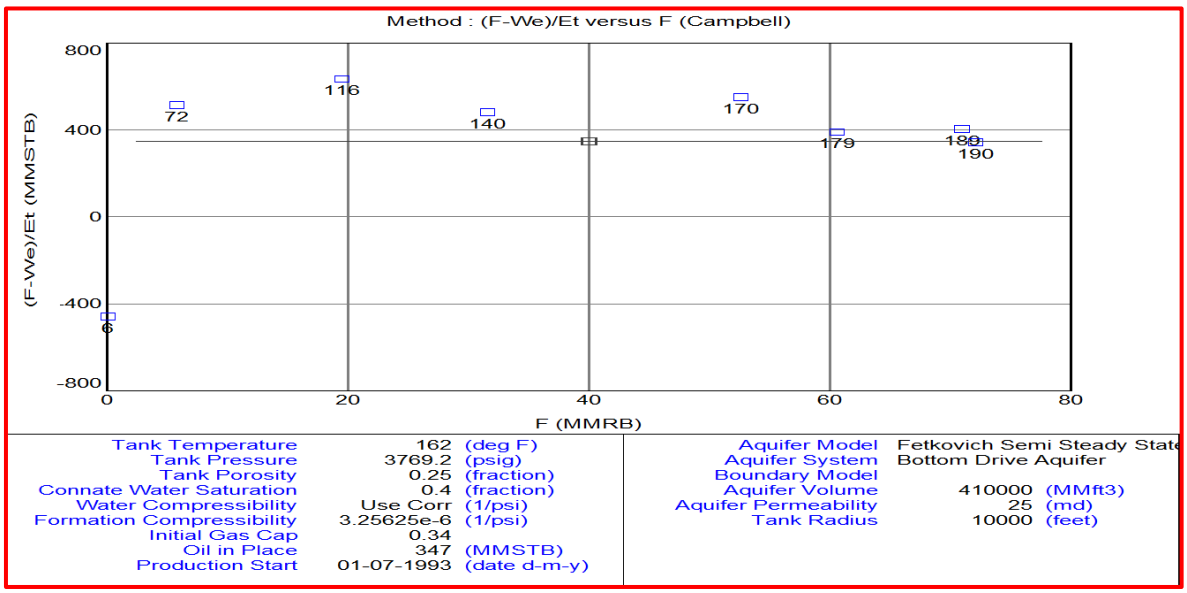

Figure 4.34:Campbell plot

4.7.2 Energy Plot

It has been observed from the output of Energy plot, material balance drive mechanism index presented in Figure 4.33 that at the beginning of the production life of the reservoir, the principal drive mechanism was water influx (60%), gas cap (20%), followed by the fluid expansion (20%). The water drive from the aquifer support then starts increasing and reaches at around 70% till end of history. The major energy support is contributed by the aquifer while 20-25% of the energy is attributed to gas cap expansion and fluid expansion.

4.7.3 Campbell Plot:

Basic material balance equation for oil is

$$F = N\,E_t + W_e \tag{4.17}$$

Where,

F = Total Production

W_e = Water Influx

E_t = Total Expansion

N = Original oil in Place

If there is no aquifer influx, then $W_e = 0$.

Rearranging the equation,

$$\frac{F}{E_t} = N \tag{4.18}$$

Now, if F / E_t versus F is plotted, a horizontal line with Y intercept equal to N should be obtained.

If there is an aquifer present,

Rearranging the equation, we get,

$$\frac{F - W_e}{E_t} = N \tag{4.19}$$

Now, if (F -W_e) / E_t versus F is plotted, a horizontal line with Y intercept equal to N should be obtained (Figure 4.34).

Plot of STOIIP along the Y-axis never changes. However, if the Campbell plot does show some variation, which indicates that, an unaccounted energy source is contributing to

the historical production. Based on the response of the Campbell plot, the presence of an aquifer is very likely (Pletcher, 2000).

4.8 CHAPTER SUMMARY

This chapter gives information on input for reservoir simulation study i.e. relative permeability, capillary pressure, PVT analysis, dynamic data (pressure and production history), porosity permeability transform. Additionally, analytical studies have also been performed for better understanding of the dynamics of reservoir such as material balance studies, contact determination, and transition zone thickness determination that are used to characterize the reservoir.

CHAPTER 5
NUMERICAL MODELING

Numerical simulation modeling involves integration of geophysical, geological and dynamic recurrent data to make a representative model for fluid flow behavior inside the reservoir. Numerical simulation model offers a rigorous and detailed manner of modeling pressure and production rate data by dividing the reservoir into smaller blocks. Rigorous material balance calculations are performed on each block to account for flow based on porosity, permeability in all three directions, oil/water/gas saturation, and fluid properties.

5.1 FLOW MODEL

A mathematical model is needed to describe fluid flow behavior. The most common models for isothermal flow are described below.

In essence, all mathematical techniques are derived from three fundamental equations of reservoir engineering viz. Darcy's law, material balance equation and fluid properties (PVT or Equation of State) (Brown, 2008). A set of equations incorporating Darcy's law and material balance is solved in the model to describe fluid flow and accounts for condition changes.

Darcy's Law (without gravity term)

$$q = -\frac{k}{\mu}\nabla P \tag{5.1}$$

Where ∇P is the applied pressure drop across the sample, μ is the viscosity of the fluid, and k is the absolute permeability of the medium

Material balance equation (Mass flux = Accumulation + Injection/Production):

$$-\nabla . M = \frac{\partial}{\partial t}(\emptyset\rho) + Q \tag{5.2}$$

Where M is mass flux in/out of control volume, ρ is the density of the fluid, $\emptyset$ is the porosity and Q is the production/injection rate.

Combining Darcy's law with material balance equation, we get simulator flow equation (with gravity term)

$$\nabla.[\lambda(\nabla P - \gamma\nabla z)] = \frac{\partial}{\partial t}\left(\frac{\emptyset}{B}\right) + \frac{Q}{\rho} \tag{5.3}$$

Where B is formation volume factor

$$\lambda = \frac{k}{\mu B}$$

Above equation is computed for all 3-Phase oil, water, and gas

$$\nabla.[\lambda_o(\nabla P_o - \gamma_o\nabla z)] = \frac{\partial}{\partial t}\left(\emptyset\frac{S_o}{B_o}\right) + q_o \tag{5.4}$$

$$\nabla.[\lambda_w(\nabla P_w - \gamma_w\nabla z)] = \frac{\partial}{\partial t}\left(\emptyset\frac{S_w}{B_w}\right) + q_w \tag{5.5}$$

$$\nabla.\left[R_s\lambda_o(\nabla P_o - \gamma_o\nabla z) + \lambda_g\left(\nabla P_g - \gamma_g\nabla z\right)\right] = \frac{\partial}{\partial t}\left(\emptyset\left[R_s\frac{S_o}{B_o} + \frac{S_g}{B_g}\right]\right) + R_sQ_o + Q_g \tag{5.6}$$

Where R_s is Solution Gas Oil Ratio, subscript o represents oil, w for water and g for gas.

5.2 WELL MODEL

Multisegment model has been selected for simulating horizontal well performance behavior. This model (Holmes et al., 1998, Stone et Al., 2002) breakdown the well into a series of connecting units termed as segments (Figure 5.1). Each segment can have no connection, one connection or more than one connection, which will be connected with grid. For every segment, there are four equations, assuming a 3-Phase black oil reservoir simulation: three (3) material balance equations and one pressure drop equation. The pressure drop equation contains acceleration, hydrostatic and friction components. These four equations are solved to get the flow rate, pressure and composition of fluid in every segment.

Multilateral topology is defined using multilateral wells, which can't be done using conventional well model. There is a good improvement in modeling of multi-phase flow as well as cross flow including inter branch crossflow, the main reason behind is that the fluid is monitored in each segment.

The main benefit of this model is that every segment can be assigned to one inflow control device, which allows multilevel branching for a multisegment well model.

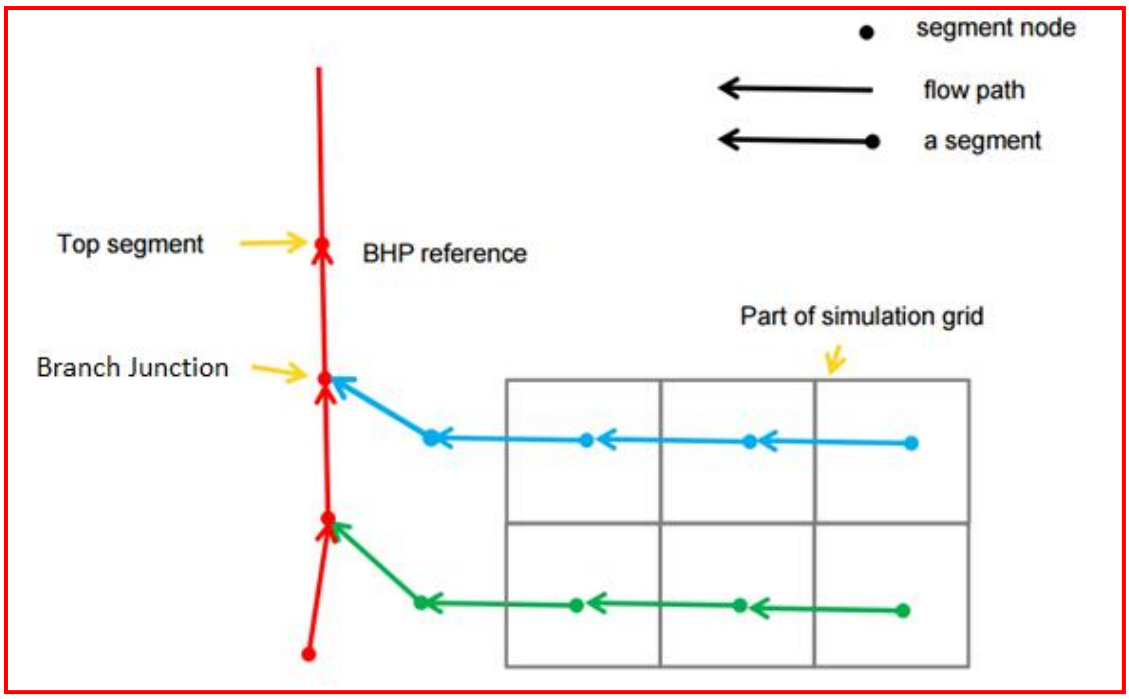

Figure 5.1: Schematic diagram illustrating the Multisegment well model (Source: OPM project website)

5.3 RESERVOIR MODEL

The 50 m by 50 m gridding of the original model was upscaled to 100 m by 100 m. The vertical resolution was reduced approximately by a factor of two, increasing average cell height from 0.5 m to 1 m. The geomodel was resampled into upscaled grid to capture Rock types, porosity, and permeability and saturation distribution. The porosity was resampled arithmetically with weighting by pore volume. The resultant upscaled simulation grid has 120x72x86 (7,43,040 cells) having 3,88,373 active cells and upscaled model was migrated into the Eclipse Simulator (Schlumberger Eclipse and Petrel, 2015). Further, reduction on active blocks was carried out by reducing the number of grid blocks in aquifer region. After reducing the number of cells in aquifer zone, number of active cell was 3,08,326.

Five Rock types are introduced in the model (Rock type 1 to 5). Rock type 1 is considered to be the best Rock type whereas Rock type 5 is worst Rock type considered for the study. Statistics of Rock type distribution in terms of oil saturation, permeability and porosity is given in Table 5.1. Porosity, permeability and Rock type distribution of the geomodel has been shown in Figure 5.2 through Figure 5.4 respectively.

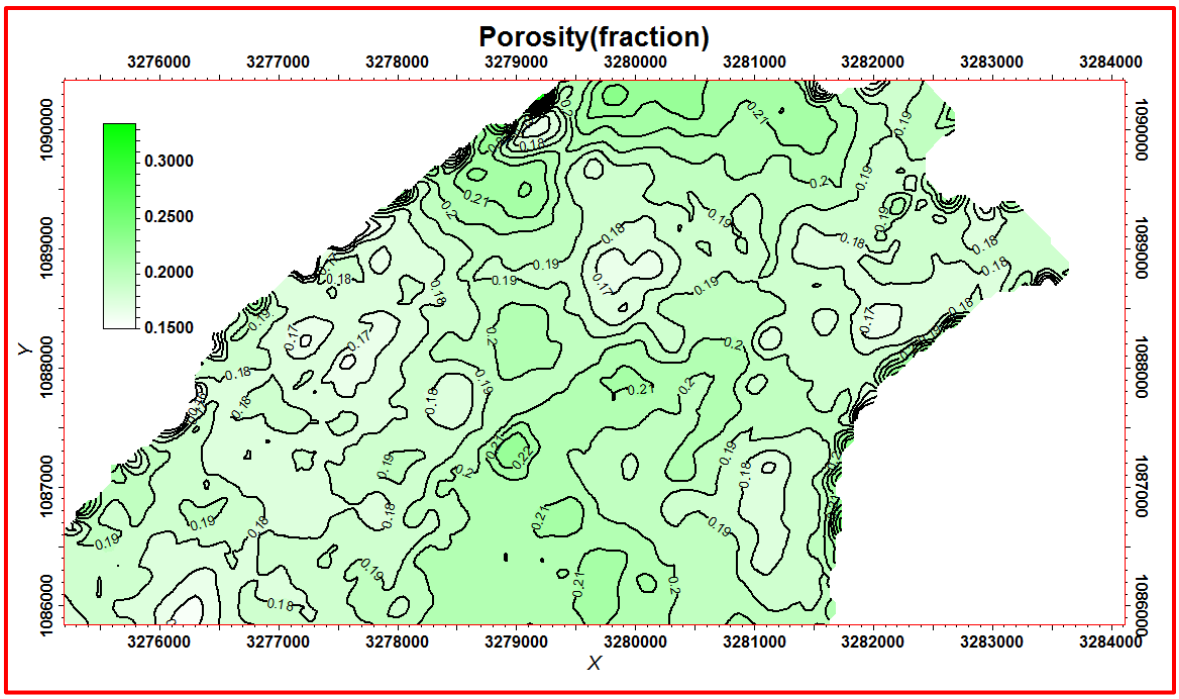

Figure 5.2: Porosity distribution of the geomodel

Average porosity map is prepared over all zones in the reservoir (Figure 5.2). From Figure 5.2, it can be seen that porosities are in the range of 15-25% in majority of the reservoir. The model clearly demonstrates the better reservoir facies distribution and its heterogeneities within the field.

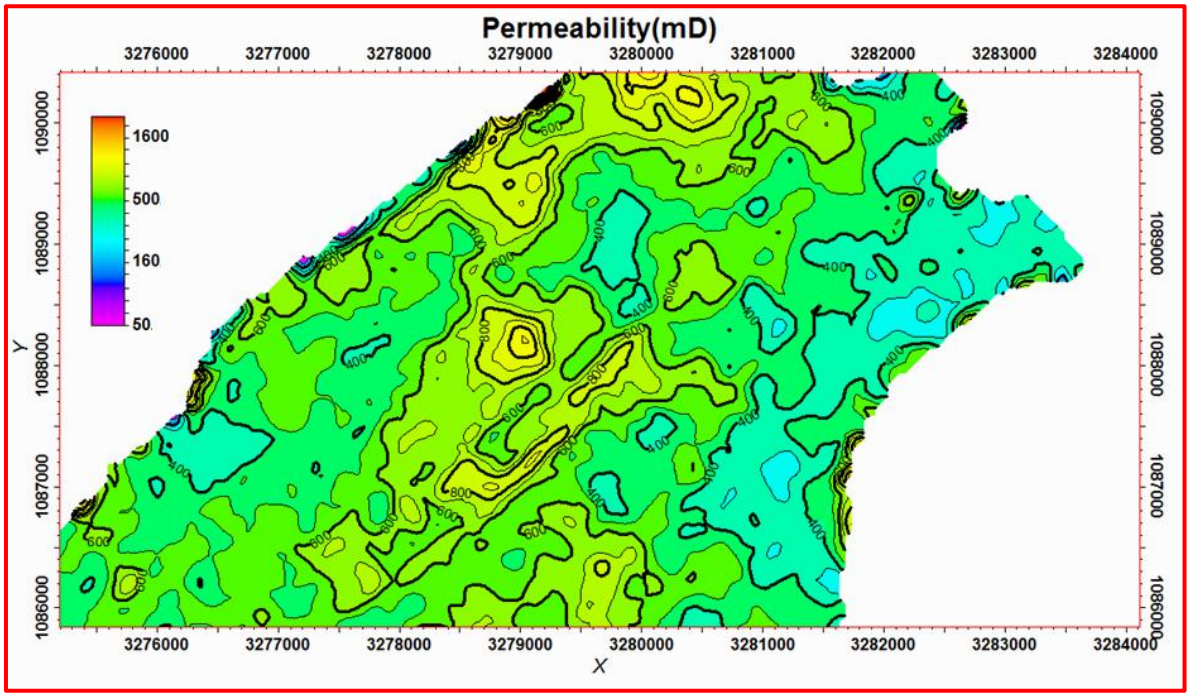

Figure 5.3: Permeability distribution of the geomodel

Average permeability map is prepared over all zones in the reservoir (Figure 5.3). From Figure 5.3, it can be seen that pemeabilities are in the range of 100-800 mD in majority of the reservoir. The model clearly demonstrates the better reservoir facies distribution and its heterogeneities within the field.

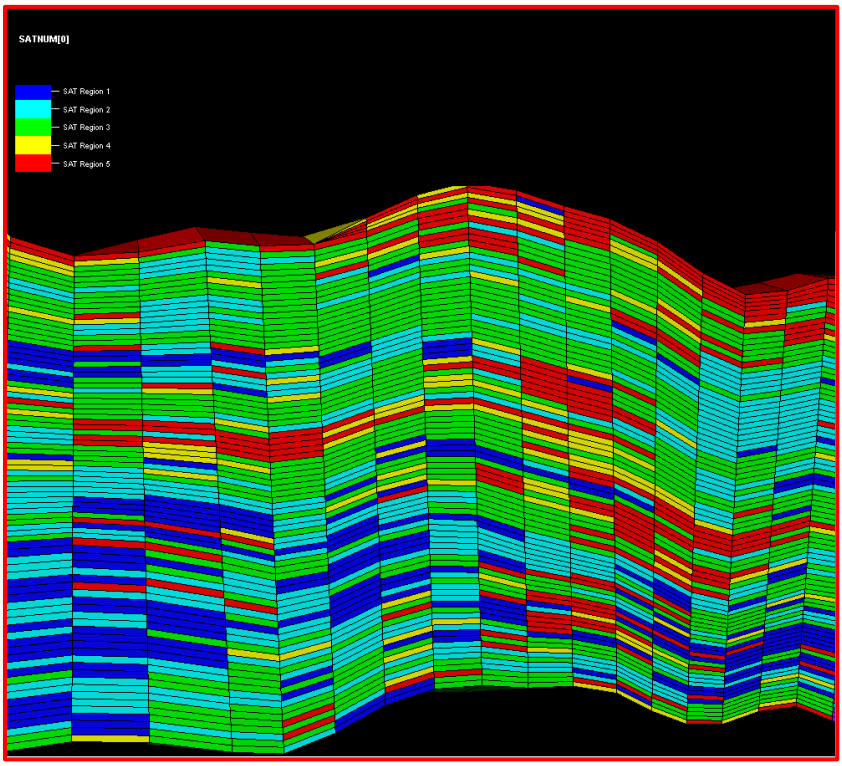

Figure 5.4: Rock type distribution of the geomodel

A representative cross section of geomodel is given in Figure 5.4, which represents five different facies in the geomodel.

Table 5.1: Statistics for different Rock type

Rock type	Percentage (%)	Oil Saturation (%)	Average permeability (mD)	Average porosity (%)
1	14.5	60.44	1157	22.25
2	28.5	51.64	502	20.73
3	33.1	37.66	220	18.29
4	8.1	7.11	180	15.44
5	15.8	1.35	157	10.96

5.4 CHAPTER SUMMARY

This chapter gives information on Flow Model (3-Dimensional, 3-Phase), Well Model and Geological Model (Porosity, Permeability and Rock type) overview, which will be used as a representative model for fluid flow behavior inside the reservoir.

CHAPTER 6

DYNAMIC MODELING

6.1 INITIALIZATION

Purpose of Initialization is to define initial conditions/solutions. For black oil case - pressure, saturation and solution GOR are calculated for each grid cell at initial time step.

Methods for Initialization in Eclipse Simulator:

- Enumeration - Directly define solutions of primary variables, for each cell, depending on the phases present. Oil, water, gas -PRESSURE, SWAT, SGAS, RS/PBUB, RV/PDEW
- Restart –A special case of enumeration where Initial solutions are read from a restart file created by an earlier ECLIPSE run. Generally used for prediction scenarios.
- Equilibration- Initial conditions are calculated based on the assumption that gas, oil and water are in hydrostatic equilibrium, and compositions are in thermodynamic equilibrium.

Here Equilibration method has been used for initialization, Data Required for Equilibration is given below:

- Pressure at datum depth
- Capillary pressure at contact depth
- Initial R_s
- Saturation end points
- Capillary pressure curves
- PVT data

The initial saturations in each zone are calculated as follows:

Gas Zone

$S_g = S_{gmax}$

$S_w = S_{wco}$

$S_o = 1 - S_{gmax} - S_{wco}$

Gas-Oil Transition Zone

S_g = Determined by inverse look-up of gas capillary pressure table

$S_w = S_{wco}$

$S_o = 1 - S_g - S_{wco}$

Oil Zone

$S_g = S_{gco}$

$S_w = S_{wco}$

$S_o = 1 - S_{gco} - S_{wco}$

Oil-Water Transition Zone

$Sg = S_{gco}$

S_w = Determined by inverse look-up of water capillary pressure table

$S_o = 1 - S_{gco} - S_w$

Water Zone

$S_g = S_{gco}$

$S_w = S_{wmax}$

$S_o = 1 - S_{gco} - S_{wmax}$

where,

S_{gco} = Connate gas saturation, the lowest gas saturation value

S_{gmax} = Maximum gas saturation

S_{wco} = Connate water saturation, the lowest water saturation

S_{wmax} = Maximum water saturation

Input in EQUIL section of Eclipse data file has been given in Table 6.1 for calculation of initial saturation and pressure distribution in the model.

Table 6.1: Input in Eclipse Simulator

Datum (m)	**Pressure (bars)**	**WOC (m)**	**P_{cwo} (bars)**	**GOC (m)**	**P_{cgo} (bars)**
2522	253.89	2568	0	2522	0

6.1.1 Initialization Results

Pressure distribution and saturation distribution in the ternary diagram at initial conditions are presented in cross sectional view with WOC and GOC in Figure 6.1 and Figure 6.2 respectively. Eclipse creates INIT file, which contains information about a static description of the model:

- Dimensions of cells, the depth of their surfaces and centers
- Properties of cells, such as porosity, permeability and pore volume
- PVT properties and saturation functions
- The distribution of the regions within the model

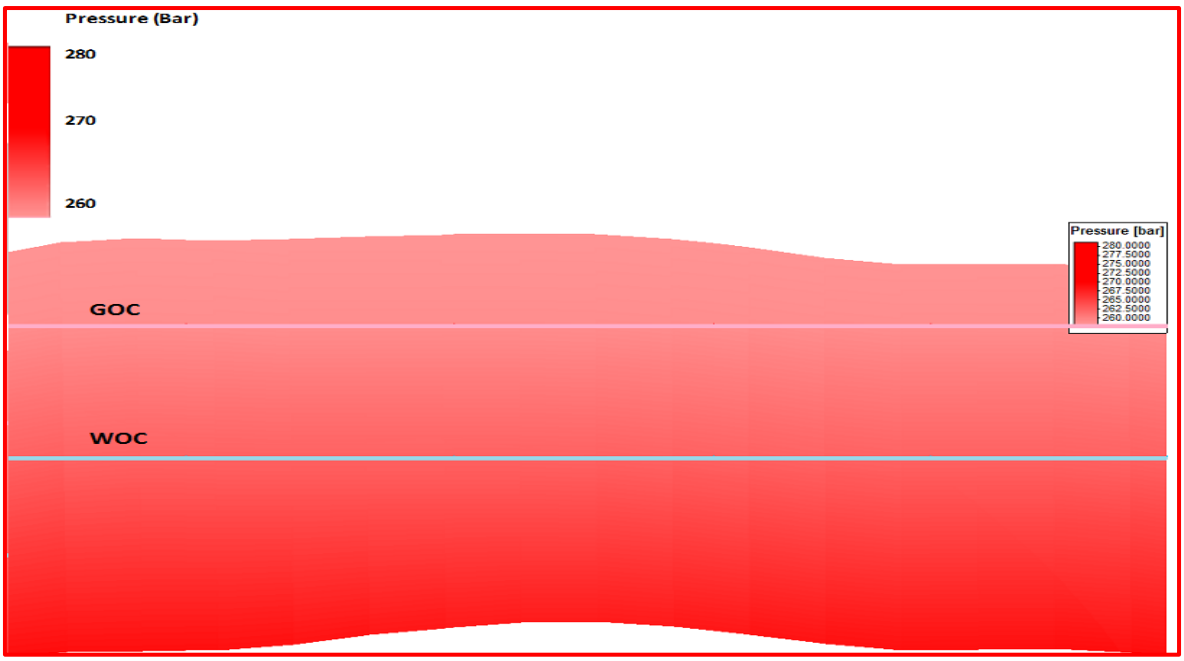

Figure 6.1: Initial pressure distribution

Pressure distribution has been shown in the above diagram at initial condition in cross section of the reservoir.

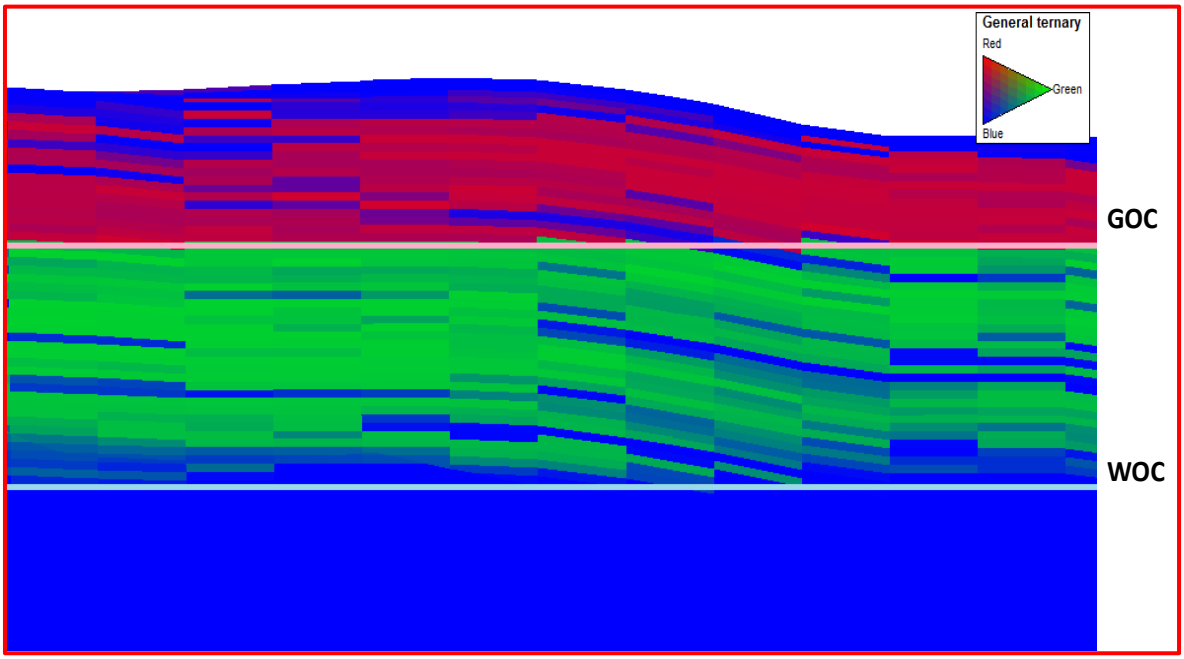

Figure 6.2: Initial saturation distribution (Ternary Diagram)

Ternary diagram shown above represents presence of oil and gas marked in green and red. Blue color is indicative of water below WOC, whereas blue color in the hydrocarbon zone represents non-reservoir.

6.2 AQUIFER MODELING

It is known from the material balance studies and well logs that aquifer is present in the reservoir. In order to model the aquifer, cells below WOC has been given a water saturation values equal to unity and a pore volume multiplier for all cells below WOC for replicating the pressure behaviors of the reservoir. The first simulation was performed in material balance mode to adjust the overall pressure behavior and to determine strength of the aquifer. To perform the simulation, all wells were defined as multirate wells, where the rate of oil, gas and water are included and put in reservoir volume control mode. The Figure 6.3 given below shows the pore volume multiplication factor and pressure responses. Here three cases were performed viz.

- Weak aquifer referred as Aquifer-3 (Pore Volume Multiplier: 1)
- Aquifer with medium strength referred as Aquifer-2 (Pore Volume Multiplier: 1.5)
- Strong aquifer referred as Aquifer-1 (Pore Volume Multiplier: 2)

Pressure behavior of all the aquifers are shown below in Figure 6.3:

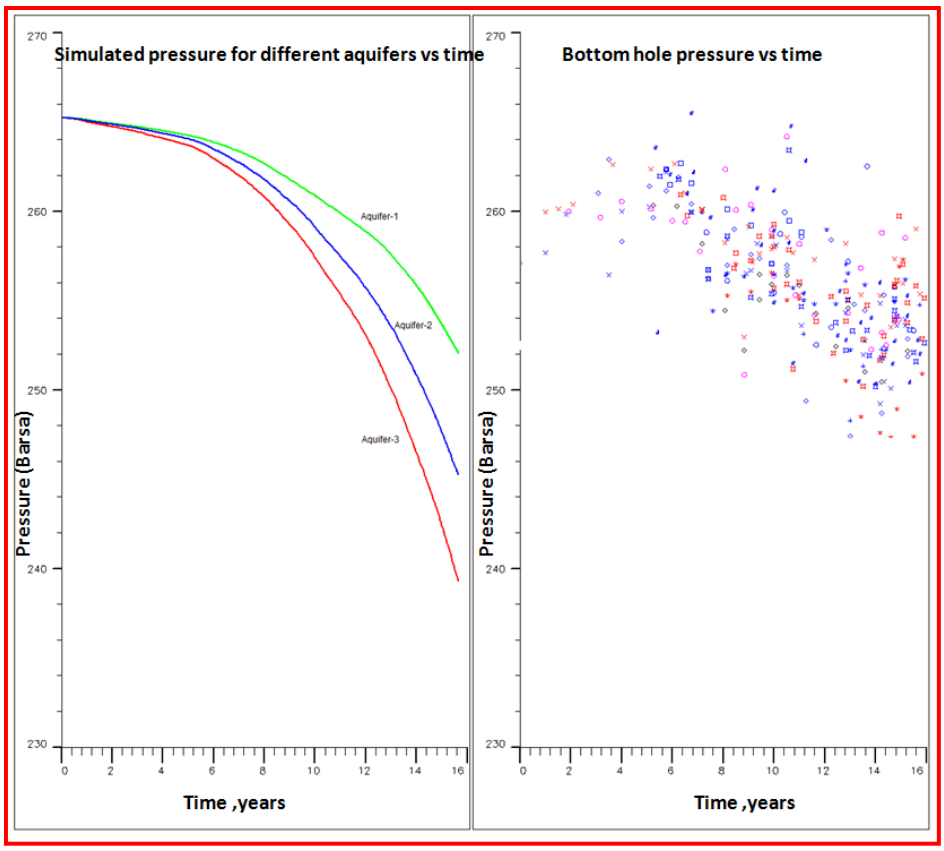

Figure 6.3: Simulated Vs actual pressure profile for various aquifer strengths

The pore volume multiplier was adjusted to get the average reservoir pressure trend that matches the historical measured bottomhole static pressure. This was confirmed by running the model in the material balance mode (by specifying the surface rates of all the three phases, which was converted to total reservoir voidage rate by the model and used to calculate the reservoir pressure) and matching the reservoir pressure trend with the actual pressures. It can be inferred that static pressure data is lying close to strong aquifer (Aquifer-1), which has been considered for further simulation studies.

6.3 HISTORY MATCHING

For predicting reservoir performance behavior, geological model needs to be tuned using dynamic data and this process is termed as history matching. It is considered that if history matching is in good agreement with dynamic data then future performance will have higher degree of confidence. The main challenge in this process is to match pressure and production rates for certain time period, as the values calculated by simulation software will not resemble the measured production rates. This process involves fine-tuning of reservoir parameters in the Dynamic Model until the simulated performance matches the observed data closely. In order to fine tune parameter, several iterations are required by changing the parameter or by doing sensitivity analysis. The efficacy of the history match must be assessed by the quality of the match at well level, some compartments of reservoir and at the field level.

Allocated oil rate and pressure data of individual production wells on a monthly averaged basis was the primary input to the simulator during history matching phase. Actual history rates and cumulative oil, water and gas for 46 wells for a period of 16 years was simulated with a commercial black oil simulator. The model response in the form of reservoir pressure, gas oil ratio, Water Cut and breakthrough time for water and gas were considered for matching with the field data.

Results of the history match on reservoir scale are illustrated in Figure 6.4. Observed historical data has been kept as marker whereas simulated data has been presented inform of a line. It can be seen that rates (oil rate and water rate), GOR and pressure have been matched quite well with the actual history by the simulator at the field level. Least square method for minimizing the difference between observed and simulated data has been used for history matching on well and field scale.

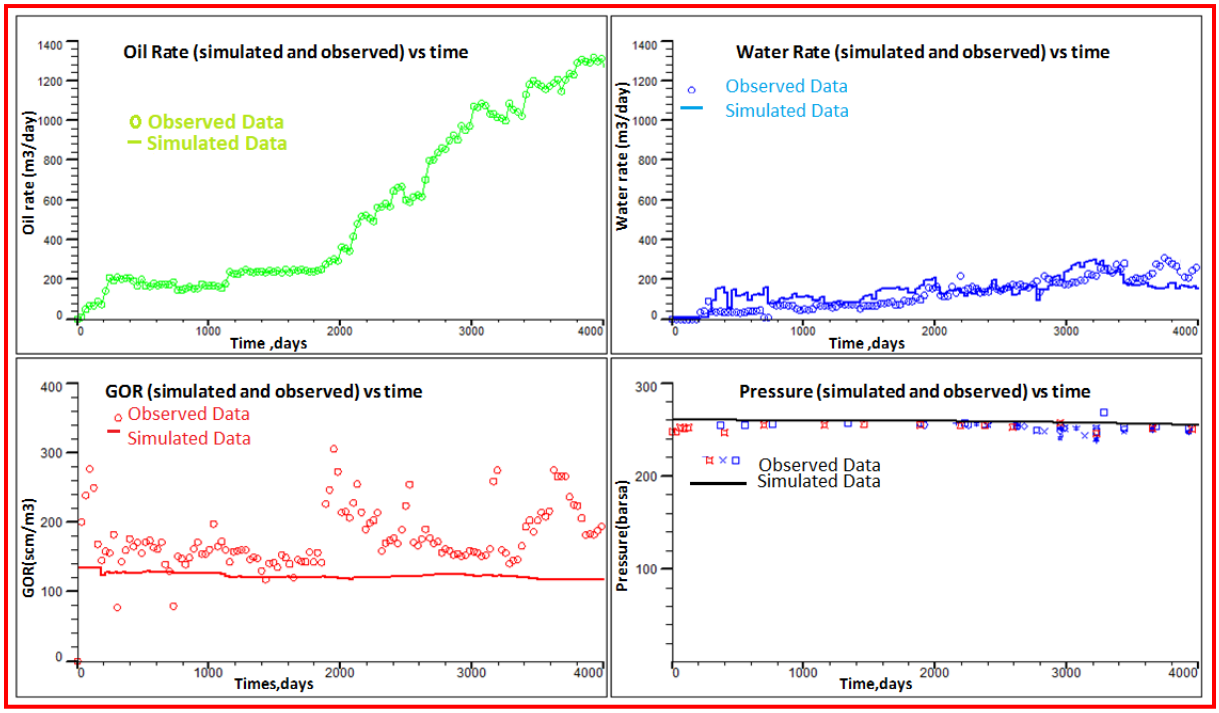

Figure 6.4: History match results

In order to see model behavior to capture coning behavior in both vertical and horizontal wells, two wells have been selected where Water Cut has been increasing. Initially, a diagnostic plot was used for analyzing the production behavior and thereafter simulation model production prediction was observed. Details of the vertical well (Well-3) and horizontal well (Well-49) are given below.

Well-3 (vertical well) is located in the North-Eastern part of the field. It was drilled and completed in the year 1998. Open-hole logs (Oil India Limited internal report, 2014) indicated that the original WOC was at a depth of 2568 m TVDSS. The bottom most perforation was kept at 2566 m TVDSS. Figure 6.5 shows the production profile of the well-3. The well started production from March 1998 to Jan 1999 at 40 m^3/d. Initially, the production rate was kept at 30 m^3/d, which was increased to 40 m^3/d. It can be seen from the graph that water started coming from the very first day due to proximity with the WOC. Well was shut-in just 5 months after the increase in fluid production due to increase in Water Cut. The historical production rate and Water Cut for Well-3 are displayed in Figure 6.5. Current offset between the WOC and the bottom perforation is 2 m, which indicates that the water production was due to a water cone.

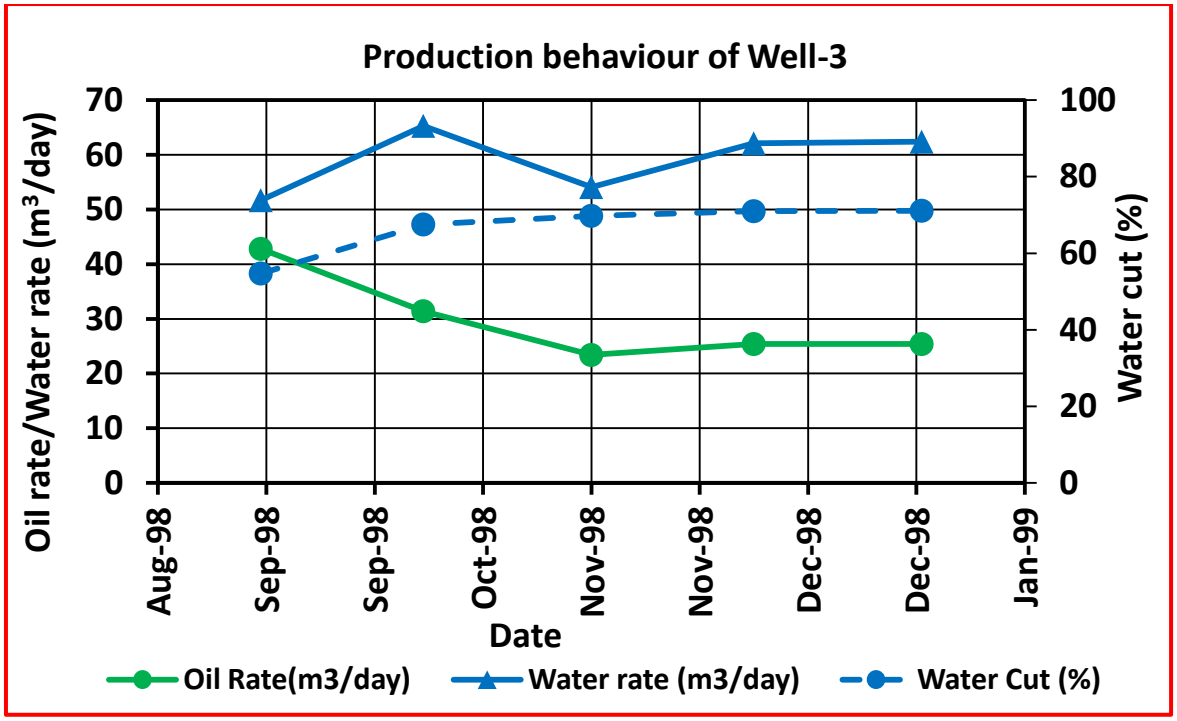

Figure 6.5: Production behavior of Well-3

A diagnostic plot (Chan, 1995) for the verification of the same has been prepared and is presented as Figure 6.6.

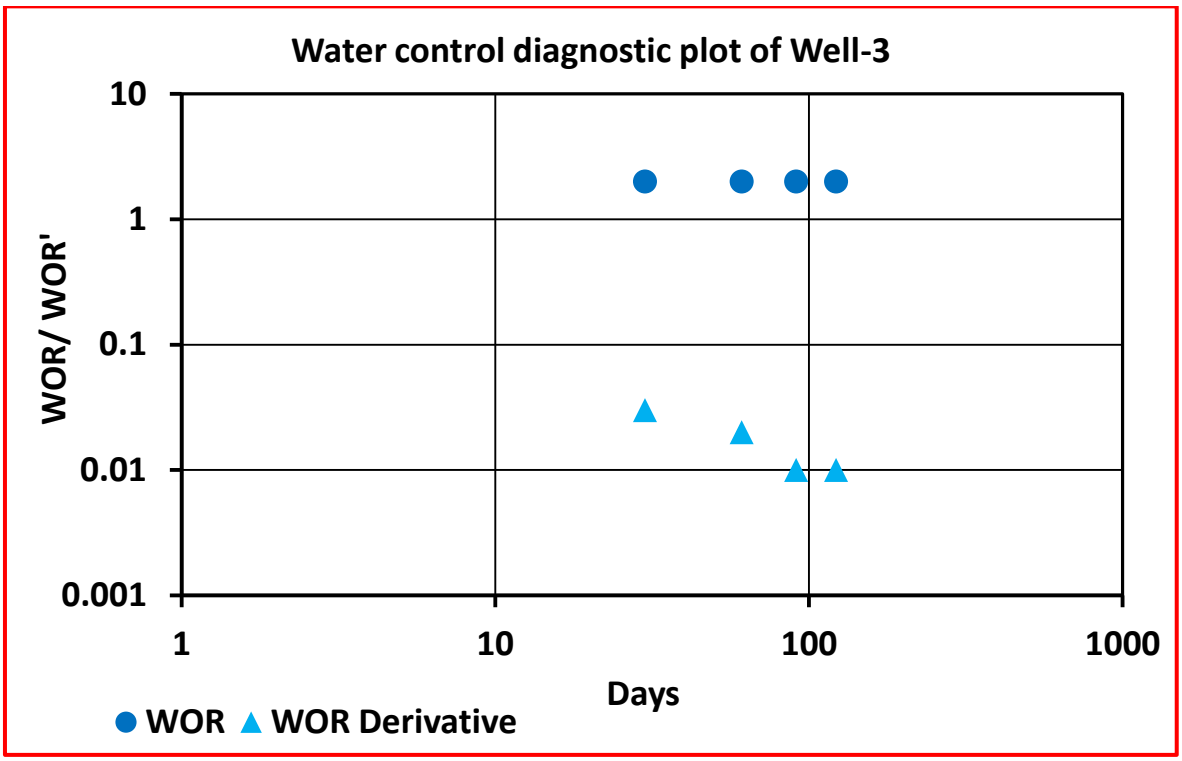

Figure 6.6: Water control diagnostic plot of Well-3

Further, simulation model production behavior was also captured for oil rate, Water Cut, pressure and GOR to see variation with the observed data. Observed historical data has been kept as marker whereas simulated data has been presented as line. It can be seen from Figure 6.7 that reservoir heterogeneity has been well captured to simulate the production behavior of well-3.

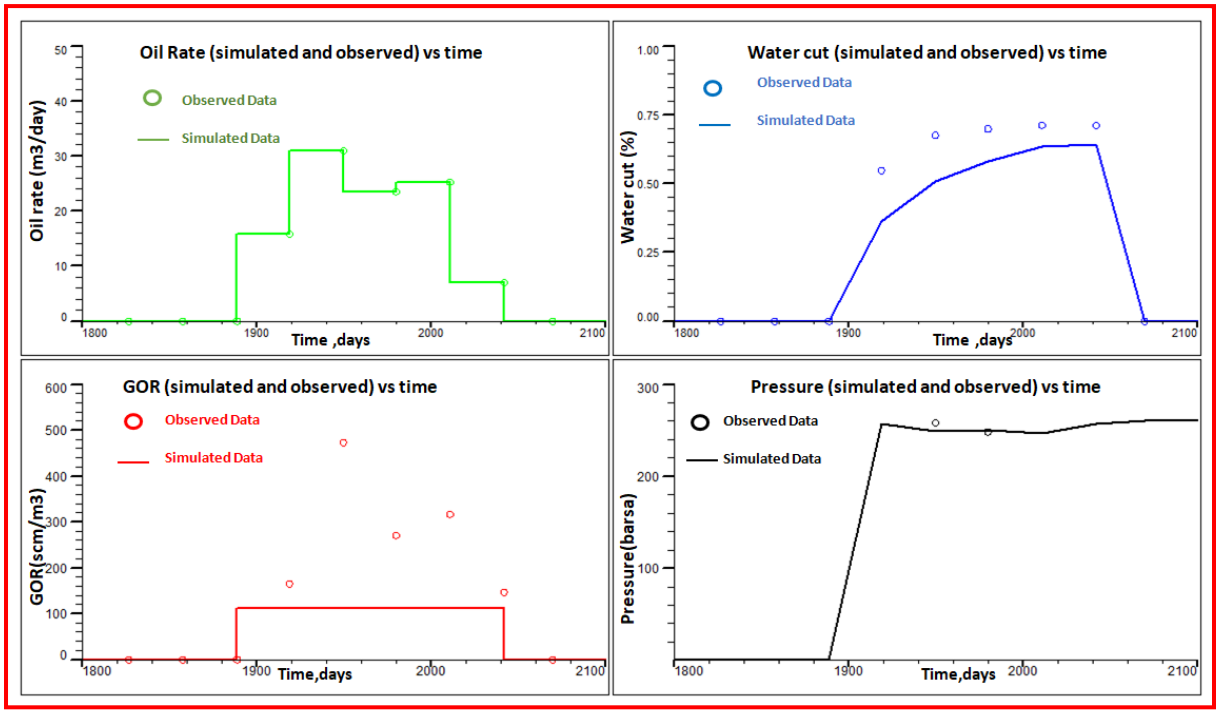

Figure 6.7: History match results of Well-3

Well-49 (horizontal well) is located in the south-western part of the field. It was drilled and completed in the year 2007. Open-hole logs (Oil India Limited internal report) indicated that the original WOC was at a depth of 2551 m TVDSS. The landing point was kept with an offset of 10 m from WOC. Figure 6.8 shows the production behavior of well-49. The well started production from April 2007 to Aug 2011 at 140 m^3/d. Initially, the production rate was kept at 140 m^3/d (7 mm bean), which was increased to 170 m^3/d (8 mm bean). It can be seen from the graph that water started coming after increasing the production rate by increasing the drawdown by increasing the bean size. Well Water Cut started thereafter, reached to a level of 50%, and finally watered out. This well produced cumulative oil of 0.152 MMm^3. A diagnostic plot (Chan, 1995) for the verification of the cone has been prepared as Figure 6.9.

Further, simulation model production behavior captured oil rate, Water Cut, pressure and GOR to see variation with observed data. Observed historical data has been kept as marker whereas simulated data has been presented as line. It can be seen from Figure 6.10 that reservoir heterogeneity has been well captured to simulate the production behavior of Well-49.

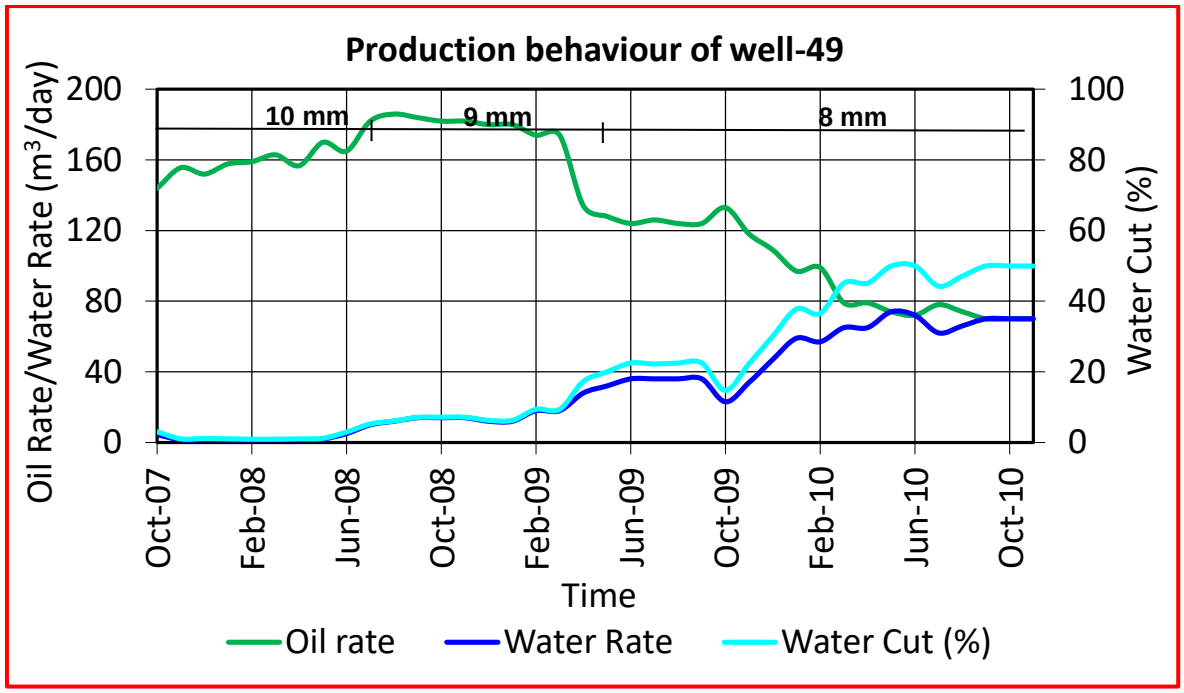

Figure 6.8: Production behavior of Well-49

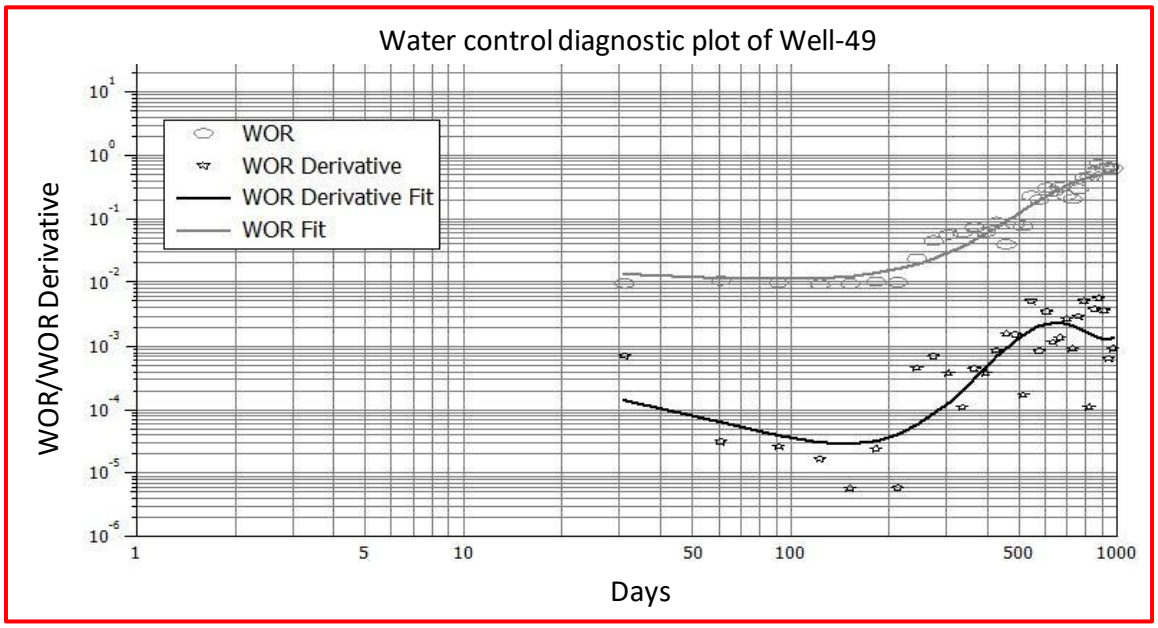

Figure 6.9: Water control diagnostic plot of Well-49

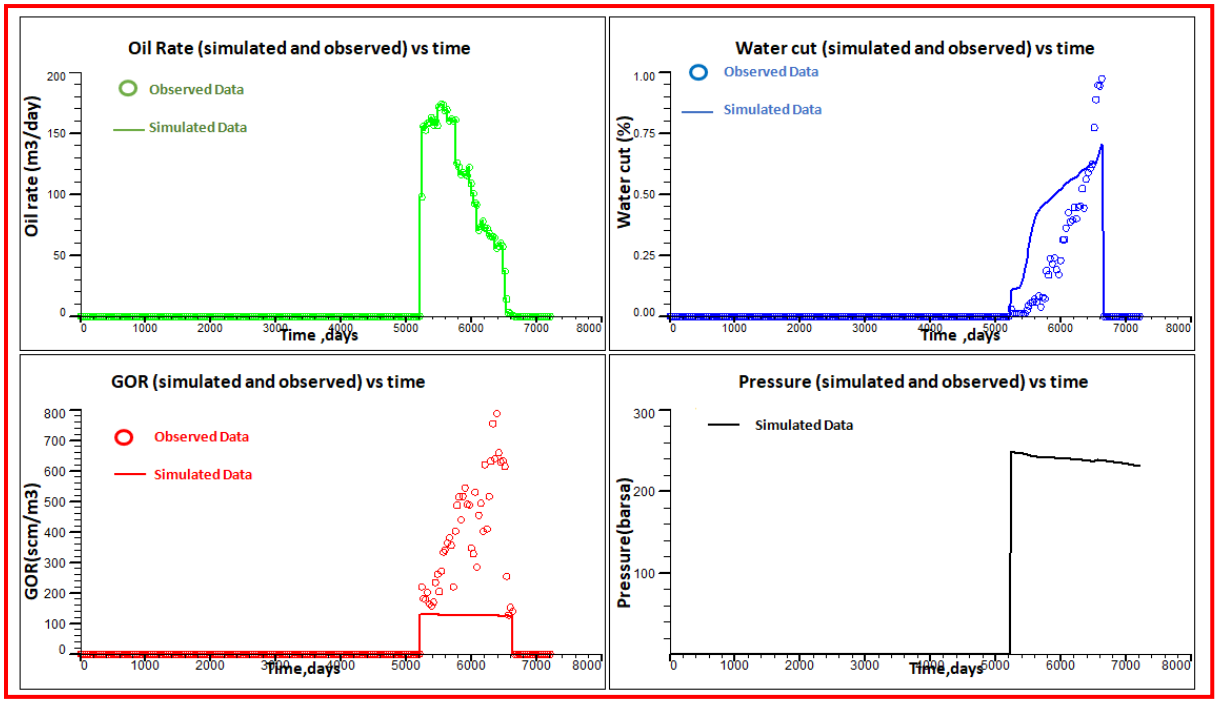

Figure 6.10: History match results of Well-49

It is evident from Figure 6.7 and Figure 6.10 that Dynamic Model is capable of predicting historical production at field level as well as at well level. This model can be used for doing sensitivity analysis for predicting hydrocarbon recovery with different variants such as liquid rate, offset from WOC etc.

6.4 PERFORMANCE PREDICTION

Performance prediction of the simulation case has been carried out in two stages.

Sensitivity study

- Sensitivity study of vertical well (Offset, Rate)
- Horizontal well (Offset, Rate, and Horizontal well length)
- Smart horizontal well (Compartment length, Nozzle sizes)
- Well spacing optimization for vertical and horizontal well

Field development

- Base case
- Well intervention case
- Infill drilling case

- Pressure maintenance case
- Simultaneous water and gas injection case

6.4.1 Sensitivity Study of Vertical Well- Offset and Withdrawal Rate

This model was used to perform sensitivity analysis on rate & offset from WOC. All variants have been mentioned in Table 6.2. From three (3) rates and five (5) offset from WOC mentioned in Table 6.2, fifteen cases (15) cases were constructed.

Table 6.2: Sensitivity parameters for vertical well

Variables	**Values**				
Rate (m^3/d)	50	100	150		
Offset (Perforation Bottom) from WOC (m)	0	5	10	15	20
***Perforation top was assumed 2 m below GOC for all cases					

The prediction cases for reservoir were run using well production-rate control mode. The well was given the production constraint as per the surface handling capacities. The well was subjected to certain other constraints which are shown in Table 6.3. From these 15 cases, 5 groups were constituted as per offset.

Group-1: With offset of 0 m from WOC (Table 6.4)

Group-2: With offset of 5 m from WOC (Table 6.4)

Group-3: With offset of 10 m from WOC (Table 6.4)

Group-4: With offset of 15 m from WOC (Table 6.4)

Group-5: With offset of 20 m from WOC (Table 6.4)

Table 6.3: Well-level constraints for prediction runs

Constraints	**Value**
Maximum individual well production rate	Decided based on historical well production
Completion type	Single Completion: bottom-to-top
Minimum well bottom-hole pressure	50 - 100 bars, depending upon the segment
Maximum Water Cut	95%
Minimum economic limit on oil-rate	1 m^3/d
Maximum GOR constraint	1500 scm/m^3

Table 6.4: Sensitivity parameters for Group-1 through Group-5(vertical well)

Variables	**Values**		
Perforation Top (m)	GOC+2 meters		
Rate (m^3/d)	50	100	150
Offset (Perforation Bottom) from WOC (m) –Group 1	0	0	0
Offset (Perforation Bottom) from WOC (m) –Group 2	5	5	5
Offset (Perforation Bottom) from WOC (m) –Group 3	10	10	10
Offset (Perforation Bottom) from WOC (m) –Group 4	15	15	15
Offset (Perforation Bottom) from WOC (m) –Group 5	20	20	20

6.4.2 Sensitivity study of Horizontal well – Offset from WOC, Withdrawal Rate and Horizontal Well Length

This model was used to perform sensitivity analysis on rate, offset from WOC and horizontal well length. All variants have been mentioned in Table 6.5. From three (3) rates, four (4) offset from WOC and five (5) horizontal well length, a total of sixty cases (60) cases were constructed. The prediction cases for reservoir were run using well production-rate control mode. The well was given the production constraint as per the surface handling capacities. These wells were subjected to certain other constraints as shown in Table 6.6. From these sixty (60) cases, 4 groups were constituted as per offset.

Group-1: With offset of 5 m from WOC (Table 6.7)
Group-2: With offset of 10 m from WOC (Table 6.7)
Group-3: With offset of 15 m from WOC (Table 6.7)
Group-4: With offset of 20 m from WOC (Table 6.7)

Table 6.5: Sensitivity parameters (horizontal well)

Variables	**Values**				
Rate (m^3/d)	200	250	300		
Offset (Perforation Bottom) from WOC (m)	5	10	15	20	
Horizontal well length (m)	400	600	800	1000	1200
***Perforation top was assumed 2 m below GOC for all cases					

Table 6.6: Well-level constraints for prediction runs

Constraints	**Value**
Maximum individual well production rate	Decided based on historical well production rate in the reservoir
Completion type	Single completion: bottom-to-top
Minimum well bottom-hole pressure	50-100 bars, depending upon the segment
Maximum Water Cut	95%
Minimum economic limit on oil-rate	1 m^3/d
Maximum GOR constraint	1500 scm/m^3

Table 6.7: Sensitivity parameters for Group-1 through Group-4(horizontal well)

Group Variable					
Group-1– (Five meters offset)					
Rate (m^3/d)	200	250	300		
Horizontal well length (m)	400	600	800	1000	1200
Group-2 (Ten meters offset)					
Rate (m^3/d)	200	250	300		
Horizontal well length (m)	400	600	800	1000	1200
Group-3 (Fifteen meters offset)					
Rate (m^3/d)	200	250	300		
Horizontal well length (m)	400	600	800	1000	1200
Group-4 (Twenty meters offset)					
Rate (m^3/d)	200	250	300		
Horizontal well length (m)	400	600	800	1000	1200

6.4.3 Sensitivity and Uncertainty Study of Inflow Control Device – Compartment length, Nozzle sizes

The necessity to produce in an economical and efficient manner has endorsed the development of multi-lateral wells and extended reach wells which enables more contact with reservoir and reduced draw down leading to achieve similar or more rates than conventional vertical wells. In a horizontal well heel and toe are beginning and end of perforated horizontal well length. Maximum production comes from heel section. Maximum pressure drawdown is around heel due to frictional pressure drop of fluid flow. This phenomenon leads to non-uniform influx of fluids around the horizontal well length which causes early water or gas break-through. Early breakthrough of oil or gas causes lower oil recovery and uneven sweep of area drained. Maximum Reservoir Contact (MRC) is obtained from longer horizontal well length which leads to more recovery but at the same time permeability contrast around the well length and heterogeneity encountered may lead to unevenly distributed pressure along the wellbore. In time, long before oil (green) from sections near the toe arrives at the wellbore, water (blue) or gas (red) is drawn to the heel (top), resulting in an early end to the well's productive life (Figure 6.11).

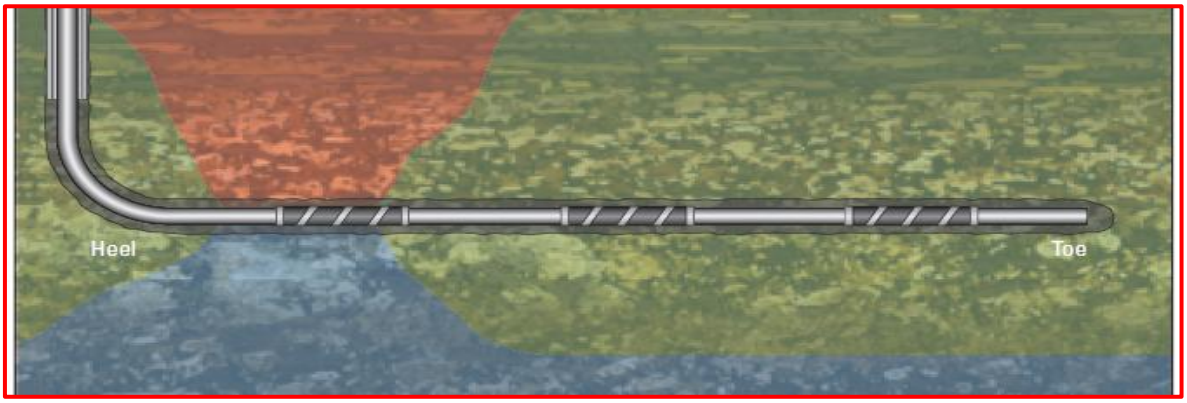

Figure 6.11: Schematics of horizontal well (heel-toe effect) (Source: Ellis et al., 2009)

To eradicate this issue, Inflow Control Device (ICD) is being used rapidly for optimizing individual well production behavior which also increases reservoir performance. The purpose of ICD is to equalize inflow along the length of the wellbore regardless of location and permeability variation. These ICDs enable the entire horizontal length of the wellbore for contributing towards total production and thereby enhance hydrocarbon recovery. ICDs are choking devices that balance inflow by adding an additional pressure drop at the sandface. They are designed to apply a specific differential pressure at a certain flow rate. Schematics of ICD with proposed contact movement have been shown in Figure 6.12.

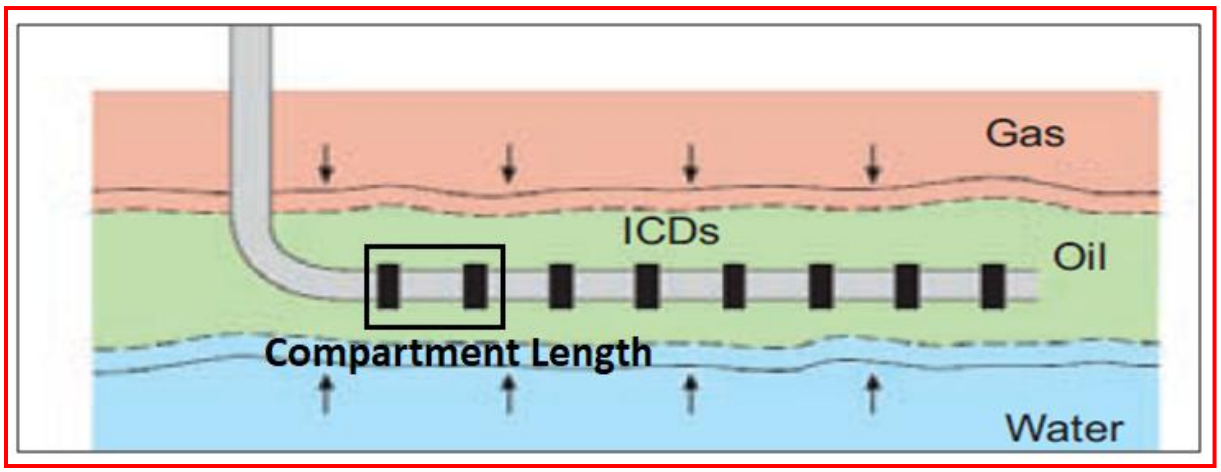

Figure 6.12: ICD Completion showing uniform contact movement, Source: Denney (2010)

Judicious selection of intelligent completions enhances the oil recovery and constraints unwanted water and gas production. Experience from field and results from the extensive dynamic reservoir simulation studies show that the oil, water and gas production are extremely dependent on the type and configuration of ICD (Mojaddam et al., 2012). A suite of optimized ICD modeling workflows and evaluation tools were developed to address these issues using a plug-in architecture in an industry leading Exploration and Production Platform (Schlumberger PETREL, 2015) and reservoir simulator (Schlumberger ECLIPSE, 2015). Historically, the most common method for designing ICD completions has been to use steady-state or pseudo steady-state (i.e. static) analytical modeling using data at one or more points in time (Ellis et al., 2009).

Design Strategies

Many parameters must be considered with uncertainty ranges during the ICD design process which includes fluid properties, contacts and saturations, porosity, vertical and horizontal permeability, drive mechanisms, reservoir pressure, fracture intensity and direction, net pay, well spacing and type, areal anisotropy, formation damage and production methods.

These parameters, their effect on production and inherent uncertainty drive the choice of modeling strategy. Main modeling strategies exist in three categories which is given below.

Equal Length Compartments with Uniform Nozzle Sizes –Sensitivity on Compartment Length

A design with equally spaced compartments and uniform nozzles sizes is preferred if there is significant uncertainty in the reservoir characterization or risk in getting the completion to total depth. Reservoir models in fractured environments, new developments or older fields often contain significant uncertainty that is difficult, impossible, or simply too expensive to reduce. In these cases, it is risky to design a completion that is strongly customized to the available data. In such cases, a design using uniform nozzle sizes and equally spaced compartments will provide useful benefits from flow equalization and increased pressure drops in the presence of water. Different compartment length (Table 6.8) with uniform nozzle sizes of 5.026E-05 m^2 has been selected for simulation runs using ICD well completion.

Table 6.8: Compartment length as an input to ICD cases

S No.	Compartment length (m)
1	100
2	125
3	150
4	25
5	50
6	75

Equal Length Compartments with Variable Nozzle Sizes –Sensitivity on Nozzle Sizes

Equally spaced compartments with variable nozzle sizes designs are the preferred option if the reservoir is homogeneous with significant heel-to-toe pressure decline along the wellbore.

High rate horizontal wells often suffer from the so-called heel-toe effect. This is caused by the frictional pressure gradient along the well, which means that the heel has a significantly lower pressure than the toe and so produces more fluid. This can lead to premature breakthrough of water or gas.

A total of 35 cases have been examined considering equal spacing sampler of nozzle sizes between 3E-05 m^2 and 5E-06 m^2 for all seven nozzles. All the seven nozzles have been

assigned a variable name $A, $B, $C, $D, $E, $F, $G for varying nozzle sizes. Details of all the seven variables for 35 cases have been given in Table 6.9.

Table 6.9: Nozzle ICD size for examined cases

Case	**$G**	**$F**	**$E**	**$D**	**$C**	**$B**	**$A**	**$RUN**
	Area of Nozzle, 10^{-5} m^2							
2548_800_300_150_1	2.00	2.00	2.00	2.00	2.00	2.00	0.50	1
2548_800_300_150_2	2.00	2.00	2.00	2.00	2.00	2.00	1.13	2
2548_800_300_150_3	2.00	2.00	2.00	2.00	2.00	2.00	1.75	3
2548_800_300_150_4	2.00	2.00	2.00	2.00	2.00	2.00	2.38	4
2548_800_300_150_5	2.00	2.00	2.00	2.00	2.00	2.00	3.00	5
2548_800_300_150_6	2.00	2.00	2.00	2.00	2.00	0.50	2.00	6
2548_800_300_150_7	2.00	2.00	2.00	2.00	2.00	1.13	2.00	7
2548_800_300_150_8	2.00	2.00	2.00	2.00	2.00	1.75	2.00	8
2548_800_300_150_9	2.00	2.00	2.00	2.00	2.00	2.38	2.00	9
2548_800_300_150_10	2.00	2.00	2.00	2.00	2.00	3.00	2.00	10
2548_800_300_150_11	2.00	2.00	2.00	2.00	0.50	2.00	2.00	11
2548_800_300_150_12	2.00	2.00	2.00	2.00	1.13	2.00	2.00	12
2548_800_300_150_13	2.00	2.00	2.00	2.00	1.75	2.00	2.00	13
2548_800_300_150_14	2.00	2.00	2.00	2.00	2.38	2.00	2.00	14
2548_800_300_150_15	2.00	2.00	2.00	2.00	3.00	2.00	2.00	15
2548_800_300_150_16	2.00	2.00	2.00	0.50	2.00	2.00	2.00	16
2548_800_300_150_17	2.00	2.00	2.00	1.13	2.00	2.00	2.00	17
2548_800_300_150_18	2.00	2.00	2.00	1.75	2.00	2.00	2.00	18
2548_800_300_150_19	2.00	2.00	2.00	2.38	2.00	2.00	2.00	19
2548_800_300_150_20	2.00	2.00	2.00	3.00	2.00	2.00	2.00	20
2548_800_300_150_21	2.00	2.00	0.50	2.00	2.00	2.00	2.00	21
2548_800_300_150_22	2.00	2.00	1.13	2.00	2.00	2.00	2.00	22
2548_800_300_150_23	2.00	2.00	1.75	2.00	2.00	2.00	2.00	23
2548_800_300_150_24	2.00	2.00	2.38	2.00	2.00	2.00	2.00	24
2548_800_300_150_25	2.00	2.00	3.00	2.00	2.00	2.00	2.00	25

Case	$G	$F	$E	$D	$C	$B	$A	$RUN
2548_800_300_150_26	2.00	0.50	2.00	2.00	2.00	2.00	2.00	26
2548_800_300_150_27	2.00	1.13	2.00	2.00	2.00	2.00	2.00	27
2548_800_300_150_28	2.00	1.75	2.00	2.00	2.00	2.00	2.00	28
2548_800_300_150_29	2.00	2.38	2.00	2.00	2.00	2.00	2.00	29
2548_800_300_150_30	2.00	3.00	2.00	2.00	2.00	2.00	2.00	30
2548_800_300_150_31	0.50	2.00	2.00	2.00	2.00	2.00	2.00	31
2548_800_300_150_32	1.13	2.00	2.00	2.00	2.00	2.00	2.00	32
2548_800_300_150_33	1.75	2.00	2.00	2.00	2.00	2.00	2.00	33
2548_800_300_150_34	2.38	2.00	2.00	2.00	2.00	2.00	2.00	34
2548_800_300_150_35	3.00	2.00	2.00	2.00	2.00	2.00	2.00	35

Equal Length Compartments with Variable Nozzle Sizes –Uncertainty on Nozzle Sizes

After determining most sensitive parameter, uncertainty analysis was carried out on variable $A, $B, $E and $F. Experimental design setup was done for the 4 variables using full factorial design, which gives a total of 16 cases to be examined, additionally one central point has also been added to make the number of simulation runs to 17. Table 6.10 lists variables for all the simulation cases to be examined.

Table 6.10: List of uncertain variables for cases examined

Case	$F	$E	$B	$A	$RUN
	Nozzle cross-sectional area, 10^{-5} m^2				
2548_800_300_150_36	1.750	1.750	1.750	1.750	1
2548_800_300_150_37	0.500	0.500	0.500	0.500	2
2548_800_300_150_38	0.500	0.500	0.500	3.000	3
2548_800_300_150_39	0.500	0.500	3.000	0.500	4
2548_800_300_150_40	0.500	0.500	3.000	3.000	5
2548_800_300_150_41	0.500	3.000	0.500	0.500	6
2548_800_300_150_42	0.500	3.000	0.500	3.000	7
2548_800_300_150_43	0.500	3.000	3.000	0.500	8
2548_800_300_150_44	0.500	3.000	3.000	3.000	9

Case	$F	$E	$B	$A	$RUN
2548_800_300_150_45	3.000	0.500	0.500	0.500	10
2548_800_300_150_46	3.000	0.500	0.500	3.000	11
2548_800_300_150_47	3.000	0.500	3.000	0.500	12
2548_800_300_150_48	3.000	0.500	3.000	3.000	13
2548_800_300_150_49	3.000	3.000	0.500	0.500	14
2548_800_300_150_50	3.000	3.000	0.500	3.000	15
2548_800_300_150_51	3.000	3.000	3.000	0.500	16
2548_800_300_150_52	3.000	3.000	3.000	3.000	17
***** valve size for remaining ICD ($C, $D and $G) is $5*10^{-6}$ m^2**					

6.4.4 Sensitivity Study on Well spacing

Sensitivity study on well spacing has been carried out in two stages viz. vertical well spacing and horizontal well spacing. For carrying out this study a sector model has been taken from the full field model and wells (vertical well, horizontal well) have been constructed with various spacing and with optimized offset from WOC, withdrawal rate and length of perforation/ horizontal well length.

Sensitivity Studies with Various Well Spacing for Vertical Well

Interference between two wells often leads to lower recovery and also impacts on economic indicators such as Net Present Value (NPV) and Internal Rate of Return (IRR). Optimization of vertical well and horizontal well completion is carried out in previous section.

Vertical well:

Offset – 20 m

Withdrawal rate- 150 m^3/d

A sector model was taken for finding the effect of well spacing on recovery. Well spacing of 100, 200, 300, 400 and 500 m were considered for testing the effect of spacing on recovery (Figure 6.13). Number of wells for all the five cases are given in Table 6.11.

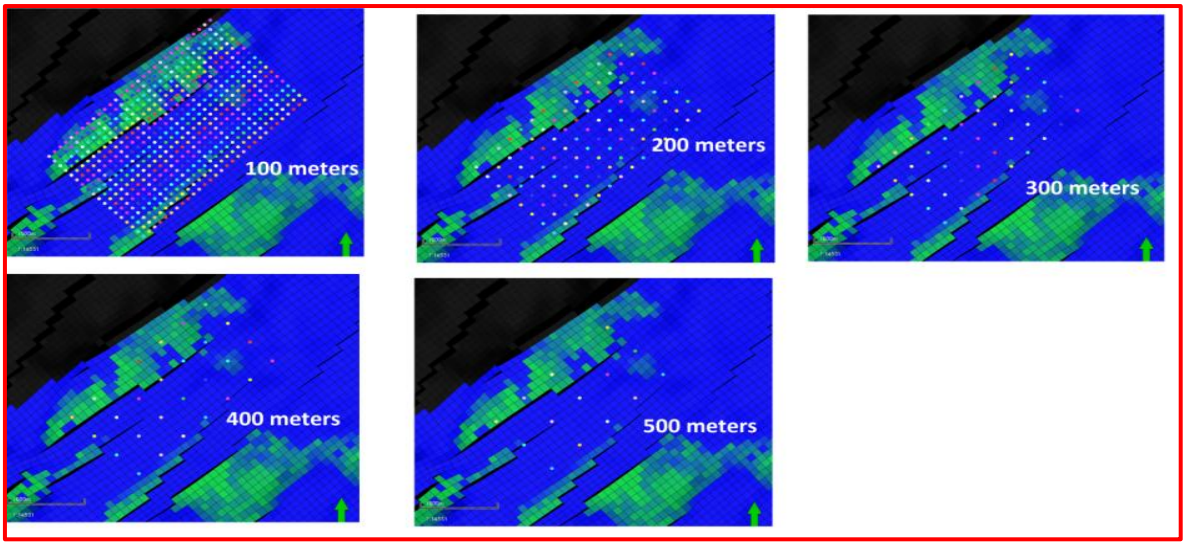

Figure 6.13: Vertical Well spacing for various development strategies

Table 6.11: Well spacing Vs number of vertical wells

Well spacing (m)	Number of vertical wells
100	540
200	112
300	45
400	28
500	15

Sensitivity Studies on Various Well Spacing for Horizontal Well

Interference between two wells often leads to lower recovery and also impacts on economic indicators such as Net Present Value (NPV) and Internal Rate of Return (IRR). Optimization of horizontal well completion is carried out in previous section.

Optimized parameter for horizontal well:

Offset – 20 m

Withdrawal rate – 300 m^3/d

Horizontal well length – 800 m

A sector model was taken for finding the effect of well spacing on recovery. Well spacing of horizontal wells has been considered in two parts namely X and Y shown in Figure 6.14. Number of well for all the five cases are given in Table 6.12. Three-Dimensional

views of all the cases with well location have been shown in Figure 6.14. Three cases were considered for testing the effect of spacing on recovery.

Table 6.12: Well spacing Vs number of horizontal wells

Well spacing, lateral (X) (m)	Well spacing, heel-toe (Y) (m)	Number of horizontal wells
400	200	12
300	150	15
200	100	24

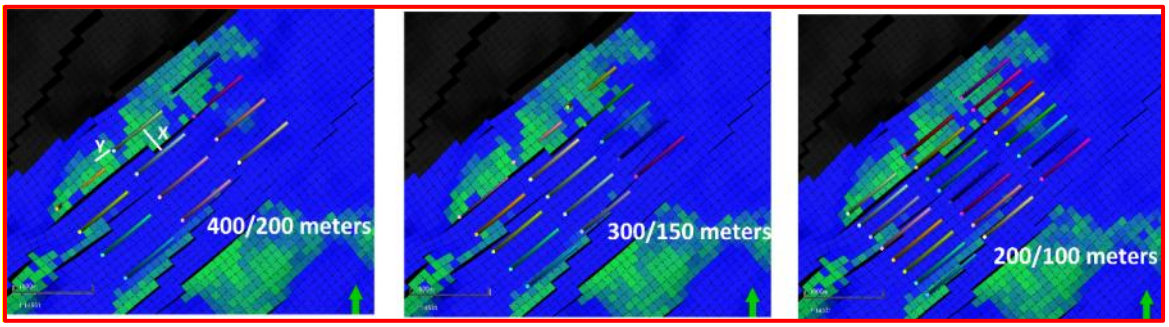

Figure 6.14: Horizontal well spacing for various development strategies

Peripheral water injection has been applied on the horizontal well with spacing of 300 (X) 150 (Y) with 15 numbers of horizontal wells. Location of water injector (32 numbers) has been shown in Figure 6.15.

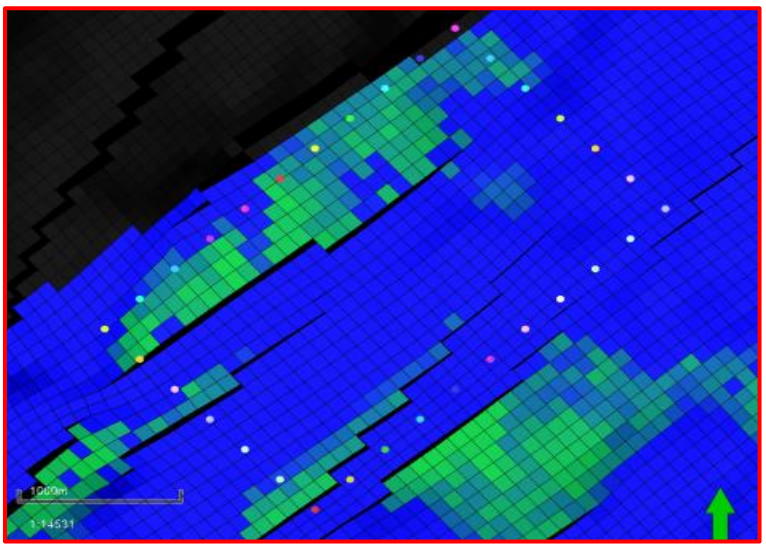

Figure 6.15: Water Injector locations

6.4.5 Field Development

Following the conclusion of the history-match exercise, sensitivity studies performed on vertical well, horizontal well, smart horizontal well and well spacing optimization for vertical and horizontal well, it is evident that additional development in terms of either well intervention in existing wells, and/or, infill wells and/or injection wells, horizontal wells and ICD completion is needed.

The Field Development Plan (FDP) exercise has been carried out for the reservoir under study after history matching and sensitivity analysis carried out for vertical well, horizontal well, smart horizontal well and well spacing optimization for vertical and horizontal well. Following stepwise procedure is used for understanding the role of different options in the development plan**.**

- Scenario-A: Base case
- Scenario-B: Well Intervention case
- Scenario-C: Infill Well case
- Scenario-D: Pressure Maintenance case
- Scenario-E: Simultaneous Water and Gas Injection case

Well intervention and infill well placement has been done based on following factors

- Mobile oil hydrocarbon pore volume (HCPV)
- Quality of history match around the wells
- Porosity, permeability and rock-type
- Connectivity around the well
- Distance from GOC and FWL
- Location of fault

The prediction cases for each reservoir were run using well production-rate control. The wells were given the production constraints as per the surface handling capacities. Overall production constraints as imposed by the group have also been defined. The wells were subjected to certain other constraints as shown in Table 6.13.

Table 6.13: Well-level constraints for prediction runs

Constraints	**Value**
Maximum individual well production rate	Based on historical well production rate reservoir
Completion type	Single Completion: bottom-to-top
Minimum well bottom-hole pressure	50-100 bars, depending upon the segment
Maximum Water Cut	95%
Minimum economic limit on oil-rate	1 m^3/d
Maximum GOR constraint	1500 scm/m^3

Scenario-A: Base case

The individual production levels established from existing wells have been used in the Base case. The wells are allowed to flow until economic limits are reached and shut in thereafter. The cut-off limit used under all prediction scenarios are given below:

- Liquid rate (oil): 1 m^3/d (For both horizontal and vertical wells)
- Max Water Cut: 95%
- Max GOR: 1500 vol/vol
- Evaluation Period: 30 years

Scenario-B: Well Intervention case

In this prediction scenario, available well intervention opportunities in all wells were evaluated to identify re-completion opportunities along with Base case. The wells, which were shut during prediction in Base case, are also evaluated to identify well intervention opportunities.

Broadly, two types of well intervention events were simulated:

- Squeeze of existing perforations and perforation in the upper section in the same zone
- Squeeze of a watered-out / gassed-out zone and perforation in a zone having no production testing

Duration of two months is taken for one well intervention. Following points are considered for scheduling the order of well intervention events.

- Existing zone recompletion/extension

- Squeeze of existing zone and perforation in a different zone
- Wells with higher incremental production from the Base case
- Nearby wells performance

Scenario-C: Infill case-Five Vertical and Eight Horizontal Wells

When deciding potential positions for well placement, zones with relatively high oil saturation and reasonable pressure at the end of the simulation were identified.

After simulations had been run, results were analyzed by looking at field cumulative oil production and bottom hole pressure, oil production rate, Water Cut where applicable for the individual wells. The grid map of the segment was also used to see how the pressure and saturation in the different grids developed.

This scenario includes the Well Intervention case along with five new vertical and eight new horizontal infill location based on mobile oil in place after Well Intervention case results. In this scenario, the same well constraints as Base case have been applied.

Location of vertical and horizontal infill wells have been shown in Figure 6.16 and Figure 6.17 respectively.

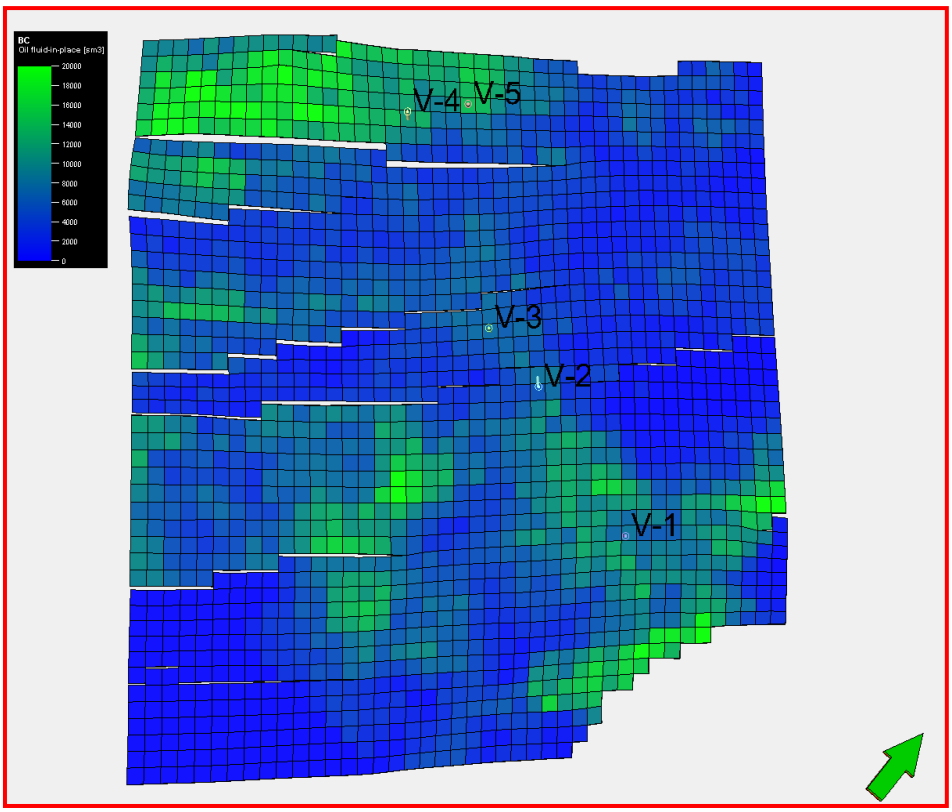

Figure 6.16: Vertical infill locations

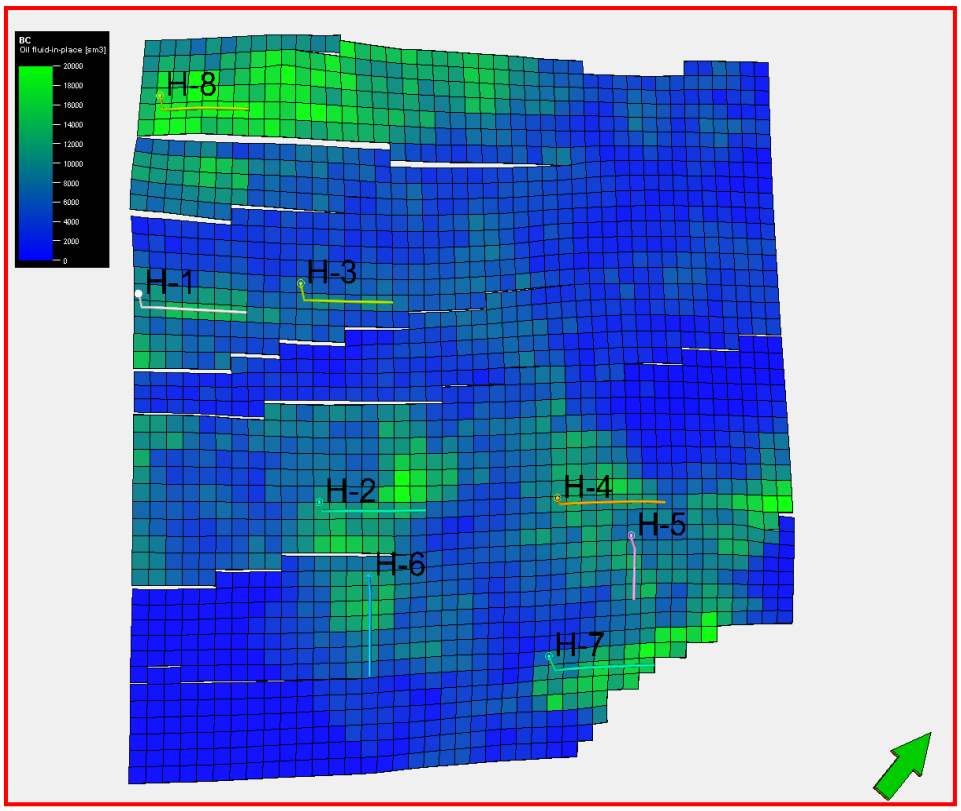

Figure 6.17: Horizontal infill locations

Scenario-D: Pressure Maintenance case

The very first step for increasing the recovery beyond primary depletion is the injection of fluid mainly water or gas for maintaining reservoir pressure. Although primary recovery mainly depends on the expansion of aquifer or gas cap, secondary recovery is dependent on injection of external fluid.

Production wells and injection wells were placed to give good drainage and sweep respectively of the areas with much remaining oil. In most cases the total production rate was matched with the total injection rate for the entire segment, ensuring that produced liquids were replaced by an equal amount of injected water.

This scenario includes Scenario-C along with identification of water injector locations for voidage replenishment and to maintain reservoir pressure. A total of twenty-six water injection wells in peripheral pattern have been drilled to maintain reservoir pressure. In this scenario, the same well constraints as in the Base case have been applied. Location of water injector has been shown in the Figure 6.18.

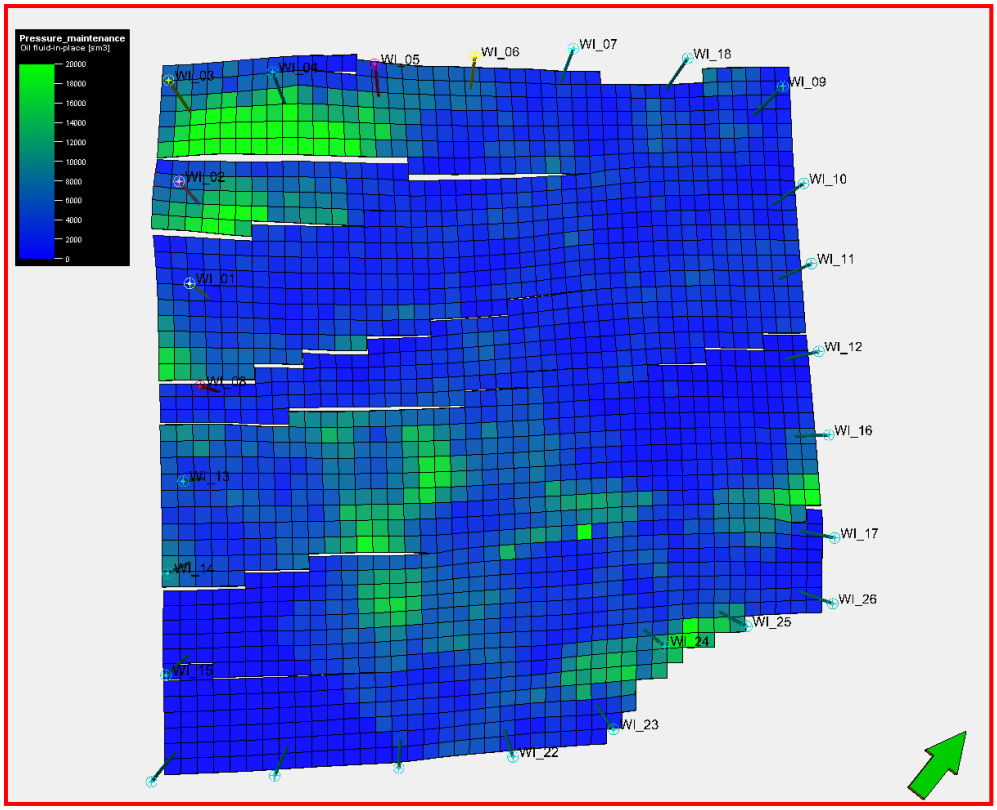

Figure 6.18: Water injection locations

Scenario-E: Simultaneous Water and Gas Injection case

Simultaneous Water and Gas Injection (SWAG) is an Enhanced Oil Recovery (EOR) process in which gas and water are mixed together and the resulting mixture is injected into the well for increasing the recovery. SWAG process incorporates the effects of microscopic sweep efficiency obtained from miscible gas injection and frontal stability obtained from waterflooding (Tunio et al., 2012).

This scenario includes Scenario-C along with identification of vertical water and gas injector locations for sweeping the unswept oil left at the end of Scenario-C and also to maintain reservoir pressure. Twenty-six SWAG injectors were placed in the simulation model based on the remaining oil saturation at the end of Scenario-C. A total of twenty-six water injector and gas injector are placed in the simulation model which is shown in Figure 6.19.

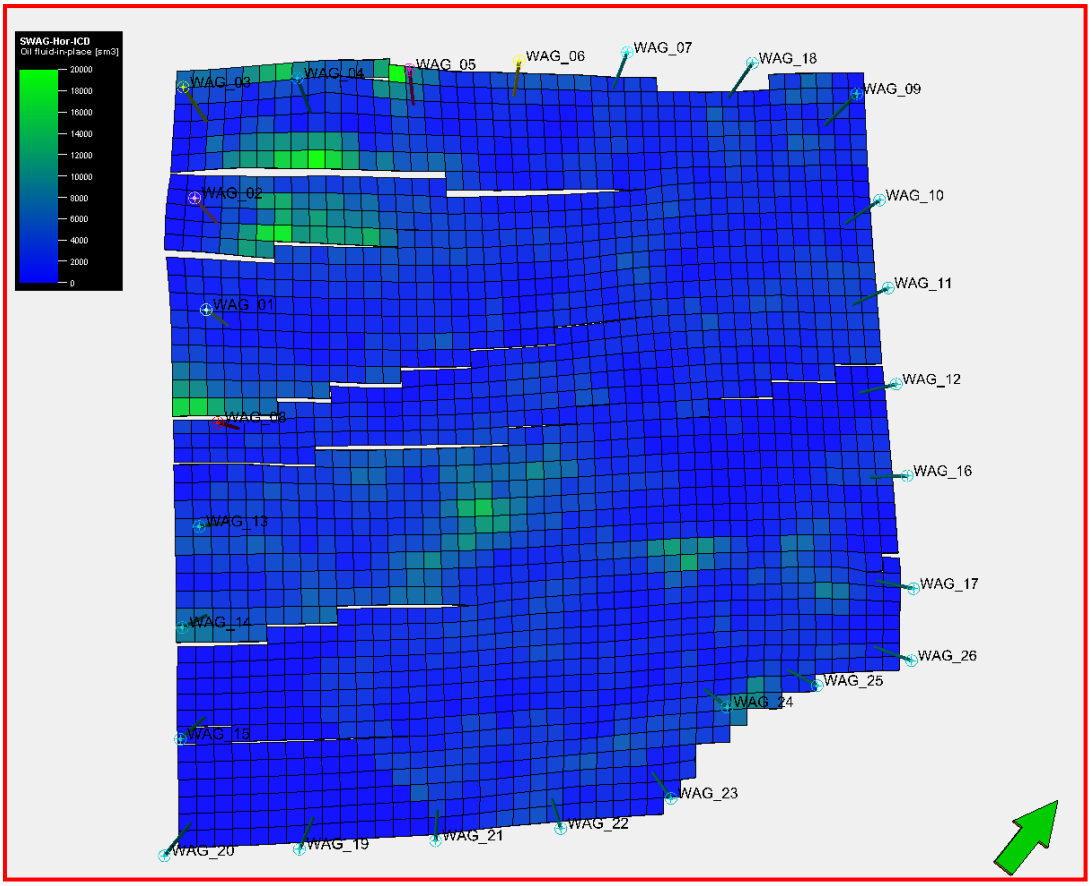

Figure 6.19: SWAG injectors

6.5 CHAPTER SUMMARY

This chapter gives information on Dynamic Modeling. Geological model is initialized using equilibration method. Aquifer model has been carried out to replicate the pressure behavior in the reservoir followed by history matching and performance prediction at well level and field scale.

CHAPTER 7
RESULTS AND DISCUSSION

7.1 RESULTS & DISCUSSION OF VERTICAL WELL SENSITIVITY ANALYSIS

In the subsequent paragraphs, discussion has been done for Group-1 through Group-5 (Table 6.4) which represents different offset from WOC. Cumulative oil, gas and water production for all the cases examined has been given in Annexure-III.

7.1.1 Group -1: Zero meter Offset from Water Oil Contact

The effect of offset and production rate on well Water Cut and cumulative oil production is presented in Figure 7.1. Variants are taken from Table 6.4.

Following conclusions can be drawn from Figure 7.1:

- Plot of Water Cut and cumulative oil production (Figure 7.1) for Group-1 shows that as rate is increased from 50 m^3/d to 100 m^3/d, Water Cut increases.
- Cumulative oil production is minimum with rate of 50 m^3/d but Water Cut remains stable at a level of around 8% for the entire production period.
- As production rate is increased from 50 m^3/d to 100 m^3/d, Water Cut rises to a level of 38% at the end of prediction (EOP).
- On increasing rate, further to 150 m^3/d Water Cut rises to a level of 54% at the EOP.

For Group-1 (0 m offset), the best case with highest cumulative oil production is with initial withdrawal rate of 150 m^3/d. Pressure and saturation distribution before and after production of the well has been given in the Figure 7.2, where it can be seen that hydrocarbon saturation has been drained efficiently in near vicinity of the wellbore.

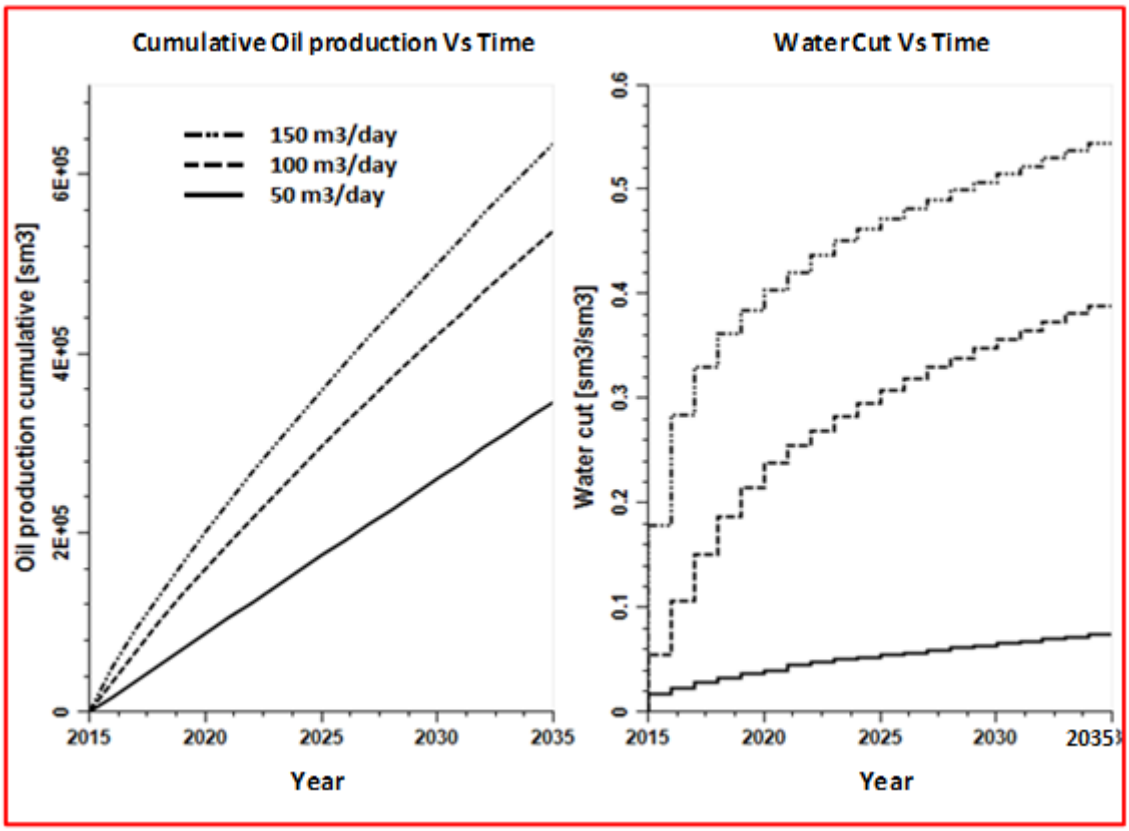

Figure 7.1: Performance prediction scenario for Group-1

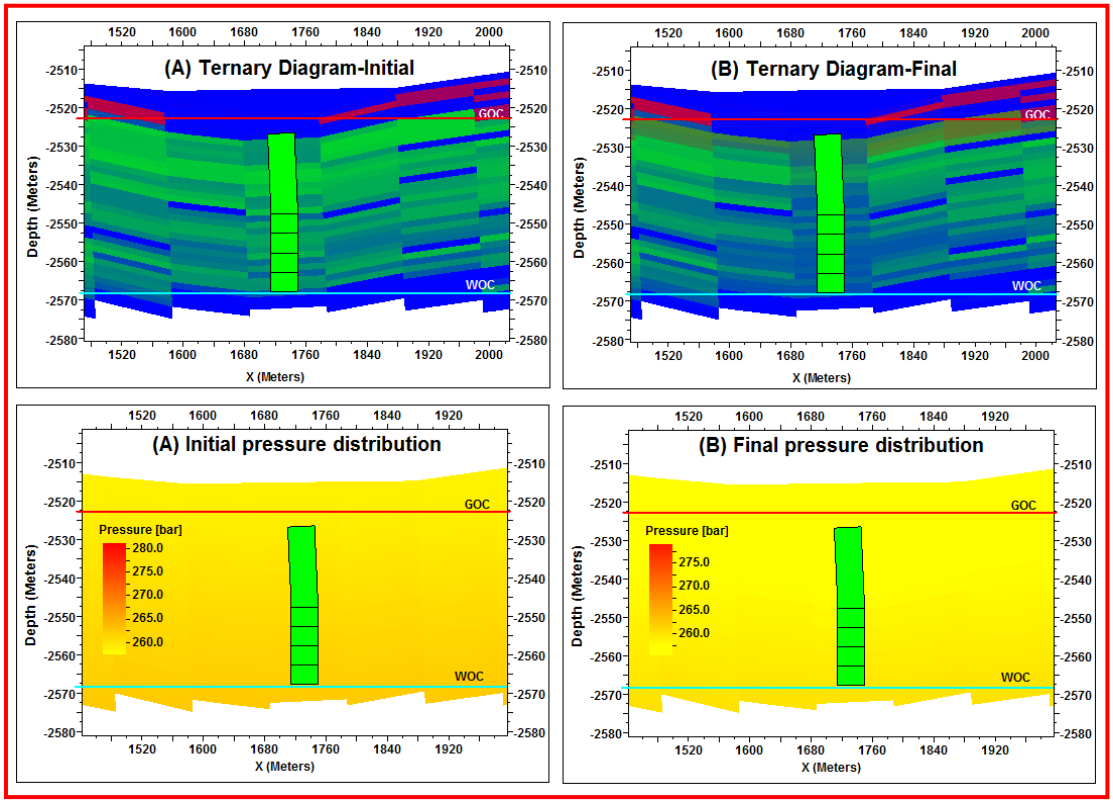

Figure 7.2 : Pressure and saturation distribution (A) *before* (B) *after for Group 1*

7.1.2 Group -2: Five meters Offset from Water Oil Contact

The effect of offset and production rate on well Water Cut and cumulative oil production are presented in Figure 7.3. Variants are taken from Table 6.4.

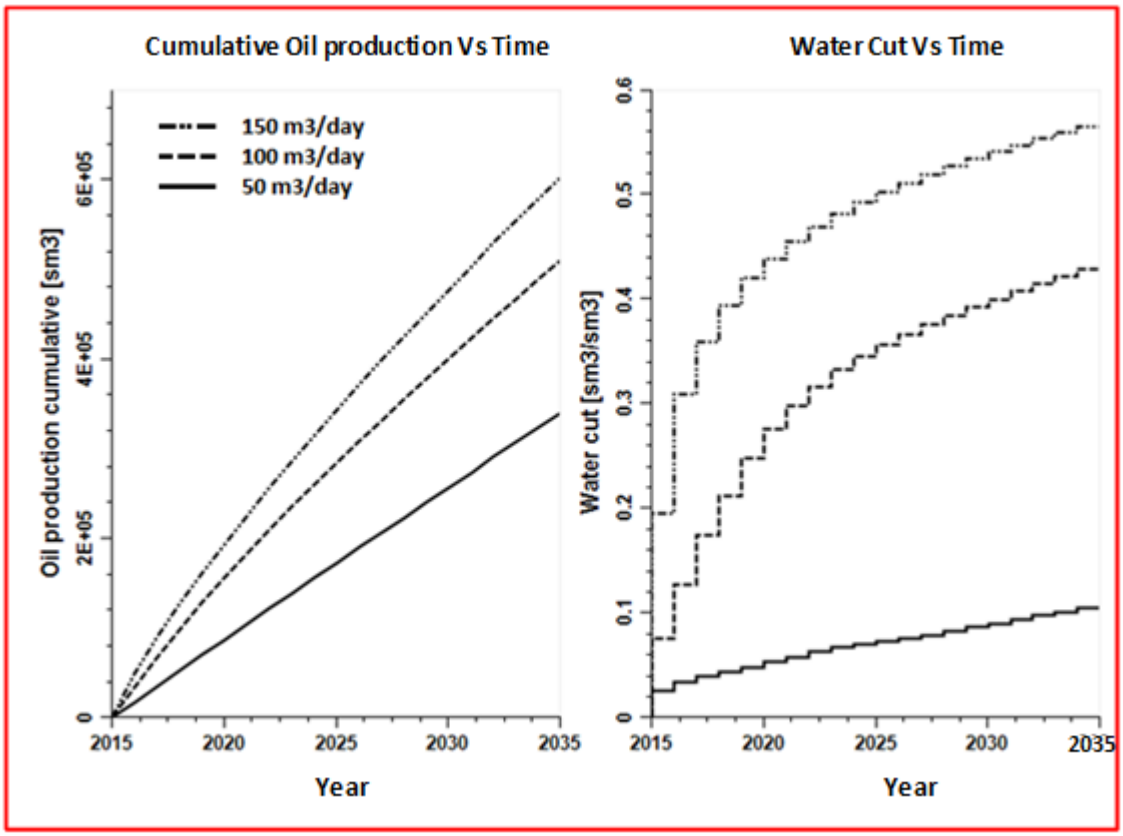

Figure 7.3: Performance prediction scenario for Group-2

Following conclusions can be drawn from Figure 7.3:

- Plot of Water Cut and cumulative oil production (Figure 7.3) for Group-2 shows that as rate is increased from 50 m^3/d to 100 m^3/d, Water Cut increases.
- Cumulative oil production is minimum with rate of 50 m^3/d but Water Cut remains stable at a level of around 10% for the entire production period.
- As production rate is increased from 50 m^3/d to 100 m^3/d Water Cut rises to a level of 43% at the EOP.
- On increasing rate, further to 150 m^3/d Water Cut rises to a level of 56% at the EOP.

For Group-2 (5 m offset) the best case with highest cumulative oil production is initial withdrawal rate of 150 m^3/d. Pressure and saturation distribution before and after production of the well has been given in the Figure 7.4, where it can be seen that hydrocarbon saturation has been drained efficiently in near vicinity of the wellbore.

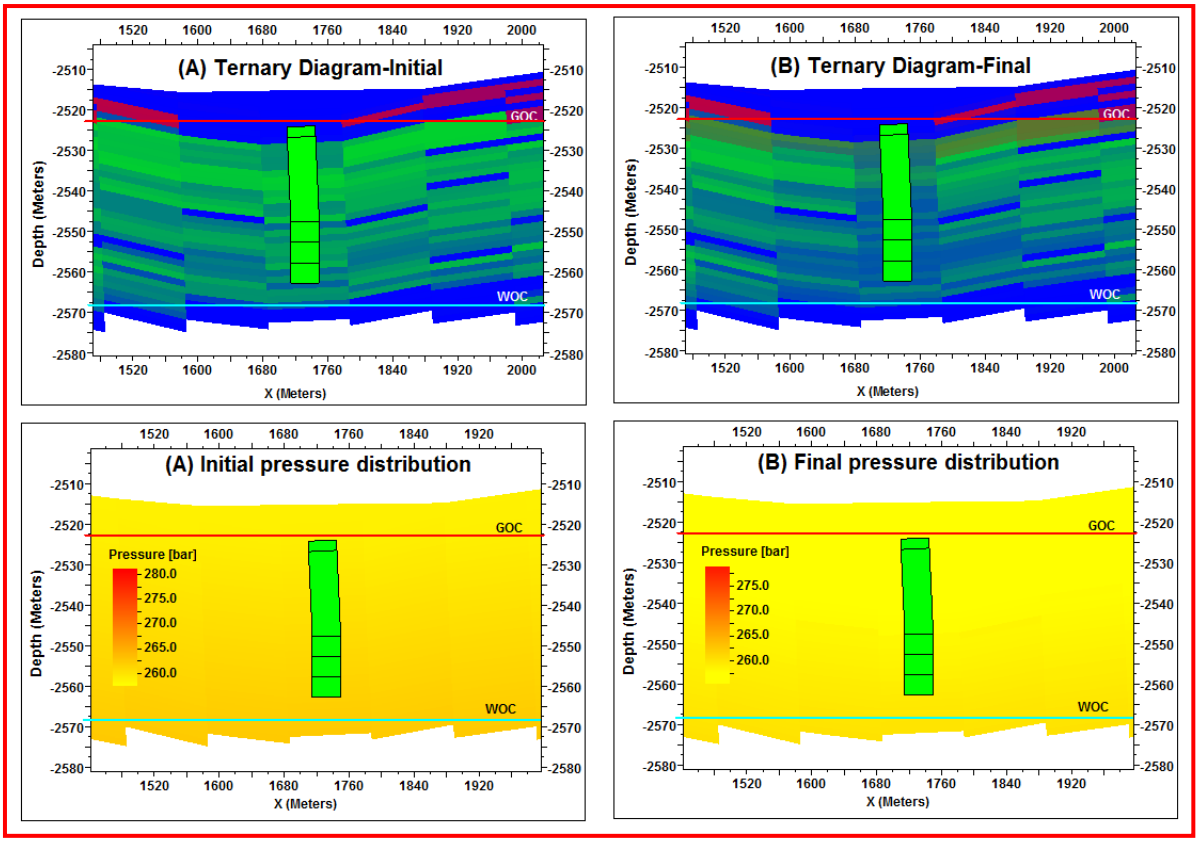

Figure 7.4: Pressure and saturation distribution (A) *before* (B) *after production Group-2*

7.1.3 Group -3: Ten meters Offset from Water Oil Contact

The effect of offset and production rate on well Water Cut and cumulative oil production are presented in Figure 7.5. Variants are taken from Table 6.4.

Following conclusions can be drawn from Figure 7.5:

- Plot of Water Cut and cumulative oil production (Figure 7.5) for Group-3 shows that as rate is increased from 50 m^3/d to 100 m^3/d, Water Cut increases.
- Cumulative oil production is minimum with rate of 50 m^3/d but Water Cut remains stable at a level of around 14% for the entire production period.
- As production rate is increased from 50 $m^{3/}$d to 100 m^3/d Water Cut rises to a level of 42% at the EOP.
- On increasing rate, further to 150 m^3/d Water Cut rises to a level of 56% at the EOP.

For Group-3 (10 m offset) the best case with highest cumulative oil production is initial withdrawal rate of 150 m^3/d. Pressure and saturation distribution before and after production of the well has been given in the Figure 7.6, where it can be seen that hydrocarbon saturation has been drained efficiently in near vicinity of the wellbore.

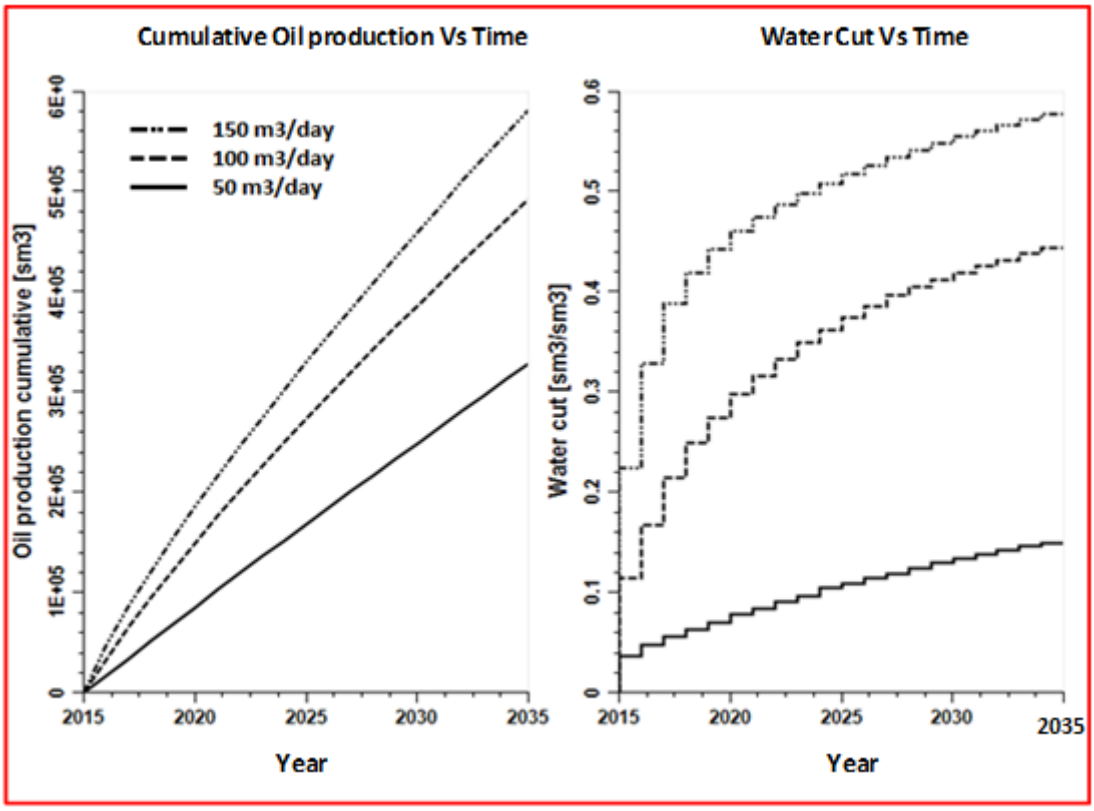

Figure 7.5: Performance prediction scenario for Group-3

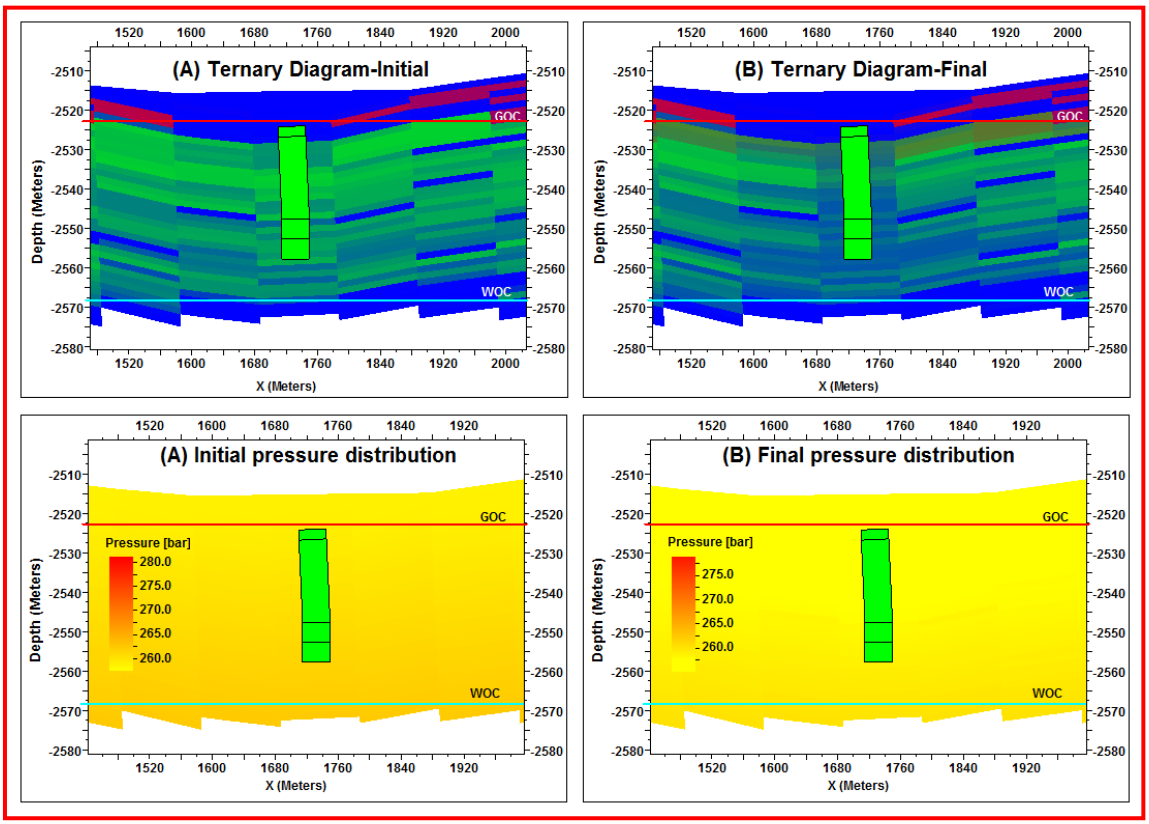

Figure 7.6: Pressure and saturation distribution (A) *before* (B) *after production Group-3*

7.1.4 Group -4: Fifteen meters Offset from Water Oil Contact

The effect of offset and production rate on well Water Cut and cumulative oil production are presented in Figure 7.7. Variants are taken from Table 6.4.

Following conclusions can be drawn from Figure 7.7:

- Plot of Water Cut and cumulative oil production (Figure 7.7) for Group-4 shows that as rate is increased from 50 m^3/d to 100 m^3/d, Water Cut increases.
- Cumulative oil production is minimum with rate of 50 m^3/d but Water Cut remains stable at a level of around 19% for the entire production period.
- As production rate is increased from 50 m^3/d to 100 m^3/d Water Cut rises to a level of 46% at the EOP.
- On increasing rate, further to 150 m^3/d Water Cut rises to a level of 59% at the EOP.

For Group-4 (15 m offset) the best case with highest cumulative oil production is initial withdrawal rate of 150 m^3/d. Pressure and saturation distribution before and after production of the well has been given in the Figure 7.8, where it can be seen that hydrocarbon saturation has been drained efficiently in near vicinity of the wellbore.

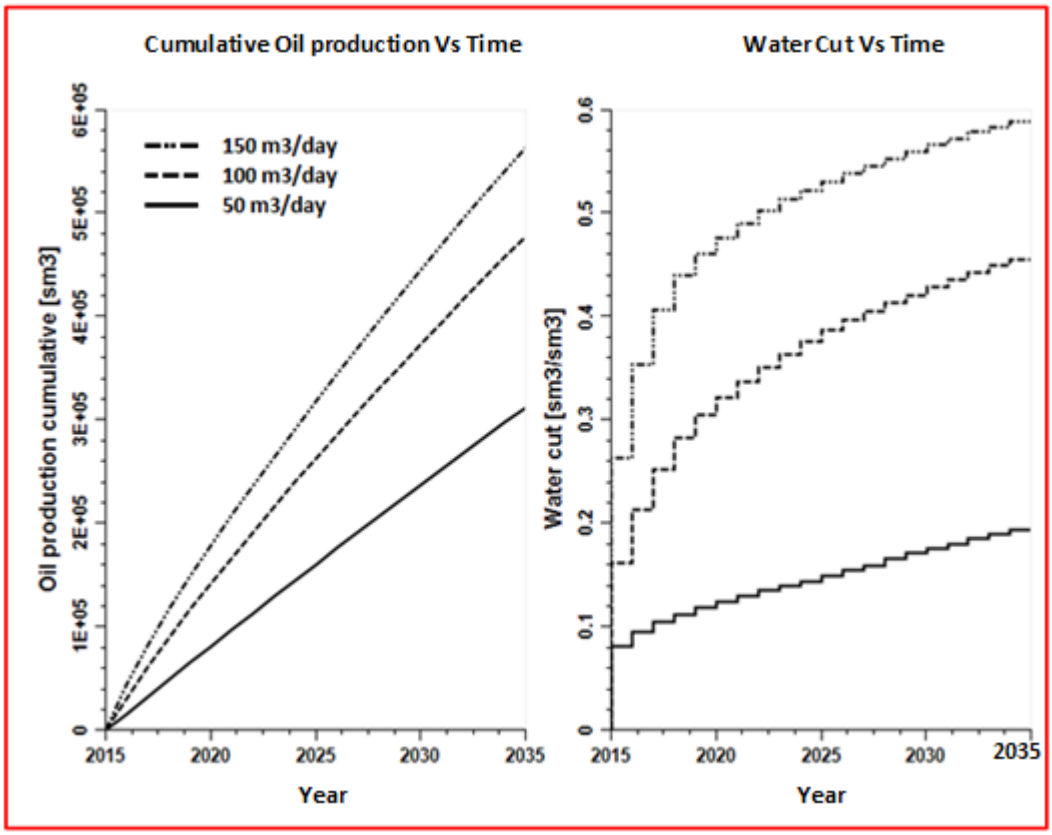

Figure 7.7: Performance prediction scenario for Group-4

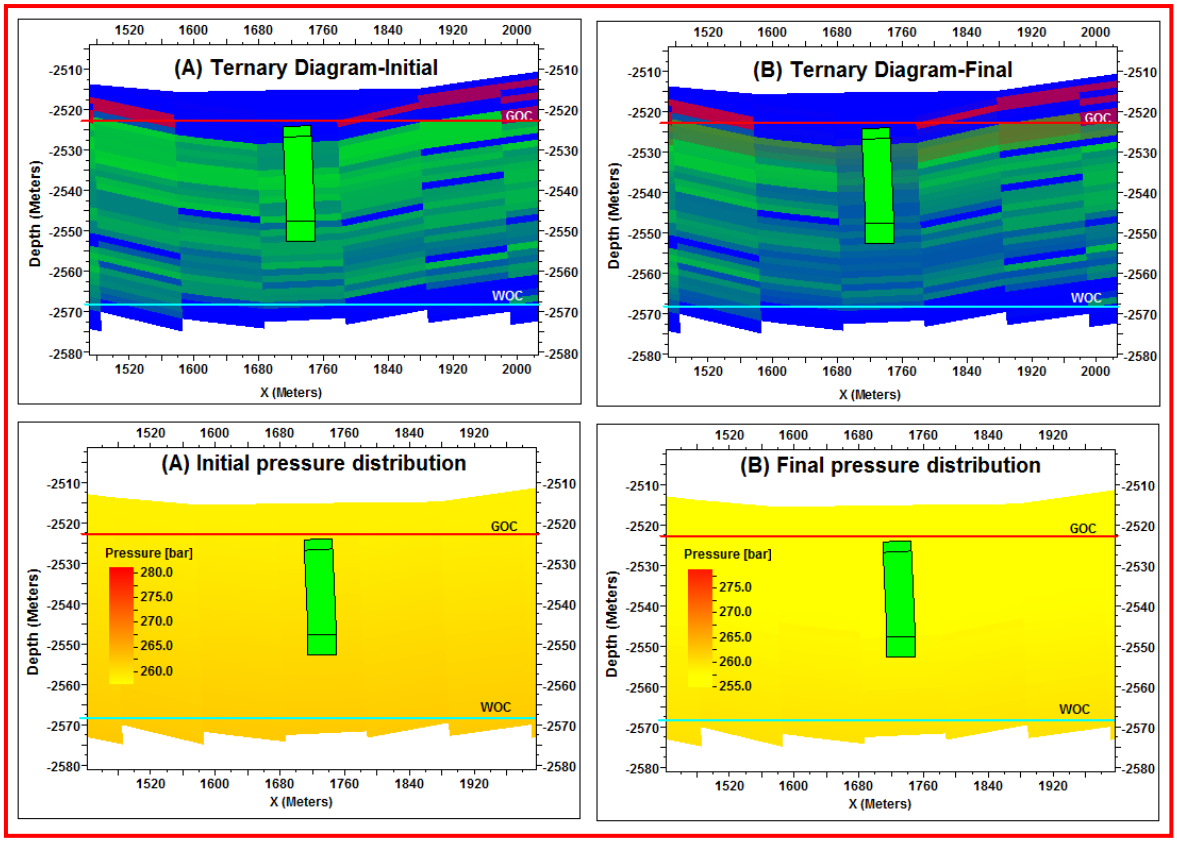

Figure 7.8: Pressure and saturation distribution (A) *before* (B) *after Production Group-4*

7.1.5 Group -5: Twenty meters Offset from Water Oil Contact

The effect of offset and production rate on well Water Cut and cumulative oil production are presented in Figure 7.9. Variants are taken from Table 6.4.

Following conclusions can be drawn from Figure 7.9 :

- Plot of Water Cut and cumulative oil production (Figure 7.9) for Group-5 shows that as rate is increased from 50 m^3/d to 100 m^3/d, Water Cut increases.
- Cumulative oil production is minimum with rate of 50 m^3/d but Water Cut remains stable at a level of around 22% for the entire production period.
- As production rate is increased from 50 m^3/d to 100 m^3/d Water Cut rises to a level of 47% at the EOP. On increasing rate further to 150 m^3/d Water Cut rises to a level of 60% at the EOP.

For Group-5 (20 m offset), the best case with highest cumulative oil production is with initial withdrawal rate of 150 m^3/d. Pressure and saturation distribution before and after production of the well has been given in the Figure 7.10, where it can be seen that hydrocarbon saturation has been drained efficiently in near vicinity of the wellbore.

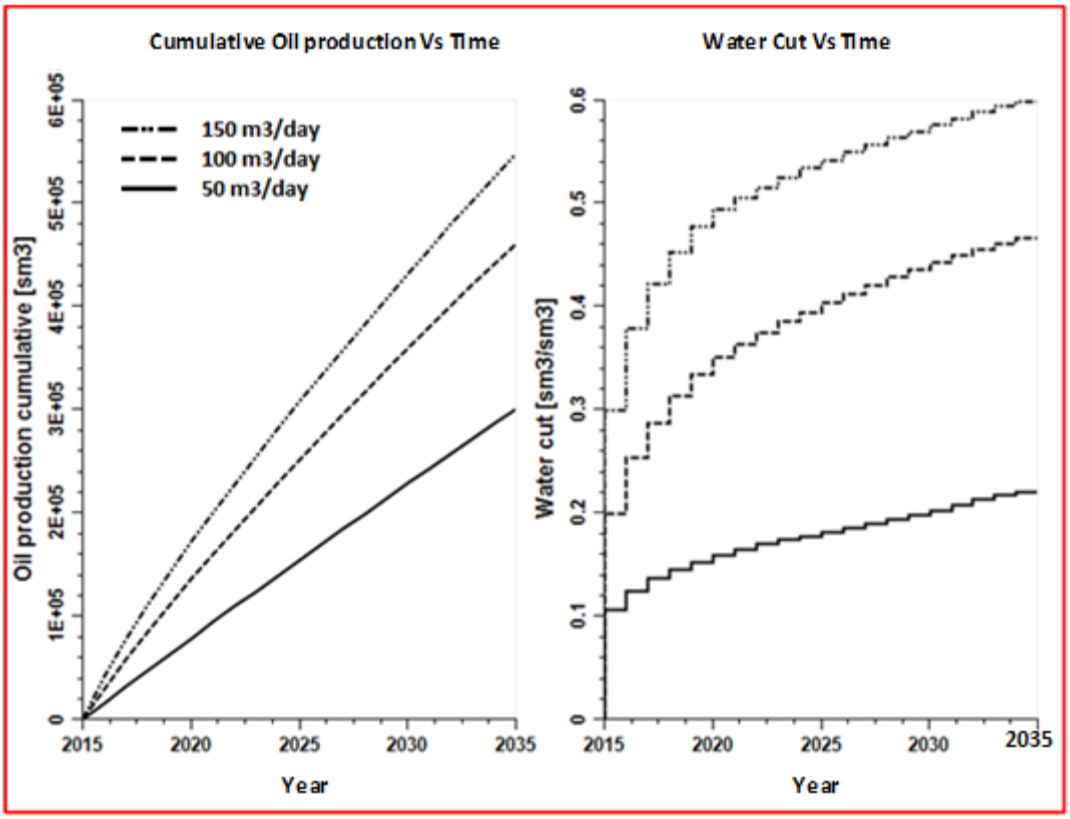

Figure 7.9: Performance prediction scenario for Group-5

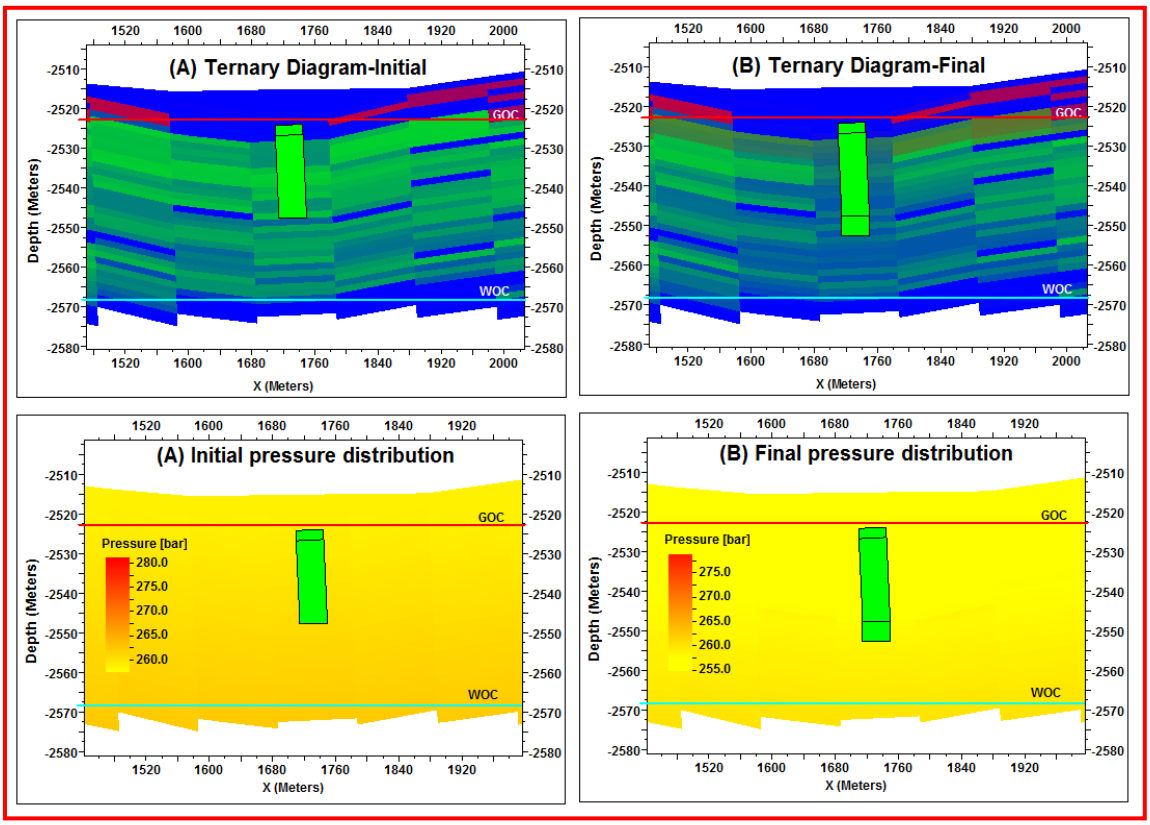

Figure 7.10: Pressure and saturation distribution (A) *before* (B) *after Production Group-5*

Apart from the variants mentioned in Group-5 lower rates than 50 m^3/d were also tested for breakthrough time, which has been presented as Figure 7.11.

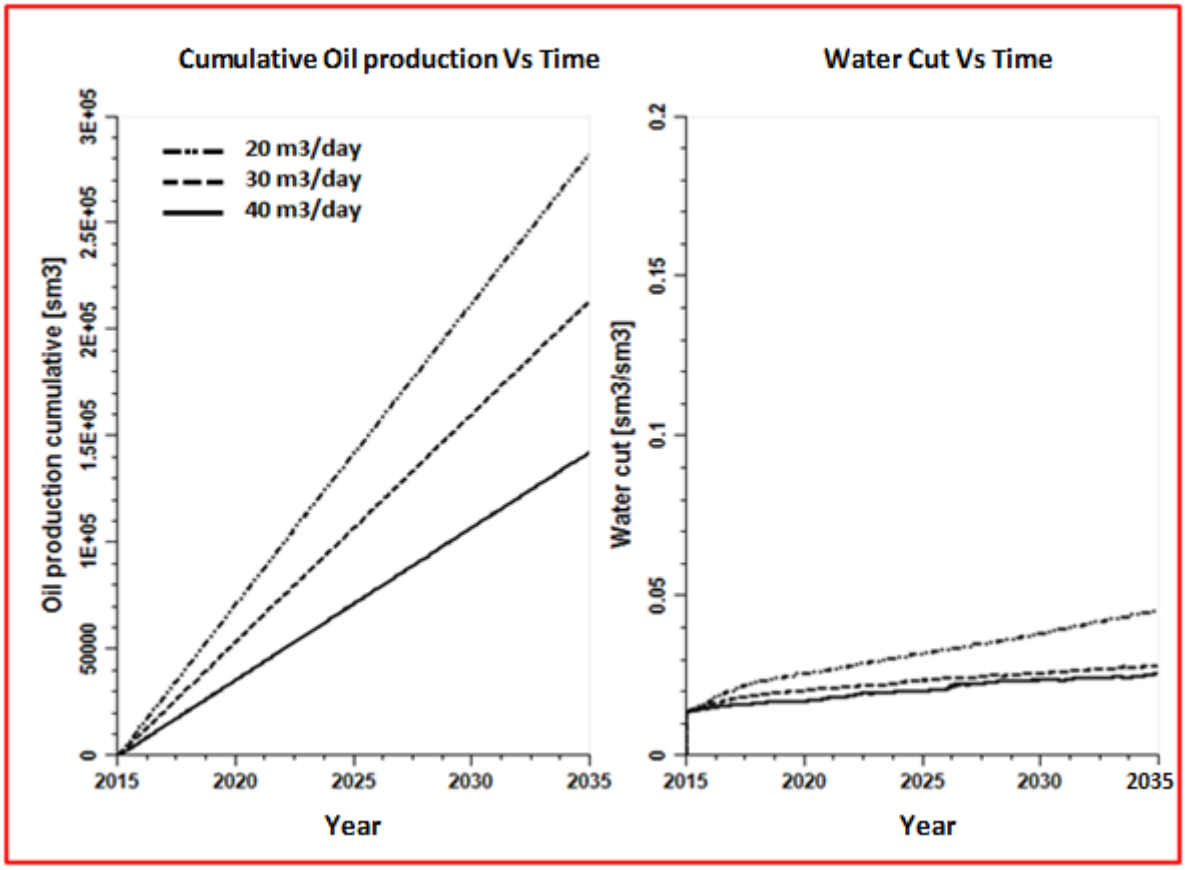

Figure 7.11: Water Cut Vs Time for lower rates for Group-5

Plot of Water Cut Vs Time (Figure 7.11) shows that as rate is increased from 20 m^3/d to 40 m^3/d Water Cut breakthrough time decreases gradually. For assigned rate of 20 m^3/d Water Cut is constant and lowest among all simulation runs.

7.2 RESULTS & DISCUSSION OF HORIZONTAL WELL SENSITIVITY ANALYSIS

In the subsequent paragraphs, discussion has been done for Group-1 through Group-4 which represents different offset from WOC (Table 6.7). Results of all simulation cases i.e. cumulative oil, gas and water production has been given in Annexure-IV.

7.2.1 Group-1: Five meters Offset from Water Oil Contact

Sensitivity analysis on three flow rates and five horizontal well lengths were carried out as per the variants listed in Table 6.7. Fifteen (15) cases were simulated for offset of 5 m

from WOC. Outcomes of the simulation runs were analyzed in Figure 7.12 under four different plots which have been listed below.

- Cumulative liquid produced at End of Prediction (EOP) Vs pressure drop for various horizontal well lengths (Figure 7.12 A)
- Water Cut at EOP Vs liquid rate for various horizontal well lengths (Figure 7.12 B)
- Cumulative oil production Vs horizontal well length for various liquid rates (Figure 7.12C)
- Cumulative oil production Vs liquid rate for various horizontal well lengths (Figure 7.12D)

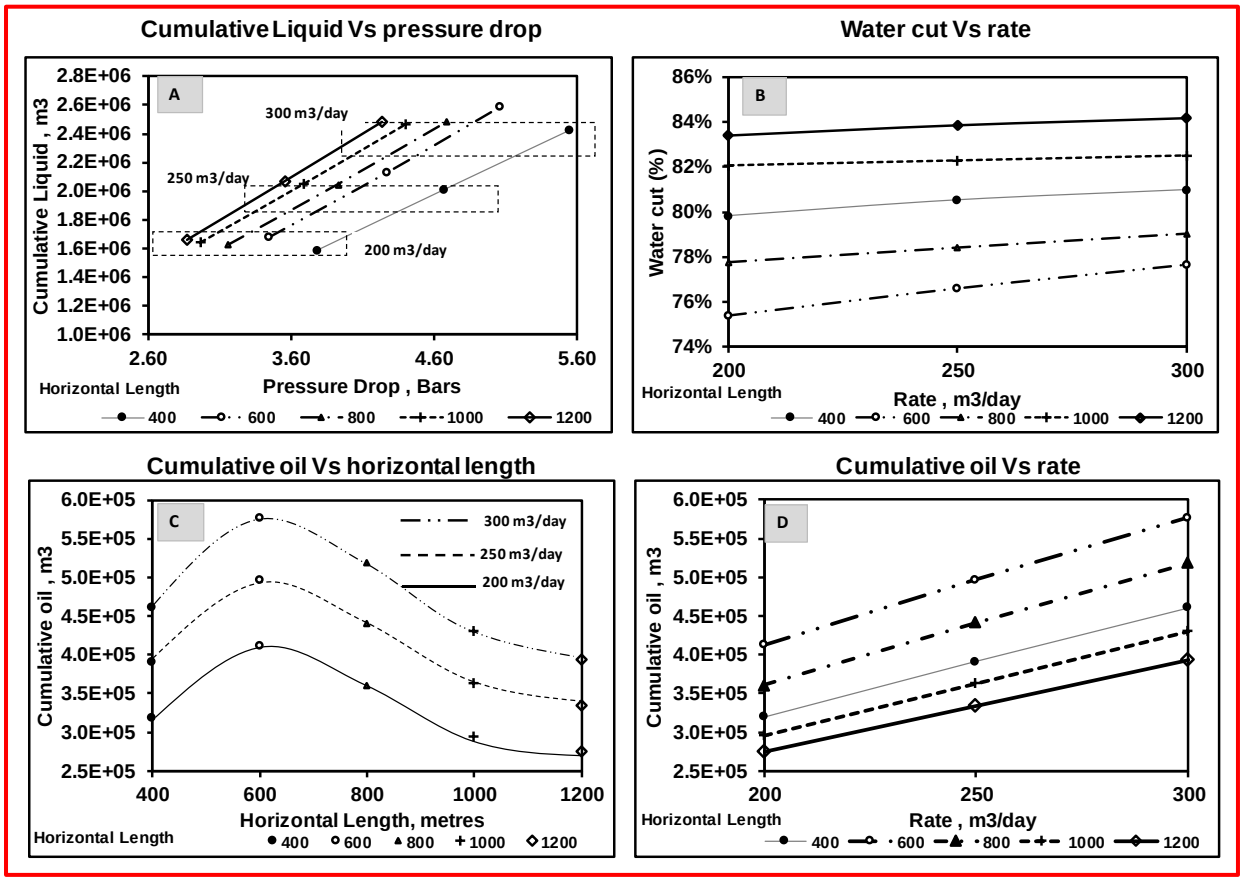

Figure 7.12: Results of Group-1 simulation runs

It can be observed from Figure 7.12 (A) that as rate is increased from 200 m^3/d to 300 m^3/d, pressure drop (Final reservoir Pressure-Initial reservoir pressure) increases for every horizontal well length. As length of horizontal section is increased, slope of cumulative liquid with pressure drop remain similar but pressure drop reduces.

It can be observed from Figure 7.12 (B) that as rate is increased from 200 m^3/d to 300 m^3/d, Water Cut increases for all horizontal well lengths. As length of horizontal section is increased, change in slope of Water Cut with liquid rate decreases.

It can be observed from Figure 7.12 (C) and Figure 7.12 (D) that as assigned liquid rate is increased from 200 m^3/d to 300 m^3/d, cumulative oil production increases for all horizontal well length sections examined. It can be seen that cumulative oil is maximum in case of 600 m horizontal well length, which decreases on increasing horizontal well length further. Horizontal wells offer higher productivity when compared to vertical wells due to increased contact area with the reservoir. An increase in horizontal well length is not proportional to higher productivity after a certain critical well length because of frictional pressure losses in the wellbore. As the well length increases, so does the frictional pressure loss (Dosunmu et al.,2015).

For Group-1 (5 m offset), the best case with highest cumulative oil production is obtained with 600 m of horizontal well length and initial withdrawal rate of 300 m^3/d. Pressure and saturation distribution before and after production of the well has been given in the Figure 7.13, where it can be seen that hydrocarbon saturation has been drained efficiently in near vicinity (below horizontal well) of the wellbore.

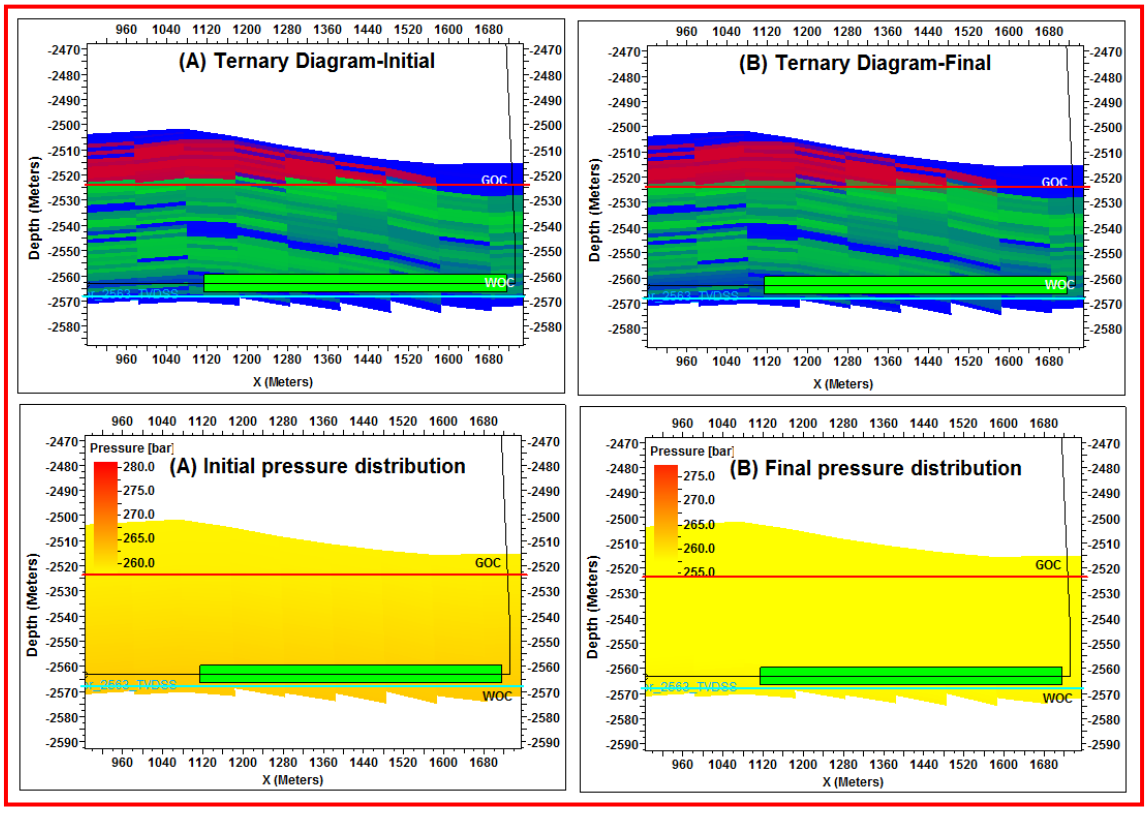

Figure 7.13: Pressure and saturation distribution (A) *before* (B) *after Production Group-1*

7.2.2 Group-2: Ten meters Offset from Water Oil Contact

Sensitivity analysis on three flow rates and five horizontal well lengths were carried out as per the variants listed in Table 6.7. Fifteen (15) cases were simulated for offset of 10 m from WOC. Outcomes of the simulation runs were analyzed in Figure 7.14 under for different plots which have been listed below.

- Cumulative liquid produced at EOP Vs pressure drop for various horizontal well lengths (Figure 7.14A)
- Water Cut at EOP Vs liquid rate for various horizontal well lengths (Figure 7.14 B)
- Cumulative oil production Vs horizontal well length for various liquid rates (Figure 7.14 C)
- Cumulative oil production Vs liquid rate for various horizontal well lengths (Figure 7.14 D)

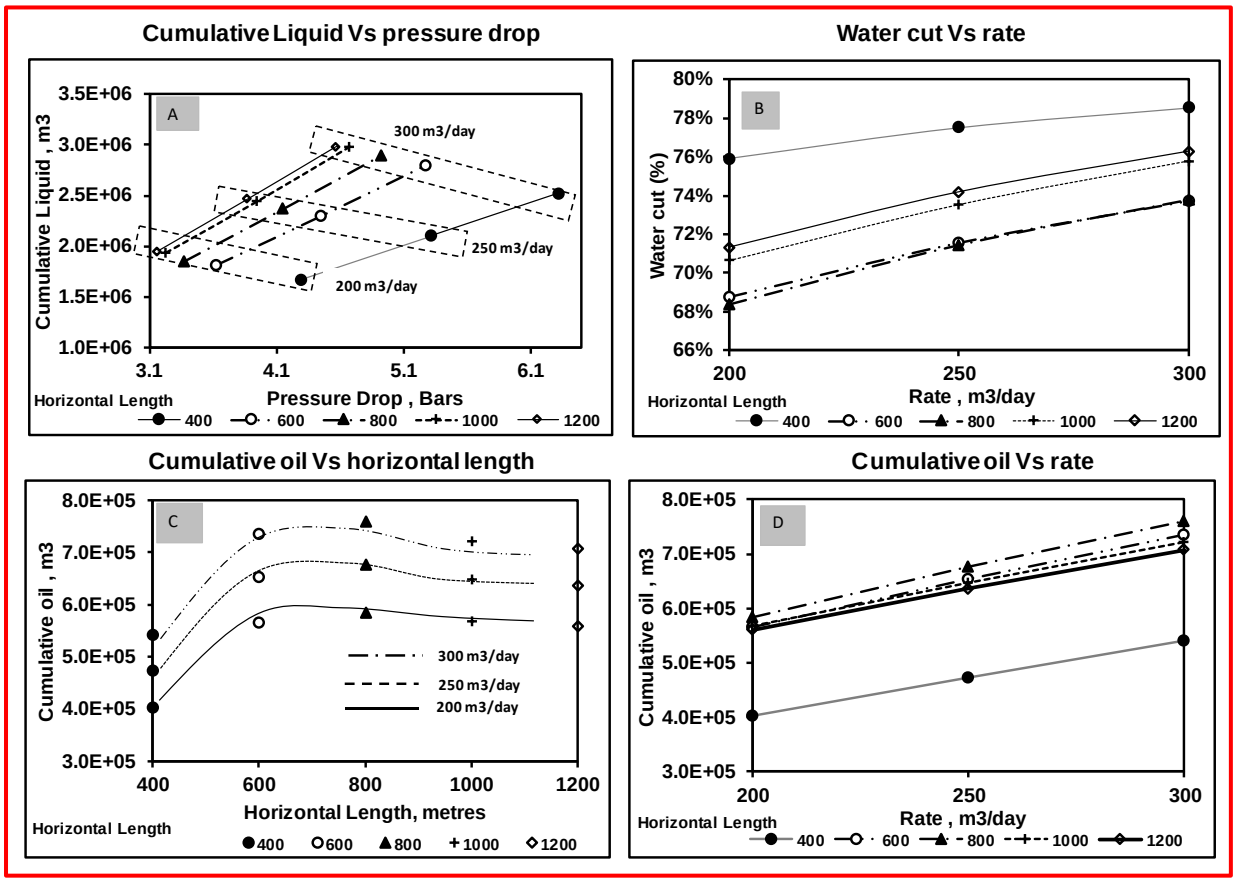

Figure 7.14: Results of Group-2 simulation runs

It can be observed from Figure 7.14 (A) that as rate is increased from 200 m^3/d to 300 m^3/d, pressure drop (Final reservoir Pressure-Initial reservoir pressure) increases for every horizontal well length. As horizontal well length is increased, slope of cumulative liquid cut with pressure drop remain similar but pressure drop reduces.

It can be observed from Figure 7.14 (B) that as rate is increased from 200 m^3/d to 300 m^3/d Water Cut increases for different horizontal well lengths. As horizontal well length is increased, change in slope of Water Cut with liquid rate decreases.

It can be observed from Figure 7.14 (C) and Figure 7.14 (D) that as assigned liquid rate is increased from 200 m^3/d to 300 m^3/d, cumulative oil production increases for every horizontal well length. It can be seen that cumulative oil is maximum in case of 800 m of horizontal well length, which decreases on increasing horizontal well length.

For Group-2 (10 m offset) the best case with highest cumulative oil production is with 800 m of horizontal well length and initial withdrawal rate of 300 m^3/d. Pressure and saturation distribution before and after production of the well has been given in the Figure 7.15, where it can be seen that hydrocarbon saturation has been drained efficiently in near vicinity of the wellbore.

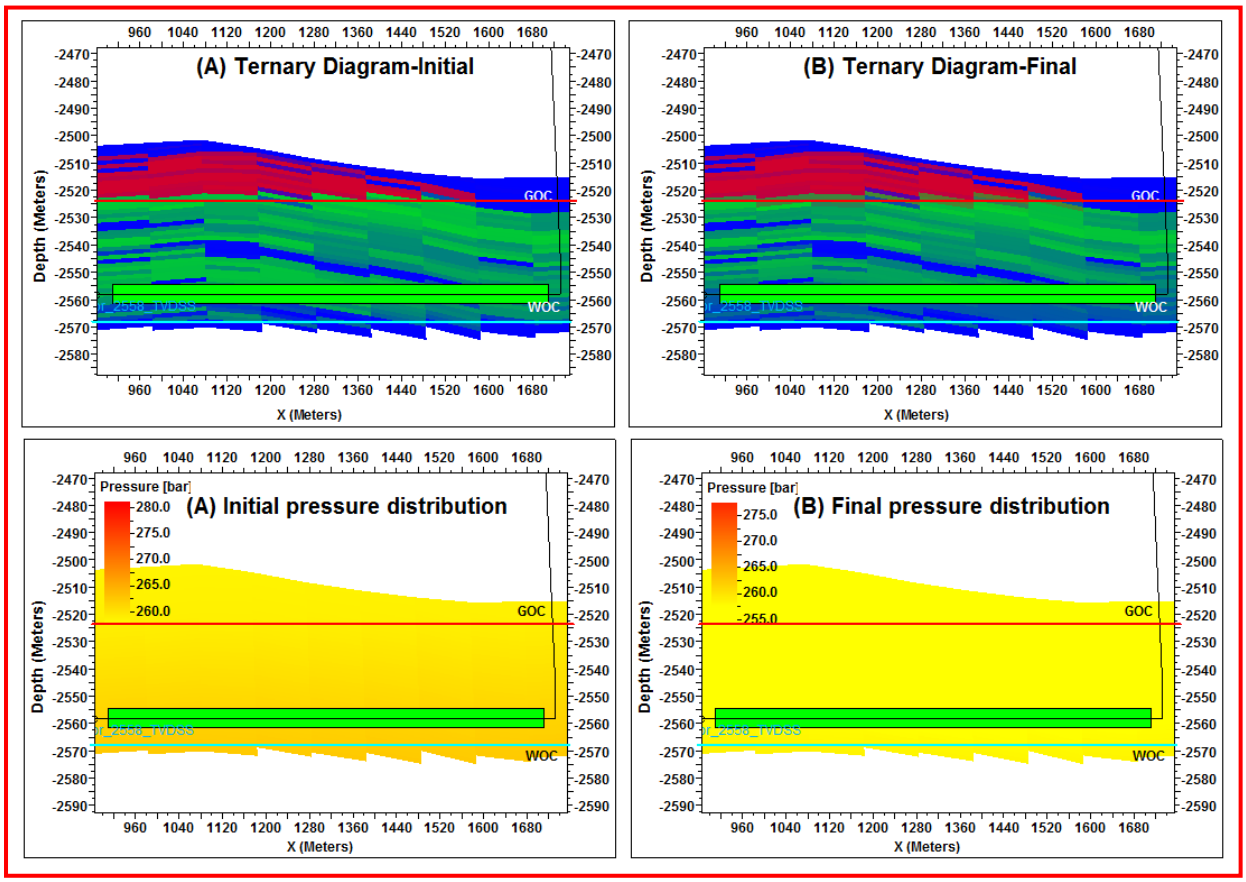

Figure 7.15: Pressure and saturation distribution (A) *before* (B) *after production Group-2*

7.2.3 Group-3: Fifteen meters Offset from Water Oil Contact

Sensitivity analysis on three flow rates and five horizontal well lengths were carried out as per the variants listed in Table 6.7. Fifteen (15) cases were simulated for offset of 15 m from WOC. Outcomes of the simulation runs were analyzed in Figure 7.16 under for different plots which have been listed below.

- Cumulative liquid produced at EOP Vs pressure drop for various horizontal well lengths (Figure 7.16 A)
- Water Cut at EOP Vs liquid rate for various horizontal well lengths (Figure 7.16 B)
- Cumulative oil production Vs horizontal well length for various liquid rates (Figure 7.16 C)
- Cumulative oil production Vs liquid rate for various horizontal well lengths (Figure 7.16 D)

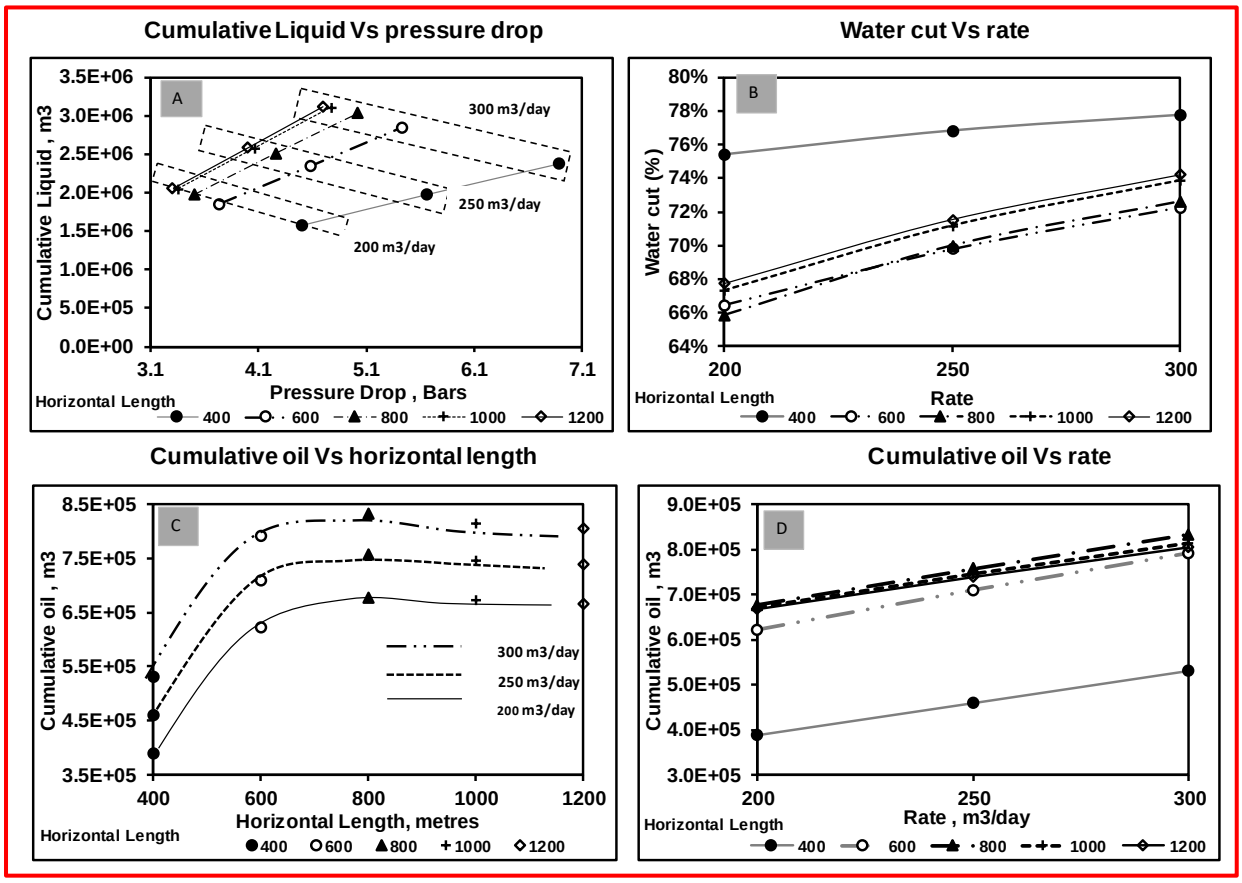

Figure 7.16: Results of Group-3 simulation runs

It can be observed from Figure 7.16 (A) that as rate is increased from 200 m^3/d to 300 m^3/d, pressure drop (Final reservoir Pressure-Initial reservoir pressure) increases for every horizontal well length. As horizontal well length is increased, slope of cumulative liquid with pressure drop remain similar but pressure drop reduces.

It can be observed from Figure 7.16 (B) that as rate is increased from 200 m^3/d to 300 m^3/d Water Cut increases for different horizontal well lengths. As length of horizontal section is increased, change in slope of Water Cut with liquid rate decreases.

It can be observed from Figure 7.16 (C) and Figure 7.16 (D) that as assigned liquid rate is increased, cumulative oil production increases for every horizontal well length. It can be seen that cumulative oil is maximum in case of 800 m horizontal well length, which decreases on increasing horizontal well length.

For Group-3 (15 m offset), the best case with highest cumulative oil production is with 800 m of horizontal well length and initial withdrawal rate of 300 m^3/d. Pressure and saturation distribution before and after production of the well has been given in the Figure 7.17, where it can be seen that hydrocarbon saturation has been drained efficiently in near vicinity of the wellbore.

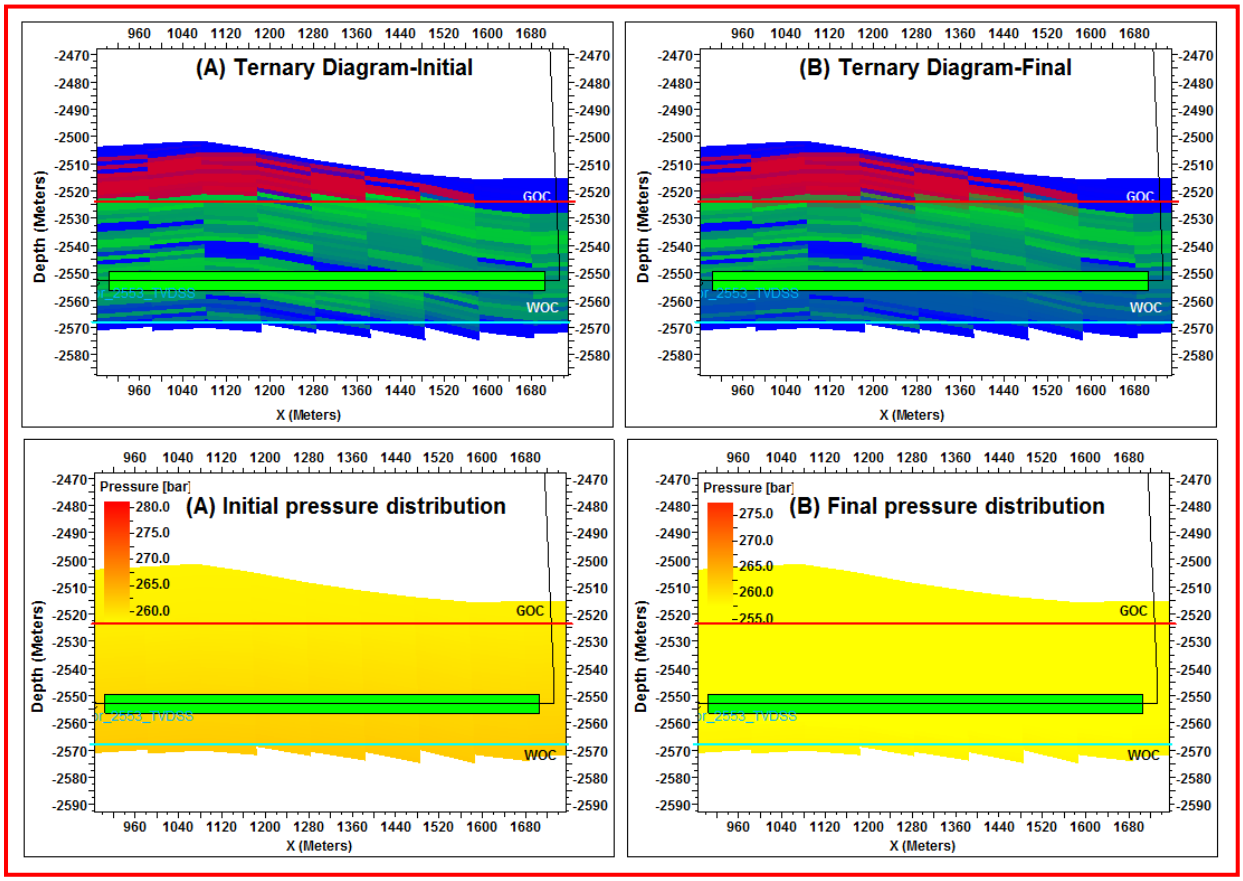

Figure 7.17: Pressure and saturation distribution (A) *before* (B) *after production Group-3*

7.2.4 Group-4: Twenty meters Offset from Water Oil Contact

Sensitivity analysis on three flow rates and five horizontal well length was carried out as per the variants listed in Table 6.7. Fifteen (15) cases were simulated for offset of 20 m from WOC. Outcome of the simulation runs were analyzed in Figure 7.18 under different plots, which have been listed below.

- Cumulative liquid produced at EOP Vs pressure drop for various horizontal well lengths (Figure 7.18A)
- Water Cut at EOP Vs liquid rate for various horizontal well lengths (Figure 7.18B)
- Cumulative oil production Vs horizontal well length for various liquid rates (Figure 7.18C)
- Cumulative oil production Vs liquid rate for various horizontal well lengths (Figure 7.18D)

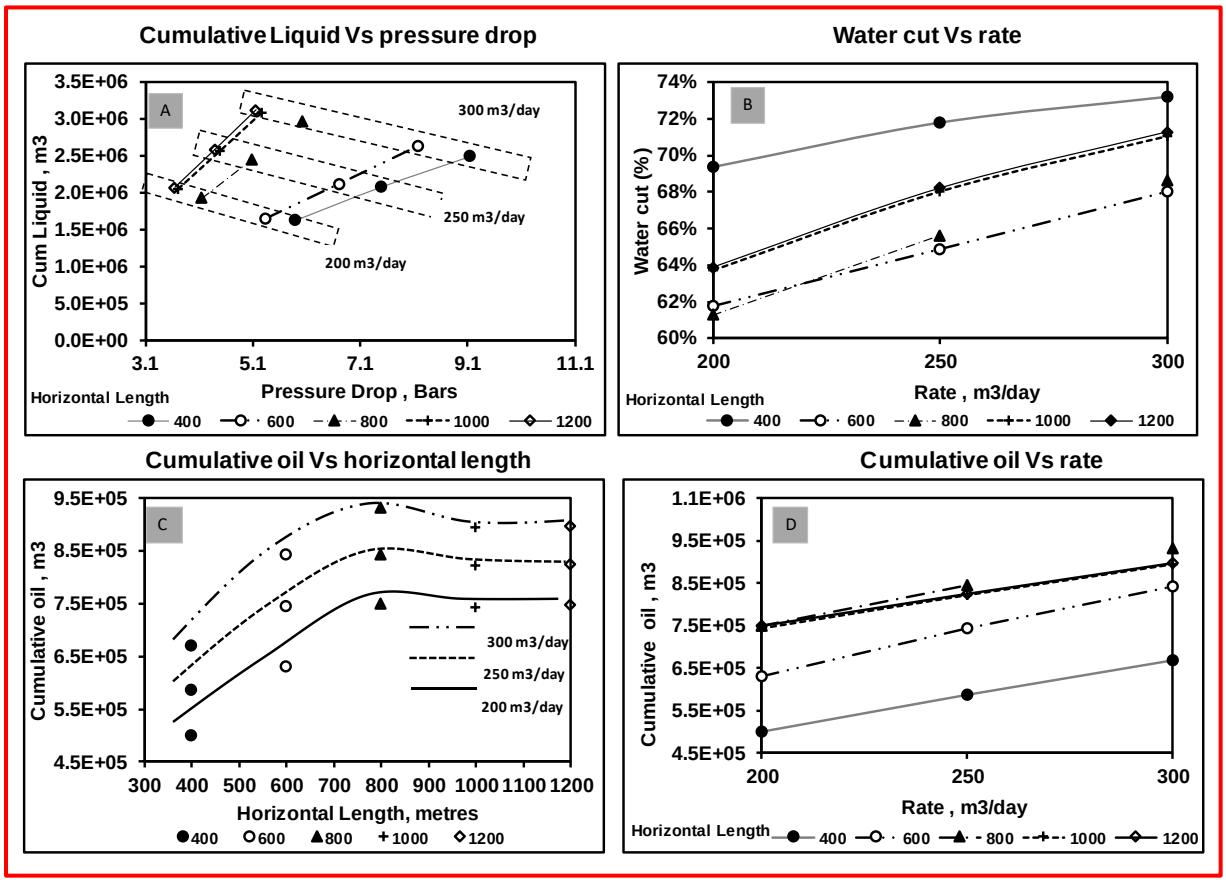

Figure 7.18: Results of Group-4 simulation runs

It can be observed from Figure 7.18 (A) that as rate is increased from 200 m^3/d to 300 m^3/d, pressure drop (Final reservoir Pressure-Initial reservoir pressure) increases for every horizontal well length. As horizontal well length is increased, slope of cumulative liquid with pressure drop remain similar but pressure drop reduces.

It can be observed from Figure 7.18 (B) that as rate is increased from 200 m^3/d to 300 m^3/d, Water Cut increases for different horizontal well length. As horizontal well length is increased, change in slope of Water Cut with liquid rate decreases.

It can be observed from Figure 7.18 (C) and Figure 7.18 (D) that as assigned liquid rate is increased cumulative oil production increases for every horizontal well length. In addition, cumulative oil is maximum in case of 800 m horizontal well length, which decreases on increasing horizontal well length.

For Group-4 (20 m offset), the best case with highest cumulative oil production is with 800 m of horizontal well length and initial rate of 300 m^3/d. Pressure and saturation distribution before and after production of the well has been given in the Figure 7.19, where it can be seen that hydrocarbon saturation has been drained efficiently in near vicinity of the wellbore.

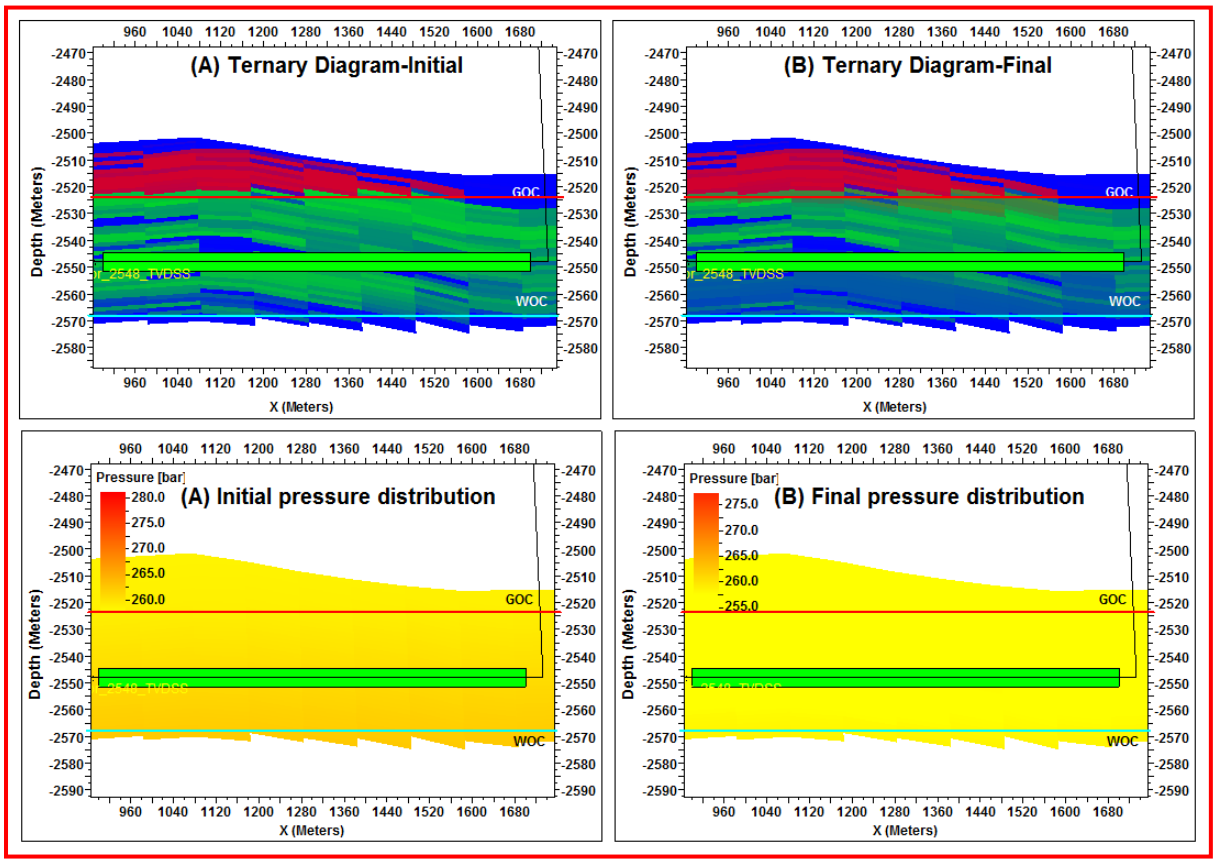

Figure 7.19: Pressure and saturation distribution (A) *before* (B) *after Production Group-4*

Additionally, rate sensitivity for lower rates (25, 40, 50, 60 & 70 m^3/d) was also carried out in the numerical simulation model to ascertain breakthrough time and Water Cut Vs time.

A plot of Water Cut Vs Time (Figure 7.20) for the above mentioned cases shows that as withdrawal rate is increased from 25 m^3/d to 70 m^3/d Water Cut breakthrough time decreases gradually. For assigned rate of 25 m^3/d Water Cut is constant and lowest among all simulation runs.

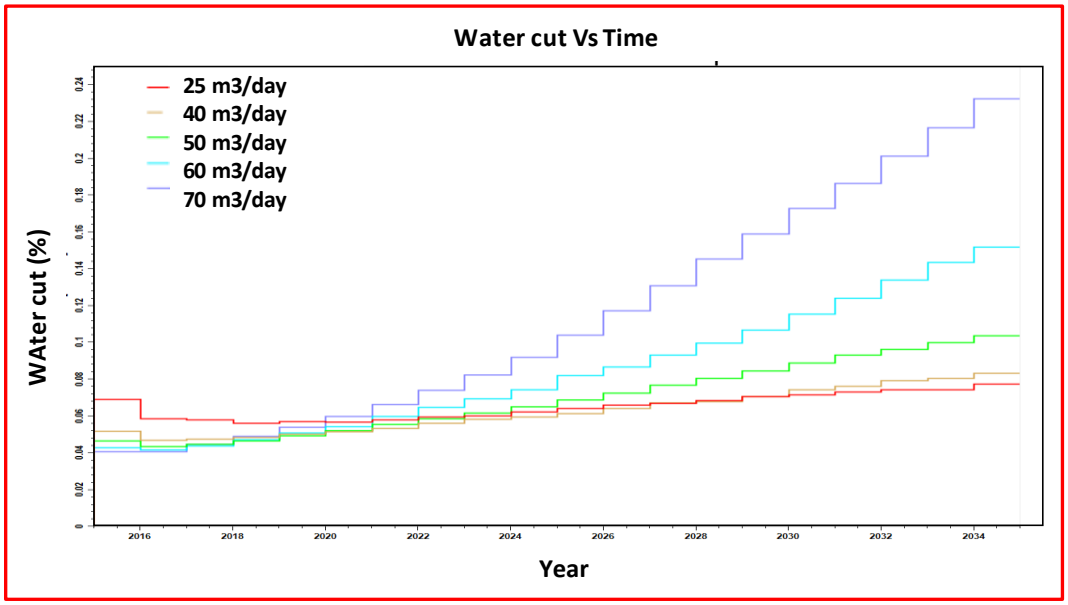

Figure 7.20: Results of Group-4 simulation runs (for lower rates)

It can be seen that well with offset of 20 m, horizontal well length between 600–800 m and withdrawal rate of 300 m^3/d drains the reservoir most efficiently in terms of cumulative oil production.

7.3 RESULTS & DISCUSSION OF ICD COMPLETION

In the subsequent paragraphs, discussion has been done for ICD completion which includes sensitivity study on compartment length, nozzle size and uncertainty analysis on nozzle size. Cumulative oil, gas and water production of the cases has been given in Annexure-V.

7.3.1 Equal Length Compartments with Uniform Nozzle Sizes - Sensitivity on Compartment Length

Horizontal well with offset of 20 m, horizontal well length of 800 m and withdrawal rate of 300 m^3/d with nozzle type ICD and packer have been simulated under the variant compartment length. Compartment length of 25, 50, 75, 100, 125 and 150 m have been selected for finding an effect of compartment length on cumulative oil production. Figure 7.21 shows production profile for various cases. In Figure 7.22 cumulative oil production Vs

compartment length has been plotted to find out the best case. It can be seen that compartment length of 150 m (case: 2548_800_300_150) gives the highest oil production. Table 7.1 summarizes the cumulative oil, gas and water production for various cases examined.

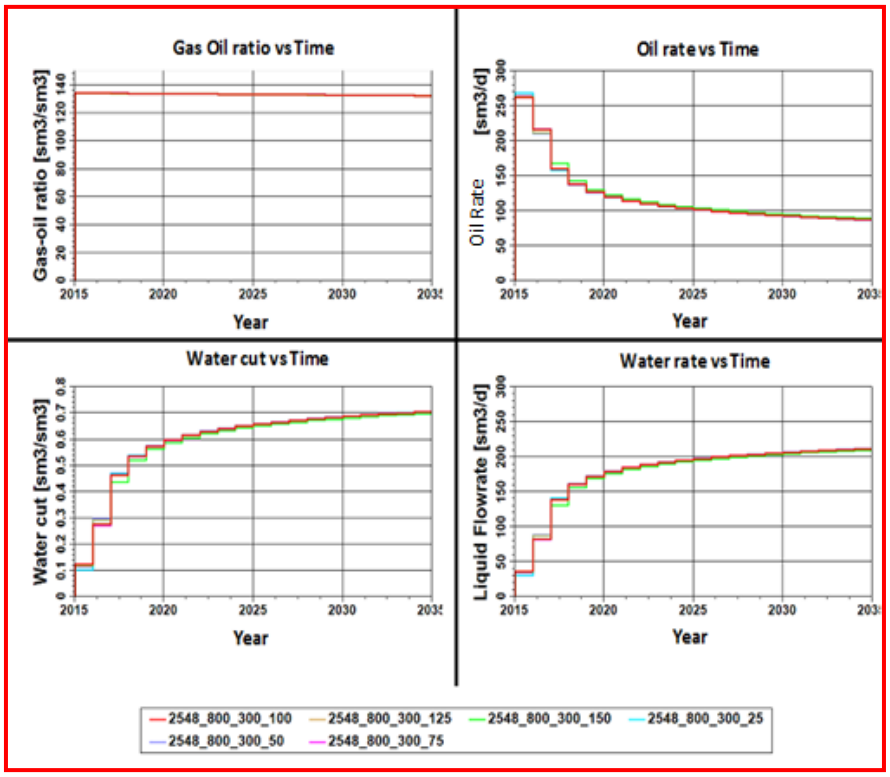

Figure 7.21: Production profile for various cases (compartment length)

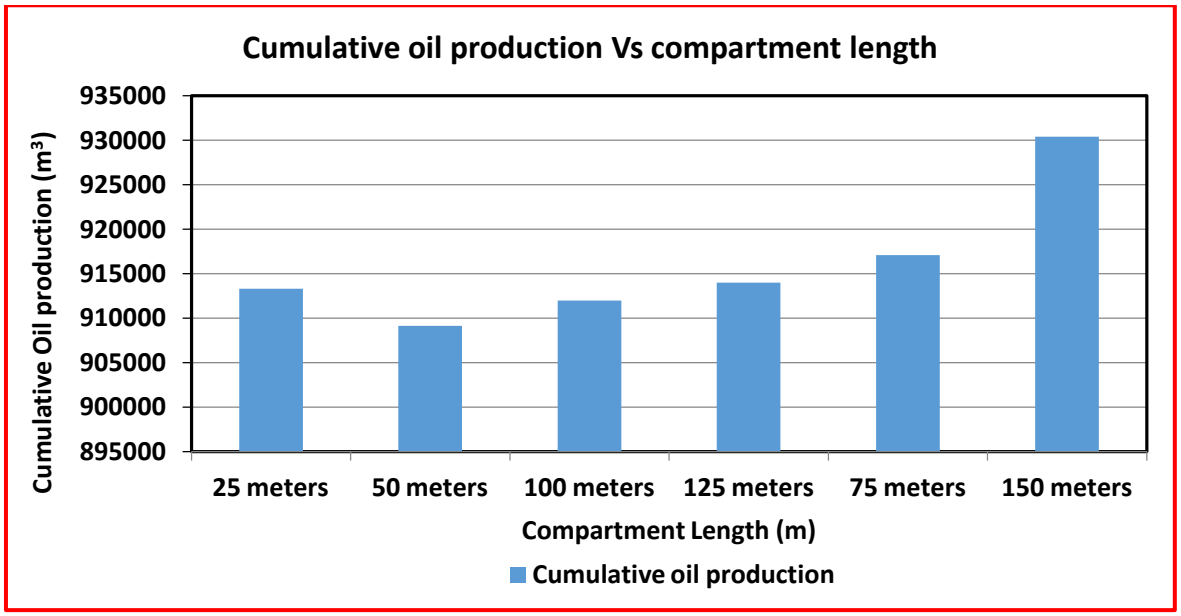

Figure 7.22: Cumulative oil production for various compartment lengths

Table 7.1: Cumulative oil, water and gas for various compartment length

Compartment length (m)	Cumulative oil (m^3)	Cumulative water (m^3)	Cumulative gas (scm)
100	911970.62	1279529.375	121974992
125	914004.25	1277495.75	122238840
150	930396.43	1261103.5	124427760
25	913312.68	1278187.375	122149712
50	909140.56	1282359.375	121594256
75	917094.56	1274405.5	122658464

Figure 7.23 and Figure 7.24 show well schematic along with property variation along horizontal well length with compartment length of 50 m and compartment length of 150 m respectively. It can be seen that only 7 number of ICD (compartment length of 150 m, case: 2548_800_300_ICD_150) are required for getting the best recovery efficiency in comparison to 18 number of ICD (compartment length of 50 m, case: 2548_800_300_ICD_50).

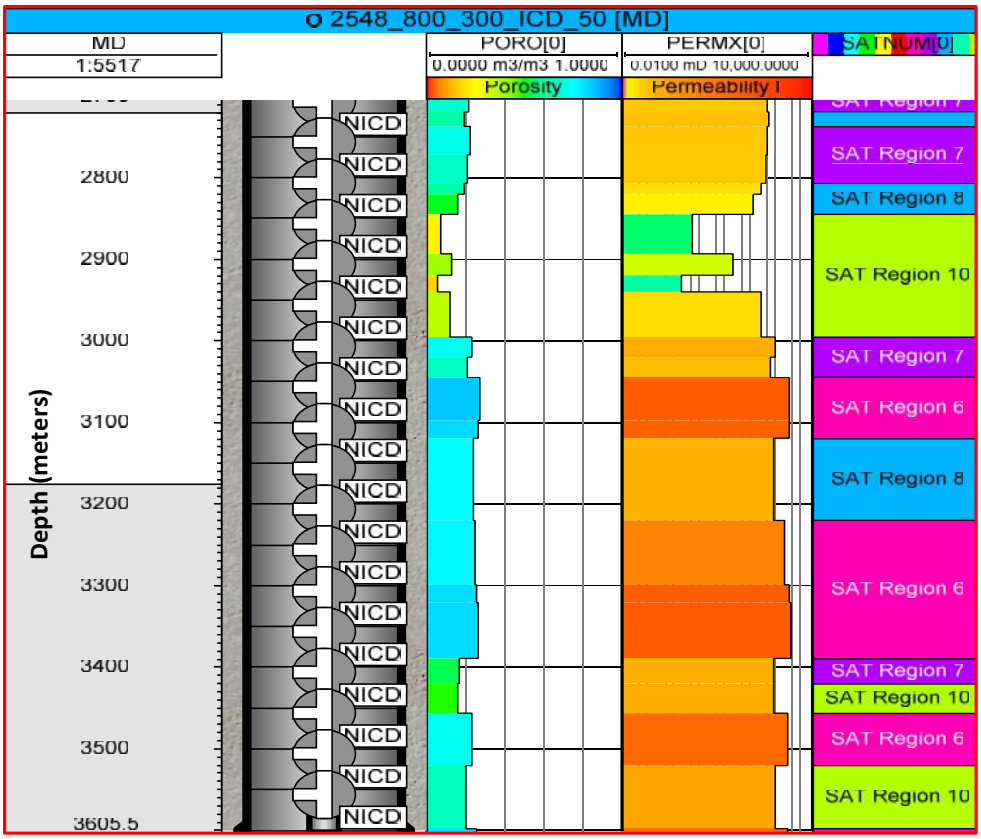

Figure 7.23: Nozzle ICD configuration for case with compartment length of 50 meters

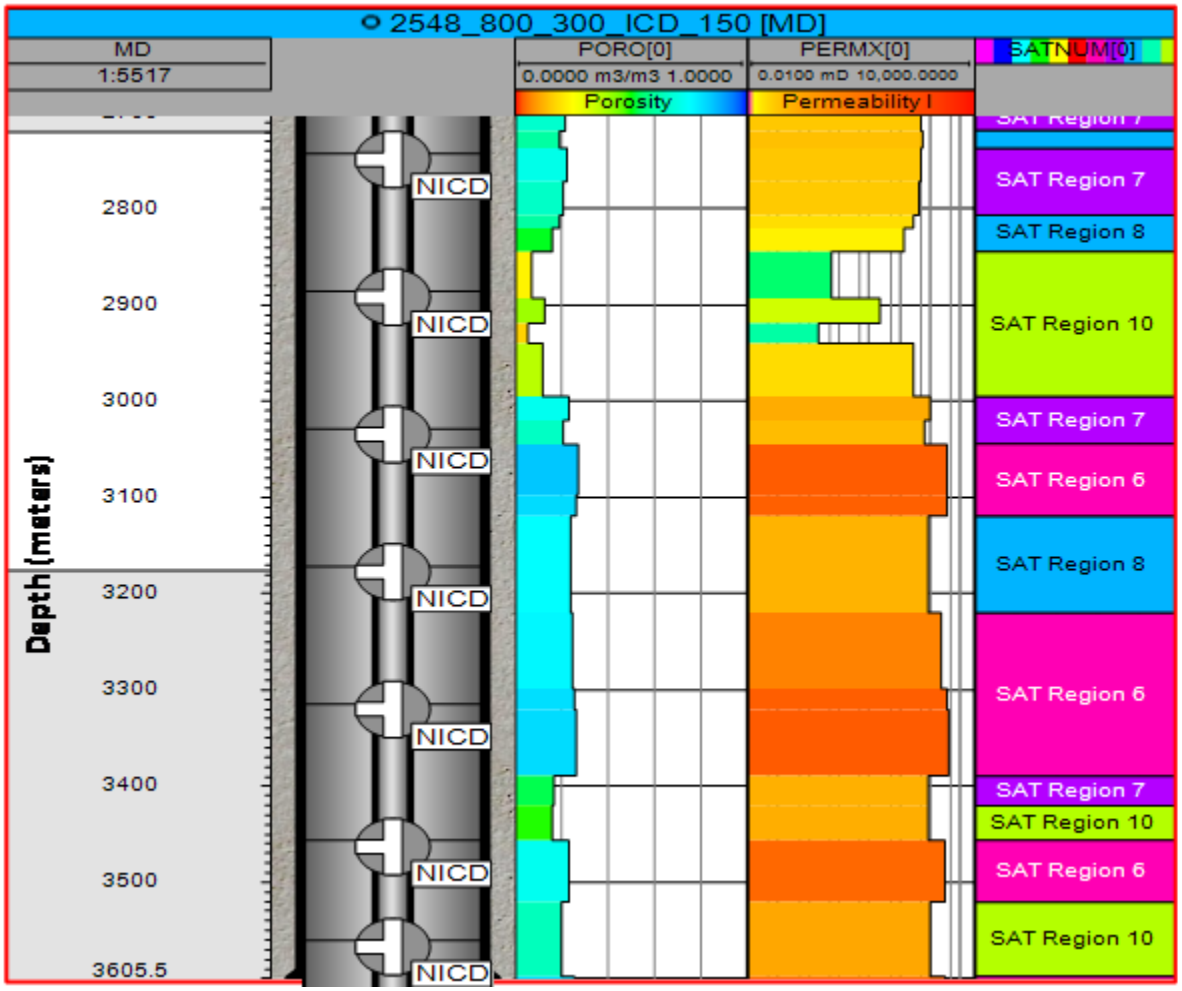

Figure 7.24: Nozzle ICD configuration for case with compartment length 150 meters

7.3.2 Equal length compartments with variable nozzle sizes – Sensitivity on nozzle sizes

In previous section, compartment length was optimized for maximum recovery (150 m of compartment length). It can be seen that seven numbers of ICD are present in the well completion of ICD with a fixed size of 5E-06 m^2. In order to find which ICD has maximum impact on recovery, a sensitivity analysis has been carried out giving a range of minimum and maximum nozzle cross-sectional area. Variable (ICD Nozzle size for seven numbers of ICD) range with base value has been defined in Figure 7.25.

A total of 35 cases have been formulated for the same, details of all the variants are given in Table 6.9. Results of these cases are plotted in form of a Tornado plot (Figure 7.26) where variable which is most sensitive to recovery efficiency is on top and variable with least sensitivity is on bottom. It can be seen that variable $A, $B, $E and $F has got the highest impact on recovery.

	Type	Pr	Int	Name	Base value	Distribution	Arguments			
1	Uncertain			$A	2E-05	Uniform	Min	5E-06	Max	3E-05
2	Uncertain			$B	2E-05	Uniform	Min	5E-06	Max	3E-05
3	Uncertain			$C	2E-05	Uniform	Min	5E-06	Max	3E-05
4	Uncertain			$D	2E-05	Uniform	Min	5E-06	Max	3E-05
5	Uncertain			$E	2E-05	Uniform	Min	5E-06	Max	3E-05
6	Uncertain			$F	2E-05	Uniform	Min	5E-06	Max	3E-05
7	Uncertain			$G	2E-05	Uniform	Min	5E-06	Max	3E-05

Figure 7.25: Sensitivity variable range for nozzle size

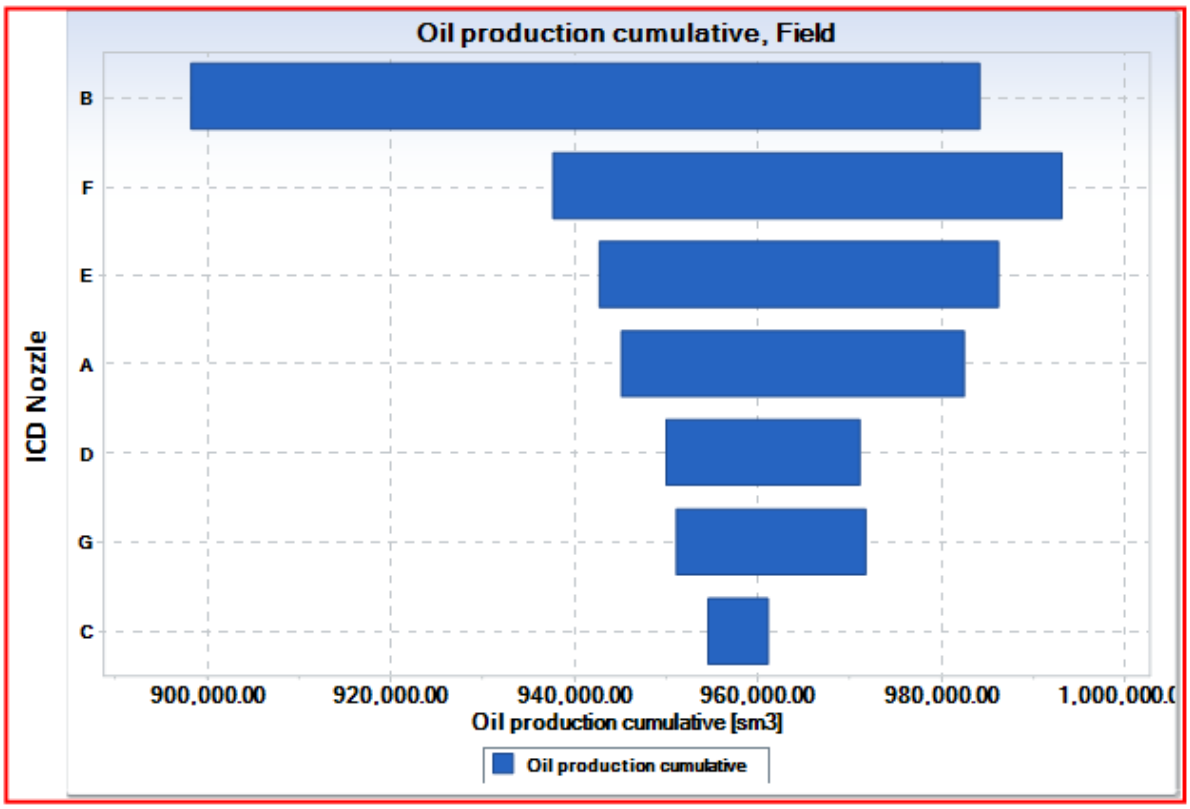

Figure 7.26: Tornado plot for nozzle ICD

7.3.3 Equal Length Compartments with Variable Nozzle Sizes – Uncertainty On Nozzle Sizes

After ascertaining the top four sensitive variables ($A, $B, $E and $F), uncertainty analysis has been carried out on the above variables. A total of seventeen cases have been examined, details of all variables are given in Table 6.10. A comparison of oil production cumulative for all seventeen cases has been presented in Figure 7.27. It can be seen that case (2548_800_300_150_39) gives maximum recovery whereas case (2548_800_300_150_50) gives minimum recovery.

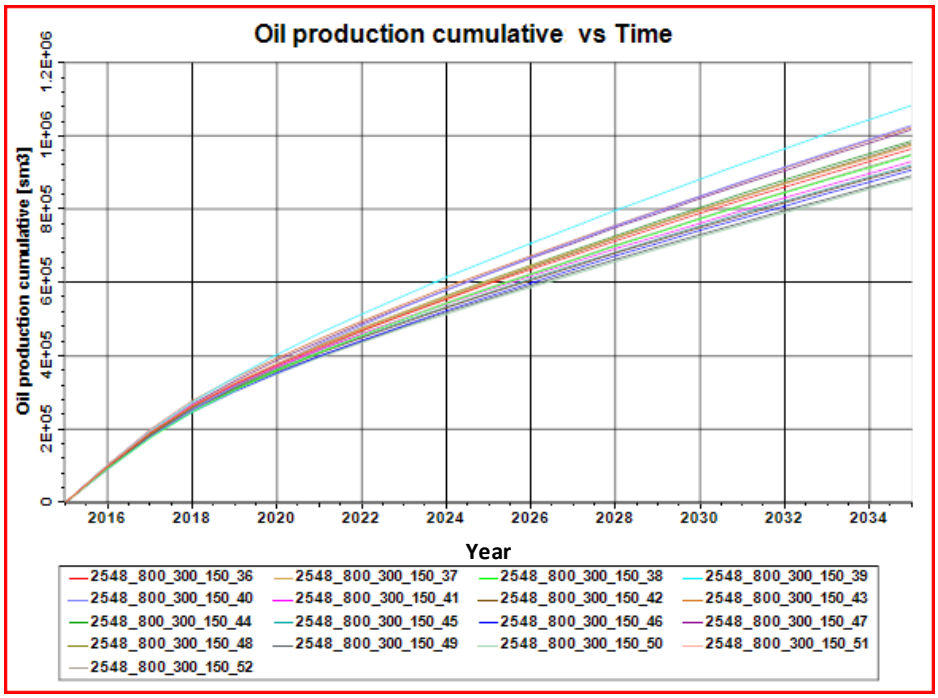

Figure 7.27: Oil production cumulative for all cases

Figure 7.28 compares the production profile of minimum (2548_800_300_150_50) and maximum recovery (2548_800_300_150_39) efficiency.

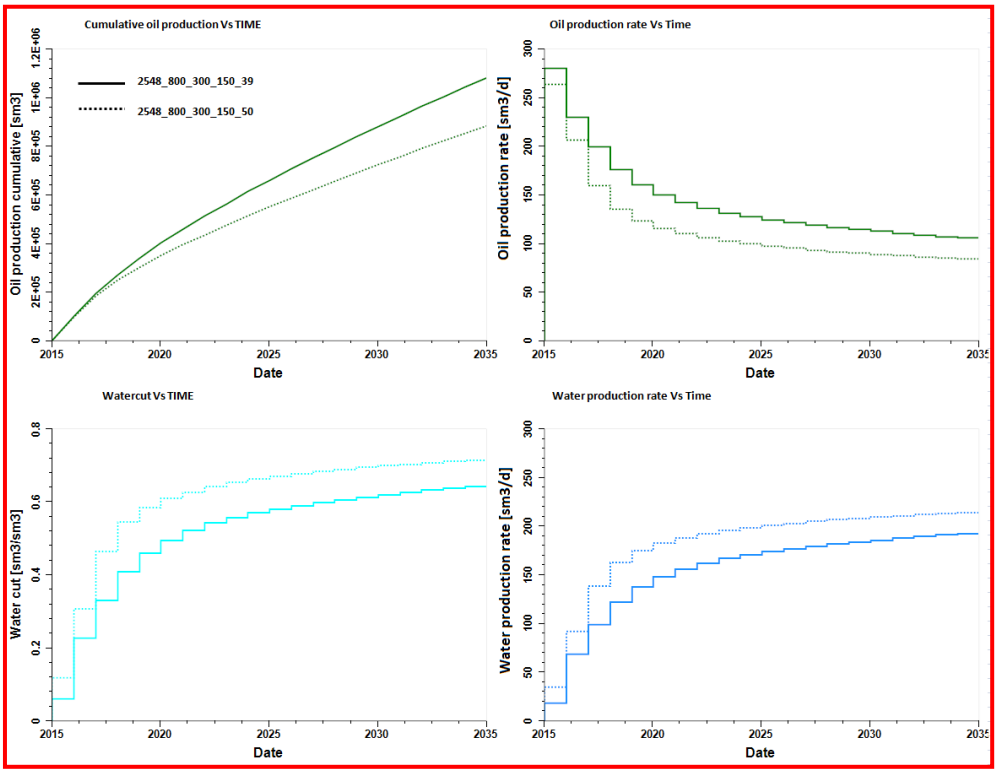

Figure 7.28: Profile comparison with minimum and maximum recovery

Different levels of recovery factor have been obtained from vertical well, horizontal well and smart horizontal well with ICD completions. A comparison of recovery from various wells (vertical, horizontal and smart horizontal well) has been done below in Table 7.2. It can be seen that maximum recovery is coming from ICD well and minimum recovery is coming from vertical well.

Table 7.2: Comparison of cumulative oil production for various completions

Case	Cumulative oil (m^3)
Horizontal Well (2548_800_300)	931630.68
Horizontal well with ICD (2548_800_300_150_39)	1086029.25
Vertical Well (HJN_023_60)	634818.75

7.4 RESULTS AND DISCUSSION OF WELL SPACING OPTIMIZATION OF VERTICAL AND HORIZONTAL WELLS

In the subsequent paragraphs, discussion has been done for well spacing optimization of vertical and horizontal wells. Cumulative oil, gas and water production for all the cases examined has been given in Annexure-VI.

7.4.1 Vertical Well Spacing Optimization

Vertical wells give maximum recovery with offset of 20 m from WOC and withdrawal rate of 150 m^3/d. A sector model was taken for examining optimum well spacing for vertical wells by using the optimum variants for vertical wells. Production profile for various well spacing of vertical wells has been presented in Figure 7.29. Cumulative oil, gas and water production of vertical well spacing optimization cases is presented below in Table 7.3.

Table 7.3: Cumulative oil, gas and water production of vertical well spacing cases

Case	Cumulative oil (m^3)	Cumulative gas (scm)	Cumulative water (m^3)
Well Spacing-100 meters	4947508	2480131840	2536377
Well Spacing-200 meters	7426815	2446394880	2268716
Well Spacing-300 meters	8124438	2772770560	1962128
Well Spacing-400 meters	8202484	2569082112	1904143
Well Spacing-500 meters	6562079	1808067456	1355007

It can be seen from Table 7.3 that vertical well with spacing of 400 m is giving the best recovery out of five cases performed.

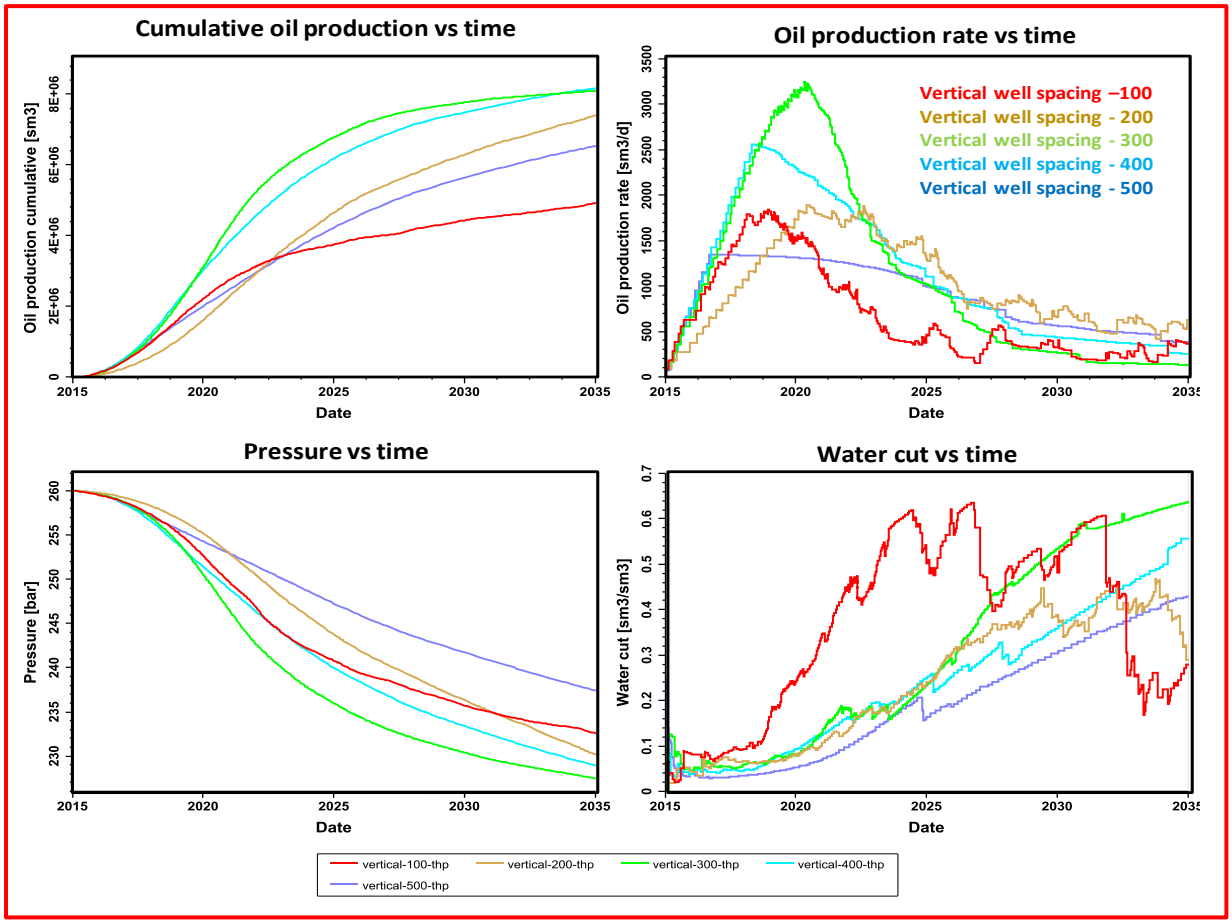

Figure 7.29: Production profile of various development strategies for various well spacing of vertical wells

7.4.2 Well Spacing Optimization of Horizontal wells

Horizontal wells gave maximum recovery with offset of 20 m from WOC, horizontal well length of 800 m and withdrawal rate of 300 m^3/d based on sensitivity results of horizontal well. A sector model was taken for examining optimum well spacing for horizontal wells by using the optimum variants for horizontal well. Production profile for various well spacing of horizontal wells has been presented in Figure 7.30. Three cases were performed in this case (400/200, 300/150, 200/100 m), out of which, case with horizontal well spacing of 300/150 m gave best cumulative oil recovery. Peripheral water injection was deployed on horizontal well spacing of 300/150 m to see the effect of water injection in periphery. Production profile comparison has been done for the horizontal well spacing of 300/150 m(solid line) and with water injection case 300/150_WI (best case with water injection) applied on the same scenario in Figure 7.31.

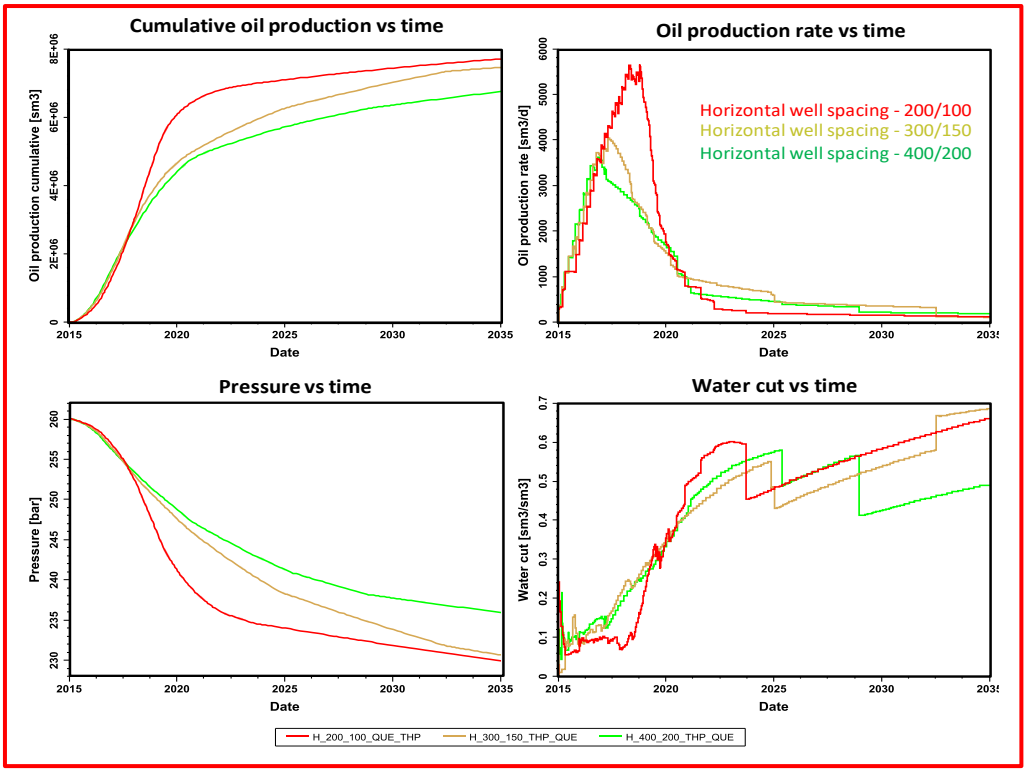

Figure 7.30: Production profile of different well spacing of horizontal wells

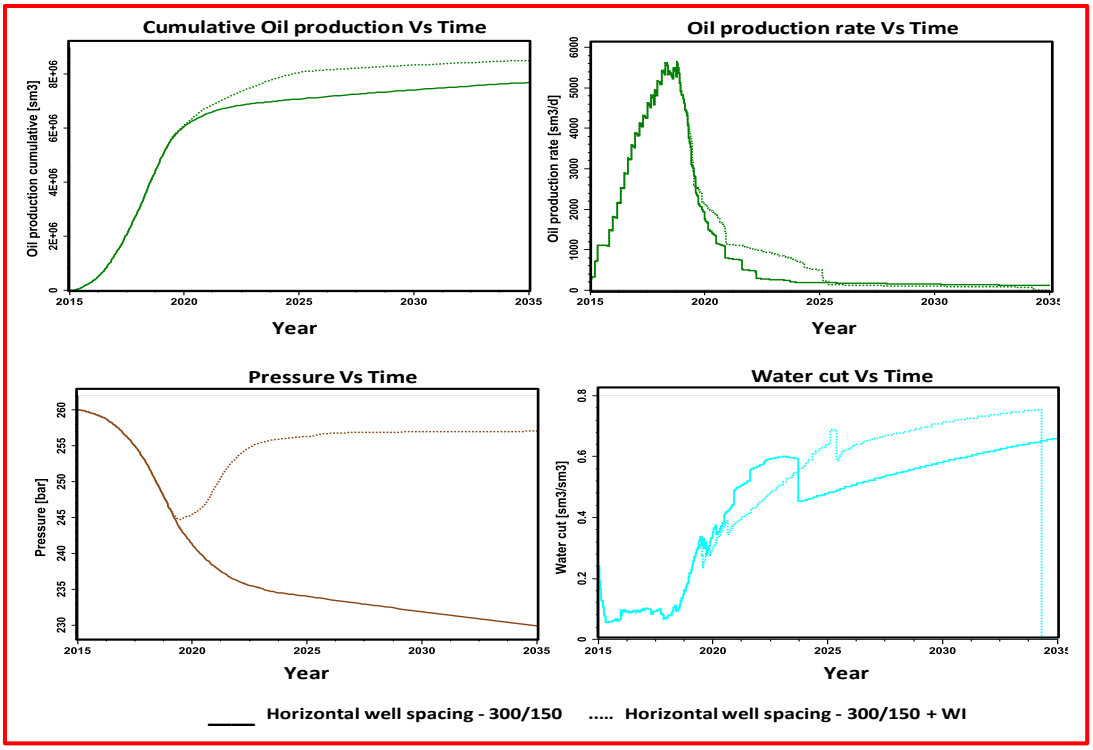

Figure 7.31: Production profile of best case and best case with water injection

Cumulative oil gas and water production for various cases has been given below in Table 7.4.

Table 7.4: Cumulative oil, gas and water production for horizontal wells with different well spacing

Case	Cumulative gas (scm)	Cumulative oil (m^3)	Cumulative water (m^3)
200_100	2336246784	7724854	2871244
300_150	2067583360	7476200	3923506
400_200	1599494784	6766218	3274979
300_150_WI	2317355264	8528678	3745869

It can be seen from Table 7.4 that out of 3 cases (200_100, 300_150 and 400_200) performed for horizontal well spacing, optimum case is 300_150. On the optimum case 300_150, peripheral water injection case (300_150_WI) has been performed which further increases recovery.

Lastly, a comparison has been made on development strategies with vertical well, horizontal well and horizontal well with water injection in Figure 7.32. It can be seen that vertical well with spacing of 400 m withdraw the same amount of oil from the reservoir as horizontal well spacing of 300/150 m. Water injection over horizontal well spacing of 300/150 m further increases the recovery.

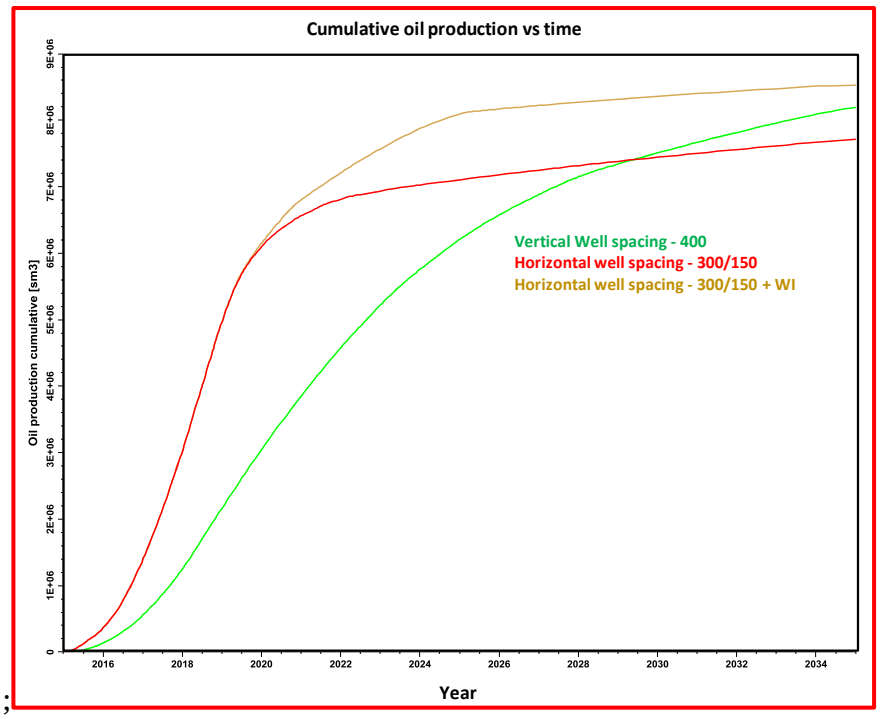

;

Figure 7.32: Cumulative oil production profile comparison

A tabulation of cumulative oil, gas and water production has been carried out in Table7.5 for vertical well with spacing of 400 m, horizontal well spacing of 300/150 m and water injection case on horizontal well spacing of 300/150 m.

Table 7.5: Cumulative oil, gas and water production for best cases of well spacing

Case	Cumulative gas (scm)	Cumulative oil (m^3)	Cumulative water (m^3)
300_150	2067583360	7476200	3923506
300_150_WI	2317355264	8528678	3745869
Vertical-400	2569082112	8202484	1904143

7.4.3 Mobile Oil In Place Calculation

In order to see how much oil is drained from the reservoir from all the cases examined above, mobile oil saturation (Eq 7.1) at the end of prediction has been given from Figure 7.33 through Figure 7.35 for all the cases mentioned in Table 7.5 above.

$$Mobile\ oil\ in\ place = \sum_{k=1}^{n} Pore\ volume * (Oil\ saturation\ at\ End\ of\ Prediction - Residual\ oil\ saturation) \quad (7.1)$$

Where k is variable and n is total no of layers

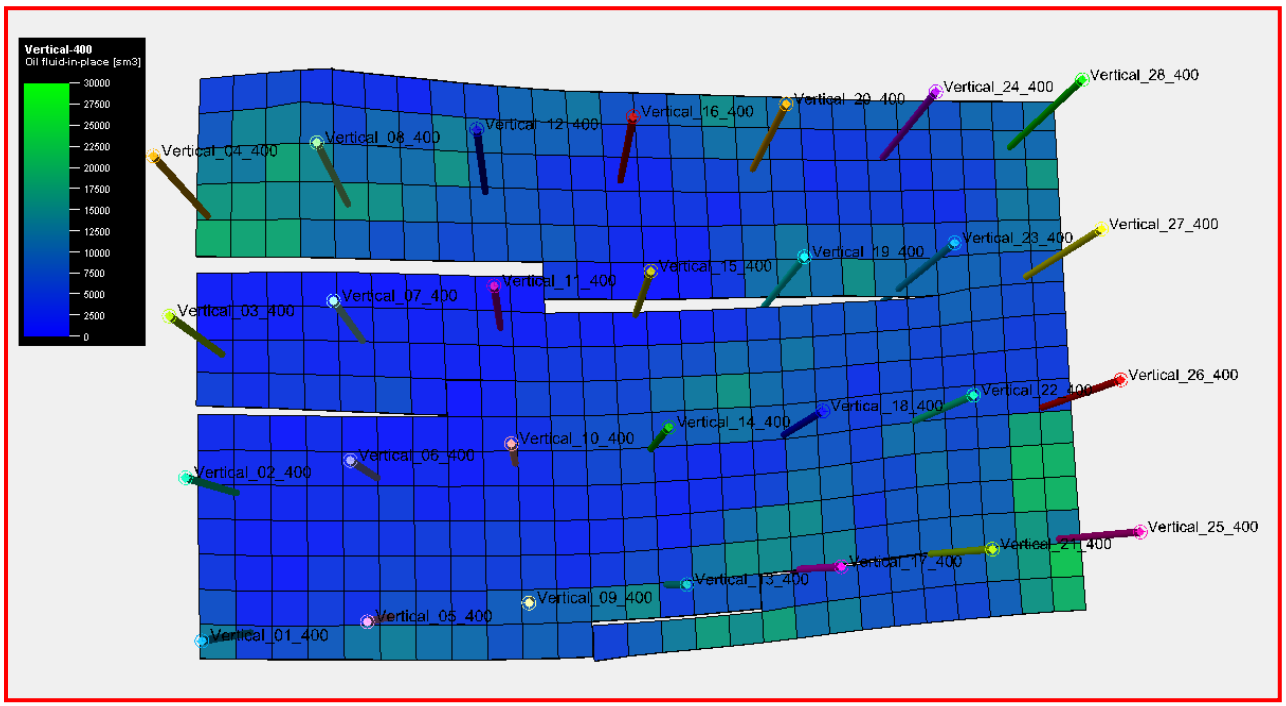

Figure 7.33: Mobile oil at end of prediction for vertical-400 case

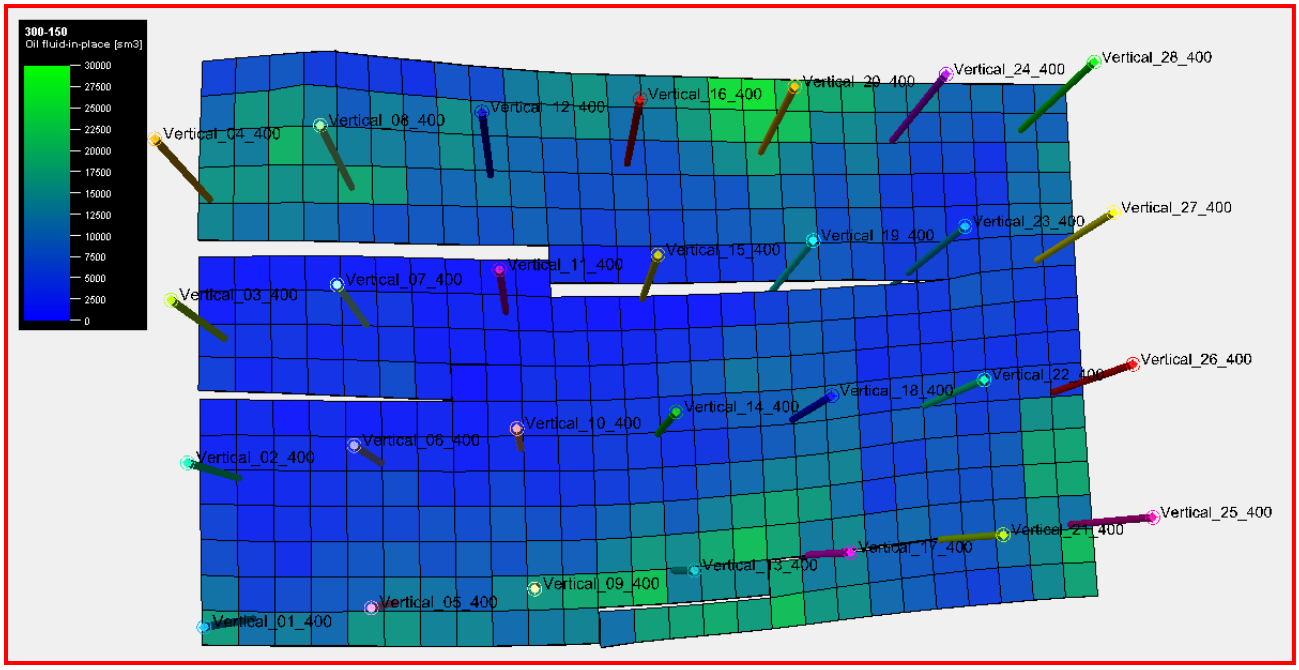

Figure 7.34: Mobile oil in place at end of prediction for horizontal well spacing of 300/150 case

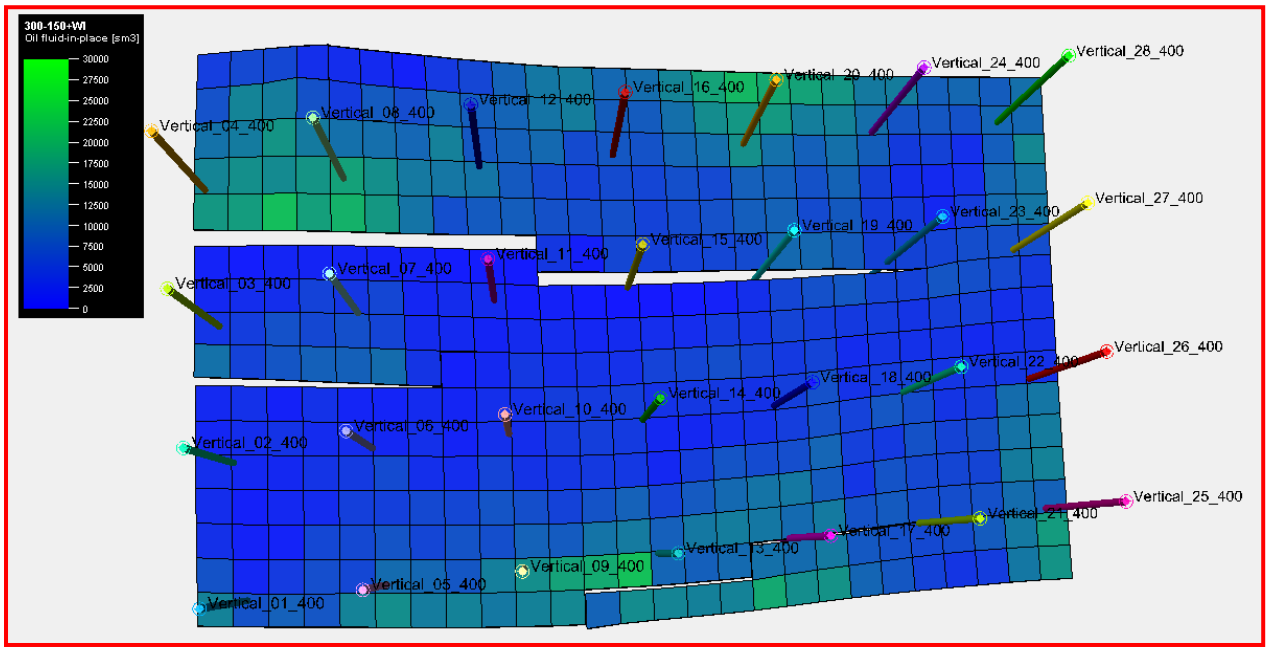

Figure 7.35: Mobile oil in place at end of prediction for horizontal well spacing of 300/150 and water injection case

It can be seen from Figure 7.33 through Figure 7.35 that mobile oil is minimum in case of horizontal well spacing of 300/150 m with water injection.

7.5 ECONOMICS AND RECOVERY FACTOR

Economics and Recovery efficiency for various cases has been compared in the form of a table which is presented in Table 7.7. Table 7.6 lists all the assumptions in working out the economics.

Table 7.6: Economic assumptions

Drilling Cost-vertical well	Rs. 60,000/m
Drilling Cost-horizontal well	Rs. 1,20,000/m
Sales price of Oil	$ 50 / bbl
Sales price Gas	$ 3 /MMBTU
Operating costs for crude oil is Rs. 2275 per m^3	
Operating costs for gas is Rs. 2025 per 1000 scm	
Tax calculated is 33.20% of [revenue - (Drilling expenditure + Workover expenditure+ operating expenditure)]	

Table 7.7: Results for various sensitivity cases

Case	**Number of oil Wells**	**Cumulative oil, (MMm^3)**	**NPV (Crores)**	**Oil in Place (MMm^3)**	**Recovery Factor (RF) (%)**
Vertical Well	1	0.6348	323	1.56	40
Horizontal Well	1	0.9316	495	2.17	43
Horizontal Well+ICD	1	1.086	589	2.17	50
Well spacing-Vertical-400	28	8.1024	4611	18.87	42
Well spacing-Horizontal-300-150	15	7.4762	5311	18.87	40
Well spacing-Horizontal-300-150-WI	15 + 35 WI	8.5287	6016	18.87	45

It can be seen from Table 7.7 that Recovery Factor (RF) from single well has been increased from a level of 40 % to 50 % by using smart horizontal well, also in sector model, 28 vertical well is giving similar recovery as 15 horizontal well. Economic indicator represented above also supports application of smart horizontal well and horizontal well spacing with optimum spacing.

7.6 FIELD DEVELOPMENT

Following the conclusion of the history-match exercise, it was evident that most of the reservoirs would have to undergo additional development in terms of either well intervention in existing wells and/or infill wells and/or injection wells, horizontal wells and ICD completion.

The Field Development Plan (FDP) exercise is carried out for the said reservoirs under study (for which the history-matched model is available).Following step-wise procedure is used for understanding the role of different options in the development plan**.**

- Scenario-A:Base case
- Scenario-B: Well Intervention case
- Scenario-C:Infill case
- Scenario-D: Pressure maintenance case
- Scenario-E: Simultaneous Water and Gas Injection case

Well intervention and infill well placement has been done based on following factors

- Mobile oil hydrocarbon pore volume (HCPV)
- Quality of history match around the wells
- Porosity, permeability and rock-type
- Connectivity around the well
- Distance from GOC and FWL
- Location of fault

The prediction cases for each reservoir were run using well production-rate control. The wells were given the production constraints as per the surface handling capacities. Overall production constraints as imposed by the Group have also been defined. The wells were subjected to certain other constraints as shown in Table 7.8.

Table 7.8: Well-level constraints for prediction runs

Constraints	Value
Maximum individual well production rate	Based on historical well production rate in the reservoir
Completion type	Single Completion: bottom-to-top
Minimum well bottom-hole pressure	50-100 bars, depending upon the segment

Maximum Water Cut	95%
Minimum economic limit on oil-rate	1 m^3/d
Maximum GOR constraint	1500 scm/m^3

7.6.1 Scenario-A: Base case

The individual production levels established from existing wells were used in the Base case. The wells are allowed to flow until economic limits are reached and shut in thereafter. The wells have constraints upon maximum Water Cut and maximum GOR, which are 95% and 1500 v/v sequentially. The field level production profile is shown in Figure 7.36.

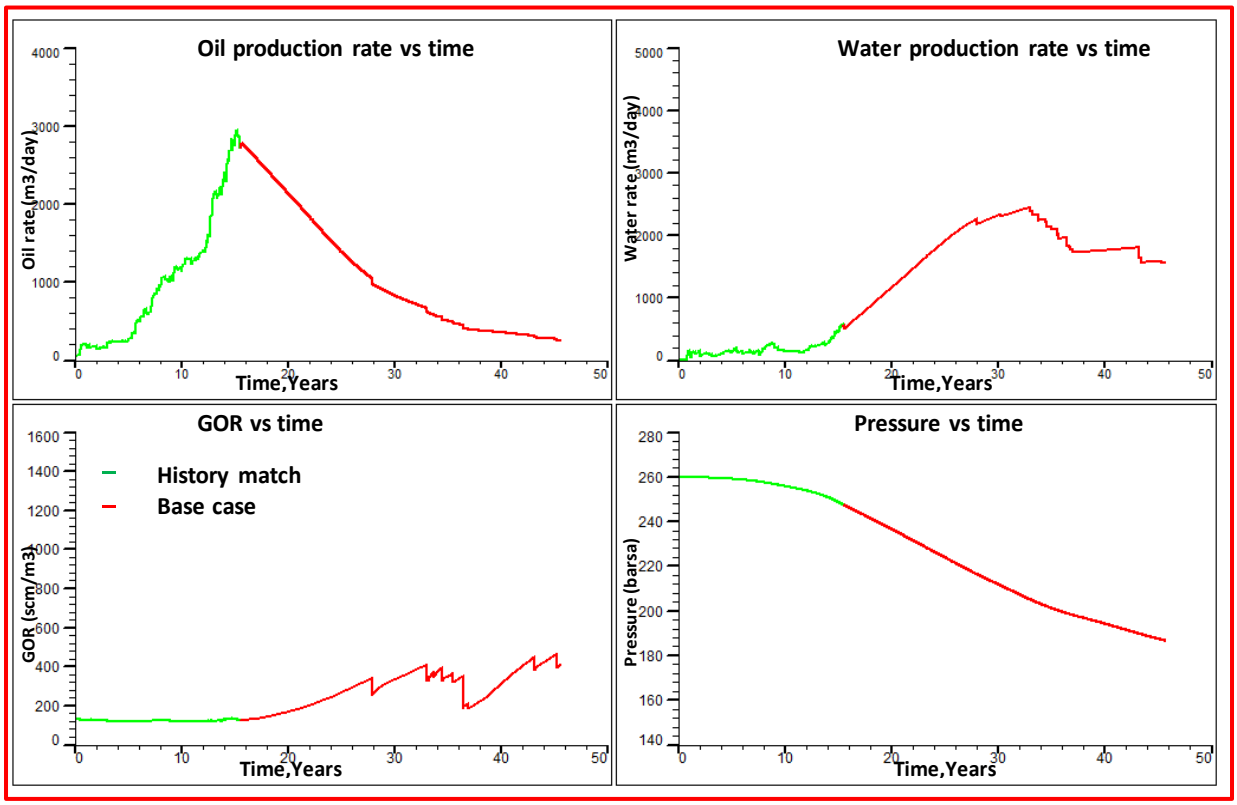

Figure 7.36: Pressure production profile for Scenario-A

This case predicts 17.48 MMm^3 oil and 3.45 BCM gas in a period of 30 years.

7.6.2 Scenario-B: Well Intervention case

For this scenario, the same well constraints as in the Base case were applied. Overall, this case predicts an incremental gain of 0.91 MMm^3 oil and 1.24 BCM gas over the Base case. Results of the Well Intervention case have been presented in Figure 7.37.

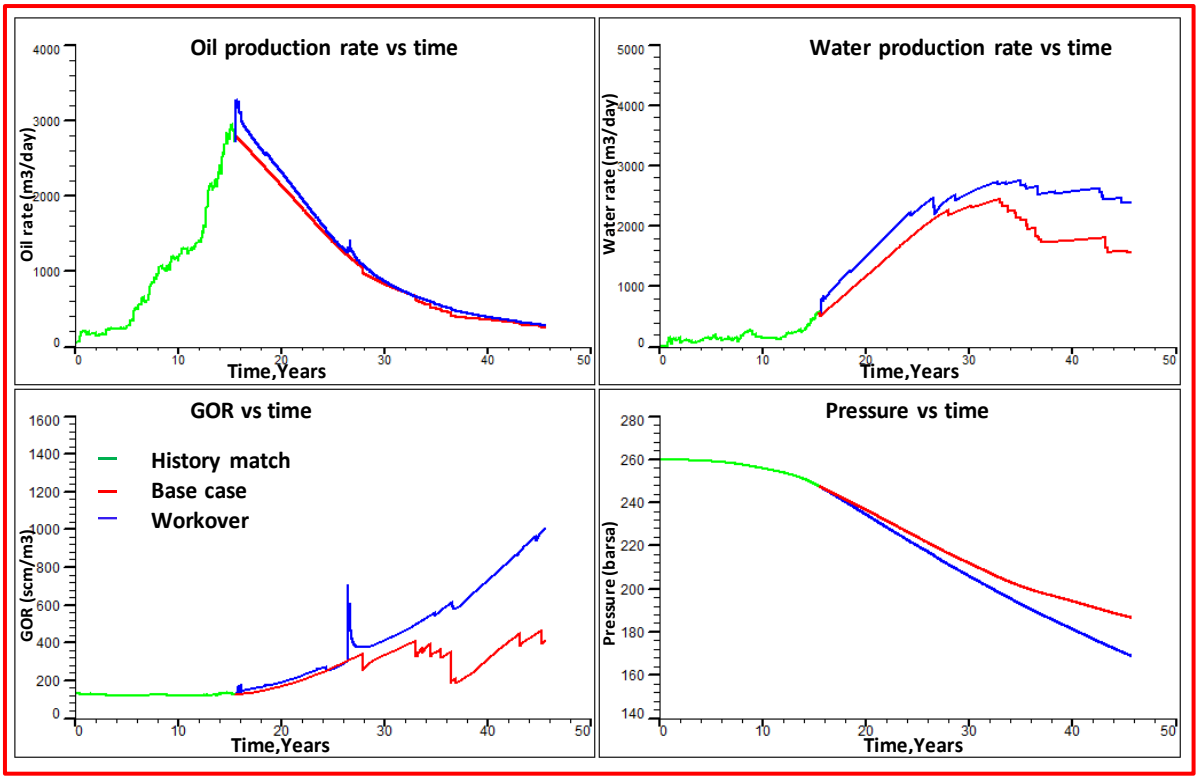

Figure 7.37: Pressure production profile comparison of scenario-B

Remaining mobile oil in place (Equation 7.1) calculated after the end of prediction has been shown below in Figure7.38.

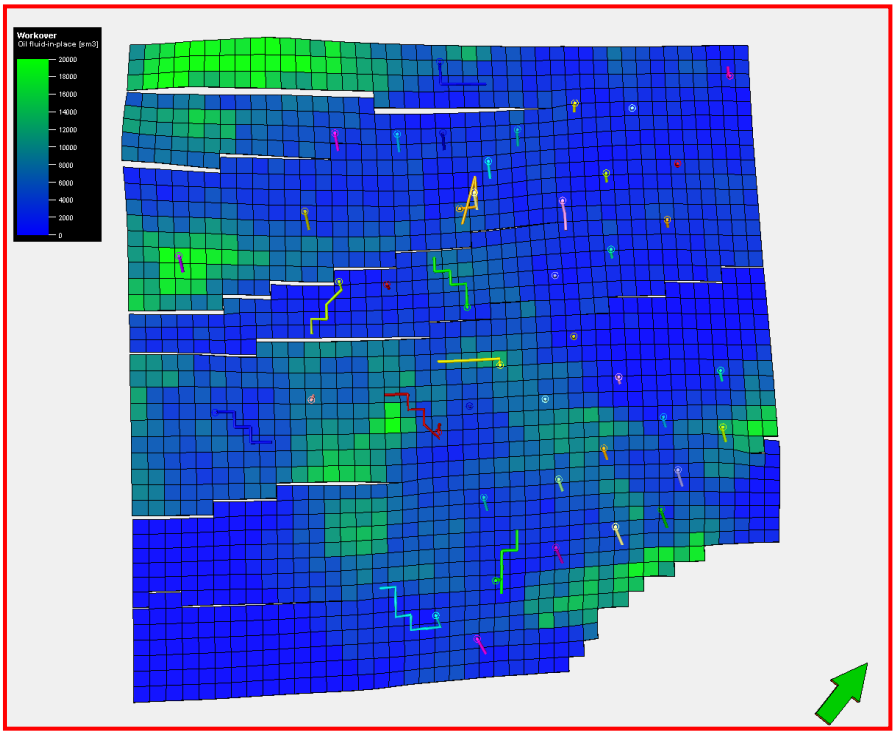

Figure 7.38: Mobile oil in place at end of prediction for Scenario-B

It can be seen that major part of the reservoir has been drained, still some oil is left, and for which infill locations have been proposed in Scenario-C.

7.6.3 Scenario-C: Infill case

Based on mobile oil saturation shown in Figure 7.37, vertical and horizontal locations have been placed in the simulation model.

With five vertical and eight horizontal locations, Scenario-C has been performed on top of well intervention case. Production profile at the field level has been shown in the Figure 7.39.

This case predicts an incremental gain of 1.57 MMm^3 oil and 2.86 BCM gas over the Base case.

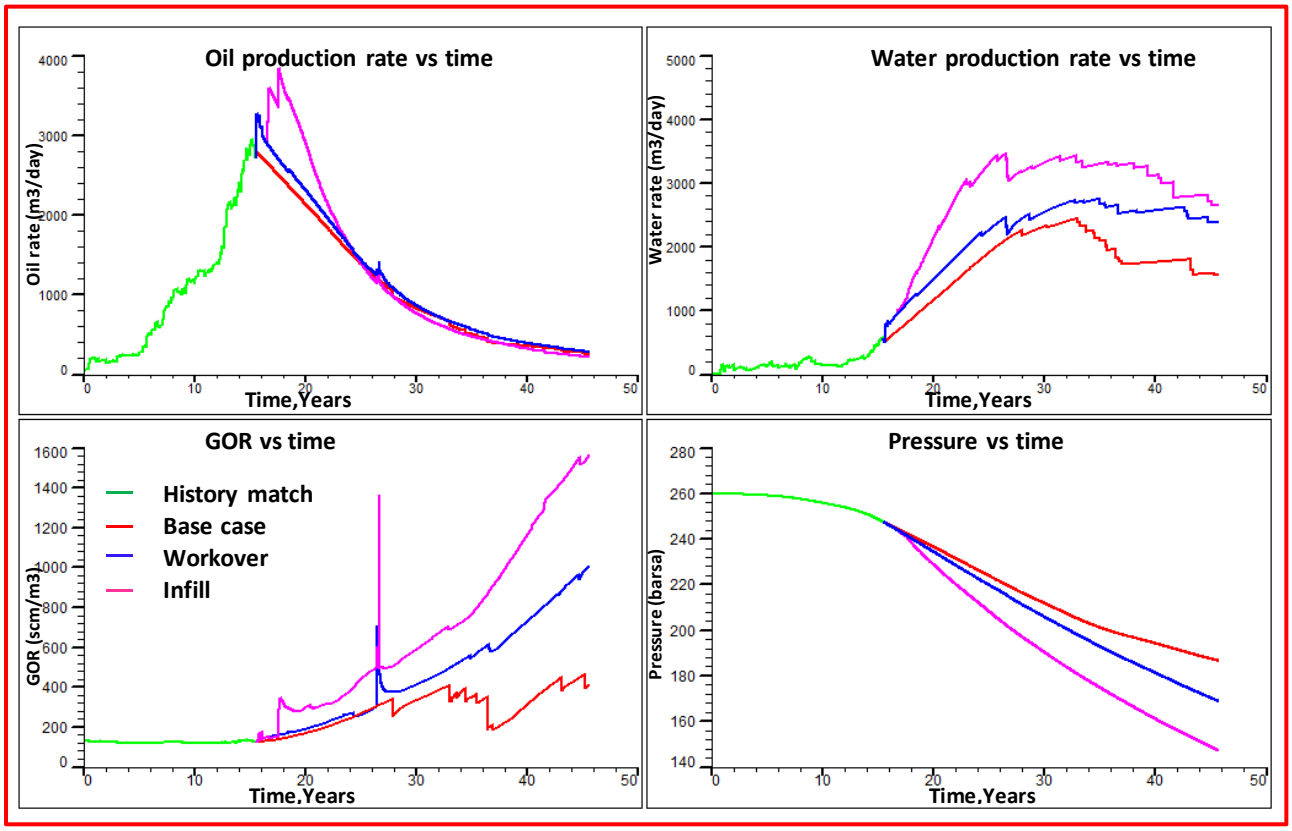

Figure 7.39: Pressure production profile comparison of Scenario-C

Mobile oil in place has been plotted in Figure 7.40 to show the drainage pattern performed by vertical and horizontal wells.

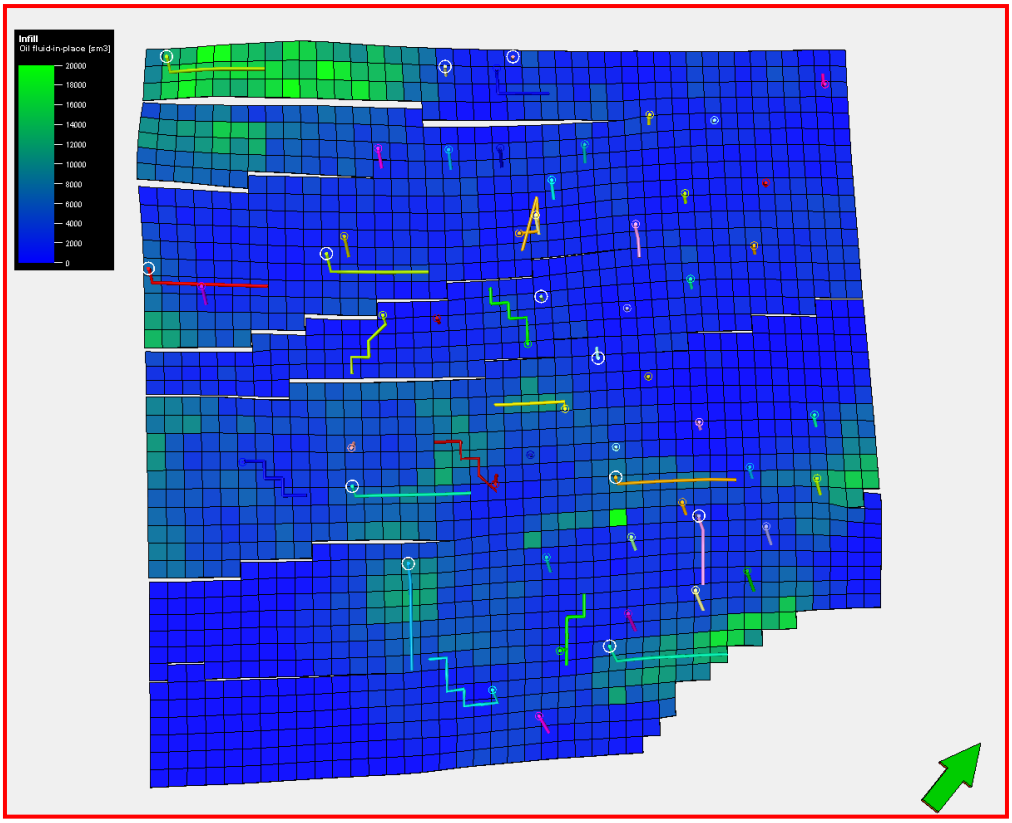

Figure 7.40: Mobile Oil Volume at the end of the Scenario-C

It can be observed that most of the mobile oil has been swept, still there are two concerns viz. pressure drop from 260 bars to 157 bars and unswept oil left. For the first concern Scenario-D has been performed, which is described below.

7.6.4 Scenario-D: Pressure Maintenance case

As there is a drop of ~98 bars (Figure 7.39) in Scenario-C, it is pertinent to compensate the voidage replenishment. A voidage of ~80 MMm^3 at reservoir condition has been created in the reservoir by taking into consideration from oil, water and gas (Figure 7.41). For compensating this large voidage, 26 water injection wells have been drilled in periphery. In order to examine the effect of introducing Pressure Maintenance scheme in the reservoir and to estimate the incremental recovery arising out of this option, Hit Squad technique was also considered (Garimella et al., 2009).

Voidage created by all cases and field water injection cumulative has been shown in Figure 7.41. It can be seen that around 70% voidage has been replenished by peripheral water injection scheme.

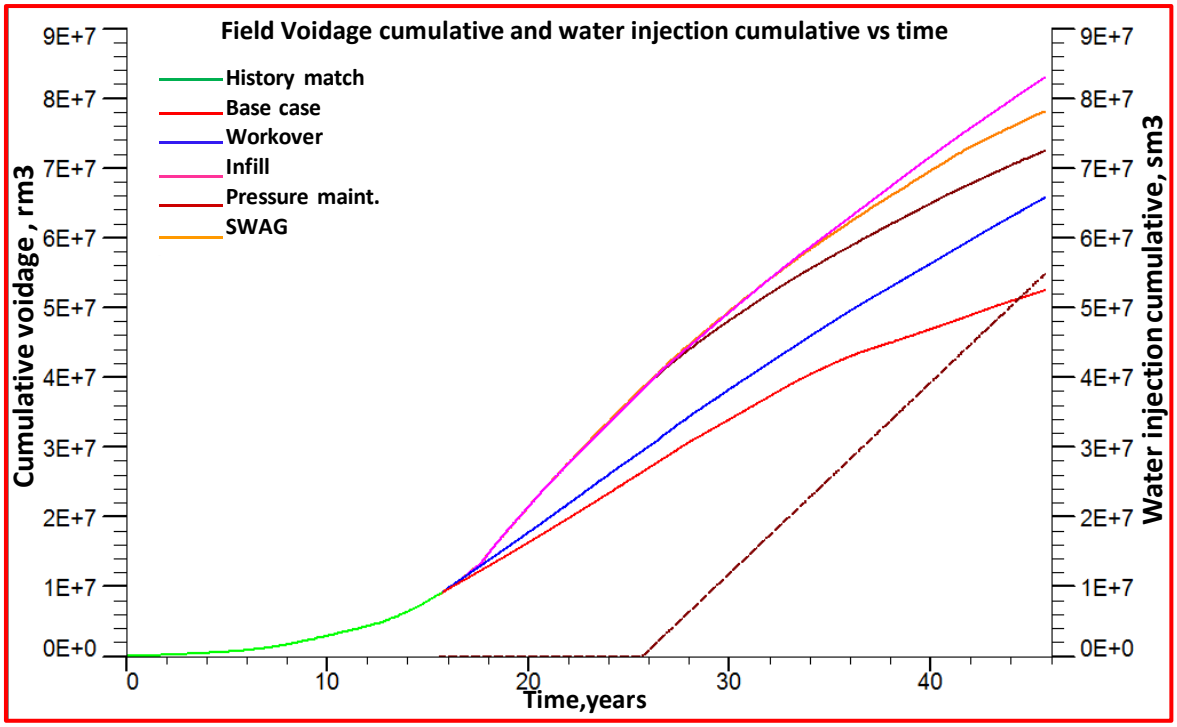

Figure 7.41: Comparison of Voidage and water injection cumulative

Production profile of Scenario-D is shown in Figure 7.42. This case predicts an incremental gain of 1.69 MMm^3 oil and 0.96 BCM gas over the Base case, also pressure at EOP is restored to a level of 232 bars by pressure maintenance.

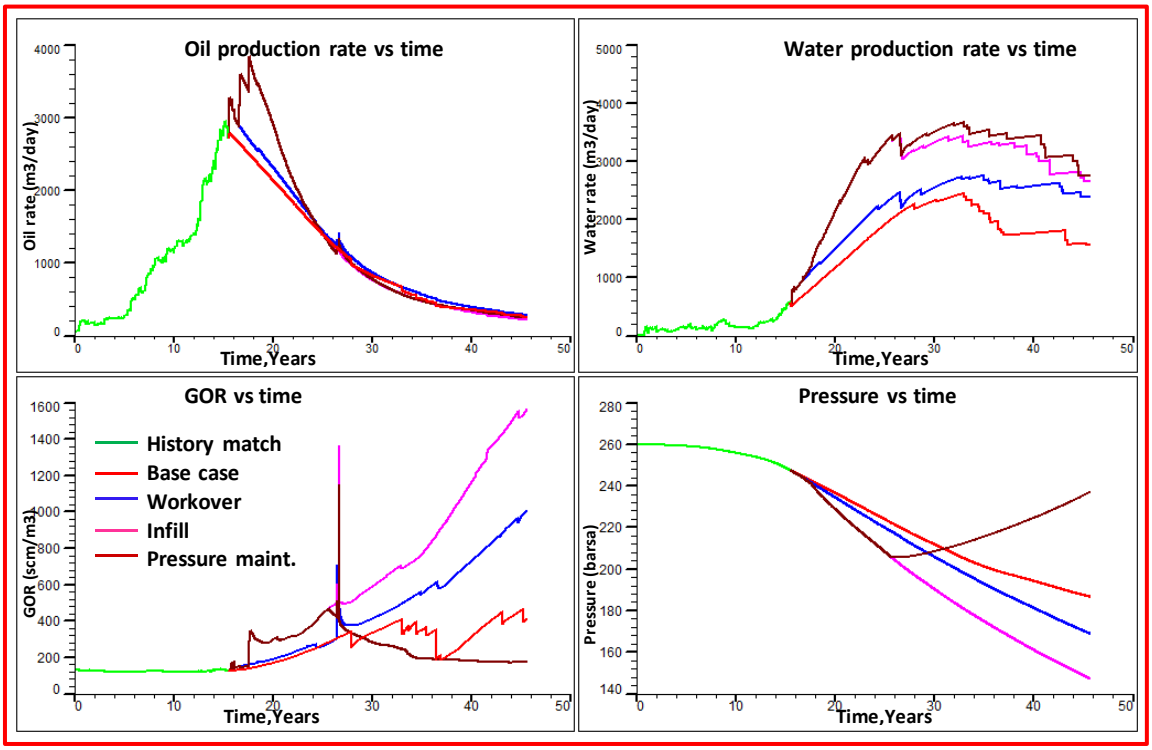

Figure 7.42: Pressure Production Profile comparison of Scenario-D

7.6.5 Scenario-E: Simultaneous Water and Gas Injection (SWAG) case

Scenario-C and Scenario-D produces almost same level of oil, but scenario D produces less gas and preserves reservoir pressure. Mobile oil in place shown at the end of Scenario-C shows some scope of productivity enhancement by tapping unswept oil. This is carried out in Simultaneous Water and Gas Injection case, where water is injected at the top part of oil column and gas is injected at the bottom part of oil column to take advantage of gravity. A total of twenty-six water injectors and gas injectors are placed in the simulation model.

Production profile of Scenario-E is shown in Figure 7.43.This case predicts an incremental gain of 3.08 MMm^3 oil and 2.04 BCM gas over the Base case. Also pressure is restored to a level of 238 bars at EOP.

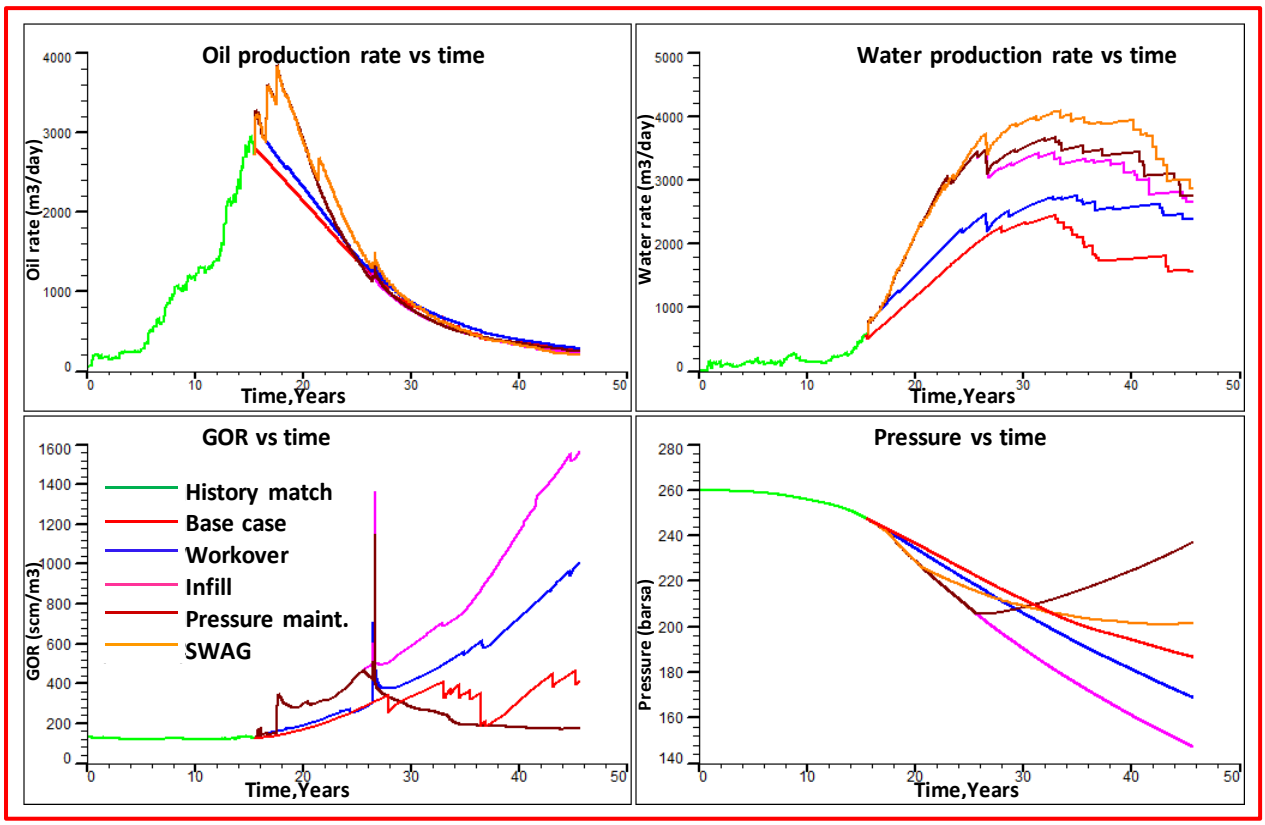

Figure 7.43: Pressure production profile comparison of Scenario-E

In this scenario, all horizontal locations viz. H-1 through H-8 (8 wells) have been converted to smart horizontal well, representative well schematic with number of compartments and nozzles have been shown in Figure 7.44 for two wells H-2 and H-7. Production profile of all eight horizontal wells (solid line) before and after conversion to smart horizontal well (dotted line) is shown in Figure 7.45 and Figure 7.46.

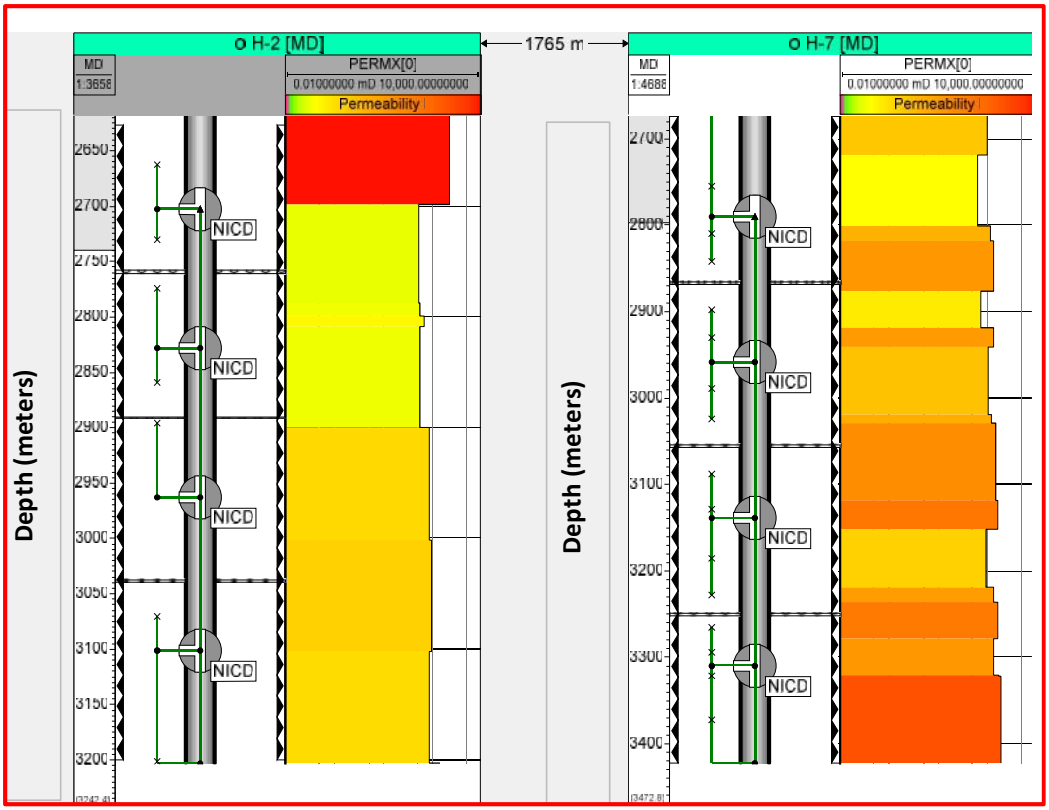

Figure 7.44: ICD completion diagram for Well H-2 and H-7

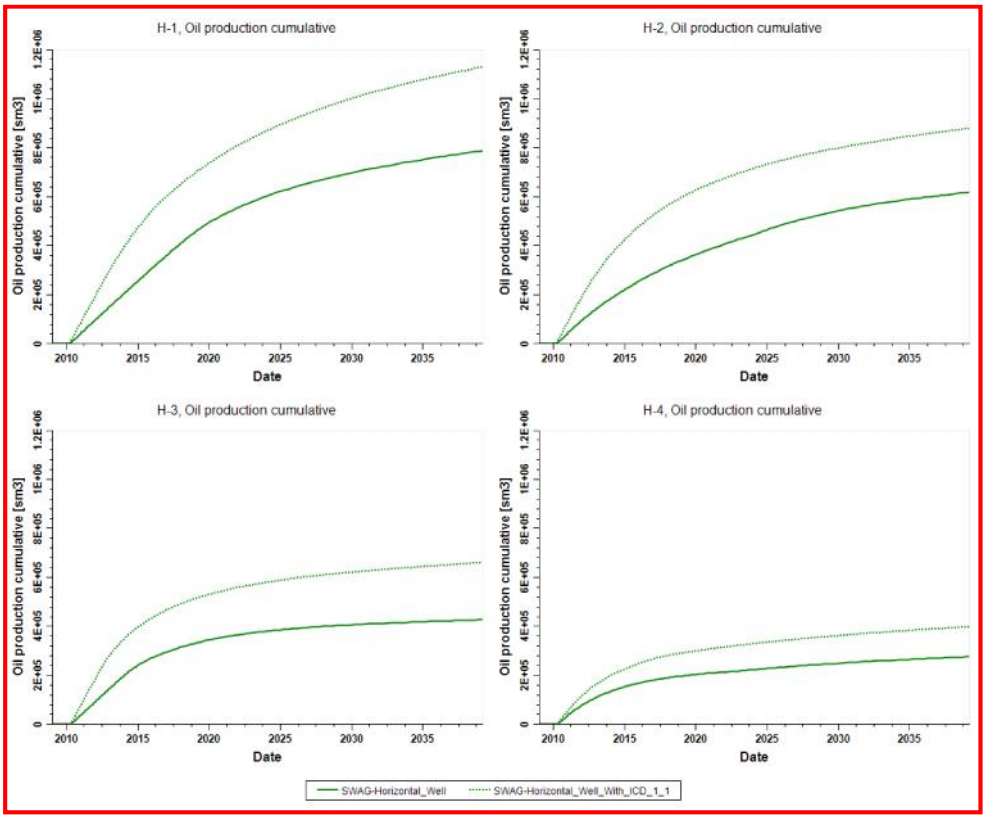

Figure 7.45: Comparison of cumulative oil production of horizontal well and horizontal well converted to ICD well (H-1 to H-4)

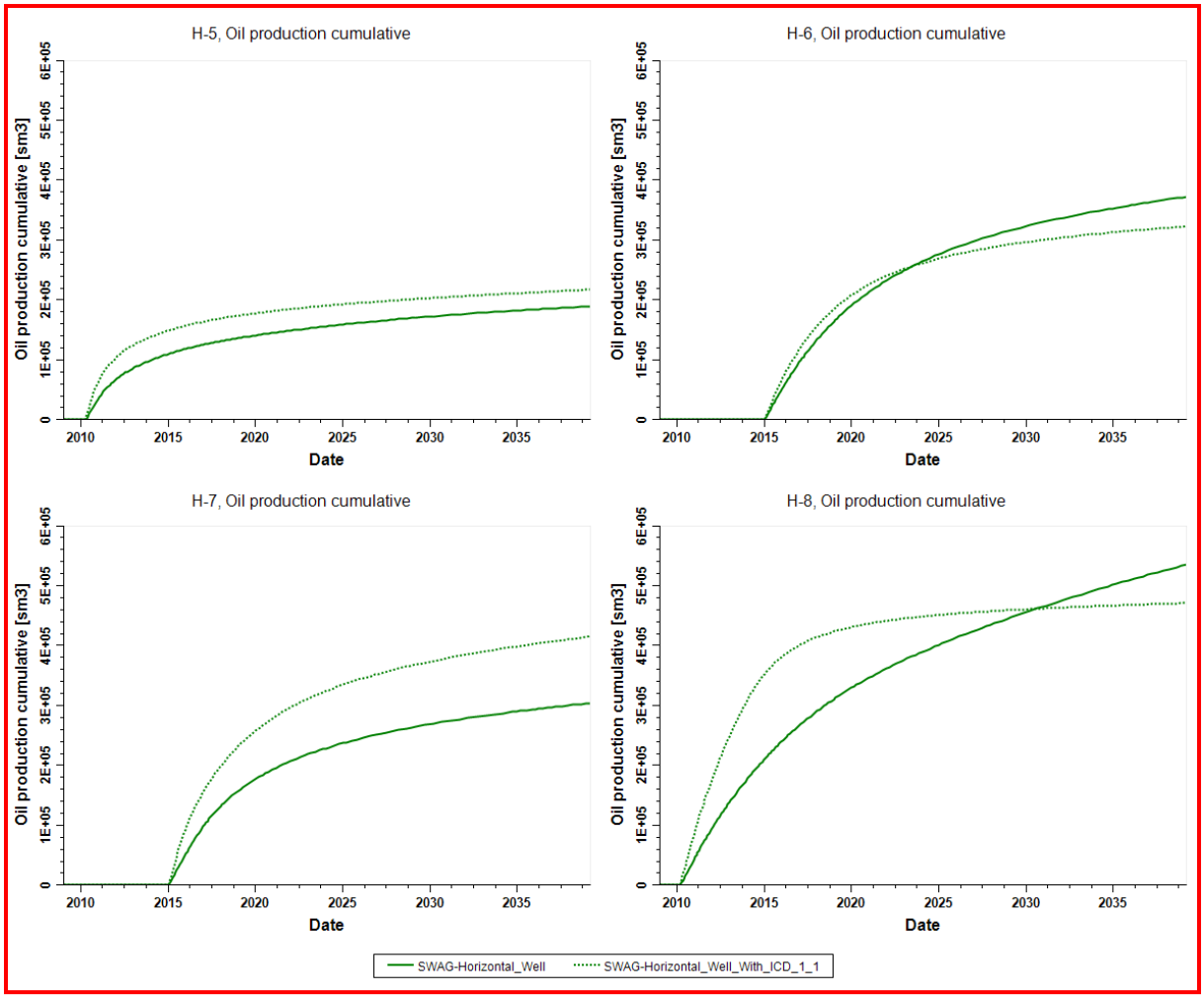

Figure 7.46: Comparison of cumulative oil production of horizontal well and horizontal well converted to ICD well (H5 to H-8)

It can be seen that there is a large change in productivity in all wells except well H-6 and H-8 after conversion to ICD completion, with the optimized parameters obtained from sensitivity results from smart horizontal well.

In order to illustrate the effectiveness of SWAG process a well schematic of infill producer without SWAG injector and infill producer with SWAG injector has been shown in Figure 7.47 and Figure 7.48 respectively. It can be seen that unswept oil in the vicinity of producer is tapped using SWAG injector, which is shown in Figure 7.47.

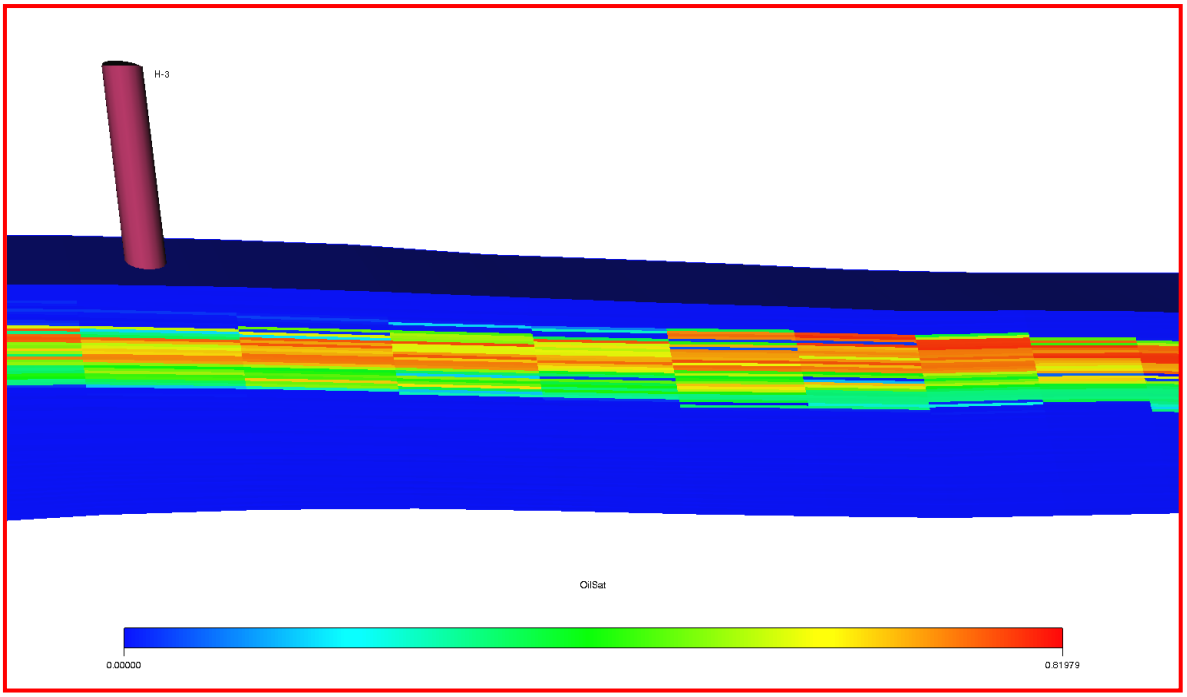

Figure 7.47: Cross section of oil saturation around the wellbore –pre-SWAG

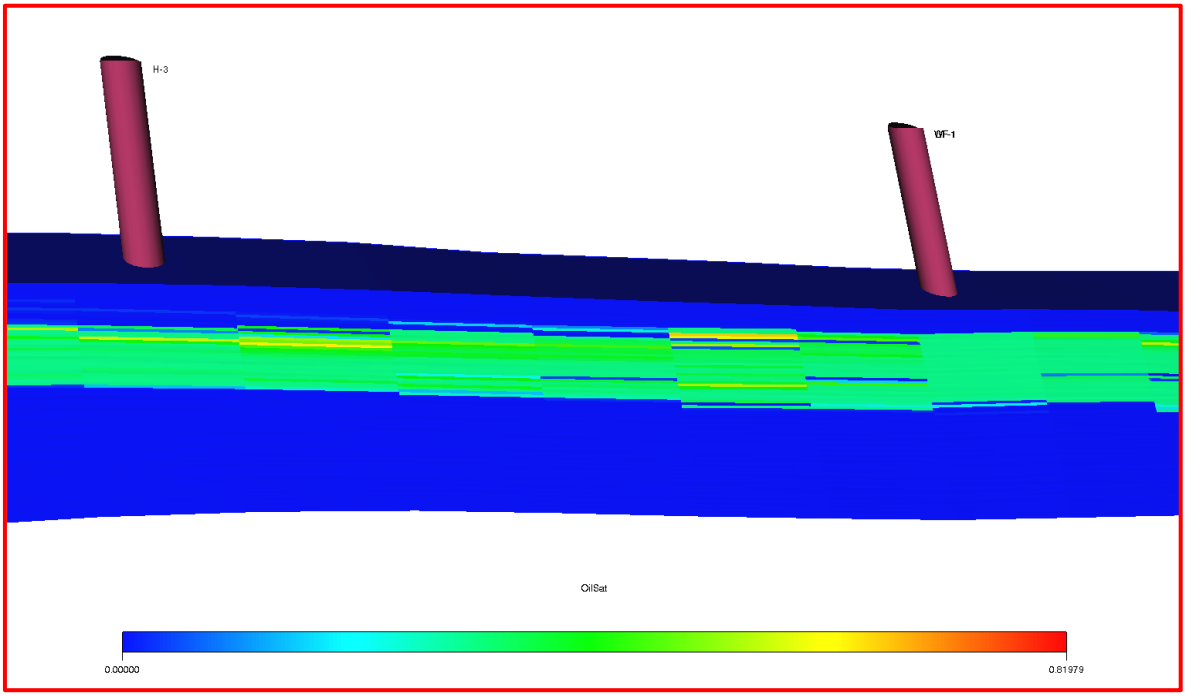

Figure 7.48: Cross section of oil saturation around the wellbore –after SWAG

Mobile oil at the end of SWAG case has been presented in Figure 7.49.

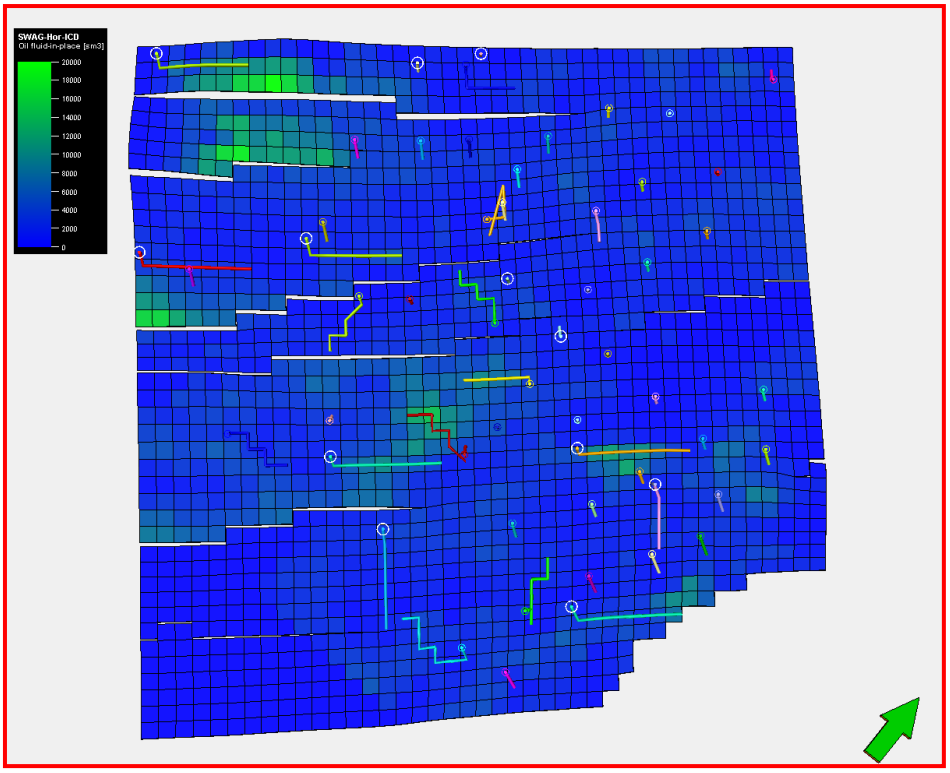

Figure 7.49: Mobile oil at the end of Scenario-E

7.7 ECONOMICS ANALYSIS

In order to compare the recovery efficiency and economic indicator of various scenarios, Table 7.10 has been prepared, which compares Recovery Factor (RF) as well as Net Present Value (NPV) for various cases examined. Results of field development cases examined have been given in Annexure-VII. Various assumptions have been made in calculating NPV for scenarios, which is presented in Table 7.9.

Table 7.9: Economic Assumptions

Drilling Cost-vertical well	Rs. 60,000/m
Drilling Cost-horizontal well	Rs. 1,20,000/m
Sales price oil	$ 50 / bbl
Sale price Gas	$ 3 /MMBTU
Operating costs for crude oil is Rs. 2275 per m^3	
Operating costs for gas is Rs. 2025 per 1000 scm	
Tax calculated is 33.20% of [Revenue - (Drilling expenditure + Workover Expenditure+ Operating Expenditure)]	

Table 7.10: Results of various prediction scenarios

Case	OIP (m^3)	Number of wells	Cumulative oil production (m^3)	Incremental over Base case (m^3)	Recovery Factor (%)	NPV (Crores)
History Match		46	5749900		11.51	
Base case	49949992	46	17489676		35.01	5894
Well Intervention case (30 Nos)		46	18386962	897286	36.81	6389
Infill case		46 + 5 V + 8 H	19055518	1565842	38.15	7334
Pressure Maintenance case		46 + 5 V + 8 H + 26 WI	19165876	1676200	38.37	7046
SWAG case		46 + 5 V+ 8 H-ICD + 26 SWAG Injector	20561430	3071754	41.16	8037
V: Vertical wells, H: Horizontal wells, H-ICD: Horizontal well converted to ICD WI- Water injector well						

7.8 CHAPTER SUMMARY

This chapter gives information on results and discussion of sensitivity cases performed on vertical well, horizontal well and smart horizontal well followed by well spacing optimization for vertical and horizontal wells. Optimized variants for vertical well, horizontal well and smart horizontal well is used in field development and planning. Calculation on productivity index/critical rate/breakthrough time for vertical, horizontal well along with horizontal well length optimization has been done in ANNEXURE-VIII along with referred literature on vertical/horizontal and smart horizontal well.

CHAPTER 8

CONCLUSION AND RECCOMENDATION FOR FUTURE WORK

8.1 CONCLUSIONS

In this thesis, reservoir characterization of a mature field having bottom water drive has been carried out using relative permeability based on Rock typing, capillary pressure, saturation-height thickness, reservoir fluid characterization (using constant composition expansion and differential liberation lab data), material balance studies (for drive mechanism determination, Oil in place, Aquifer strength determination). After doing analytical studies, a three-dimensional, three-phase numerical simulation model has been developed for a bottom water drive reservoir using all static properties i.e. porosity, permeability in all three direction, facies distribution and dynamic data i.e. pressure, production history and well events (perforation, plug etc.).

This developed static model was validated for a mature field having bottom water drive using pressure production history of sixteen years over forty six numbers of individual wells using industry standard software. This validated model was used for doing various sensitivity analyses on vertical, horizontal and smart horizontal well.

Firstly, the effect of withdrawal rate and offset from WOC on cumulative oil production was studied for a vertical well. From this study, it was concluded that offset from WOC and withdrawal rate has an impact on cumulative oil production in case of vertical well. From sensitivity study on offset & withdrawal rate it, was observed that offset has more impact on cumulative oil production than withdrawal rate.

Next, effect of withdrawal rate, offset from WOC and horizontal well length on cumulative oil production was analyzed for horizontal well. From this study, it was concluded that offset from WOC, horizontal well length and withdrawal rate has an impact on cumulative oil production in case of horizontal well. Maximum impact on cumulative oil production is given by offset from WOC followed by withdrawal rate and lastly on horizontal well length. With optimized variant for horizontal well, increased recovery has been obtained when compared to vertical well cumulative oil production.

Next, effect of compartment length was studied with optimized variants (withdrawal rate, offset from WOC and horizontal well length) of horizontal well on cumulative oil production, which was analyzed for smart horizontal well. Also, effect of nozzle size and number of nozzles were studied with optimized variants (withdrawal rate, offset from WOC and horizontal well length) of horizontal well and optimized compartment length on cumulative oil production, which was analyzed for smart horizontal well. Compartment length and Nozzle size has an impact on cumulative oil production in case of smart horizontal well (ICD). Maximum impact on cumulative oil production is given by nozzle size in each ICD followed by compartment length. Maximum recovery was obtained with smart horizontal well with ICD completion when compared with vertical and horizontal well.

Next, with optimized variants (offset from WOC and withdrawal rate) obtained for vertical well and optimized variants (offset from WOC, horizontal well length and withdrawal rate) for horizontal well, effect of well spacing for vertical well and horizontal well on cumulative oil production was analyzed in a sector model. Well spacing has an impact on cumulative oil production for vertical as well as horizontal wells. With optimal number of wells, approximately same amount of oil can be recovered. Application of horizontal well with optimized spacing gave similar recovery when compared to vertical well, but with less number of wells, which resulted in better economics.

Next, field development study of mature field having bottom water drive and 16 years of production history was carried out on full field using various development strategies i.e. Base case, well intervention case, infill vertical and horizontal wells, pressure maintenance and application of SWAG. In FDP, SWAG case gave the best recovery and profitable solution among five prediction cases examined. Large amount of oil remains untrapped after history match, which is recovered by well intervention operations targeting remaining sand, infill drilling by identifying mobile oil in place and voidage replenishment by pressure maintenance.

8.2 RECOMMENDATIONS

Some recommendations for future scope of work in a mature field having bottom water drive reservoir are given below:

- Optimized variant should be determined for vertical, horizontal and smart horizontal well before field implementation.

- Well spacing should be optimized taking into consideration the optimized variants for vertical and horizontal well.
- Pressure maintenance should be deployed in the field from start of production for avoiding cessation of flow due to reduced THP.
- EOR methods such as WAG or SWAG should be deployed in the field after performing suitable laboratory studies.

8.3 FUTURISTIC SCOPE

The global average recovery factor for a typical oilfield is approximately 35%. More oil can be recovered over this easy oil by proper reservoir characterization, reservoir management and incorporating proper technology. Significant amount of oil production comes from mature field and reserve replenishment ratio is decreasing gradually over the last decades. On the other side, there is less probability of discovering giant fields.

In order to meet the demand supply gap presently in India, known oil in mature field should be produced in a techno economic efficient manner by applying good reservoir management from early periods of production and maximizing production from individual well.

There is a big gap in demand and supply in case of crude oil, which is increasing on day to day basis. As there are less discoveries in the last decade, it is pertinent to increase the recovery factor by maximizing oil production from individual well as well as on field scale. This can help India in reducing the demand supply gap of crude oil.

BIBILOGRAPHY

- **Abdul-Latif, B. L., Kwesi, D. C., Ernest, A., and Fahd, K. 2015.** Optimizing Spacing of Horizontal Wells in Gas and Gas-Condensate Reservoirs, SPE Russian Petroleum Technology Conference, 26-28 October, Moscow, Russia, doi:10.2118/176586-MS.
- **Ahmed, T. 2010.** Water and gas coning, Reservoir Engineering Handbook. 4th ed, Oxford, United Kingdom, Elsevier science & technology, pp. 574-605, print.
- **Al Qahtani, A., Al Hashim, H., and Al Yousef, H. 2015.** A New Approach for Optimization of Long Horizontal Wells' Performances, Paper IPTC-18372-MS, International Petroleum Technology Conference. Doha, Qatar, 6-9 Dec.
- **Al-Attar, A.E., 2004.** A review of upstream development policies in Kuwait. OPEC Rev. 28, 275–288.
- **Algharabi, M.K., Gharbi, R.B., Malallah, A., and Al-Ghanim, W. 2007.** Parametric investigations of a Modified SWAG Injection Technique, SPE 105071, SPE Middle East Oil and Gas Show and Conference, 11-14 March, Manama, Bahrain.
- **Amaefule, J. O., Altunbay, M., Tiab, D., Kersey, D. G. and Keelan, D. K. 1993.** Enhanced Reservoir Description: Using Core and Log Data to Identify Hydraulic (Flow) Units and Predict Permeability in Uncored Intervals/Wells, SPE Annual Technical Conference and Exhibition, 3-6 October, Houston, Texas, doi:10.2118/26436-MS.
- **Anietie Ndarake Okon and Dulu A. 2018.** Water Coning Prediction: An Evaluation of Horizontal Well Correlations. Engineering and Applied Sciences. Vol. 3, No. 1, 2018, pp. 21-28. doi: 10.11648/j.eas.20180301.14
- **Anietie Ndarake Okon, Dulu Appah and Julius Udo A. 2018.** A Critical Evaluation of Water Coning Correlations in Vertical Wells. American Journal of Science, Engineering and Technology. Vol. 3, No. 1, 2018, pp. 1-9. doi: 10.11648/j.ajset.20180301.11
- **Ansari, R.Z. and Johns R.T. 2006.** Steady-State Coning Solutions with Multiple Wells and Reservoir Boundaries. SPE paper 99896-MS, presented on SPE/DOE Symposium on Improved Oil Recovery, Tulsa, Oklahoma, USA. 22-26 April.

- **Archer J.S. and Wall C. G. 2012.** Petroleum Engineering Principles and Practice, Springer Science & Business Media, pp.362, 173.
- **Awotunde, A. A., and Naranjo, C. 2014.** Well Placement Optimization Constrained to Minimum Well Spacing, Paper SPE-169272-MS, SPE Latin America and Caribbean Petroleum Engineering Conference, Maracaibo, Venezuela, 21-23 May.
- **Bahadori, A. 2010.** Determination of well placement and breakthrough time in horizontal wells for homogeneous and anisotropic reservoirs. Journal of Petroleum Science and Engineering, 75 (1–2), 196–202.
- **Bailey, W. J., Couët, B., and Wilkinson, D. 2004.** Field Optimization Tool for Maximizing Asset Value, SPE Asia Pacific Conference on Integrated Modelling for Asset Management, 29-30 March, Kuala Lumpur, Malaysia, doi:10.2118/87026-MS.
- **Birchenko, V., Al-Khelaiwi, F., Konopczynski, M. and Davies, D. 2008.** Advanced wells: how to make a choice between passive and active inflow-control completions, SPE Annual Technical Conference and Exhibition, 21-24 September, Denver, Colorado, USA, doi: http://dx.doi.org/10.2118/115742-MS.
- **Black, G. and LaFrance, J.T. 1998.** Is Hotelling's rule relevant to domestic oil production? J. Environ. Econ. Manage. 36, 149–169.
- **Brown, D. 2008.** Reservoir Simulation Overview. Petroleum Reserve Estimation, Production, and Production Sharing Contract (PSC) Short Course. April 29-30.
- **Carpenter, C. 2015.** Smart Horizontal Wells for Development of Thin-Oil-Rim Reservoirs.,Journal of Petroleum Technology,67(11).
- **Chan, K.S 1995.** Water Control Diagnostic Plots, SPE 30775, SPE Annual Technical Conference and Exhibition, 22-25 October, Dallas, Texas, doi:http://dx.doi.org/10.2118/30775-MS.
- **Chen, P., Al Sowaidi, A. K., Patel, H., Brantferger, K., Bin Buang, K. A., Syed, F. I. and Shehhi, R. A. 2016.** Assessment of Simultaneous Water and Gas Injection SWAG Pilot in a Giant Offshore Carbonate Reservoir, Paper SPE-183223-MS, Abu Dhabi International Petroleum Exhibition & Conference, Abu Dhabi, UAE,, 7-10 November.
- **Cho, Hyun, 2003.** Integrated Optimization on a Long Horizontal Well Length, SPE Reservoir Evaluation & Engineering, Volume 06, Issue 02, pp. 81-88.

- **Chodhury A. 2003.** Well testing handbook by amanat chodhury, website:https://books.google.co.in/books/about/Oil_Well_Testing_Handbook.html?id=50VW0ZZ_
- **Christensen, J. R., Stenby, E. H. and Skauge, A. 2001.** A Review of WAG field experience, SPE Reservoir Evaluation & Engineering, Volume 4, Issue 02,pp.97-106,doi:http://dx.doi.org/10.2118/71203-PA.
- **Davis, E. F., and Shepler, J. C. 1969.** Reservoir Pressure Data Used To Justify Infill Drilling in a Low Permeability Reservoir. Journal of Petroleum Technology, Vol 21, issue 03, doi:10.2118/2260-PA.
- **Denney, D. 2010.** Intelligent-Well Completions in Agbami: Value Added and Execution Performance', J. Petro. Technology, Vol. 62, Issue 5, pp. 49-51.doi: http://dx.doi.org/10.2118/0510-0049-JPT.
- **DGH India website**:dghindia.gov.in/assets/downloads/56cc43934337fAssam-Arakan_Basin.pdf
- **Dikken, B.J. 1990.** Pressure drop in horizontal well and its effects on their production performance; Paper SPE19824; Journal of Petroleum Technology, Vol 42, Issue 11, pp. 1426-1433.
- **Dosunmu, I., and Osisanya, S. 2015.** An Economic Approach to Horizontal Well Length Optimization, Society of Petroleum Engineers, paper SPE-177866-MS, Abu Dhabi International Petroleum Exhibition and Conference, Abu Dhabi, UAE, 9-12 November.
- **Ellis, T., Erkal, A. Jokela T., Kvernstuen, S., Leung, E., Moen, T., Porturas, F., Skillingstad, T., Vorkinn, P.B., Raffn, A.G. and Gordon, G. 2009.** 'Inflow Control Devices-Raising Profile', Oilfield Review Winter 2009, pp.30-37.
- **Fabusuyi Oluwatosin John, 2015.** Optimization of a Water Alternating Gas Injection, P.h.D. thesis. website:https://fenix.tecnico.ulisboa.pt/downloadFile/1126295043834228/Tosin%20Fabusuyi%20Final%20thesis.pdf (accessed on 07 Feb 2017)
- **Fahim Forouzanfar and Reynolds A.C. 2013.** Well-placement optimization using a derivative-free method, Journal of Petroleum Science and Engineering, Volume 109, September 2013, Pages 96-116.
- **Fan Z. and Fang, H. 1997.** On the design method of optimal horizontal wellbore, Acta petrotel sinica, no.4, pp.117-121.

- **Flewitt, W. E. 1975.** Refined reservoir description to maximize oil recovery, SPWLA-1975-X, SPWLA sixteen annual logging symposium SPWLA 16th Annual Logging Symposium, 4-7 June, New Orleans, Louisiana.
- **Gamal, M., Khairy, M., El-Banbi, A. H. and Saad, S. M. 2016.** An Approach for Determination of the Economically Optimal Production Controlling Parameters from Water Drive Oil Reservoirs. Society of Petroleum Engineers. doi:10.2118/182842-MS
- **Garimella, S. V. S., Kloosterman, H. J., Horstmann, D. and Algheithy, A. A. 2009.** FDP-Revisions: Keeping Your FDP's Green in a Fit-For-Purpose Manner' Paper SPE 120319-MS Presented at SPE Middle East Oil and Gas Show and Conference, 15-18 March, Manama, doi: http://dx.doi.org/10.2118/120319-MS.
- **Helfferich, F. G. 1981.** Theory of Multicomponent, Multiphase Displacement in Porous Media, Society of Petroleum Engineer Journal, Volume 21 issue 01,pp.51-62,doi:10.2118/8372-PA.
- **Holmes, J. A., Barkve, T. and Lund, O. 1998.** Application of a Multi-segment Well Model to Simulate Flow in Advanced Wells, SPE 50646,SPE European Petroleum Conference, European Petroleum Conference, 20-22 October, The Hague, Netherlands, doi:10.2118/50646-MS.
- **Ivanhoe, L. F. 1997.** King Hubbert updated. http://hubbert.mines.edu/news/Ivanhoe_97-1.pdf.
- **Johansen, T.E. and Khoriakov, V. 2007.** Iterative techniques in modeling of multi-phase flow in advanced wells and the near well region, J. Petrol. Sci. Eng., Volume 58, Issue(1–2), pp.49–67,doi:URL http://www.dx.doi.org/10.1016/j.petrol.2006.11.013.
- **Johnson, A. 1987.** Permeability Averaged Capillary Data: A Supplement To Log Analysis In Field Studies, Paper SPWLA-1987-EE presented at SPWLA 28th Annual Logging Symposium, 29 June-2 July, London, England.
- **Joshi, S. D. 2003.** Cost/Benefits of Horizontal Wells, SPE-83621-MS,SPE Western Regional/AAPG Pacific Section Joint Meeting, 19-24 May, Long Beach, California, doi:http://dx.doi.org/10.2118/83621-MS.
- **Kalla, S. and White, C. D. 2007.** Efficient design of reservoir simulation studies for development and optimization, SPE-95456, SPE Annual Technical Conference and Exhibition, 9-12 October, Dallas, Texas,doi:10.2118/95456-MS.

- **Khasanov, M. M., Ushmaev, O. S., Samolovov, D. A., Ovcharov, V. V., Dmitruk, D. N., Timofeeva, T. N., and Andjukaev, C. V. 2013.** A Method to Determine Optimum Well Spacing for Oil Rims Gas-Oil Zones (Russian), SPE Arctic and Extreme Environments Technical Conference and Exhibition, 15-17 October, Moscow, Russia, doi:10.2118/166898-RU.
- **Kolchanova, I. 2014.** Application of the Intelligent Control Systems for Horizontal Well Placement, Paper SPE-171279-MS, SPE Russian Oil and Gas Exploration & Production Technical Conference and Exhibition, Moscow, Russia, 14-16 October.
- **Kumar M., Sharma P. and Gupta D. K. 2017.** Optimization of vertical well completion in a saturated reservoir with bottom water drive for maximizing recovery, Biofuels, DOI: 10.1080/17597269.2017.1284472
- **Kumar M., Sharma P. and Gupta D. K. 2016.** Integrated approach for maximizing recovery from Oligocene reservoir under bottom water drive, International Journal of oil, gas and coal technology
- **Kumar M., Sharma P. and Gupta D. K. 2017.** Sensitivity study of horizontal length, offset from water oil contact and withdrawal rate of horizontal well in bottom water drive reservoir, Journal of Petroleum Exploration and Production Technology, Volume 8, Issue 2, pp 577–588,DOI 10.1007/s13202-017-0348-9
- **Leung, E., Nukhaev, M., Gottumukkala, V., Samosir, H., El-Fattah, M. A., Ogunsanwo, O., and Gonzalez, A. 2010.** Horizontal Well Placement and Completion Optimisation in Carbonate Reservoirs, SPE-140048-MS, SPE Caspian Carbonates Technology Conference, 8-10 November, Atyrau, Kazakhstan,doi:10.2118/140048-MS.
- **Leverett, M. C. 1941.** Capillary Behaviour in Porous Solids, Transactions of the AIME, Vol. 142, Issue 1, pp. 152-169. doi: http://dx.doi.org/10.2118/941152-G.
- **Lyons W. and Plisga, B. S. 2005.** Standard Handbook of Petroleum & Natural Gas Engineering (Second edition). Burlington, MA: Elsevier Inc. ISBN-13:978-0-7506-7785-1.
- **Maalouf, C. B., Zidan, M., Uijttenhout, M., Hernandez, E. J., Al-Jaberi, S., Saeed, Y. and Graham R. A. 2017.** Responsive Design of Inflow Control Devices Completions for Horizontal Wells. Society of Petroleum Engineers. doi:10.2118/188794-MS

- **Magzoub, M. I. and Hossain, M. E. 2015.** A Dual Multilateral Completion as an Alternative to Un-Wanted Water Control in Horizontal Wells,Paper SPE-175703-MS, SPE North Africa Technical Conference and Exhibition, Cairo, Egypt, 14-16 September.
- **Mazen, T. B. 2008.** A Simulation Study to verify Stone's Simultaneous water and Gas Injection Performance in 5-spot Pattern, Master of Science thesis, Texas A&M University.
- **Menouar, H. 2013.** Effect of Heterogeneity on Formation Damage in Long Horizontal Wells: An Experimental Study, Paper SPE-165313-MS, SPE Western Regional & AAPG Pacific Section Meeting 2013 Joint Technical Conference, Monterey, California, USA, 19-25 April.
- **Meshal, A., G. Rida and M. Adel 2007.** A parametric Investigations of SWAG injection technique, SPE paper 105071,15th SPE Oil and Gas Show, Bahrain 11-14th March.
- **Mezzomo, C. C. and Schiozer, D. J. 2003.** Methodology for water injection strategies planning optimization using reservoir simulation, Journal of Canadian Petroleum Technology, Vol. 42, no. 7, pp. 9-11.
- **Mojaddam Zadeh, A., Slotte, P. A., Gyllensten, A. J., Aasheim, R. and Arland, K. 2012.** Optimal Inflow Control Devices Configurations for Oil Rim Reservoirs, Paper OTC-22963-MS presented at Offshore Technology Conference, 30 April-3 May, Houston, Texas, USA doi: http://dx.doi.org/10.4043/22963-MS.
- **Moradi Dowlatabad, M., Zarei, F. and Akbari, M. 2015.** The Improvement of Production Profile While Managing Reservoir Uncertainties with Inflow Control Devices Completions, Paper SPE-173841-MS, SPE Bergen One Day Seminar, Bergen, Norway,22 April.
- **NCBI website**: https://www.ncbi.nlm.nih.gov/pmc/articles/PMC3866386/
- **Neylon, K., Reiso, E., Holmes, J. and Nesse, O. 2009.** Modeling well inflow control with flow in both annulus and tubing, SPE Reservoir Simulation Symposium, 2-4 February, The Woodlands, Texas, doi:http://www.dx.doi.org/10.2118/118909-MS.
- **NPTEL website:** http://nptel.ac.in/courses/101103004/pdf/mod3.pdf
- **Oil India Limited internal report, 2014.**

- **OPM project website :** http://opm-project.org/wp-ontent/uploads/2016/06/opm2016-bao-multi-segment-wells.pdf
- **Ouyang, L.B. 2009.** Practical Consideration of Inflow Control Device Application for Reducing Water Production, SPE124154, SPE Technical Conference and Exhibition, New Orleans, Louisiana, U.S.A., October 2009.
- **Pang, W., Zhang, T., Chen, D., Jiang, L. and Li, C. 2013.** Perforation Optimisation for Long Horizontal Wells in Heterogeneous Reservoirs, Paper IPTC-17023-Abstract,International Petroleum Technology Conference,Beijing,China,26-28 march.
- **Pedroso JR., C. and Schiozer, D. J. 2000.** Optimizing locations of wells in Field Development using Reservoir Simulation and Parallel Computing (PVM), RIO OIL AND GAS, 2000, Rio de Janeiro.
- **PETROTEL website**: http://www.petrotel.com/whydigitaloilfield.html
- **Pletcher, J. L. 2000.** Improvements to Reservoir Material Balance Methods, SPE Annual Technical Conference and Exhibition, 1-4 October, Dallas, Texas, doi:10.2118/62882-MS.
- **Popa, A. S. 2013.** Identification of Horizontal Well Placement Using Fuzzy Logic, Paper SPE-166313-MS. PE Annual Technical Conference and Exhibition, New Orleans, Louisiana, USA, 30 September-2 October.
- **Pordel Shahri, M., Shi, Z., Zhang, H., Akbari, B., and Mohammadnia Firoozabad, M. R. 2013.** Generalized Inflow Performance Relationship (IPR) for Horizontal Wells, Paper SPE-165691-MS, SPE Eastern Regional Meeting, Pittsburgh, Pennsylvania, USA, 20-22 August.
- **Raju, S.V. and Mathur, N. 1995.** Petroleum geochemistry of a part of Upper Assam Basin, India: a brief overview, Organic Geochemistry, Vol. 23, Issue 1, pp. 55-70, doi:10.1016/0146-6380(94)00104-9.
- **Rouzbeh Ghanbarnezhad, SPE, Larry W. and Lake, 2010.** Simultaneous Water-Gas-Injection Performance under Loss of Miscibility. Paper SPE-129966, presented at SPE Improved Oil Recovery Symposium held in Tulsa, Oklahoma, USA, 24-28 April.

- **Sadana, A. K., Agrawal, D. K. and Noui-Mehidi, M. N. 2016.** Modified Intervention-Less Inflow Control Device for Water Management, Paper SPE-183151-MS, Abu Dhabi International Petroleum Exhibition & Conference, Abu Dhabi, UAE, 7-10 November.
- **Schlumberger ECLIPSE* E&P Software Platform, 2015.** Eclipse Technical Description.
- **Schlumberger PETREL* E&P Software Platform, 2015.** User Manual, Version 2015.1
- **Shehadeh, K. M., H., Hillgartner, R. AlMjeni and X.D. Jing, 2010.** Simultaneous Injection of Miscible Gas and Polymer (SIMGAP) to Improve Oil Recovery and Sweep Efficiency from Layered Carbonate Reservoirs, Paper SPE-129645, SPE EOR Conference at Oil & Gas West Asia, Muscat, Oman, 11-13 April 2010.
- **Skelt, C. 1996.** A Relationship between Height, Saturation, Permeability and Porosity, Paper E018 presented at 17th European Formation Evaluation Symposium (SPWLA), 3-7 June, Amsterdam, Netherland, doi: 10.3997/2214-4609.201409015.
- **Skelt, C. and Harrison, B. 1995.** An Integrated Approach to Saturation Height Analysis, Paper SPWLA-1995-NNN presented at SPWLA 36th Annual Logging Symposium, 26-29 June, Paris, France.
- **SPE website:** https://www.spe.org/industry/increasing-hydrocarbon-recovery-factors.php
- **Stone, H.L. 1970.** Probability Model for Estimating Three-Phase Relative Permeability, SPE-2116-PA,J Pet Technol, Volume 22, Issue 02,pp.214–218. http://dx.doi.org/10.2118/2116-PA.
- **Stone, T. W., Bennett, J., Law, D. H.-S. and Holmes, J. A. 2002.** Thermal Simulation with Multisegment Wells, SPE 78131-PA, SPE Reservoir Simulation Symposium, 11-14 February, Houston, Texas.
- **Tabatabaei N.S.A. 2007.** Estimating Optimum Well Spacing in a Middle East Onshore Oil Field Using a Genetic Algorithm Optimization Approach, SPE Middle East Oil and Gas Show and Conference, 11-14 March, Manama, Bahrain, doi: http://dx.doi.org/10.2118/105230-MS.

- **Temizel, C., Kirmaci, H., Wijaya, Z., Balaji, K., Suhag, A., Ranjith, R. and Yegin, C. 2016.** Production Optimization Through Voidage Replacement Using Triggers for Production Rate,Paper SPE-184131-MS, SPE Heavy Oil Conference and Exhibition, Kuwait City, Kuwait, 6-8 December.
- **Tokunaga, H., and Hise, B. R. 1966 .** A Method to Determine Optimum Well Spacing, SPE California Regional Meeting, 17-18 November, Santa Barbara, California, doi:10.2118/1673-MS.
- **Tunio, S. Q., Chandio, Chandio, T.A. and Memon, M.K. 2012.** Comparative study of FAWAG and SWAG as an effective EOR technique for a Malaysian field, Research Journal of Applied Sciences, Engineering and Technology 4(6):645.
- **Wan, J., Dale, B.A., Ellison, T.K., Benish, T.G. and Grubert M.A. 2008.** Coupled well and reservoir simulation models to optimize completion design and operations for subsurface control, Europec /EAGE Conference and Exhibition, 9-12 June 2008, Rome, Italy,doi:http://www.dx.doi.org/10.2118/113635-MS.
- **Wanga,J., Liua, H., Liub, Y., Jiaoc, Y., Wud, J. and Kange, A. 2016.** Mechanism and sensitivity analysis of an inflow control devices (ICD) for reducing water production in heterogeneous oil reservoir with bottom water, J. Petrol. Sci. Eng., vol: 146,pp.971-982.
- **Wilson, A. 2016.** Completion and Well-Spacing Optimization for Horizontal Wells in Pad Development, Journal of petroleum technology, 68(10).

Rock Quality Index (RQI), Flow Zone Indicator (FZI) and Porosity Permeability transform

Rock Quality Index (RQI) and Flow Zone Indicator (FZI)

Porosity (%)	Air Permeability (mD)	RQI	FZI
25.28	514	1.41587	4.18488
28.54	771	1.63204	4.08638
26.1	963	1.90732	5.40041
28.02	1235	2.08463	5.35516
26.12	236	0.94384	2.66964
26.39	224	0.91482	2.55171
24.56	286	1.07152	3.29133
22.01	272	1.10384	3.91132
30.12	1469	2.19287	5.08758
31.11	2003	2.51953	5.57926
31.41	1966	2.48421	5.42476
26.84	1234	2.1291	5.80346
30.13	1226	2.00297	4.6448
26.39	384	1.19778	3.34097
23.64	640	1.63379	5.27733
23.37	95	0.63309	2.07588
23.83	108	0.66847	2.13668
26.35	127	0.68935	1.92679
27.23	90.13	0.57127	1.52667

Permeability values for various Rock Quality Index (RQI)

	Permeability (mD)				
	RQI = 0.9	RQI =1.1	RQI=1.5	RQI=2	RQI=2.5
Porosity (%)	0.9	1.1	1.5	2	2.5
20	164.307	245.446	456.408	811.392	1267.8
22	180.738	269.991	502.049	892.531	1394.58
24	197.168	294.535	547.69	973.67	1521.36
26	213.599	319.08	593.33	1054.81	1648.14
28	230.03	343.624	638.971	1135.95	1774.92
30	246.46	368.169	684.612	1217.09	1901.7
32	262.891	392.714	730.253	1298.23	2028.48

ANNEXURE-II

Relative permeability & Capillary Pressure of Oil-Water and Oil-Gas System

Relative Permeability of Oil-Water System

Core no.	S_{wi} %	Porosity %	S_w %	K_{rw}	K_{ro}	N_o	N_w	K_{rwe}	K_{roe}	S_{wc} %	S_{or} %
AH1	17.46	27.93	0.17	0	1	2.03	2	0.05	1	0.17	0.31
AH1	17.46	27.93	0.31	0.02	0.6	2.03	2	0.05	1	0.17	0.31
AH1	17.46	27.93	0.47	0.03	0.2	2.03	2	0.05	1	0.17	0.31
AH1	17.46	27.93	0.55	0.04	0.07	2.03	2	0.05	1	0.17	0.31
AH1	17.46	27.93	0.6	0.04	0.03	2.03	2	0.05	1	0.17	0.31
AH1	17.46	27.93	0.65	0.05	0.01	2.03	2	0.05	1	0.17	0.31
AH1	17.46	27.93	0.69	0.06	0.01	2.03	2	0.05	1	0.17	0.31
BH2	12.1	21.6	0.12	0	1	2.61	1.9	0.24	1	0.25	0.33
BH2	12.1	21.6	0.35	0.01	0.81	2.61	1.9	0.24	1	0.25	0.33
BH2	12.1	21.6	0.37	0.04	0.48	2.61	1.9	0.24	1	0.25	0.33
BH2	12.1	21.6	0.44	0.06	0.2	2.61	1.9	0.24	1	0.25	0.33
BH2	12.1	21.6	0.48	0.07	0.1	2.61	1.9	0.24	1	0.25	0.33
BH2	12.1	21.6	0.52	0.09	0.05	2.61	1.9	0.24	1	0.25	0.33
BH2	12.1	21.6	0.56	0.11	0.03	2.61	1.9	0.24	1	0.25	0.33
BH2	12.1	21.6	0.6	0.11	0.02	2.61	1.9	0.24	1	0.25	0.33
BH2	12.1	21.6	0.65	0.12	0.01	2.61	1.9	0.24	1	0.25	0.33
CH1	13.08	29.63	0.13	0	1	4.06	1.7	0.14	1	0.13	0.32
CH1	13.08	29.63	0.34	0.02	0.56	4.06	1.7	0.14	1	0.13	0.32
CH1	13.08	29.63	0.42	0.06	0.12	4.06	1.7	0.14	1	0.13	0.32
CH1	13.08	29.63	0.46	0.06	0.04	4.06	1.7	0.14	1	0.13	0.32
CH1	13.08	29.63	0.48	0.06	0.01	4.06	1.7	0.14	1	0.13	0.32
CH1	13.08	29.63	0.5	0.07	0.01	4.06	1.7	0.14	1	0.13	0.32
CH1	13.08	29.63	0.52	0.07	0.01	4.06	1.7	0.14	1	0.13	0.32
CH1	13.08	29.63	0.55	0.07	0	4.06	1.7	0.14	1	0.13	0.32
EH1	6.5	29.14	0.07	0	1	3.04	1.4	0.14	1	0.15	0.5
EH1	6.5	29.14	0.21	0.03	0.56	3.04	1.4	0.14	1	0.15	0.5
EH1	6.5	29.14	0.27	0.05	0.2	3.04	1.4	0.14	1	0.15	0.5
EH1	6.5	29.14	0.32	0.06	0.09	3.04	1.4	0.14	1	0.15	0.5
EH1	6.5	29.14	0.36	0.07	0.04	3.04	1.4	0.14	1	0.15	0.5
EH1	6.5	29.14	0.41	0.09	0.03	3.04	1.4	0.14	1	0.15	0.5
EH1	6.5	29.14	0.46	0.1	0.02	3.04	1.4	0.14	1	0.15	0.5
EH1	6.5	29.14	0.5	0.07	0	3.04	1.4	0.14	1	0.15	0.5

ANNEXURE-II

Relative permeability & Capillary Pressure of Oil-Water and Oil-Gas System

Relative Permeability of Oil-Gas System

Core	S_{wi} %	Porosity %	S_g %	K_{rg}	K_{ro}	N_o	N_g	K_{rge}	K_{ro}	S_{wc} %	S_{org} %
AH1	24.2	27.93	0.017	0.00	1	2.7	3.1	0.2	1	0.1	0.4
AH1	24.2	27.93	0.042	0.00	0.554	2.7	3.1	0.2	1	0.1	0.4
AH1	24.2	27.93	0.057	0.00	0.413	2.7	3.1	0.2	1	0.1	0.4
AH1	24.2	27.93	0.072	0.01	0.314	2.7	3.1	0.2	1	0.1	0.4
AH1	24.2	27.93	0.093	0.01	0.235	2.7	3.1	0.2	1	0.1	0.4
AH1	24.2	27.93	0.122	0.02	0.169	2.7	3.1	0.2	1	0.1	0.4
AH1	24.2	27.93	0.153	0.02	0.122	2.7	3.1	0.2	1	0.1	0.4
AH1	24.2	27.93	0.182	0.03	0.094	2.7	3.1	0.2	1	0.1	0.4
AH1	24.2	27.93	0.209	0.04	0.069	2.7	3.1	0.2	1	0.1	0.4
AH1	24.2	27.93	0.234	0.06	0.049	2.7	3.1	0.2	1	0.1	0.4
AH1	24.2	27.93	0.257	0.08	0.029	2.7	3.1	0.2	1	0.1	0.4
AH1	24.2	27.93	0.275	0.09	0.022	2.7	3.1	0.2	1	0.1	0.4
AH1	24.2	27.93	0.292	0.11	0.015	2.7	3.1	0.2	1	0.1	0.4
AH1	24.2	27.93	0.311	0.15	0.009	2.7	3.1	0.2	1	0.1	0.4
AH1	24.2	27.93	0.329	0.18	0.006	2.7	3.1	0.2	1	0.1	0.4
AH1	24.2	27.93	0.346	0.23	0.002	2.7	3.1	0.2	1	0.1	0.4
AH1	24.2	27.93	0.355	0.26	0.002	2.7	3.1	0.2	1	0.1	0.4
BH2	17.5	21.6	0.042	0.00	1	2.7	2.3	0.5	1	0.2	0.1
BH2	17.5	21.6	0.094	0.00	1	2.7	2.3	0.5	1	0.2	0.1
BH2	17.5	21.6	0.116	0.00	0.632	2.7	2.3	0.5	1	0.2	0.1
BH2	17.5	21.6	0.142	0.01	0.406	2.7	2.3	0.5	1	0.2	0.1
BH2	17.5	21.6	0.170	0.01	0.312	2.7	2.3	0.5	1	0.2	0.1
BH2	17.5	21.6	0.203	0.02	0.233	2.7	2.3	0.5	1	0.2	0.1
BH2	17.5	21.6	0.238	0.04	0.208	2.7	2.3	0.5	1	0.2	0.1
BH2	17.5	21.6	0.272	0.06	0.175	2.7	2.3	0.5	1	0.2	0.1
BH2	17.5	21.6	0.304	0.08	0.133	2.7	2.3	0.5	1	0.2	0.1
BH2	17.5	21.6	0.335	0.10	0.099	2.7	2.3	0.5	1	0.2	0.1
BH2	17.5	21.6	0.368	0.13	0.075	2.7	2.3	0.5	1	0.2	0.1
BH2	17.5	21.6	0.398	0.16	0.058	2.7	2.3	0.5	1	0.2	0.1
BH2	17.5	21.6	0.424	0.20	0.039	2.7	2.3	0.5	1	0.2	0.1
BH2	17.5	21.6	0.460	0.26	0.030	2.7	2.3	0.5	1	0.2	0.1
BH2	17.5	21.6	0.496	0.33	0.018	2.7	2.3	0.5	1	0.2	0.1
BH2	17.5	21.6	0.531	0.42	0.012	2.7	2.3	0.5	1	0.2	0.1
BH2	17.5	21.6	0.561	0.54	0.006	2.7	2.3	0.5	1	0.2	0.1

ANNEXURE-II

Relative permeability & Capillary Pressure of Oil-Water and Oil-Gas System

Core	S_{wi} %	Porosity %	S_g %	K_{rg}	K_{ro}	N_o	N_g	K_{rge}	K_{ro}	S_{wc} %	S_{org} %
BH2	17.5	21.6	0.579	0.669	0.003	2.7	2.3	0.5	1	0.2	0.1
BH2	17.5	21.6	0.590	0.783	0.001	2.7	2.3	0.5	1	0.2	0.1
CH1	15.5	29.63	0.051	0.002	1	3.8	4	0.5	1	0.1	0.3
CH1	15.5	29.63	0.114	0.005	0.356	3.8	4	0.5	1	0.1	0.3
CH1	15.5	29.63	0.139	0.007	0.262	3.8	4	0.5	1	0.1	0.3
CH1	15.5	29.63	0.174	0.008	0.205	3.8	4	0.5	1	0.1	0.3
CH1	15.5	29.63	0.205	0.025	0.150	3.8	4	0.5	1	0.1	0.3
CH1	15.5	29.63	0.238	0.021	0.107	3.8	4	0.5	1	0.1	0.3
CH1	15.5	29.63	0.276	0.034	0.062	3.8	4	0.5	1	0.1	0.3
CH1	15.5	29.63	0.301	0.044	0.040	3.8	4	0.5	1	0.1	0.3
CH1	15.5	29.63	0.324	0.058	0.032	3.8	4	0.5	1	0.1	0.3
CH1	15.5	29.63	0.347	0.073	0.024	3.8	4	0.5	1	0.1	0.3
CH1	15.5	29.63	0.369	0.094	0.014	3.8	4	0.5	1	0.1	0.3
CH1	15.5	29.63	0.388	0.119	0.013	3.8	4	0.5	1	0.1	0.3
CH1	15.5	29.63	0.407	0.142	0.008	3.8	4	0.5	1	0.1	0.3
CH1	15.5	29.63	0.427	0.183	0.005	3.8	4	0.5	1	0.1	0.3
CH1	15.5	29.63	0.443	0.24	0.002	3.8	4	0.5	1	0.1	0.3
CH1	15.5	29.63	0.456	0.32	0.001	3.8	4	0.5	1	0.1	0.3
CH1	15.5	29.63	0.466	0.423	0.000	3.8	4	0.5	1	0.1	0.3
EH1	9.8	29.14	0.021	0.000	1	1.4	3.8	0.7	1	0.1	0.3
EH1	9.8	29.14	0.057	0.001	1.250	1.4	3.8	0.7	1	0.1	0.3
EH1	9.8	29.14	0.083	0.003	0.855	1.4	3.8	0.7	1	0.1	0.3
EH1	9.8	29.14	0.111	0.003	0.599	1.4	3.8	0.7	1	0.1	0.3
EH1	9.8	29.14	0.141	0.007	0.432	1.4	3.8	0.7	1	0.1	0.3
EH1	9.8	29.14	0.166	0.016	0.352	1.4	3.8	0.7	1	0.1	0.3
EH1	9.8	29.14	0.195	0.019	0.315	1.4	3.8	0.7	1	0.1	0.3
EH1	9.8	29.14	0.222	0.037	0.246	1.4	3.8	0.7	1	0.1	0.3
EH1	9.8	29.14	0.243	0.053	0.217	1.4	3.8	0.7	1	0.1	0.3
EH1	9.8	29.14	0.270	0.073	0.249	1.4	3.8	0.7	1	0.1	0.3
EH1	9.8	29.14	0.304	0.102	0.218	1.4	3.8	0.7	1	0.1	0.3
EH1	9.8	29.14	0.337	0.138	0.202	1.4	3.8	0.7	1	0.1	0.3
EH1	9.8	29.14	0.371	0.184	0.151	1.4	3.8	0.7	1	0.1	0.3
EH1	9.8	29.14	0.408	0.254	0.109	1.4	3.8	0.7	1	0.1	0.3
EH1	9.8	29.14	0.444	0.361	0.071	1.4	3.8	0.7	1	0.1	0.3
EH1	9.8	29.14	0.476	0.507	0.044	1.4	3.8	0.7	1	0.1	0.3
EH1	9.8	29.14	0.502	0.694	0.023	1.4	3.8	0.7	1	0.1	0.3

Relative permeability & Capillary Pressure of Oil-Water and Oil-Gas System

Capillary pressure for well M-5

Well	P_c (psi)	S_w (Plug-1)
M-5	0.704166667	84.67
M-5	2.813055556	54.02
M-5	6.333888889	45.26
M-5	11.25944444	39.79
M-5	17.59333333	35.41
M-5	25.33194444	33.22
M-5	34.47888889	32.12

Well	P_c (psi)	S_w (Plug-2)
M-5	0.725833333	85.23
M-5	2.899722222	53.59
M-5	6.525277778	44.09
M-5	11.59888889	38.82
M-5	18.12055556	35.65
M-5	26.09388889	33.54
M-5	35.51888889	32.49

Well	P_c (psi)	S_w (Plug-3)
M-5	0.693333333	100
M-5	2.776944444	71.34
M-5	6.243611111	60.59
M-5	11.10055556	53.43
M-5	17.34416667	49.84
M-5	24.97805556	46.26
M-5	33.99861111	45.07

Well	P_c (psi)	S_w (Plug-4)
M-5	0.693333333	97.84
M-5	2.776944444	67.64
M-5	6.243611111	56.85
M-5	11.10055556	50.38
M-5	17.34416667	46.06
M-5	24.97805556	43.91
M-5	33.99861111	42.83

Relative permeability & Capillary Pressure of Oil-Water and Oil-Gas System

Capillary pressure for well M-8

Well	P_c (atm)	S_w (Plug-C)
M-8	0	100
M-8	0.014168937	95
M-8	0.028337875	79
M-8	0.042506812	55
M-8	0.056675749	50
M-8	0.070844687	47
M-8	0.085013624	45
M-8	0.113351499	41
M-8	0.141689373	36
M-8	0.283378747	32
M-8	0.42506812	28
M-8	0.566757493	25
M-8	0.708446866	23
M-8	1.133514986	19
M-8	1.416893733	17
M-8	2.125340599	15
M-8	2.833787466	14
M-8	4.250681199	12
M-8	4.959128065	11
M-8	5.667574932	10.5

Well	P_c (atm)	S_w (Plug-A)
M-8	0	100
M-8	0.014168937	99
M-8	0.028337875	98
M-8	0.042506812	74
M-8	0.056675749	59
M-8	0.070844687	51
M-8	0.085013624	48
M-8	0.113351499	45
M-8	0.141689373	39
M-8	0.283378747	38
M-8	0.42506812	30
M-8	0.566757493	27
M-8	0.708446866	25
M-8	1.133514986	20
M-8	1.416893733	18
M-8	2.125340599	18
M-8	2.833787466	18
M-8	4.250681199	12.47

Relative permeability & Capillary Pressure of Oil-Water and Oil-Gas System

Well	P_c (atm)	S_w (Plug-B)
M-8	0	100
M-8	0.014168937	91
M-8	0.028337875	63
M-8	0.042506812	46
M-8	0.056675749	42
M-8	0.070844687	40
M-8	0.085013624	38
M-8	0.113351499	35
M-8	0.141689373	31
M-8	0.283378747	26
M-8	0.42506812	23
M-8	0.566757493	21
M-8	0.708446866	19
M-8	1.133514986	16
M-8	1.416893733	15
M-8	2.125340599	13
M-8	2.833787466	12
M-8	4.250681199	10

Sensitivity Results for Vertical Well

Case	Oil production cumulative (m^3)	Gas production cumulative (scm)	Water production cumulative (m^3)	Perforation (m)	Withdrawal rate (m^3/d)
HJN_023_58	346908	47466212	18342	22	50
HJN_023_59	538806	85317488	198999	22	100
HJN_023_60	634819	114850848	475541	22	150
HJN_023_61	340452	46363640	24798	29	50
HJN_023_62	510183	77809240	227622	29	100
HJN_023_63	603607	102790608	506753	29	150
HJN_023_64	328929	44572520	36321	34	50
HJN_023_65	493371	73148200	244434	34	100
HJN_023_66	582694	94966408	527666	34	150
HJN_023_67	313148	42185948	52102	39	50
HJN_023_68	478373	69529144	259432	39	100
HJN_023_69	564697	88930752	545663	39	150
HJN_023_70	302005	40556548	63245	44	50
HJN_023_71	461790	66214140	276015	44	100
HJN_023_72	548455	84160504	561905	44	150

Sensitivity Results for Horizontal Well

Case	Offset (m)	Rate (m^3/d)	Horizontal length (m)	Oil production cumulative (m^3)	Gas production cumulative (scm)	Water production cumulative (m^3)
2548_1200_300	20	300	1200	897094	119984632	1294406
2553_1200_300	15	300	1200	804976	107855600	1386524
2558_1200_300	10	300	1200	707280	94883344	1484220
2563_1200_300	5	300	1200	393734	52907044	1797766
2548_1200_250	20	250	1200	824891	110464304	1001359
2553_1200_250	15	250	1200	737770	98964448	1088480
2558_1200_250	10	250	1200	636158	85439032	1190093
2563_1200_250	5	250	1200	334346	44978996	1491904
2548_1200_200	20	200	1200	748501	100359248	712499
2553_1200_200	15	200	1200	666143	89460416	794857
2558_1200_200	10	200	1200	560133	75314624	900867
2563_1200_200	5	200	1200	275147	37058276	1185853
2548_1000_300	20	300	1000	895495	119749760	1296005
2553_1000_300	15	300	1000	813627	109000464	1377873
2558_1000_300	10	300	1000	721457	96764512	1470043
2563_1000_300	5	300	1000	430670	57843728	1760830
2548_1000_250	20	250	1000	821816	110037352	1004434
2553_1000_250	15	250	1000	744892	99908784	1081358
2558_1000_250	10	250	1000	647700	86972936	1178551
2563_1000_250	5	250	1000	362903	48800948	1463347
2548_1000_200	20	200	1000	743851	99725704	717149
2553_1000_200	15	200	1000	671296	90144168	789704
2558_1000_200	10	200	1000	568013	76362264	892987
2563_1000_200	5	200	1000	295275	39754848	1165725
2548_800_300	20	300	800	931631	124486440	1259869
2553_800_300	15	300	800	832689	111487880	1358811
2558_800_300	10	300	800	760179	101885832	1431322
2563_800_300	5	300	800	518891	69651240	1672609
2548_800_250	20	250	800	843511	112875064	982739
2553_800_250	15	250	800	756748	101448664	1069502
2558_800_250	10	250	800	677048	90857056	1149202
2563_800_250	5	250	800	441238	59302056	1385012
2548_800_200	20	200	800	748715	100336864	712285
2553_800_200	15	200	800	676320	90782296	784680

Sensitivity Results for Horizontal Well

Case	Offset (m)	Rate (m^3/d)	Horizontal length (m)	Oil production cumulative (m^3)	Gas production cumulative (scm)	Water production cumulative (m^3)
2558_800_200	10	200	800	584627	78554984	876373
2563_800_200	5	200	800	360902	48567096	1100098
2548_600_300	20	300	600	843058	112453440	1348442
2553_600_300	15	300	600	791322	105892800	1400178
2558_600_300	10	300	600	736342	98648040	1455158
2563_600_300	5	300	600	577370	77467016	1614130
2548_600_250	20	250	600	744050	99421456	1082200
2553_600_250	15	250	600	708931	94997616	1117319
2558_600_250	10	250	600	654123	87749952	1172127
2563_600_250	5	250	600	496794	66741044	1329456
2548_600_200	20	200	600	630353	84379472	830647
2553_600_200	15	200	600	621267	83366328	839733
2558_600_200	10	200	600	565626	75978496	895374
2563_600_200	5	200	600	412345	55468220	1048655
2563_400_200	5	200	400	319300	42938300	1141700
2558_400_200	10	200	400	402200	53976900	1058800
2553_400_200	15	200	400	387800	52014500	1073200
2548_400_200	20	200	400	499400	66793700	961600
2563_400_250	5	250	400	390800	52476600	1435500
2558_400_250	10	250	400	472800	63376300	1353400
2553_400_250	15	250	400	458900	61467200	1367300
2548_400_250	20	250	400	587200	78389100	1239100
2563_400_300	5	300	400	460600	61772000	1730900
2558_400_300	10	300	400	541400	72473500	1650100
2553_400_300	15	300	400	529600	70842400	1661900
2548_400_300	20	300	400	669300	89213300	1522200

ANNEXURE-V

Sensitivity Results for ICD Well on Compartment Length, Nozzle Size and Uncertainty on Nozzle Size

Sensitivity Results on Compartment Length

Case	Compartment length (m)	Water production cumulative (m^3)	Oil production cumulative (m^3)	Gas production cumulative (scm)
2548_800_300_25	25	1278187	913313	122149712
2548_800_300_50	50	1282359	909141	121594256
2548_800_300_75	75	1274406	917095	122658464
2548_800_300_100	100	1279529	911971	121974992
2548_800_300_125	100	1277496	914004	122238840
2548_800_300_150	150	1261104	930396	124427760

Sensitivity Analysis on Nozzle Sizes

Case	Water production cumulative (m^3)	Oil production cumulative (m^3)	Gas production cumulative (scm)
2548_800_300_150_1	1209083	982417	131349584
2548_800_300_150_2	1218842	972658	130055376
2548_800_300_150_3	1227809	963691	128864824
2548_800_300_150_4	1238579	952921	127434712
2548_800_300_150_5	1246336	945164	126404152
2548_800_300_150_6	1293253	898247	120145312
2548_800_300_150_7	1264417	927083	123993272
2548_800_300_150_8	1239784	951716	127273000
2548_800_300_150_9	1221733	969767	129672088
2548_800_300_150_10	1207345	984155	131581304
2548_800_300_150_11	1230978	960523	128427160
2548_800_300_150_12	1230364	961136	128520376
2548_800_300_150_13	1230577	960924	128496520
2548_800_300_150_14	1235503	955997	127844272
2548_800_300_150_15	1236911	954589	127657992
2548_800_300_150_16	1220451	971049	129836352
2548_800_300_150_17	1224826	966674	129259440
2548_800_300_150_18	1229267	962233	128671496

ANNEXURE-V

Sensitivity Results for ICD Well on Compartment Length, Nozzle Size and Uncertainty on Nozzle Size

Case	Water production cumulative (m^3)	Oil production cumulative (m^3)	Gas production cumulative (scm)
2548_800_300_150_19	1235853	955647	127796176
2548_800_300_150_20	1241501	949999	127043880
2548_800_300_150_21	1205354	986146	131843408
2548_800_300_150_22	1216953	974547	130304728
2548_800_300_150_23	1227229	964271	128941208
2548_800_300_150_24	1239315	952185	127336328
2548_800_300_150_25	1248730	942770	126084616
2548_800_300_150_26	1198398	993102	132774016
2548_800_300_150_27	1213344	978156	130788056
2548_800_300_150_28	1226262	965238	129071472
2548_800_300_150_29	1240793	950707	127138840
2548_800_300_150_30	1253831	937669	125402848
2548_800_300_150_31	1236672	954828	127681208
2548_800_300_150_32	1240374	951126	127195104
2548_800_300_150_33	1238937	952563	127387496
2548_800_300_150_34	1226508	964992	129040656
2548_800_300_150_35	1219766	971734	129945000

Uncertainty Analysis on Nozzle Sizes

Case	Water production cumulative (m^3)	Oil production cumulative (m^3)	Gas production cumulative (scm)
2548_800_300_150_50	1304304	887196	118670032
2548_800_300_150_49	1297913	893587	119501472
2548_800_300_150_46	1282205	909295	121612960
2548_800_300_150_42	1273720	917780	122748216
2548_800_300_150_45	1268779	922721	123378896
2548_800_300_150_41	1259955	931545	124559760
2548_800_300_150_38	1241963	949537	126974008
2548_800_300_150_52	1238968	952532	127380400
2548_800_300_150_36	1224008	967492	129376256
2548_800_300_150_37	1215042	976459	130529688
2548_800_300_150_51	1213987	977513	130694872

ANNEXURE-V

Sensitivity Results for ICD Well on Compartment Length, Nozzle Size and Uncertainty on Nozzle Size

Case	Water production cumulative (m^3)	Oil production cumulative (m^3)	Gas production cumulative (scm)
2548_800_300_150_48	1209534	981966	131285992
2548_800_300_150_44	1202310	989190	132253704
2548_800_300_150_47	1171979	1019521	136275824
2548_800_300_150_43	1165266	1026234	137175936
2548_800_300_150_40	1160862	1030638	137754000
2548_800_300_150_39	1105471	1086029	145109520

ANNEXURE-VI

Sensitivity Results for Well Spacing Optimization

Vertical well spacing

Case	Well spacing (m)	Water production cumulative (m^3)	Oil production cumulative (m^3)	Gas production cumulative (scm)
VERTICAL-300-THP	300	1962128	8124437	2772770560
VERTICAL-400-THP	400	1904143	8202483	2569082112
VERTICAL-500-THP	500	1355006	6562079	1808067456
VERTICAL-200-THP	200	2268715	7426815	2446394880
VERTICAL-100-THP	100	2536377	4947508	2480131840

Horizontal well spacing

Case	Well spacing (m)	Water production cumulative (m^3)	Oil production cumulative (m^3)	Gas production cumulative (scm)
H_300_150_THP_QUE	300/150	3923506	7476200	2.068E+09
H_200_100_QUE_THP	200/100	2871244	7724854	2.336E+09
H_300_150_QUE_THP_WI	200/150	3745869	8528678	2.317E+09
H_400_200_THP_QUE	400/200	3274979	6766218	1.599E+09

Annexure-VII

Field Development Results for Various Strategies

Case	Oil production cumulative (m^3)	Water production cumulative (m^3)	Gas production cumulative (scm)	Pressure at EOP (bars)	Water Cut at EOP (%)	Oil Rate at EOP (m^3/day)
Base case	17489676	20227268	3.459E+09	183	86%	254
Well intervention case	18386962	25527094	4.696E+09	166	89%	285
Infill case	19055518	32205866	6.316E+09	144	92%	218
Pressure maintenance case	19165876	33594628	4.422E+09	232	92%	248
SWAG case	19816294	36349572	4.874E+09	198	93%	201
EOP- End of prediction						

Calculations and Referred Literature used in Present Research Work

Calculations and references:

1. Calculation of Productivity Index (PI) for vertical and horizontal wells
2. Calculation of horizontal well length optimization for horizontal well
3. Calculation of critical rate for vertical and horizontal well
4. Calculation of Breakthrough time for vertical and horizontal well
5. Inflow control device referred results

1. Calculation of PI for vertical and horizontal wells

Comparison of Productivity index for Vertical, Horizontal and ICD completion has been given in Table-A. The input data for calculation has been given in Table-B.

Table-A: PI comparison of different well

Method	**Well**	**Productivity Index Formulae**	**PI (STB/D/psi]**
Pseudo steady State	Vertical Well	$PI = \frac{0.00708\, K\, h}{\mu_o\, B_o\, \ln\frac{r_e}{r_w}}$	61
Joshi, 1991	Horizontal Well	$PI = \frac{0.00708\ K\, h}{\mu_o\, B_o\, [\ln[\, a + \sqrt{\frac{a^2 - \left(\frac{L}{2}\right)^2}{\frac{L}{2}}}] + \frac{h}{L}\beta^2\, \ln\frac{h}{2\, r_w}}$ $a = \frac{L}{2}[\frac{1}{2} + \sqrt{\frac{1}{4} + \left(\frac{2r_{eh}}{L}\right)^4}\,]^{0.5}$ $\beta = \sqrt{\frac{K_h}{K_v}}$ $r_{eh} = \sqrt{a'b}$	727

Calculations and Referred Literature used in Present Research Work

Method	Well	Productivity Index Formulae	PI (STB/D/psi]
Borisov, 1954* Horizontal Well	Horizontal Well	$PI = \frac{0.00708\, k\, h}{\mu_o\, B_o\, [\ln(4\frac{r_{eh}}{L}) + \frac{h}{L}\ln(\frac{h}{2\Pi\, r_w})}$	904
Where K = permeability, mD r_{eh} = drainage radius of well r_w= wellbore radius, ft L= horizontal well length , ft h = payzone thickness , ft K_v= vertical permeability K_h=horizontal permeability μ_o= oil viscosity ,cP B_o = oil formation volumen factor			

Table-B: Input Data for PI calculation

Property	Value	Unit
K_h	500	mD
K_v	25	mD
H	98.4252	ft
μ_o	0.62	cP
B_o	1.12	RB/STB
L	2296.59	ft
r_w	0.23	ft
A	50.27	Acres

It can be seen that Productivity Index (PI) for vertical well is less than that of the horizontal well, which causes more productivity in case of horizontal well deliverability. In case of ICD completion PI will remain same , but Inflow will be reduced because Q = PI (P_r - P_{wf} - ΔP) due to Nozzle, This will lead to reduction in liquid flow rate but at the same time the drawdown will be controlled near heel and in high permeability zones which will cause late breakthrough.

Calculations and Referred Literature used in Present Research Work

2. Calculation of horizontal well length optimization for horizontal well

Horizontal well length is critical in terms of recovery and economics, hence it needs to be optimized. An optimum horizontal length can be defined as length after which incremental recovery starts reducing. Table-C below is given below for input data used for calculation.

Table-C: Input for well deliverability for horizontal well

K_h, Horizontal Permeability (mD)	500
h, Reservoir Thickness (ft)	164.0419948
Pressure Difference (psi)	80
Viscosity oil (cP)	0.4
FVF oil (RB/STB)	1.12
r_w (ft)	0.229166667
r_{eh}, effective radius of horizontal well (ft)	1476.377953
K_v, vertical permeability (mD)	25
L, horizontal well length (ft)	328.0839895

Table-D below summarizes the steps used for calculation as well as formulae used for the same.

Table-D : Calculation for horizontal well productivity

$$Q = \frac{0.00708\ K\ h\ \Delta P}{\mu_o\ B_o\ [\ln[\ a + \sqrt{\frac{a^2 - \left(\frac{L}{2}\right)^2}{\frac{L}{2}}}] + \frac{h}{L}\ \ln\frac{h}{2r_w}}$$

Where,

$$a = \frac{L}{2}[\frac{1}{2} + \sqrt{\frac{1}{4} + \left(\frac{2r_{eh}}{L}\right)^4}\ ]^{0.5}$$

$$\beta = \sqrt{\frac{K_h}{K_v}}$$

$$r_{eh} = \sqrt{a'b}$$

Calculations and Referred Literature used in Present Research Work

Where K = permeability, mD r_{eh} = drainage radius of well r_w= wellbore radius, ft L= horizontal well length , ft h = payzone thickness , ft K_v= vertical permeability, mD K_h=horizontal permeability, mD μ_o= oil viscosity ,cP B_o = oil formation volumen factor	
Beta	4.47
a, Half major axis of drainage ellipse (ft)	1480.94
Productivity Index (STB/D.psi)	66.875959
Flow Rate (STB/D)	5350.08
Flow Rate (m^3/d)	850.57

Above calculation has been done for one horizontal well length. The same process has been repeated for different horizontal well lengths. The results have been mentioned in the Table-E below.

Table-E: Horizontal well productivity calculation for different horizontal well lengths

Horizontal length (m)	**Rate (m^3/d)**	**Change in Rate (m^3/d)**
100	851	0
200	1563	712
300	2201	638
400	2787	586
500	3332	545
600	3843	511
700	4324	481
800	4779	455
900	5211	432
1000	5621	410

A graphical representation for the above calculation has been made below as Figure-A.

Calculations and Referred Literature used in Present Research Work

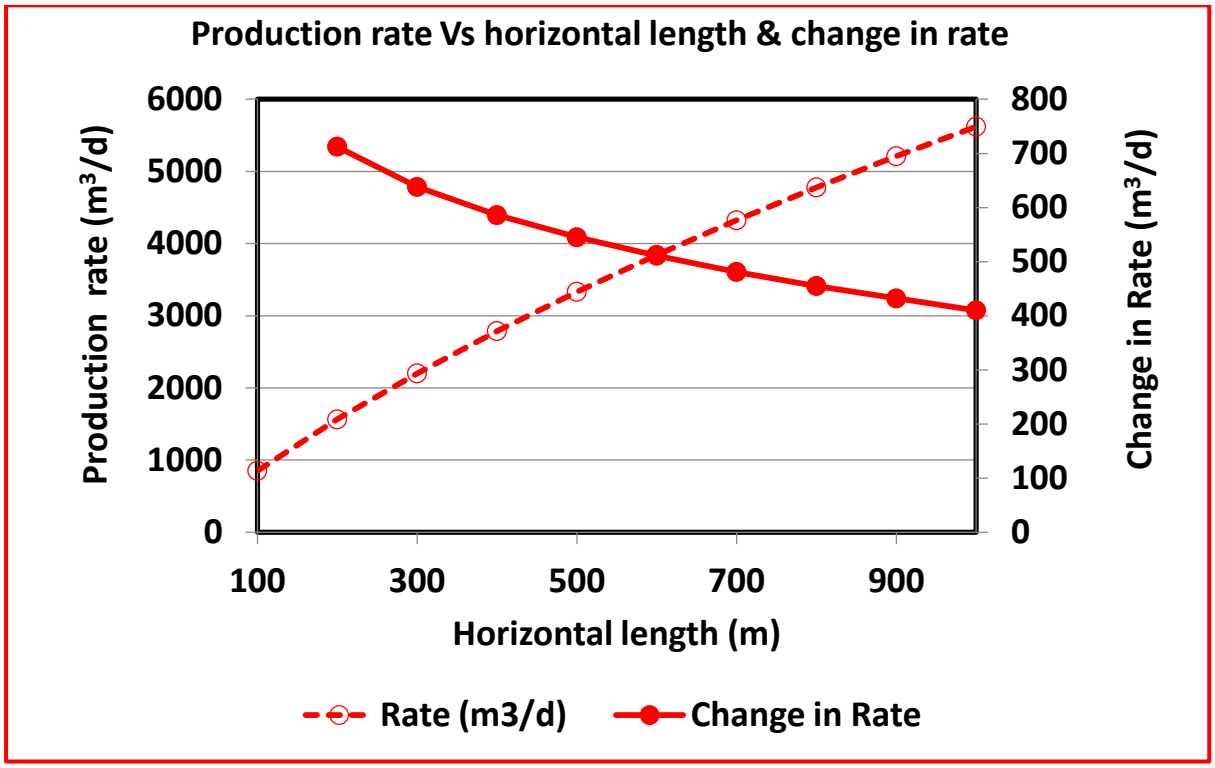

Figure-A: Production rate Vs Horizontal length

Oaikhena (2013) study shows that productivity index of horizontal well increases with increase in horizontal length and anisotropy value (High K_v/K_h ratio favorable for horizontal well). Figure-B represents productivity index determined from various methods vs horizontal length.

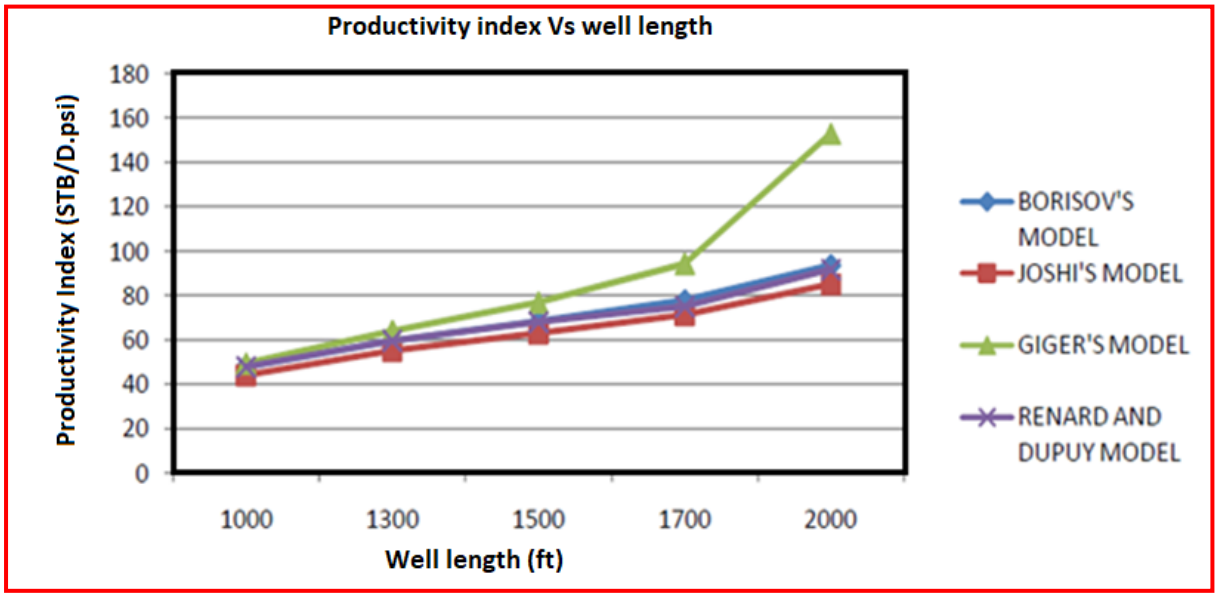

Figure-B: Productivity Index vs Horizontal length

Calculations and Referred Literature used in Present Research Work

Folefac (1991) study showed the following observation:

- Deliverability of horizontal well is affected by pressure drop along wellbore. This effect has serious implication on perforated well length because PI is no longer proportional to horizontal well length. If the wellbore pressure drop is significant as compared to the reservoir drawdown (DD), the reservoir DD , and consequently , the production rate along the well length will change.
- Well length, diameter and perforated interval have most significant impact on pressure drop along wellbore. The consequence of ignoring this wellbore pressure drop is to over predict the well deliverability. It is also shown the wellbore pressure drop increases dramatically with increase in reservoir productivity.
- The calculation of productivity index (PI) for horizontal wells has been addressed by several authors. However, a common simplification to the well model is to assume that the wellbore is at a constant pressure - In other words, the along-well pressure gradient is negligible. Whilst this assumption may be reasonable for conditions where single phase laminar flow in the wellbore occurs, it is no longer valid when turbulent or two phase flow is considered. A simple calculation using typical wellbore conditions: fluid density 800 kg/m^3, viscosity of 1.0 cP, wellbore diameter of 0.1968 m and well rate of 5000 RB/D gives a Reynolds Number (R_e = 4000). This is well above the turbulence transition limit of 2000.
- There is very little discussion on multiphase pressure drop in horizontal wells. Folefac (1991) studied the effect of two phase flow (hydrocarbon liquid and water are treated as one phase with identical velocity but averaged properties). The pressure drop along the horizontal wellbore was similar to that for single phase flow. However, the pressure drop was higher than for single phase flow for the same volume of fluid intake.

Productivity of horizontal well is dependent on horizontal length, thickness of reservoir and fluid properties (Pipesim , 2015 , Technical description**)**

Elizabeth (2001) study showed the following observation:

- For a vertical well, assumption of constant pressure at the middle of perforation is valid, as length of perforation is small, on the other hand horizontal well length is

Calculations and Referred Literature used in Present Research Work

large, and assumption of constant pressure is not valid. The pressure drop due to gravity, friction and other effects, over the perforated interval is negligible compared to the pressure drop that occurs over the tubing length, and to the drawdown between the reservoir and the wellbore. The length of the horizontal section is much greater than the thickness of the zone, and can approach the length of the vertical section.

- As fluid flow from the toe , the end of the bottom of the horizontal well, to the heel , the start of the horizontal section several things occur
  - Kinetic pressure losses
  - Gravity changes
  - Momentum changes from influx

  These all causes changes in the pressure distribution within the horizontal section over the entire length. Therefore, the pressure in the wellbore cannot be assumed to be constant over the length of the horizontal section.
- From basic fluid mechanics, in order to have flow there should be a pressure gradient from toe to heel. As the pressure is decreasing, the pressure difference between the reservoir and the wellbore at the influx points along the wellbore is increasing, implying an increase in the specific influx per unit length from the toe to the heel (Figure-C).

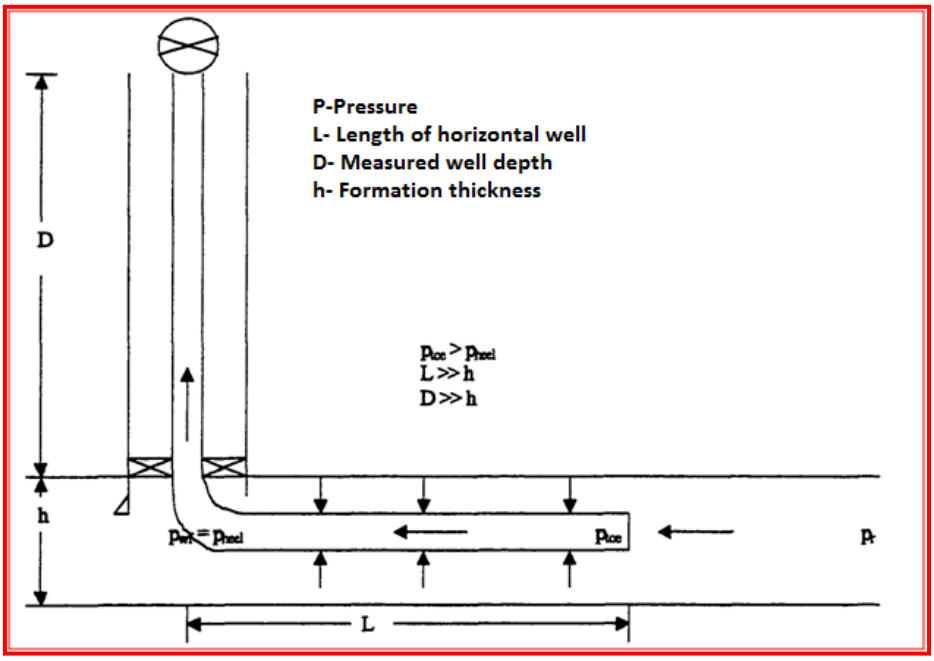

Figure-C: Schematic of horizontal well

Calculations and Referred Literature used in Present Research Work

Grassi (2015) study showed the following observation:

- The flow rate obtained from horizontal well increases till a maximum value (critical value of reservoir length) and then decreases with increases in reservoir length, assuming well length is parallel to the reservoir length, no frictional pressure losses along the wellbore, uniform flux along the wellbore, homogeneous reservoir. The slopes on both sides are dependent on many factors viz: Bo , Oil viscosity , Oil density , pressure drawdown, wellbore radius etc. A plot of flow rate vs reservoir length has been shown in Figure-D below.

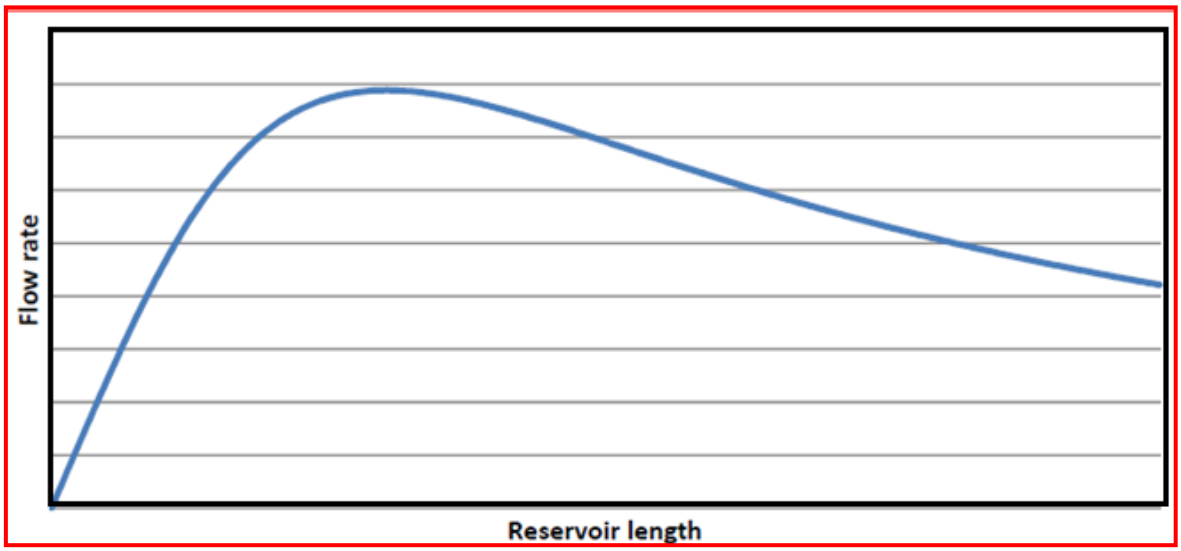

Figure-D: General behavior of Flow rate vs Reservoir length

3. Calculation of critical rate for vertical well and horizontal well

Critical rate has been calculated for vertical and horizontal well with correlations. Results of the calculation and input data have been shown in Table-F through Table-I below:

Table-F : Input data for critical rate calculation for vertical well

Property	**Data**
α"	2.98
q_c	1.38
r_e(ft)	1312.34
ρ_w(lbm/ft^3)	62.30
Oil API gravity	22.00

Calculations and Referred Literature used in Present Research Work

Property	**Data**
ρ_o (lbm/ft^3)	44.23
K_h(mD)	500.00
K_v(mD)	25.00
h(ft)	98.43
μ_o(cP)	0.60
B_o	1.12
h_p	32.81

Table-G : Input data for critical rate calculation for horizontal well

Parameter	**Data**
r_w(ft)	0.3
Area (A)-Acres	80
a	1396.1696
r_{eh}	1052.995726
r_w'	443.6505499
α"	1.49
q_c	4.05
L(ft)	2296.59
Y_e(ft)	656.17
ρ_w (lbm/ft^3)	63.76
Oil API gravity	22.00
ρ_o (lbm/ft^3)	45.27
K_h(mD)	500.00
K_v(mD)	25.00
h(ft)	98.43
D_b(ft)	65.62
μ_o(cP)	0.60
B_o	1.12

Calculations and Referred Literature used in Present Research Work

Table-H: Critical rate calculation for vertical well

Critical Rate (m^3/d)	**Method**	**Formulae**
99.63	Chaperson Method	$Qoc = \frac{0.0783 * 10^{-4}\ K\ h\ (h-h_p)^2 q_c^*}{\mu_o\ B_o}\Delta\rho$ $q_c^* = 0.7311 + (\frac{1.943}{\alpha^{"}})$ $\alpha^{"} = \left(\frac{r_e}{h}\right)\sqrt{\frac{K_v}{K_h}}$
52.32	Meyer-Gardener	$Qoc = \frac{0.246* 10^{-4}\ K_o\ (h^2-{h_p}^2)}{\mu_o\ B_o \ln\frac{r_e}{r_w}}\Delta\rho$
79.74	Schol's Method	$Q_{oc} = \frac{0.246* 10^{-4}\ Ko\ (h^2-{h_p}^2)}{\mu_o\ B_o}\Delta\rho$ X $\left[0.432 + \frac{3.142}{\ln\frac{r_e}{r_w}}\right](\frac{h}{r_e})^{0.14}$
Where, Q_{oc}= critical oil rate, STB/D K_h= horizontal permeability, mD $\Delta\rho=\rho_w-\rho_o$, density difference , lbm/ft^3 h=oil column thickness , ft h_p = perforated interval, ft r_e, r_w = drainage and wellbore radius ,ft		

Table-I: Critical rate calculation for horizontal well

Critical Rate (m^3/d)	**Method**	**Formulae**
129	Efros Method	$Qoc = \frac{0.0783 * 10^{-4}\ K_h\ (\rho_w - \rho_o)[h-(h-D_b)]^2 L}{\mu_o\ B_o\ \left[Y_e + \sqrt{{Y_e}^2 + \left(\frac{h^2}{3}\right)}\right]}$
128	Kracher Method	$Qoc = \frac{0.0783 * 10^{-4}\ K_h\ (\rho_w - \rho_o)[h-(h-D_b)]^2 L}{\mu_o\ B_o\ (2Y_e)\ \left[1-(\frac{h-(h-D_b)}{Y_e})^2\ \frac{1}{24}\right]^{-1}}$
536	Joshi Method	$Qoc = \frac{0.0246 * 10^{-3}\ K_h\ (\rho_w - \rho_o)[h^2-(h-D_b)^2]}{\mu_o\ B_o\ \ln\frac{r_{eh}}{r_w}}$

Calculations and Referred Literature used in Present Research Work

1046	Chaperson Method	$Qoc = \frac{0.0783 * 10^{-4}\ K_h\ L\ Q_c^*(\rho_w - \rho_o)[h-(h-D_b)]^2}{\mu_o\ B_o\ Y_e}$

Where,

L = length of the horizontal well, ft

Ye= half distance between two lines of horizontal wells

ρ = density , lbm/ft^3

h= net pay thickness, ft

k = permeability ,mD

B=h-D_b

D_b=distance between WOC and horizontal well , ft

Q_{oc}= critical oil rate , STB/D

Q_c* = dimensionless function

μ_o = Viscosity ,cP

B_o= Formation volume factor

r_{eh} = Well drainage radius , ft

4. Calculation of Breakthrough time for horizontal and vertical well

Breakthrough time is calculated for vertical and horizontal well using Ozkan method for horizontal well and Sobocinski-Cornelius method for vertical well:

Input for vertical well and horizontal well breakthrough time calculation is given in Table-J and Table-K below. Table-L lists the outcome of critical rate for vertical and horizontal well.

Table- J: Input data for breakthrough time for vertical well

Parameter	**Data**
Q_o (BPD)	943.5
r_w(ft)	0.229166667
R_e(ft)	1312.34
ρ_w (lbm/ft^3)	62.30
Oil API gravity	22.00
ρ_o (lbm/ft^3)	44.23
K_v (mD)	25.00
K_h (mD)	500.00

Calculations and Referred Literature used in Present Research Work

Parameter	**Data**
h(ft)	98.43
μ_o(cP)	0.60
μ_w(cP)	0.40
Bo	1.12
h_p	32.81
ϕ	0.22
Mobility	0.642857143
K_v,mD	25.00
$(K_{rw})_{Sor}$	0.30
$(K_{ro})_{Swc}$	0.70
Alpha	0.50

Table- K: Input data for breakthrough time for horizontal well

Input	**Data**
α"	1.49
qc	4.05
L(ft)	2296.59
Ye(ft)	656.17
ρ_w (lbm/ft^3)	62.30
Oil API	22.00
ρ_o (lbm/ft^3)	44.23
K_h(mD)	500.00
K_v(mD)	25.00
h(ft)	98.43
D_b(ft)	65.62
μ_o(cP)	0.60
B_o	1.12
ϕ	0.22
S_{wc}	0.20
S_{or}	0.32
Q_o	1887

Calculations and Referred Literature used in Present Research Work

Table- L: Breakthrough time calculation for horizontal and vertical well

Breakthrough time for horizontal well (Ozkan method**)**

$$tBT = \left[\frac{f_{d\,h^3\,E_s}}{5.615\,Q_o\,B_o}\right]\left(\frac{k_h}{k_v}\right)$$

With the parameter f_d as defined by :

$$f_d = \emptyset(1 - s_{wc} - s_{or})$$

t_{BT} = time to breakthrough , days

K_v= vertical permeability, mD

K_h= horizontal permeability , mD

$\emptyset$ = porosity, fraction

s_{wc} = connate water saturation , fraction

s_{or} = residual oil saturation, fraction

Q_o= oil flow rate , STB/D

E_s = Sweep efficiency

Dimensionless breakthrough time $(t_D)_{BT}$	7.6
Breakthrough time in days	2466.2
Breakthrough time in years	6.7

Breakthrough time for vertical well (Sobocinski-Cornelius method)

Dimensionless cone height Z

$$Z = 0.492\,X\,10^{-4}\,\frac{(\rho_w - \rho_o)k_h h(h - h_p)}{\mu_o\,B_o\,Q_o}$$

Where

ρ = density ,lbm/ft^3

Q_o= oil production rate, STB/D

h_p= perforated interval ,ft

h= oil column thickness ,ft

Dimensionless breakthrough time

$$(t_D)_{BT} = \frac{4Z + 1.75Z^2 - 0.75\,Z^3}{7 - 2Z}$$

$$tBT = \frac{20{,}325\,\mu_o\,h\,\emptyset\,(t_D)_{BT}}{(\rho_w - \rho_o)K_v(1 + M^{\alpha})}$$

Where

t_{BT} = time to breakthrough ,days

Calculations and Referred Literature used in Present Research Work

φ = porosity,fraction K_v= vertical permeability , mD M= mobility ratio	
t_{BT},Days	848.48
Breakthrough time, years	2.32

Moradi (2010) showed the following observation:

- Critical flow rate calculations frequently show low rates that, for economic reasons, cannot be imposed on production wells. Therefore, if a well produces above its critical rate, the cone will break through after a given time period. This time is called time to breakthrough t_{BT}. Two of the most widely used correlations are documented below
  - The Sobocinski-Cornelius Method
  - The Bournazel-Jeanson Method
- It can be seen that as dimensionless cone height increases breakthrough time also increases taking into consideration equation below for calculation of breakthrough time, which is dependent on Offset from WOC.
- Also with increase in withdrawal rate, dimensionless cone height (Z) decreases leading towards early water breakthrough. For pre breakthrough performance to be optimal Rate should be low and offset should be more.
- Critical oil rate is directly dependent on offset from WOC.

Procon Manual (2015) refers to following observation below:

- In all of vertical well, the assumption for coning calculations is that, the perforations are always located at the top of the oil zone, thereby maximizing the distance between the perforations and the oil-water contact.

- It is important to note that these correlations are valid for a continuous oil pay zone with oil-water contact or gas-oil contact or both. These correlations show that the critical rate depends upon effective oil permeability, oil viscosity, density difference between oil and water or oil and gas, well penetration ratio, and vertical permeability.

Calculations and Referred Literature used in Present Research Work

- The advantages of using a horizontal well over a conventional vertical well are their larger capacity to produce oil for the same drawdown, together with a longer breakthrough time at a given production rate.
- Several horizontal well critical rate correlations are available in the literature, most of which are included within these routines. The method of Kuo and Desbrisay has been used within this routine, for horizontal wells, to predict the performance after water breakthrough.

5. Inflow control device referred results

OGES website supports the following facts about Inflow Control Device (ICD):

- An inflow control device is a completion hardware that is deployed as part of well completions aimed at distributing the inflow evenly.
- High pressure losses regions
  - High viscous crude
  - Long length of wellbore
  - High withdrawal rate
  - Permeability variations along wellbore
- ICD is use to Maximizing recovery from horizontal well by slowing down the water and gas encroachment and help to reduce bypassed reserves. In a horizontal well the flowing pressure is less in heel than at the toe, due to which water /gas arrives early in the heel resulting in an early well's productive life. ICD equalize the pressure drop along the entire length of the horizontal section, promoting uniform flow of oil & gas through the formation so that the arrivals of water and gas are delayed and simultaneous.
- In a horizontal well the flowing pressure is less in heel than at the toe, due to which water /gas arrives early in the heel resulting in an early well's productive life. ICD equalize the pressure drop along the entire length of the horizontal section, promoting uniform flow of oil & gas through the formation so that the arrivals of water and gas are delayed and simultaneous.

Calculations and Referred Literature used in Present Research Work

- The way ICD's improve well recovery is that it severely limits the influx from high permeability zones so that the flow is uniform along the wellbore. By restricting inflow
- recovery from the lower permeability zones are increased. In the design analysis a choke value is assigned to the ICD, run the model and rates are monitored along with uniformity of flow. Same process is repeated again till uniform influx is obtained.
- ICD completion is used to obtain higher cumulative recovery (not higher production rates) in a bottom water aquifer setting, compared to a horizontal well. This is due to better vertical sweep of the bottom water, which is via a more uniform movement of the OWC along the length of the entire lateral of the well and not a skewed movement that gives faster breakthrough to the heel region of the horizontal well earlier in the life of the producing life of the well.
- The basic principle of using ICD is to impose additional pressure drop between the sandface and the interior of the tubing, in varying amounts, depending on the relative location of the ICD segment in the lateral. This additional pressure drop is engineered for each individual ICD in each section of the horizontal well in a such a fashion that effectively ensures similar pressure in the sandface along the entire length of the lateral, under flowing conditions, for a reservoir with homogeneous, anisotropic permeability distribution. This ensures a near horizontal OWC movement and better sweep, which leads to ultimately higher recovery on a per well basis.
- ICD'S mainly work upon lowering down the differential pressure due to the the friction between Toe and heel point of the horizontal wells. They normally have orifice point that is designed as per the expected differential pressure in the bottom hole flowing pressures which in turn manages the friction differential pressures and thus avoid the chances of water coning by lowering the difference in the production draw down between heel and toe.
- In horizontal well completion, we use several ICD with isolation packer-swell packer to complete one horizontal section. The exact number of ICD- swell packer set is arrived after analysis of log motives of horizontal section and analyzing those sections which have passed through water encroached section or which may approach water

section soon. These are isolated with swell packer and ICD are placed only in productive section.

The number of swell packer or ICD again varies depending on well condition. ICD and swell packer combination is very important for thin as well as water drive fields/wells. ICD is mechanical device to allow production from those sections. Before installation of ICD and swell packer, the well will produce with higher percentage of water. There will be higher back pressure on sand face due to this. After installation of ICD, we isolate water, reduce water percent, reduce back pressure, give higher draw down with increased production.

Birchenko (2010) showed that

- For the same rate BHP is less in case of ICD well as compared to normal horizontal well which leads towards high drawdown and hence water production through coning.
- Also, the approximate analytical solution highlights the dependencies between the key parameters influencing the resulting ICD completion design (e.g. nozzle diameter dependence on the drawdown at the heel).
- The Specific Productivity Index, j and hence the inflow, U, changes stochastically along the completion interval. A coefficient of variation will be used to quantify the degree of these changes. Recall that the coefficient of variation of a random variable is defined as the ratio of its standard deviation and its mean.
- In case of conventional completion (no ICD), the coefficient of variation(CoV) of specific inflow is equal to that of the specific PI:

CoV U = CoV j

ICD application reduces the variation of inflow so that:

CoV U < CoV j

- Let us consider the ratio of the two coeffient of variation, CoV U= CoV j. This ratio equals unity for a conventional completion and decreases monotonically with increasing ICD strength. The magnitude of this decrease is a quantitative measure of the equalisation of the inflow along the completion length due to the ICD.
- The objective of this work is to develop a mathematical model linking the ratio of the two coefficient of variation (CoV) with the well parameters (such as ICD \strength", drawdown, etc.). Figure-E depicts variation of well flow rate and CoV ratio with nozzle size.

Calculations and Referred Literature used in Present Research Work

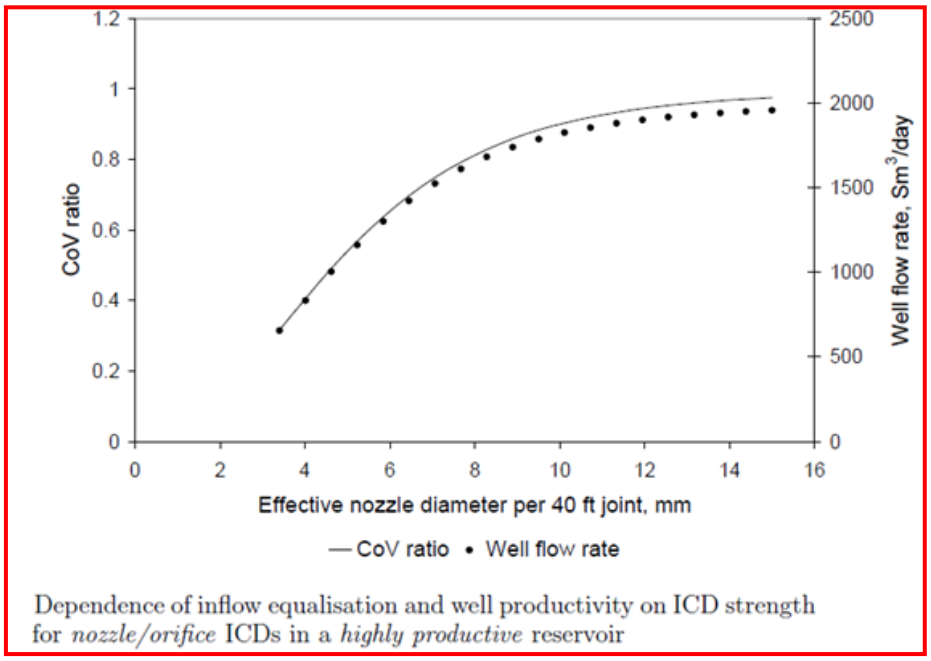

Figure-E: CoV ratio and flow rate vs nozzle size

- Flow through the ICD depends on pressure drop. The pressure drop is proportional to density and to the square of flow rate. The entire flow system may be defined as follows.
  - Flow is from the reservoir into the completion system, and usually is laminar.
  - Flow through the ICD is turbulent.
  - Cumulative flow is from the toe to the heel of a horizontal well; this flow is laminar at the toe but often turbulent at the heel. The degree of turbulence will decrease with reservoir depletion. (JPT, May 2010)
- Youngs et al. (2009) showed that dor implementing ICD in whole horizontal length, it is very important to know how many segments need to be created in the horizontal wellbore. Thumb rule is to assign each grid as one segment but grid with similar properties can be clubbed together for placing ICDs. These segments are practically created in the wellbore by placing packers so that there should not be any flow through annulus, only flow may occur through orifices. Thus determination of optimum no of segments is also necessary in order to reduce no of ICDs and hence cost component. Figure-F represents schematic of horizontal well with ICD.

Calculations and Referred Literature used in Present Research Work

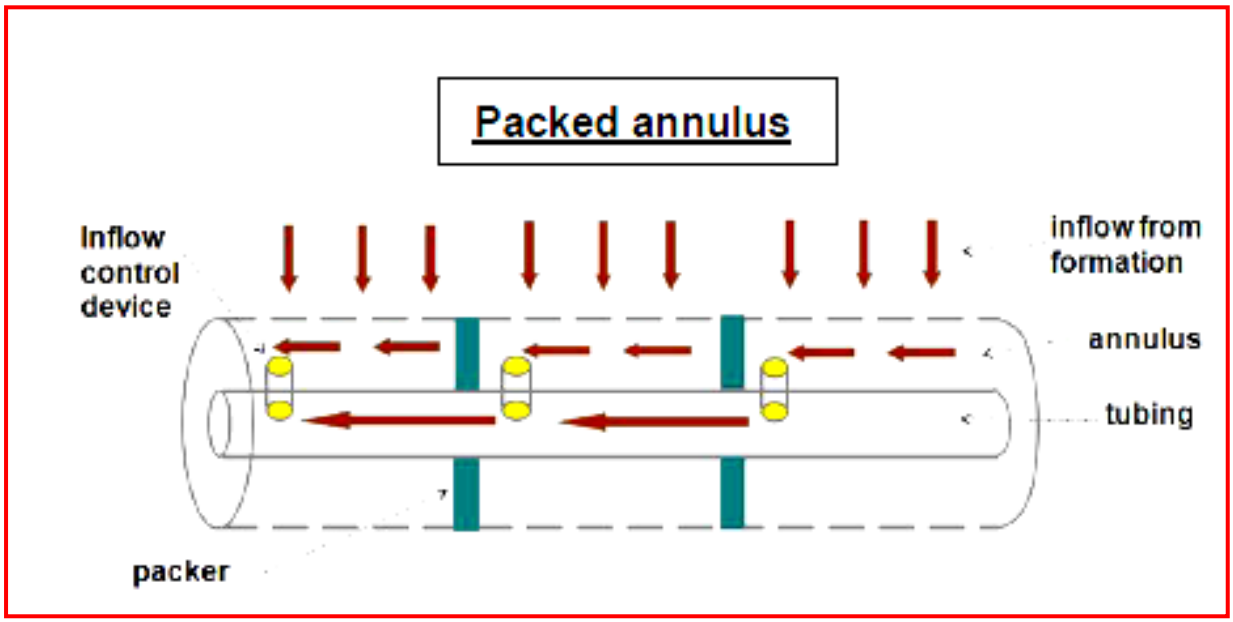

Figure-F: ICD schematic

References:

Birchenko Vasily Mihailovich., **2010.** Analytical Modelling of Wells with Inflow Control Devices, Thesis, Institute of Petroleum Engineering Heriot-Watt University

Elizabeth G. A. 2001. Horizontal well productivity and wellbore pressure behavior incorporating wellbore hydraulics, , Norman, Oklahoma

Folefac, A. N., Archer, J. S., Issa, R. I., and Arshad, A. M. 1991. Effect of Pressure Drop Along Horizontal Wellbores on Well Performance. Society of Petroleum Engineers. doi:10.2118/23094-MS

Grassi E. A. 2015. Analysis of Babu and Odeh's Model, Texas A&M University, USA

JPT, May 2010. Analysis of Inflow-Control Devices

Moradi, B., Dastkhan, Z., Roozbehani, B., and Montazeri, G. H. 2010. Modeling of Water Coning Phenomena in a Fractured Reservoir and Design a Simulator Trinidad and Tobago Energy Resources Conference, 27-30 June, Port of Spain, Trinidad

Oaikhena E. Emmanuel Oloro J. 2013. A Comparative Study of the Productivity Index of Horizontal Well , Vol. 3 (3), pp. 097-109, Delta State University, Department of Petroleum and Gas Engineering, Oleh, Delta State, Nigeria.

ANNEXURE-VIII

Calculations and Referred Literature used in Present Research Work

OGES website (Website: http://oges.info/question/147132/Analytical-Explanation-to-why-ICD-completion-gives)

Procone Manual, 2015

Youngs, B., Neylon, K. J., and Holmes, J. A. 2009. Recent Advances In Modeling Well Inflow Control Devices In Reservoir Simulation. International Petroleum Technology Conference. doi:10.2523/IPTC-13925-MS)

Resume

MANISH KUMAR
Chief Reservoir Engineer
CoEES, Oil India Limited
Guwahati, Assam, India
Mobile: +91-9678006146
E-mail: manish.7417@outlook.com; manish@oilindia.in

Qualifications

2018 Pursuing Part time Ph.D. from University of Petroleum and Energy studies, Dehradun

2003 B. Tech in Petroleum Engineering from Indian School of Mines, Dhanbad

Professional experience

June 2003 till date

- A practicing Reservoir engineer having about 10 years overall experience in Oil and Gas Fields with strong fundamentals in numerical & analytical Reservoir Simulation studies - black oil & gas using Eclipse 100 and MBAL
- Preparation of Field development plan for various oil fields
- Reservoir monitoring and management
- Reservoir data acquisition, Pressure transient design, Interpretation & analysis of oil, gas and water injection wells
- Production performance studies, decline curve analysis, material balance studies, selection of tubing size, vertical lift performance, artificial lift, PLT planning (Software: OFM , MBAL , VFPI)
- IOR/EOR screening, Water flood planning and monitoring of oil wells
- Overseas onshore block evaluation for exploration/production potential
- Mentoring of new team members

Current research interest

- Field development and planning
- Reservoir simulation
- Reservoir management

LIST OF PUBLICATIONS

LIST OF JOURNAL PUBLICATION

Mr. Manish Kumar, Dr. Pushpa Sharma, Dr. D.K. Gupta, 2016. Optimization of vertical well completion in a saturated reservoir with Bottom Water Drive for maximizing recovery, Biofuels , DOI: http://dx.doi.org/10.1080/17597269.2017.1284472

Mr. Manish Kumar, Dr. Pushpa Sharma, Dr. D.K. Gupta, 2016. Integrated approach for maximizing recovery from Oligocene reservoir under bottom water drive, International Journal of oil, gas and coal technology

Mr. Manish Kumar, Dr. Pushpa Sharma, Dr. D.K. Gupta, 2017. Sensitivity study of horizontal length, offset from water oil contact and withdrawal rate of Horizontal well in Bottom Water Drive reservoir, Journal of Petroleum Exploration and Production Technology (PEPT) , DOI: https://doi.org/10.1007/s13202-017-0348-9

Mr. Manish Kumar, Dr. Pushpa Sharma, Dr. D.K. Gupta, 2015. Application of Inflow control devices in Horizontal well in bottom water drive reservoir using Reservoir Simulation, International Journal of Engineering Research and Technology (IJERT), DOI: http://dx.doi.org/10.17577/IJERTV4IS041092 , Volume 4, Issue 4

Mr. Manish Kumar, Dr. Pushpa Sharma, Dr. D.K. Gupta, 2016. Completion design optimization of multilateral well to maximize hydrocarbon production in a bottom water drive reservoir, International Journal Of Engineering Development And Research (IJEDR) , Volume 4 ,Issue 2 ,pp. 897-906

Dr. Pushpa Sharma, Mr. Manish Kumar, Dr. D.K. Gupta, 2018. 3D numerical simulation of clastic reservoir with bottom water drive using various IOR techniques for maximizing recovery, Journal of Petroleum Exploration and Production Technology (PEPT)

LIST OF CONFERENCES

Mr. Manish Kumar, Dr. Pushpa Sharma, Dr. D.K. Gupta, 2016. Investigation of water breakthrough in a bottom water drive reservoir using reservoir simulation: a case study of oligocene sand of upper assam basin, India , The paper was presented at Chemcon-2015 , 27-30 December 2015 , IIT-Guwahati, Assam

LIST OF JOURNAL ACCEPTED AND UNDER PUBLICATION

Dr. Pushpa Sharma, Dr. Vamsi Krishna Kudapa and Manish Kumar, 2018. Screening Criteria for Selecting Appropriate Enhanced Oil Recovery Method, DEW Journal